DOCTOR OF PHILOSOPHY

Effects of hypercapnic acidosis on the primary cells relevant to acute respiratory distress syndrome pathophysiology and the therapeutic potential of Mesenchymal Stem Cells

Fergie, Nicola

Award date:
2018

Awarding institution:
Queen's University Belfast

Effects of hypercapnic acidosis on the primary cells relevant to Acute Respiratory Distress Syndrome pathophysiology and the therapeutic potential of Mesenchymal Stem Cells

Nicola Fergie, BSc

A thesis submitted for the Degree of Doctor of Philosophy

School of Medicine, Dentistry and Biomedical Sciences

Queen's University Belfast

November 2017

Contents

Declaration

I declare that the work presented in this thesis and its composition is based entirely on my own work and that all results and statements presented herein are correct and to the best of my knowledge. None of the material in this thesis has been submitted for which a degree has been or will be conferred by any other university or institution nor has this thesis already been submitted to obtain a degree by this university.

Acknowledgements

Firstly, I would like to thank my supervisors Anna Krasnodembskaya, Danny McAuley, and Cecilia O'Kane for the opportunity to carry out this research and for their guidance throughout the project. The time, patience and effort put into their supervision is truly appreciated.

I would also like to thank the members of the ARDS research group, past and present, for all their help, support and friendship over the past few years. I would especially like to thank Dr. Thomas Morrison and Dr. Megan Jackson for their guidance throughout the duration of the project. Thanks also to Samantha Gallaher who assisted in staining of small airway epithelial cells for identification of cell populations, and to Dr. Marianne Fitzgerald and Dr. Andrew Boyle for their help in obtaining human lungs.

I would also like to acknowledge the Department for the Economy (DfE) who provided funding which enabled me to undertake this project.

Above all else, I would like to thank my family who have been a constant source of support and have always encouraged me to do the best I can.

Abstract

Acute Respiratory Distress Syndrome (ARDS) is an inflammatory disorder in which the integrity of the alveolar epithelial-capillary endothelial barrier breaks down, facilitating the accumulation of a protein-rich oedema fluid within the alveoli. Despite years of clinical trials, no effective pharmacological therapy exists for the condition. Its management therefore remains largely supportive. Low tidal volume ventilation is a central component of supportive care, but may result in the development of hypercapnic acidosis (HCA). While it was once believed that HCA exerts protective effects in such an environment, more recent data are controversial. However, much of these data have been derived from *in vitro* experiments using cell types which are of limited relevance to the pathophysiology of ARDS. The first aim of this project was therefore to determine the effects of HCA on the inflammatory and reparative responses of primary human pulmonary microvascular endothelial cells (HPMECs) and primary human small airway epithelial cells (SAECs) – two of the primary cell types most relevant to the pathophysiology of ARDS – in an *in vitro* model of the condition. Inflammatory responses and wound repair by HPMECs and SAECs were attenuated in HCA, demonstrating its beneficial, but also potentially detrimental effects. This is the first time that the effects of HCA on the reparative response of HPMECs and SAECs has been demonstrated in an inflammatory environment.

Efforts to identify an effective therapy for ARDS are ongoing. Mesenchymal Stem Cells (MSCs) are among the promising candidates currently in early-phase clinical trials. However, no data are currently available on how HCA might influence the therapeutic efficacy of such a cell-based therapy. Identification of any alterations to the MSC therapeutic capacity could aid decision-making in the emerging era of stratified medicine and may facilitate future development of a more effective cell-based therapy. The second aim of this project was therefore to determine the influence of HCA on the biology and therapeutic potential of MSCs in an *in vitro* model of ARDS. MSCs promoted SAEC wound repair in normocapnia, but this effect was lost in HCA. This is the first time that the therapeutic capacity of MSCs in HCA – an environmental factor of great importance in ARDS – has been reported.

The third and final aim of the project was to elucidate the mechanism behind the effects of HCA on the inflammatory and reparative responses of HPMECs and SAECs, and on the therapeutic potential of MSCs. Surprisingly, NFκB activation was not altered by HCA, as it has been in many previous reports. However, HCA was, for the first time, associated with significant attenuation of mitochondrial membrane potential in all three cell types, highlighting a generalised effect of HCA on cell biology. Functional mitochondria were required for the therapeutic potential of MSCs to enhance SAEC wound repair. Mitochondrial transfer from MSCs to SAECs was observed in both normocapnia and HCA. These data support the concept that MSCs transfer functional mitochondria to SAECs to promote wound closure, but that mitochondria transferred in HCA are less functional, resulting in attenuation of the therapeutic capacity of MSCs. This is the first demonstration that the transfer of functional mitochondria is responsible and required for the therapeutic effects of MSCs on repair of the distal lung epithelium, revealing a novel mechanism for the effects of MSCs in ARDS.

Presentations and publications

Oral Presentations at National/International Conferences

- Elucidation of the effects of hypercapnia on distal lung epithelial and endothelial cells, and on mesenchymal stem cells in a model of ARDS
  Intensive Care Society of Ireland and Northern Ireland Intensive Care Society Joint Sumer Meeting, Belfast UK, June 2017

Poster Presentations at National/International Conferences

- Hypercapnic acidosis attenuates endothelial proinflammatory cytokine secretion in an in vitro model of Acute Respiratory Distress Syndrome
  3rd Annual REMERGE Symposium, Belfast UK, June 2015
- Effects of hypercapnia on the inflammatory and reparative response of primary human distal lung epithelial and endothelial cells in the context of ARDS
  4th Annual REMERGE Symposium, Belfast UK, June 2016
- Hypercapnia impairs the ability of Mesenchymal Stem Cells to promote epithelial wound repair
  5th Annual REMERGE Symposium, Belfast UK, June 2017
- Effects of hypercapnic acidosis on the primary cells relevant to ARDS pathophysiology and the therapeutic potential of mesenchymal stem cells
  European Respiratory Society International Congress 2017, Milan Italy, September 2017
- Hypercapnia impairs the ability of mesenchymal stem cells to promote distal lung epithelial wound repair in ARDS
  British Thoracic Society Winter Meeting, London UK, scheduled for December 2017

Prizes and Awards

- Third placed poster presentation – Queen's University Belfast School of Medicine Education and Research Forum, Belfast UK, October 2015
- First placed oral presentation - Intensive Care Society of Ireland and Northern Ireland Intensive Care Society Joint Sumer Meeting, Belfast UK, June 2017
- BTS best practice conference award – British Thoracic Society Winter Meeting, London UK, December 2017

Published Abstracts

NF Fergie, DF McAuley, CM O'Kane and AD Krasnodembskaya. P47 – Hypercapnia impairs the ability of mesenchymal stem cells to promote distal lung epithelial wound repair in ARDS. Thorax, 2017, 72: Suppl 3 A108.

N Fergie, D McAuley, C O'Kane and A Krasnodembskaya. Effects of hypercapnic acidosis on the primary cells relevant to ARDS pathophysiology and the therapeutic potential of mesenchymal stem cells. ERJ, 2017.

Publications in preparation

Nicola Fergie, Daniel McAuley, Cecilia O'Kane and Anna Krasnodembskaya. Hypercapnic acidosis diminishes inflammatory responses but attenuates tissue repair and negatively affects the therapeutic potential of mesenchymal stem cells in ARDS. In preparation for submission to Thorax.

Abbreviations

AFC	Alveolar fluid clearance
Ang-1	Angiopoietin-1
ARDS	Acute Respiratory Distress Syndrome
ATI	Alveolar type I epithelial cell
ATII	Alveolar type II epithelial cells
ATP	Adenosine triphosphate
AQP-5	Aquaporin-5
A549	ATII-like cell line
BALF	Bronchoalveolar lavage fluid
BSA	Bovine serum albumin
CLP	Caecal Ligation and Puncture
COPD	Chronic obstructive pulmonary disease
CO_2	Carbon dioxide
CXCL5	C-X-C motif chemokine ligand 5
CXCL8	C-X-C motif chemokine ligand 8
DMSO	Dimethyl sulfoxide
DPBS	Dulbecco's phosphate buffered saline
E. coli	*Escherichia coli*
ELISA	Enzyme-linked immunosorbent assay
E-selectin	Endothelial-selectin
ETC	Electron transport chain
EV	Extracellular vesicle

EVLP	*Ex vivo* lung perfusion
FBS	Foetal bovine serum
FCCP	Carbonyl cyanide p-trifluoromethoxyphenylhydrazone
FITC	Fluorescein isothiocyanate
HCA	Hypercapnic acidosis
HCO_3^-	Bicarbonate
HPAEC	Human pulmonary artery endothelial cell
HPMEC	Human pulmonary microvascular endothelial cell
HUVEC	Human umbilical vein endothelial cell
H_2O_2	Hydrogen peroxide
ICAM-1	Intercellular adhesion molecule-1
IFNγ	Interferon gamma or gamma interferon
IκB	Inhibitor of kappa B
IKK	IκB kinase
IL1β	Interleukin 1 beta
IL-1ra	Interleukin-1 receptor antagonist
IL-10	Interleukin-10
IT	Intratracheal
IV	Intravenous
JC-1	5,5',6,6'-tetrachloro-1,1',3,3'-tetraethylbenzimidazolylcarbocyanine iodide
KGF	Keratinocyte growth factor
LDH	Lactate dehydrogenase
LG	L-glutamine

LPS	Lipopolysaccharide
MFI	Median fluorescence intensity
miR	microRNA
MSC	Mesenchymal stem cell
$NaHCO_3$	Sodium bicarbonate
Na,K-ATPase	Sodium, Potassium-ATPase
NFκB	Nuclear factor kappa B
NGS	Normal goat serum
$paCO_2$	Partial pressure of CO_2
P. aeruginosa	*Pseudomonas aeruginosa*
PBS	Phosphate buffered saline
PBW	Predicted body weight
PFA	Paraformaldehyde
PS	Pencillin-Streptomycin
ROS	Reactive oxygen species
R6G	Rhodamine 6 G
SAEC	Small airway epithelial cell
S. aureus	*Staphylococcus aureus*
SPC	Surfactant protein C
TCA	Tricarboxylic acid
TEER	Trans-epithelial/endothelial electrical resistance
TNFα	Tumour necrosis factor alpha
VCAM-1	Vascular cell adhesion molecule-1
VE-cadherin	Vascular endothelial-cadherin

Chapter One - Introduction

1.1 Acute Respiratory Distress Syndrome (ARDS)

1.1.1 Definition of ARDS

Acute Respiratory Distress Syndrome (ARDS) is a devastating inflammatory disorder in which alveolar epithelial-capillary endothelial barrier integrity is compromised, facilitating accumulation of protein-rich oedema fluid within the alveoli[1–3]. Clinically, it has been recognised as the acute onset of hypoxaemic respiratory failure since its first description in 1967[4]. However, the precise definition used to clinically diagnose the condition has evolved over time. The American-European Consensus Conference (AECC) Definition, published in 1994, was the first widely-used definition of ARDS but had multiple limitations[5,6]. It was subsequently refined and replaced in 2012 with the introduction of the Berlin Definition[7]. This new definition covers a clinical spectrum in which ARDS is stratified into mild, moderate and severe forms based on the degree of hypoxaemia. Other diagnostic criteria include the presence of bilateral opacities on chest radiograph which appear within 7 days of a known clinical insult or new/worsening respiratory symptoms. Cardiac failure and/or fluid overload must not be the sole cause of respiratory failure.

1.1.2 Pathophysiology of ARDS

The most distal portion of the lung, and specifically the alveoli, is the area most affected in ARDS. The alveoli are small air sacs where gas exchange occurs. Their wall is lined primarily by two cell types – alveolar type I (ATI) and alveolar type II (ATII) epithelial cells. Surrounding, and in close contact with the alveoli are a network of pulmonary capillaries formed by microvascular endothelial cells. In health, the alveolar epithelium and capillary endothelium work together to form a barrier across which effective gas exchange occurs.

Alveolar macrophages ordinarily reside within the healthy alveoli where they play a key role in host defence by facilitating removal of invading microorganisms through the process of phagocytosis. However, in ARDS, upon recognition of an insult such as infection or trauma, they are activated to secrete a plethora of proinflammatory

cytokines, particularly tumour necrosis factor alpha (TNFα)[8,9]. Additionally, among the secreted cytokines are chemokines, such as C-X-C motif chemokine ligand 8 (CXCL8), which promote neutrophil recruitment from the peripheral blood to the alveoli[9–11]. While, like macrophages, neutrophils are phagocytic cells of the innate immune system, they are also an important source of inflammatory cytokines and reactive oxygen species (ROS) which not only further exacerbate the inflammatory response, but also induce tissue damage[10]. These effects are not helped by enhanced neutrophil survival in ARDS[12,13].

The inflammatory response within the alveoli during ARDS – particularly that driven by neutrophils – promotes death of alveolar epithelial and capillary endothelial cells[14–16]. Inflammation also induces destabilisation of the intercellular junctions which normally maintain the integrity of the epithelial and endothelial barriers, and activates the actomyosin contractile apparatus of the cells. This, together with increased cell death, increases alveolar epithelial and capillary endothelial permeability to promote leucocyte recruitment from the peripheral blood and the formation of a protein-rich oedema fluid within the alveoli which impairs effective gas exchange[3,17–19]. To complicate matters further, the ability of remaining ATII cells to clear the excess fluid accumulating within the alveoli (a process termed alveolar fluid clearance or AFC) is impaired in ARDS[20].

The early phase of ARDS described, in which inflammation and the accumulation of a protein-rich oedema fluid resulting from impaired barrier integrity and function are the key hallmarks, is referred to as the acute or exudative phase. These hallmarks are summarised in **Figure 1.1** which illustrates the key differences between the alveoli of healthy individuals and those with ARDS.

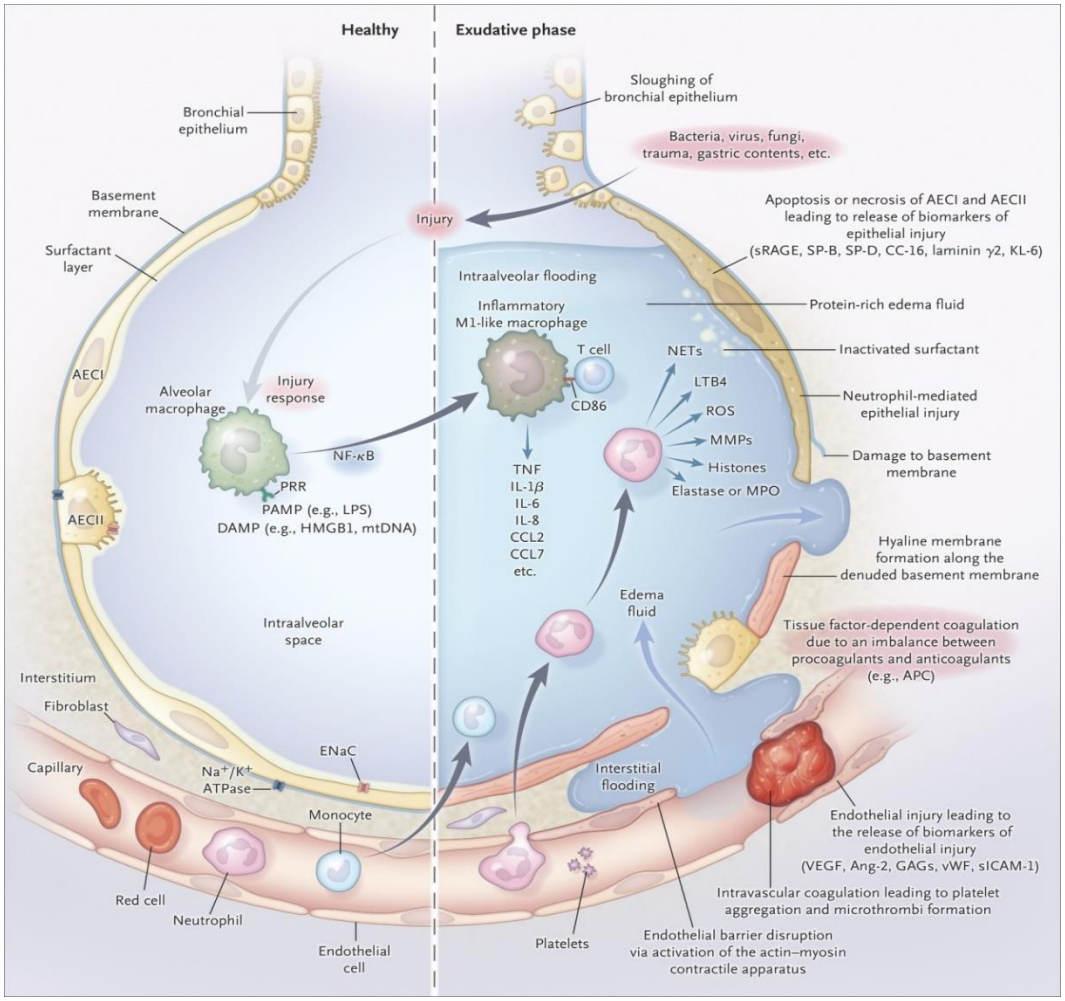

Figure 1.1: Hallmarks of the acute/exudative phase of ARDS in comparison to a healthy alveolus. Reproduced from Thompson *et al.* 2017[3].

Following the acute/exudative phase, there are two possible outcomes in those who survive. The first is functional recovery of the damaged alveolar compartment following re-cellularisation of denuded basement membranes. Human lung regeneration is a complex process, the cellular regulation of which is incompletely understood. It is a long-held belief that migration and subsequent proliferation and differentiation of remaining ATII cells to ATI cells drives re-epithelialisation in the alveolar compartment[21,22], but, more recently, a number of endogenous adult stem and progenitor cells have been identified within the lung which may also contribute[23,24]. Importantly, however, regardless of whether re-epithelialisation is driven by ATII cells or stem/progenitor cells, the regenerated alveolar epithelium consists of

functional epithelial cells. This permits recovery of epithelial functions including limitation of further oedema formation and removal of excess alveolar fluid by AFC to allow progression towards recovery from ARDS[1,25]. Endothelial barrier function is also restored in a similar manner by proliferation of both endothelial cells and endothelial progenitor cells[26].

If injury persists following the acute/exudative phase, however, regeneration may be impaired and fibrous tissue deposited in place of functional epithelial/endothelial cells. In this case, the alveolar compartment may be structurally repaired, but complete functional recovery is unlikely[25]. While the factors influencing the path taken following the acute/exudative phase remain poorly understood, progression to this fibrotic stage is associated with unfavourable outcome in ARDS[27].

1.1.3 Epidemiology of ARDS

The aetiology of ARDS is highly variable. Although multiple risk factors, including both direct and indirect insults to the alveolar compartment may coexist, the most commonly reported are sepsis and pneumonia[28]. Others include, but are not limited to, smoke inhalation, thoracic trauma, and pancreatitis to name a few[29].

With almost 200,000 cases reported *per annum* in the United states alone[30], ARDS is a common condition, particularly in intensive care units where it accounts for approximately 10% of admissions and almost 25% of patients requiring mechanical ventilation[28]. It is predicted that without major advances in the treatment of ARDS, its incidence will increase further as a result of continuing population growth[30], placing an ever-increasing burden on healthcare systems.

Unfortunately, despite decades of research, morbidity and mortality from ARDS remain a concern; mortality rates of up to 40% are not unheard of[7,28], and even in those who do survive, significant physical and psychological impairments are still common years after diagnosis[31–36]. These longer-term effects have wider-reaching

consequences too, affecting not only the patients themselves, but also those providing their care. Advances in the treatment of ARDS and subsequent management of post-ARDS morbidities are therefore urgently required in order to limit the impact of morbidity and mortality on both healthcare systems and those affected, either directly or indirectly, by ARDS.

1.1.4 Management of ARDS

Despite decades of research, there remains no successful pharmacological therapy for the treatment of ARDS[37]. Promising preclinical data have been difficult to translate to the clinic and so, to date, multiple pharmacological interventions investigated clinically - including corticosteroids, β-agonists, and statins to name a few – have not progressed past clinical trials[29,38–43]. For example, while preclinical data suggested that β-agonists (salbutamol, salmeterol, albuterol) enhance epithelial wound repair, improve AFC and reduce pulmonary oedema[44–46], aerosolised albuterol did not improve clinical outcomes in patients with ARDS[40] while administration of intravenous salbutamol worsened 28-day mortality[47].

The heterogeneity of ARDS, coupled with its complex pathophysiology, is believed to contribute to the lack of clinical translation from preclinical studies. As a result, interest in stratified medicine aimed at identifying subphenotypes of patients with ARDS who may be more responsive to specific therapies than others, is now emerging[48,49]. Although still early in the evolution of stratified medicine, two phenotypes of ARDS – hyper-inflammatory and hypo-inflammatory – have been identified on the basis of clinical and biomarker data. Retrospective analysis of clinical trial data suggests that these phenotypes may differ in their response to supportive care strategies, including conservative fluid management and ventilation with high positive end-expiratory pressure (PEEP)[50,51]. The individual responses of these phenotypes to pharmacological intervention have not yet been determined.

As work in identifying ARDS phenotypes emerges, the search for an effective therapy for ARDS continues. While investigations into the use of pharmacological therapies

(for example, the use of aspirin, clinicaltrials.gov NCT02326350) continue, considerable interest in the potential use of a mesenchymal stem cell (MSC)-based therapy exists. MSCs are multipotent adult stem cells which have consistently demonstrated therapeutic potential towards the major hallmarks of ARDS **(Table 1.1)**. Early phase clinical trials have suggested that their application in the condition is safe[52,53], but data on their clinical therapeutic efficacy is awaited (clinicaltrials.gov NCT03042143 and NCT02097641). Despite their progress to clinical trials however, there are still considerable gaps in knowledge with relation to the use of MSCs for the treatment of ARDS. Currently, much is still to be learned about the optimal isolation, expansion, screening, and ultimately use of MSCs as a potential therapeutic for the condition. Additionally, incomplete understanding of MSC biology and the factors which influence it may have important implications for the clinical translation of promising preclinical data if the heterogeneity of ARDS and the presence of subphenotypes are considered. These knowledge gaps will narrow with time, but, for now, it is important that they are recognised as limitations in the interpretation of clinical trial data.

Meanwhile, in the absence of successful pharmacological therapies, the management of ARDS relies on supportive care approaches. Among these include conservative fluid management strategies and low tidal volume ventilation[54,55].

	Mechanism of Injury	Source of MSCs and route of administration	Effects of MSCs
In vivo models of ARDS			
Gupta *et al.* 2007[56]	*E. coli* endotoxin-induced pneumonia in mice	Mouse MSCs; IT	Improved survival Inflammation: ↓ BALF and plasma MIP-2 and TNFα; ↑ BALF and plasma IL-10 Permeability and oedema: ↓ BALF protein concentration and excess lung water
Nemeth *et al.* 2009[57]	Sepsis induced by caecal ligation and puncture (CLP) in mice	Mouse MSCs; IV	Improved survival Inflammation: ↓ serum TNFα and IL-6, and bacterial load in blood; ↑ serum IL-10 and number of circulating neutrophils
Krasnodembskaya *et al.* 2010[58]	*E. coli*-induced pneumonia in mice	Human MSCs; IT	Inflammation: ↓ BALF neutrophil counts, and bacterial counts in BALF and lung homogenates Permeability and oedema: ↓ BALF protein concentration
Curley *et al.* 2012[59]	Ventilator-induced lung injury in rats	Rat MSCs; IV	Improved oxygenation and lung compliance Inflammation: ↓ BALF TNFα and neutrophil counts Permeability and oedema: ↓ BALF protein concentration and wet:dry ratio Reduced histologic lung injury
Gupta *et al.* 2012[60]	*E. coli*-induced pneumonia in mice	Mouse MSCs; IT	Improved survival Inflammation: ↓ BALF TNFα, neutrophil degranulation, and lung bacterial load; ↑ bacterial clearance Permeability and oedema: ↓ excess lung water Reduced histologic lung injury
Krasnodembskaya *et al.* 2012[61]	*P. aeruginosa*-induced sepsis in mice	Human MSCs; IV	Improved survival ↑ phagocytic capacity of blood monocytes; ↓ bacterial load in blood
Asmussen *et al.* 2014[62]	P. *aeruginosa* pneumonia in sheep	Human MSCs; IV	Improved oxygenation Permeability and oedema: ↓ excess lung water
Curley *et al.* 2017[63]	*E. coli*-induced pneumonia in rats	Human MSCs; IV	Improved survival, lung compliance Inflammation: ↓ BALF TNFα and alveolar neutrophil recruitment, and lung tissue ROS Permeability and oedema: improved wet:dry ratio Reduced histologic lung injury

	Mechanism of Injury	Source of MSCs and route of administration	Effects of MSCs
Human ex vivo lung perfusion (EVLP) model of ARDS			
Lee *et al*. 2009[64]	*E. coli* endotoxin	Human MSCs; IT	Permeability and oedema: Improved endothelial permeability; ↓ lung water content; ↑ AFC
Lee *et al*. 2013[65]	Live *E. coli*	Human MSCs; IT and IV	Inflammation: ↓BALF IL1β and CXCL8, neutrophil counts, and bacterial load in alveoli; ↑ phagocytic capacity of macrophages Permeability and oedema: ↑ AFC Reduced histologic lung injury
McAuley *et al*. 2014[66]	Human lungs rejected for transplantation with around 50% demonstrating impaired AFC	Human MSCs; IV	Permeability and oedema: ↑ AFC

Table 1.1 (continued): Therapeutic potential of MSCs in *in vivo* and *ex vivo* models of ARDS

This table highlights some, but not all, of the key *in vivo* and *ex vivo* studies which contribute to a substantial body of evidence supporting the therapeutic potential of MSCs for ARDS. The results of each are related to the key hallmarks of ARDS: inflammation and permeability / oedema. (*E. coli* = *Escherichia* coli; *P. aeruginosa* = *Pseudomonas* aeruginosa; IV = intravenous; IT = intratracheal; ↑ = increased; ↓ = decreased/reduced; IFNγ = interferon gamma; IL = interleukin; MIP-2 = macrophage inflammatory protein-2; BALF = bronchoalveolar lavage fluid; ROS = reactive oxygen species; AFC = alveolar fluid clearance)

1.2 Mechanical Ventilation

1.2.1 Ventilator-Induced Lung Injury (VILI)

Mechanical ventilation is a key component of life support for patients experiencing acute respiratory failure[28]. Traditionally, high tidal volumes of 10-15ml/kg body weight were used to maintain adequate blood gas and pH parameters[67]. However, from the 1980s, clinicians began to realise that this traditional approach to mechanical ventilation was actually harming patients[68,69].

In ARDS, much of the lung is too injured to participate in gas exchange, but an area of healthy lung, known as the 'baby lung', remains[70]. Such areas of normal tissue may be over distended (volutrauma) as a result of exposure to tidal volumes which are significantly higher than those in the lungs of healthy individuals (7ml/kg)[54]. In these areas, volutrauma induces ventilator-induced lung injury (VILI) which manifests as an intense inflammatory response exhibiting many of the characteristic features of the exudative phase of ARDS[69,71–74]. It is concerning to note that, in addition to worsening of lung injury in ARDS, high tidal volume ventialtion may also induce *de novo* lung injury in mechanically ventilated patients not previously presenting with ARDS[75,76].

1.2.2 Low tidal volume ventilation

The use of low tidal volumes was introduced to mechanical ventialtion to address the issues surrounding the use of higher tidal volumes and reduce the potential for VILI caused by mechanically-induced alveolar over distension. This is the only intervention to have demonstrated a survival benefit in ARDS to date. An early randomised trial by Amato *et al.* suggested that ventilation strategies involving the use of low tidal volumes (<6ml/kg predicted body weight) improved mortality[77]. Later, the results of the landmark ARMA trial which compared low (6ml/kg predicted body weight) with high (12ml/kg predicted body weight) tidal volume ventilation in patients with ARDS, were published. These demonstrated a 9% reduction in mortality and an increase in the number of ventilator-free days in the low tidal volume group compared to the high tidal volume group[54]. Lower levels of inflammatory markers and reduced

likelihood of extrapulmonary organ failure were also observed[54]. The use of a low tidal volume ventilation strategy subsequently became, and remains, the mainstay of supportive care approaches in the management of ARDS[78].

1.2.3 Permissive hypercapnia

The use of lower tidal volumes in mechanical ventilation can impair carbon dioxide (CO_2) removal, resulting in increased arterial CO_2 ($paCO_2$) and a fall in pH, otherwise known as hypercapnic acidosis (HCA)[54,79]. This is an unintended side effect of the low tidal volume approach. However, while hypercapnia is a recognised negative prognostic indicator in chronic obstructive pulmonary disease (COPD) and cystic fibrosis, data suggest that its effects in ARDS may be more beneficial that harmful[80,81]. This possibility arises from a retrospective, secondary analysis of the data obtained from >800 patients enrolled in the ARMA study which suggested that HCA (defined as pH <7.35 and $paCO_2$ >45mmHg on Day 1) may reduce mortality in patients receiving high tidal volume, but not low tidal volume, mechanical ventilation[82]. The authors postulated that the lack of effect in the low tidal volume group may be explained by the presence of less-pronounced VILI[82].

While no human trials have yet assessed the direct effects of hypercapnia and HCA on clinical outcomes in ARDS, the HCA associated with low tidal volume ventilation is often now accepted by clinicians and has come to be known as 'permissive hypercapnia'. However, emerging pre-clinical data **(Section 1.4)** raise concerns regarding the true implications of HCA in ARDS. Additionally, recent retrospective analysis of data from more than 250,000 mechanically ventilated patients suggested that HCA is actually associated with increased hospital mortality[83]. Further randomised trials designed specifically to investigate the association between HCA and clinical outcomes are therefore required.

1.3 CO_2 transport and cellular sensing of CO_2 and pH

1.3.1 CO_2 transport

Carbon dioxide (CO_2) can be carried in the blood in one of three forms[84]. Firstly, CO_2 is a highly soluble molecule and approximately 10% is carried in a dissolved form[84]. The remaining 90% enters erythrocytes. This is generally thought to occur via passive diffusion, but more recently a role for channels such as aquaporins has been identified[84–86]. Regardless of how it enters erythrocytes however, CO_2 either binds within the cell to proteins – particularly haemoglobin – or combines with water in a reaction catalysed by carbonic anhydrase. The latter reaction generates carbonic acid which then freely dissociates into H^+ and bicarbonate (HCO_3^-). H^+ is retained within the cell, but HCO_3^- diffuses out of the cell to be carried within the plasma[84]. CO_2 bound to haemoglobin on the other hand is retained and transported within the erythrocyte[84].

1.3.2 CO_2 sensing

The mechanisms by which mammalian cells sense CO_2 appear to be indirect and predominantly mediated by direct sensors of HCO_3^- coupled with carbonic anhydrases[87]. The best characterised CO_2 sensor is soluble adenylyl cyclase (sAC). This is an enzyme expressed both within the cell cytoplasm and in numerous organelles, including the mitochondria[88,89]. sAC acts as a direct sensor of HCO_3^- which can either be directly transported into the cell or can be produced following hydration of CO_2 by carbonic anhydrase[87]. Activation of sAC by HCO_3^- results in enhanced production of the intracellular messenger, cyclic adenosine monophosphate (cAMP) and subsequent activation of protein kinase A (PKA)[90]. CO_2 sensing in this way increases ciliary beat frequency in isolated airway epithelial cells *in vitro*[90,91] and has been associated with a number of effects relevant to the key hallmarks of ARDS, particularly with regards to barrier function and alveolar fluid clearance. For example, HCO_3^- sensing by sAC in rat pulmonary capillary endothelial cells increases cAMP production and is associated with impaired barrier integrity[92]. Additionally, while the involvement of sAC sensing of HCO_3^- was not investigated, PKA activation in response to elevated CO_2 has been associated with endocytosis of Na,K-ATPase – an

ion channel mediating AFC - in alveolar epithelial cells[93]. Together these data suggest that indirect CO_2 sensing by sAC within the alveolar compartment could have important implications for the pathophysiology of, and recovery from, ARDS.

1.3.3 pH sensing

Sensing of extracellular pH by mammalian cells is primarily mediated by G protein-coupled receptors, such as GPR4 which is expressed in the lung[87,94]. Like CO_2, sensing of acidic extracellular pH by GPR4 enhances intracellular production of cAMP[95]. While the involvement of GPR4 in the alveolar compartment has not been directly investigated, its sensing of acidic pH attenuates inflammatory cell adhesion molecule expression on human umbilical vein endothelial cells (HUVECs) in a manner associated with Epac activation downstream of enhanced cAMP production[95]. Additionally, activation of GPR4 by acidosis has been associated with enhanced cytokine and chemokine secretions by HUVECs[96], and with inhibition of tumour cell migration *in vitro*[97]. Together these reports suggest that pH sensing via G protein-coupled receptors, specifically GPR4, may have important implications for inflammation and for processes which involve cell migration, for example re-epithelialisation.

1.4 Physiologic effects of HCA

A diverse range of physiologic effects can be exerted by HCA throughout the human body, including the cardiovascular, cerebrovascular, and respiratory systems.

1.4.1 Cardiovascular system

Targeting of the cardiovascular system by HCA is well-characterised. It impairs the rate and force of myocardial and vascular smooth muscle contraction, attenuating peripheral vascular resistance. This stimulates the sympathoadrenal system to increase heart rate and subsequently cardiac output[98]. Increased cardiac output,

together with a HCA-induced reduction in the oxygen-binding affinity of haemoglobin (Bohr effect), promotes oxygen delivery to the peripheral tissues[84,99–101].

1.4.2 Cerebrovascular system

The systemic vascular response to HCA also applies to the cerebrovascular system where it induces vasodilation at the level of the arterioles and increases cerebral blood flow by approximately 4% for every 1mmHg increment in $paCO_2$[102,103]. While this effect is mediated by pH rather than CO_2 *per se*, the ultimate result is improved cerebral oxygenation[104]. Change in $paCO_2$ may therefore alter the course of ischemic brain injury[105–107].

1.4.3 Respiratory system

Numerous physiologic effects are also exerted by HCA within the lung. Importantly, these include improved arterial oxygenation[108–110]. HCA may also improve lung compliance via both surfactant-dependent and surfactant-independent mechanisms. Surfactant is a phospholipoprotein synthesised and stored in ATII cells. Its secretion into the alveolar space reduces alveolar surface tension to prevent alveolar collapse[111], but its function is impaired in ARDS[112–114]. Exposure of the alveolar epithelium to HCA enhances surfactant secretion. In the presence of acidosis, the function of this surfactant is also enhanced[115]. A surfactant-independent role for the motor protein, myosin, has also been suggested in improving lung compliance[115,116].

In addition to its effects on arterial oxygenation and lung compliance, HCA is additionally thought to influence airway resistance. However, while hypocapnia is associated with airway constriction[117], the effects of HCA on lung resistance are varying and uncertain[115,118–120].

1.5 Effects of HCA in preclinical models of ARDS

To date, a considerable body of experimental work has been performed to demonstrate the effects of HCA in ARDS. The models used in these studies can be broadly divided into those in which lung injury is associated with infection (i.e. sepsis or pneumonia), and those in which lung injury occurs in the absence of infection. Overall, the results demonstrate that the effects exerted by HCA may vary depending on factors such as the severity of lung injury and the context in which it occurs.

1.5.1 Effects of HCA in *in vivo* and *ex vivo* models of ARDS in the absence of infection

A number of *in vivo* and *ex vivo* models of ARDS not associated with infection have been developed. Of these, the two most commonly used are those of ventilator-induced lung injury (VILI) and ischemia-reperfusion (IR)-induced lung injury. The concept of VILI was introduced in **Section 1.2.1**. Ischemia-reperfusion is a common cause of ARDS following thoracic surgeries including lung transplantation, but can also induce lung injury indirectly from other sites within the body[121,122]. Common markers analysed in assessing the degree of lung injury in these models can also be broadly divided into two categories. These relate to the major hallmarks of ARDS: inflammation (leucocyte counts, inflammatory cytokine concentrations, and activation of the NFκB pathway), and barrier integrity and function (BALF protein concentrations which are indicative of barrier function, and lung wet:dry ratio which is indicative of the extent of oedema accumulation).

The results of studies in which models of VILI and IR-induced lung injury were utilised to assess the effects of HCA are summarised in **Table 1.2**. Overall, HCA attenuated inflammation and improved the function of the alveolar epithelial-capillary endothelial barrier, attenuating pulmonary oedema. Given that aberrant inflammation and barrier integrity are key hallmarks of ARDS[3], these data suggest that in a non-infectious setting, HCA benefits lung injury.

	Type of model and degree of HCA	Effect of HCA (compared to normocapnia)
Models of ischemia-reperfusion (IR)-induced lung injury		
Shibata *et al.* 1998[123]	Model: *ex vivo* rabbit lung HCA: 5% CO_2 vs 25% CO_2	• Prevented increase in capillary permeability
Laffey *et al.* 2000[124]	Model: *in vivo* rabbits; direct lung IR HCA: $FiCO_2$ 0.00 vs. 0.12, delivered therapeutically	• Improved oxygenation and lung compliance • Inflammation: ↓ BALF TNFα concentration • Permeability and oedema: ↓ BALF protein concentration and lung wet:dry ratio
Laffey *et al.* 2003[125]	Model: *in vivo* rats; indirect lung injury induced by mesenteric IR HCA: $FiCO_2$ 0.00 vs. 0.05, delivered therapeutically	• Improved oxygenation and lung compliance • Permeability: ↓ BALF protein concentration • Effects dose-dependent
Wu *et al.* 2012[126]	Model: *ex vivo* rat lung HCA: 5% CO_2 vs. 10% CO_2	• Inflammation: ↓ BALF and perfusate TNFα concentrations, inflammatory cell infiltration, and NFκB activation • Permeability and oedema: ↓ BALF protein concentration and lung weight
Wu *et al.* 2013[127]	Model: *ex vivo* rat lung HCA: 0% CO_2 vs. 5% CO_2	• Inflammation: ↓ BALF TNFα concentration and neutrophil counts in lung interstitium • Permeability and oedema: ↓ BALF protein concentration, lung wet:dry ratio and weight

Table 1.2: Summary of the effects of HCA in *in vivo* and *ex vivo* models of ARDS not associated with infection (continued overleaf)

(↓ = decreased/reduced; BALF = bronchoalveolar lavage fluid; TNFα = tumour necrosis factor alpha; $FiCO_2$ = fraction of inspired CO_2; NFκB = nuclear factor kappa B).

	Type of model and degree of HCA	Effect of HCA (compared to normocapnia)
Models of ventilator-induced lung injury (VILI)		
Broccard *et al.* 2001[128]	Model: *ex vivo* rabbit lungs HCA: Target pCO_2 40 vs. 70-100 mmHg	• Permeability and oedema: ↓ BALF protein concentration, ultrafiltration coefficient, and wet:dry ratio
Sinclair *et al.* 2002[129]	Model: *in vivo* rabbits HCA: 4-5% CO_2 (40mmHg) vs 12% CO_2 (80-100mmHg)	• Improved oxygenation • Inflammation: ↓ BALF cell count • Permeability and oedema: ↓ BALF protein concentration and lung wet:dry ratio • Reduced histologic lung injury
Halbertsma *et al.* 2008[130]	Model: *in vivo* mice HCA: 0.06% CO_2 vs. 2% or 4% CO_2	• Inflammation: ↓ IL1β, TNFα and IL-6 in lung tissue, and lung leucocyte infiltration
Peltekova *et al.* 2010[131]	Model: *in vivo* mice HCA: $FiCO_2$ 0.00 vs. 0.12	• Inflammation: ↓ BALF IL-6, MCP-1 and KC • Permeability: ↓ microvascular leak of Evans blue dye (dose-dependent effect)
Contreras *et al.* 2012[132]	Model: *in vivo* rats HCA: $FiCO_2$ 0.00 vs. 0.05	• Improved oxygenation (moderate and severe VILI) and lung compliance (severe VILI only) • Inflammation: ↓ BALF IL-6 and CINC-1 concentrations (both in severe VILI only), BALF neutrophil count, and NFκB activation • Permeability: ↓ BALF protein (severe VILI only) • Reduced histologic lung injury

Table 1.2 (continued): Summary of the effects of HCA in *in vivo* and *ex vivo* models of ARDS not associated with infection

(↓ = decreased/reduced; BALF = bronchoalveolar lavage fluid; TNFα = tumour necrosis factor alpha; $FiCO_2$ = fraction of inspired CO_2; NFκB = nuclear factor kappa B; pCO_2 = partial pressure of CO_2; IL1β = interleukin-1 beta; IL-6 = interleukin-6; MCP-1 = monocyte chemoattractant protein-1; KC (mouse homolog of human CXCL8; CINC-1 = cytokine-induced chemoattractant-1 (rat homolog of human CXCL8).

1.5.2 Effects of HCA in *in vivo* and *ex vivo* models of infection-associated ARDS

Pulmonary and systemic infections account for the majority of ARDS diagnoses[133]. The effects of permissive hypercapnia on the host response to infection are therefore of particular interest in ARDS. A number of models exist in which infection-associated ARDS can be studied. These can be broadly divided, *in vivo*, into models of pulmonary pneumonia and systemic sepsis.

1.5.2.1 Pulmonary pneumonia

Escherichia coli and *Pseudomonas aeruginosa* are common causes of pneumonia in the clinical setting[134]. Their administration, usually via intratracheal instillation, is often used to model pneumonia *in vivo*. Such a model was utilised in the demonstration that the effects exerted by HCA may vary according to the duration of exposure, as well as the duration and severity of pneumonia (results summarised in **Table 1.3**).

Early in the course of less severe *E. coli*-induced pneumonia, HCA did not alter physiologic parameters, the degree of histologic injury, or inflammation when investigated using these models[135]. In more severe, evolving *E. coli*-induced pneumonia, both oxygenation and lung compliance were improved by HCA in comparison to normocapnia. Bronchoalveolar lavage fluid (BALF) protein and TNFα concentrations were also attenuated, but only in the setting of neutrophil depletion[136]. These results suggest that the severity of infection and/or lung injury may be important factors in determining the effects of HCA in the setting of infection. However, as HCA was present at the initiation of infection in both these models, they are of limited clinical relevance to ARDS. In the clinical setting, HCA arises as a result of the ventilation strategy used in the management of the patient's condition. Therefore, established (not early) pneumonia is likely to be present at the time of ventilation and subsequent induction of HCA. In an *in vivo* model more clinically relevant in this context, *E. coli*-induced pneumonia was allowed to develop over 6 hours before the introduction of HCA. Lung compliance, but not histologic injury or inflammation, was improved in hypercapnic animals. When antibiotic therapy was initiated,

bacterial counts were reduced and HCA attenuated the degree of lung injury[137], suggesting that the presence of bacteria may interfere with the protective effects of HCA.

In the setting of infection, one of the biggest concerns regarding HCA is its potential to alter bacterial growth. This is because immunocompetence is required for bacterial clearance by the host immune system, but potent anti-inflammatory effects of HCA are well-documented. *E. coli* has been shown to grow better in culture medium acidified by the addition of hydrochloric acid (HCl), while its growth was inhibited in medium in which pH was artificially increased by the addition of sodium hydroxide (NaOH)[138]. Growth of numerous clinical isolates from the lungs of patients with ventilator-associated pneumonia also grew better at acidic pH. These isolates included *E. coli*, *P. aeruginosa*, *Klebsiella pneumoniae*, and *Staphylococcus aureus*[138]. However, despite these observations, in the *in vivo* models discussed, bacterial loads in the BALF and blood of hypercapnic animals did not differ significantly from normocapnia.

Taken together, the above results demonstrate that the protective effects of HCA observed in models of infection-independent ARDS are not as apparent, and possibly even absent, in the setting of early bacterial pneumonia. However, HCA did not worsen the hallmarks of ARDS, suggesting that even if not protective, its presence is at least safe during the early stage of infection.

In comparison to early pneumonia, the effects of HCA may be very different when present throughout the course of prolonged *E. coli*-induced pneumonia. In such a model, while inflammation was not affected by HCA, lung compliance was reduced and structural damage worsened. Of particular concern, bacterial colony counts were also increased[139]. However, these detrimental effects could be abrogated by daily antibiotic therapy post-infection[139], suggesting that the detrimental effects of HCA in prolonged bacterial pneumonia relate more to complication by infection than the duration of exposure to HCA.

More worryingly, however, when mice were exposed to 10% CO_2 for three days prior to early *P. aeruginosa*-induced pneumonia, mortality increased; all mice in the hypercapnic group were dead by 48 hours in comparison to 50% at 48 hours and 70% at 72 hours in normocapnic controls[140]. This was associated with increased bacterial counts in the liver, lung and spleen. While the contribution of bacterial growth to this effect was not determined, it appears that attenuation of the phagocytic capacity of neutrophils in HCA may have contributed, at least in part, to this effect by impairing bacterial clearance[140]. While these findings are of limited clinical relevance in ARDS given that bacterial pneumonia would normally be established at the time of mechanical ventialtion and subsequent development of HCA in patients with ARDS, they do raise concerns with regards to prolonged exposure to HCA in the setting of ARDs associated with bacterial pneumonia.

	Type of model and degree of HCA	**Effect of HCA (compared to normocapnia)**
	Models of pneumonia	
O'Croinin *et al.*[135]	Model: less severe *E. coli* pneumonia in rats HCA: $FiCO_2$ 0.00 vs. 0.05	• No effect on oxygenation or lung compliance • No effect on degree of histologic lung injury • Inflammation: no effect on BALF neutrophil counts or BALF IL1β or MIP-2 concentrations • Bacterial load: colony counts not altered in lung homogenate

Table 1.3: Summary of the effects of HCA in *in vivo* models of pneumonia (continued overleaf)

(E. coli = Escherichia coli; $FiCO_2$ = fraction of inspired CO_2; BALF = bronchoalveolar lavage fluid; IL1β = interleukin-1 beta, MIP-2 = macrophage inflammatory protein-2)

	Type of model and degree of HCA	Effect of HCA (compared to normocapnia)
Models of pneumonia		
Ni Chonghaile *et al.*[136]	Model: more severe evolving *E. coli* pneumonia in rats HCA: $FiCO_2$ 0.00 vs. 0.05	• Improved oxygenation and lung compliance • No effect on degree of histologic lung injury • Inflammation: no effect on BALF neutrophil counts or BALF TNFα concentrations* • Permeability and oedema: no effect on BALF protein concentrations* • Bacterial load: not altered in lungs or blood **** BALF protein and TNFα concentrations ↓ in HCA mice with depleted neutrophils vs. normocapnic mice with no depletion***
Ni Chonghaile *et al.*[137]	Model: established *E. coli* pneumonia in rats (6 hours before HCA) HCA: $FiCO_2$ 0.00 vs. 0.05	• No effect on oxygenation or lung compliance • No effect on degree of histologic lung injury* • Inflammation: no effect on BALF neutrophil counts or BALF TNFα concentrations • Bacterial load: not altered in BALF or blood **** Degree of histologic injury ↓ in mice which received antibiotics***
O'Croinin *et al.*[139]	Model: prolonged (2 days) *E. coli* pneumonia in rats HCA: 0% CO_2 vs. 5% CO_2	• No effect on oxygenation, ↓ lung compliance • ↑ degree of histologic lung injury • Inflammation: no effect on BALF neutrophil counts or BALF IL1β or MIP-2 concentrations • Bacterial load: ↑ counts in lung homogenate, ↓ neutrophil phagocytic capacity **(No difference between groups in any of the above parameters when administered antibiotics)**
Gates *et al.*[140]	Model: *P. aeruginosa* pneumonia in mice HCA: 10% CO_2 vs. air (for 3 days before infection)	• ↑ mortality* • No effect on degree of histologic lung injury • Inflammation: no effect on BALF neutrophil counts, no effect on BALF and lung tissue TNFα • Bacterial load: ↑ in lung, liver and spleen; ↓ phagocytic capacity of neutrophils *** Effects of HCA on mortality were reversible, especially if recovery in air was permitted before infection**

Table 1.3 (continued): Summary of the effects of HCA in *in vivo* models of pneumonia

(E. coli = Escherichia coli; P. aeruginosa = Pseudomonas aerginosa; $FiCO_2$ = fraction of inspired CO_2; BALF = bronchoalveolar lavage fluid; TNFα = tumour necrosis factor alpha; IL1β = interleukin1 beta, MIP-2 = macrophage inflammatory protein-2; ↑ = increased; ↓ = decreased)

1.5.2.2 Systemic sepsis

A number of models of sepsis-associated ARDS exist[141]. Among these include the caecal ligation and puncture (CLP) model in which the ceacum is ligated and subsequently punctured with a needle. This results in ischemic damage to the caecum but, importantly, promotes polymicrobial sepsis owing to faecal leakage into the peritoneum[141,142]. The severity of sepsis resulting from CLP can be adjusted according to the area of caecum ligated, as well as the size and number of puncture wounds[141,143].

Using this model, Higgins *et al*. demonstrated that HCA improved arterial oxygenation and attenuated lung tissue damage and inflammation in early systemic sepsis. While HCA delayed the appearance of bacteria in the blood, bacterial counts did not differ at the end of the study[144]. Similarly, Costello *et al*. also demonstrated attenuated pulmonary inflammation, barrier permeability and oedema formation in HCA using a CLP-induced model of early systemic sepsis[145]. In contrast, despite a moderately reduced histologic degree of lung injury, there was no evidence that HCA affected inflammation, barrier permeability or oedema formation in the setting of more prolonged sepsis with simultaneous HCA exposure. However, it is important to highlight that, in contrast to prolonged pneumonia, these parameters and bacterial loads within the lungs and blood were not worsened by HCA[145]. When compared to prolonged pneumonia, these results suggest that the site of initial infection might be an important determinant of the effects of HCA.

Sepsis can also be modelled *in vivo* by the induction of peritonitis following direct injection of faecal contents into the abdominal cavity[141,146]. Using this model, the abilities of HCA to improve oxygen delivery and reduce the accumulation of pulmonary oedema have been demonstrated in established sepsis[147].

Taken together, these results (which are summarised in **Table 1.4**) are strongly suggestive of a protective effect of HCA in sepsis-associated lung injury. Importantly, the lack of detrimental effects in any of the septic models discussed attests to the safety of HCA in this setting.

	Type of model and degree of HCA	Effect of HCA (compared to normocapnia)
Models of sepsis		
Higgins *et al.*[144]	Model: early systemic sepsis induced by CLP in rats HCA: 0% CO_2 vs. 5% CO_2	• No effect on oxygenation or lung compliance • Inflammation: ↓ BALF neutrophil counts and BALF TNFα concentration • Bacterial load: Not altered in BALF, delayed appearance in blood but no significant difference at end of the protocol *** Renal buffering for 96 hours prior to infection ameliorated effects on BALF neutrophil counts and TNFα concentrations**
Costello *et al.*[145]	Model: early systemic sepsis induced by CLP in rats HCA: $FiCO_2$ 0.00 vs. 0.05	• No effect on oxygenation or lung compliance at end of protocol • Inflammation: ↓ BALF neutrophil counts, no effect on BALF TNFα concentration • Permeability and oedema: ↓ wet:dry ratio and BALF protein concentration, no effect on histologic lung injury • Bacterial load: Not altered in BALF, peritoneum, or blood
	Model: prolonged (96h) systemic sepsis induced by CLP in rats HCA: $FiCO_2$ 0.00 vs. 0.05	• No effect on survival, oxygenation or lung compliance at end of protocol • Inflammation: no effect on BALF neutrophil counts or BALF TNFα concentration • Permeability and oedema: ↓ histologic lung injury, no effect on wet:dry ratio or BALF protein concentration • Bacterial load: Not altered in BALF, peritoneum, or blood
Wang *et al.*[147]	Model: faecal peritonitis-induced systemic sepsis established 2 hours before HCA exposure in sheep HCA: 35-45mmHg vs. 55-65mmHg	• ↑ oxygen delivery, no effect on survival or lung compliance • Permeability and oedema: ↓ wet:dry ratio

Table 1.4 Summary of the effects of HCA in *in vivo* models of sepsis

(CLP = caecal ligation and puncture; $FiCO_2$ = fraction of inspired CO_2; BALF = bronchoalveolar lavage fluid; TNFα = tumour necrosis factor alpha; ↑ = increased, ↓ = decreased)

1.5.3 Limitations of *in vivo* models

When interpreting the effects of HCA in *in vivo* models of ARDS, it is important to consider that these studies were carried out predominantly in small animals, primarily rats. Small animals are often used for *in vivo* research due to their availability and lower cost when compared to the use of larger animals. However, it is important to consider that in these models, the degree of lung injury is often much less severe than that in human ARDS as the animals do not survive severe impairment of gas exchange[148]. Importantly, although small animal models have provided invaluable insights into the impact of HCA at the level of the whole organism, the cellular responses of rodents may differ considerably from those of human cells. Further studies in more relevant models, for example *ex vivo* lung perfusion, are therefore warranted.

1.5.4 Effects of HCA at the cellular level

In vitro work has provided further insight into the effects of HCA at the cellular level in the cell types implicated in the pathophysiology of ARDS.

1.5.4.1 Macrophages

As the first line of defence to infection and injury, macrophages are key cells of the innate immune system[149]. As discussed in **Section 1.1.2**, macrophages are central to the pathogenesis of ARDS; in response to insult they respond by secreting proinflammatory cytokines. In *in vivo* and *ex vivo* models of ARDS, HCA was associated with attenuated BALF proinflammatory cytokine concentrations **(Section 1.5)**. While the contributions of individual cell types to this response have not been directly determined, HCA attenuates macrophage secretion of proinflammatory cytokines, including TNFα, *in vitro*[150,151], suggesting that alveolar macrophages may contribute to the reduction in BALF proinflammatory cytokine concentrations observed *in vivo*.

As part of the innate immune system, the capacity of alveolar macrophages to phagocytose bacteria is important in the context of pneumonia- and sepsis-induced ARDS. *In vitro*, uptake of *S. aureus* by human alveolar macrophages is impaired in HCA, suggesting that macrophage phagocytic activity may be impaired in the setting of hypercapnic infection[152]. It is possible that impaired phagocytosis by macrophages could reduce bacterial clearance and subsequently play a role in the HCA-mediated increase in bacterial counts observed in some *in vivo* models of bacterial pneumonia[139,140]. However, more recent work in macrophages derived from differentiation of the monocytic THP-1 cell line and exposed to *E. coli* or *S. aureus* bioparticles suggests that although the number of phagosomes is reduced, hypercapnia exerts a greater effect on autophagy by macrophages than on their phagocytic capacity[153]. Autophagy is a process classically involved in the removal of the cell's own damaged organelles and proteins, but it also plays a role in host defence against pathogens[154]. In hypercapnia, binding of the anti-apoptotic proteins Bcl-2 and Bcl-xL to the BH3 domain of Beclin-1 – a protein with a key role in the assembly of autophagosomes – is attenuated. The function of Beclin-1 and subsequently autophagy and bacterial killing is thus reduced[153]. Together these results suggest that macrophages may play a key role in mediating the effects of HCA on bacterial counts in some *in vivo* models of bacterial pneumonia, and that their involvement may extend beyond simply reducing the phagocytic capacity of alveolar macrophages.

1.5.4.2 Neutrophils

Neutrophils are another key cell of the innate immune system. As discussed in **Section 1.1.2**, their infiltration into the alveoli is a key hallmark of ARDS. Like macrophages, neutrophils are phagocytic cells and *in vitro* data suggest that the effects of HCA on the two cell types may follow a similar pattern. Similar to macrophages, HCA attenuated the secretion of proinflammatory cytokines, including CXCL8, by neutrophils[155], suggesting that neutrophils may also contribute to attenuation of BALF proinflammatory cytokine concentrations *in vivo*. However, alveolar neutrophils isolated from mice pre-exposed to 10% CO_2 for 3 days prior to induction of bacterial pneumonia were capable of phagocytosing fewer bacteria *in vitro* than those from mice exposed to air[140]. During phagocytosis, oxygen consumption is increased and

neutrophil production of reactive oxygen species (ROS), including superoxide and hydrogen peroxide (H_2O_2), is enhanced in a process termed the 'respiratory burst'. These ROS may subsequently be released to exert anti-microbial functions, but may also induce further tissue damage[156]. Intracellular production of superoxide by neutrophils is attenuated in HCA[155]. Additionally, neutrophils from mice pre-exposed to 10% CO_2 prior to induction of bacterial pneumonia produced less H_2O_2 than neutrophils from air-exposed mice *in vitro*[140]. These findings further support the suggestion that neutrophil phagocytosis is impaired in HCA, raising concerns that while ROS-mediated damage may be attenuated by HCA in the setting of infection, the capacity of neutrophils to clear bacteria is impaired.

1.5.4.3 Endothelial cells

Current knowledge regarding the effects of HCA on endothelial cells *in vitro* are discussed in more detail in **Section 3.2**. However, in overview, little is known about the response of the pulmonary capillary endothelium to HCA, despite its contributions to the alveolar oedema and neutrophil recruitment which are characteristic of ARDS. Only two studies exist to date in which the response of endothelial cells to HCA has been investigated, and these have given rise to conflicting results. The first of these studied the effects of HCA in human pulmonary artery endothelial cells (HPAECs), demonstrating that HCA attenuated inflammatory cytokine secretion. The results also suggested that the contribution of the endothelium to neutrophil extravasation may also be attenuated as a result of reduced expression of the adhesion molecule intercellular adhesion molecule-1 (ICAM-1)[157]. However, the endothelial cells used in this study were not derived from the pulmonary capillary endothelium and in a later study which did utilise these more relevant cells, all of the parameters which were reduced in HPAECs, were increased[158]. While the discrepancy between the two studies could be explained by differences in the endothelial cell type used, the latter study was reported alongside *in vivo* data which also contradicted a large body of previous *in vivo* findings, raising concerns regarding the validity of these results[158]. Further investigations are therefore required before it can be said with confidence that HCA enhances the contribution of pulmonary capillary endothelial cells to inflammation.

1.5.4.4 Epithelial cells

As discussed in **Section 1.1.2**, disruption to the integrity of the alveolar epithelial barrier, together with impaired alveolar fluid clearance by alveolar epithelial cells, is central to the formation of pulmonary oedema – one of the key hallmarks of ARDS. Current knowledge regarding the effects of HCA on alveolar epithelial cells *in vitro* are discussed in more detail in **Section 4.2**. In overview, the response of the epithelium to HCA is somewhat better understood when compared to the response of the endothelium. However, much of this knowledge has been obtained from work in cancer cell lines and is limited by lack of experimental work in the most clinically relevant primary cell types *in vitro*. While the ability of the ATII-like cell line, A549, to secrete proinflammatory cytokines is attenuated in HCA[127,159], concerns have arisen regarding the reparative capacity of the alveolar epithelium; A549 wound closure is attenuated in HCA as a result of impaired migration[160], while HCA also attenuates cell proliferation[161]. This is concerning as the integrity of the alveolar epithelial barrier is central to the regulation of alveolar permeability. These results suggest that HCA may impair restoration of the alveolar epithelial barrier in ARDS by attenuating the potential for re-epithelialisation.

The capacity of epithelial cells to facilitate alveolar fluid clearance in HCA has also been studied, extensively, *in vitro*. However, the results consistently demonstrate impairment of alveolar fluid clearance by A549 cells (reviewed by Vadasz *et al.*[162]), adding further concern to the effects of HCA on the alveolar epithelium.

Taken together, the *in vitro* results obtained in epithelial cells, largely the A549 cell line, raise concerns regarding the contribution of the alveolar epithelium to repair and resolution of ARDS in a hypercapnic acidotic environment. It is noteworthy however, that permeability and pulmonary oedema were rarely increased in HCA in *in vivo* models of ARDS **(Sections 1.5.1 and 1.5.2)**. While O'Toole *et al*. confirmed that HCA also impaired wound closure by distal lung epithelial cells *in* vitro[160], this has been the only demonstration of the effects of HCA on primary human lung epithelial cells to date. It is possible that the discrepancies between *in vitro* and *in vivo* results could be explained by differences in the responses of rodent versus human cells, and

by the limitation of the use of immortalised cell lines in which cell biology may markedly differ from primary cells of the same origin. Confirmation of the response of epithelial cells to HCA in primary cell types relevant to the pathophysiology of ARDS is therefore required.

1.6 Effects of hypercapnic acidosis - pH vs. CO_2 *per se*?

When investigating the effects of HCA, it is important to consider that the results may arise from either the pH or the CO_2 *per se*, and not necessarily from the combined effect of the two. This is important as buffering of acidosis is often permitted in clinical trials[54] and may have the potential to negate any protective effects of HCA if they are mediated by acidosis. To investigate the effects of pH and CO_2 as separate entities *in vitro*, the medium pH in HCA is usually buffered using sodium bicarbonate, sodium hydroxide or Tris-Hydroxymethyl aminomethane (THAM). Additionally, the pH of cell culture medium may be artificially reduced by the addition of acid in normocapnia. Buffers may also be used to increase pH *in vivo* or time may be given to allow renal buffering to occur. As illustrated in **Table 1.5**, the results of investigations into the individual contributions of pH and CO_2 to HCA-mediated effects have yielded conflicting results.

	Model	Method of Buffering	Parameters measured	pH or CO_2-mediated effect?
Laffey *et al.* 2000[163]	*Ex vivo* IR-induced lung injury	Sodium hydroxide	Capillary permeability and oedema	Acidosis
Coakley *et al.* 2002[155]	*In vitro* neutrophils	Bufferall	CXCL8 secretion and superoxide production	Acidosis
Briva *et al.* 2007[164]	*In vivo* rat lungs	Tris base	Na,K-ATPase endocytosis	CO_2
Caples *et al.* 2009[165]	*Ex vivo* and *in vivo* VILI	THAM and sodium bicarbonate	Plasma membrane injury	Acidosis
Higgins *et al.* 2009[144]	*In vivo* rat CLP-induced sepsis	Renal buffering	Inflammation, tissue damage and bacterial counts in blood	Acidosis
O'Toole *et al.* 2009[160]	*In vitro* A549 cells	Sodium bicarbonate	Wound repair	CO_2
Wang *et al.* 2010[151]	*In vitro* macrophages	Sodium bicarbonate (or acidification with HCl in normocapnia)	IL6 mRNA expression	CO_2
Gates *et al.* 2013[140]	*In vivo* pneumonia	Acute vs. chronic respiratory acidosis	Mortality	CO_2

Table 1.5: Summary of experiments performed to investigate the individual contributions of pH and CO_2 to the effects of HCA

The conflicting data which have arisen as a result of experimental work aiming to investigate the individual contributions of pH and CO_2 to HCA-mediated effects may be explained by differences in experimental design. The results presented in **Table 1.5** clearly demonstrate the existence of considerable variations in the design of individual studies. Firstly, some of these studies are *in vivo* studies while others have been performed *in vitro*. Variation between the results of *in vivo* and *in vitro* studies may arise as buffering (e.g. renal buffering) naturally occurs in *in vivo* systems, but it is difficult to replicate its contributions in *in vitro* models. Differences also exist in the type of buffer administered. Sodium bicarbonate is a widely used buffer. Its use was permitted in the ARMA study[54]. However, a number of concerns exist with regard to its use as it has the potential to increase CO_2 and reduce intracellular pH, and may therefore exert biologic effects of its own[166]. THAM on the other hand does not exert

these effects as it differs in its mechanism of action by assisting excretion of protons via the renal system[167,168]. Optimisation and standardisation of experimental buffering will therefore be required before the contributions of pH and CO_2 to HCA-mediated effects can be accurately determined.

1.7 Mechanisms of HCA-mediated effects

The precise mechanism of HCA-mediated effects (whether protective or detrimental) are unknown. Experimental work has ruled out the involvement of hypoxia-responsive genes such as vascular endothelial growth factor (VEGF), and heat shock proteins such as Hsp70[152]. However, with few exceptions[152], the effects of HCA have consistently been associated with altered activation of the nuclear factor kappa B (NFκB) pathway (where studied). This is unsurprising given that many of the inflammatory proteins altered by HCA (CXCL8[169], TNFα[170] and ICAM-1[171,172]) are regulated by this pathway. Some evidence also points towards the involvement of a second mechanism – altered mitochondrial function – in mediating the effects of HCA. Again, this would be unsurprising given the central role which mitochondria play in cell biology, not least in their capacity to facilitate the oxidative phosphorylation required to meet cellular energy demands.

1.7.1 The Nuclear Factor kappa B (NFκB) pathway

The NFκB pathway is one of the main transcriptional activators of inflammatory genes. This is important in ARDS where one of the key hallmarks is alveolar inflammation. In mammalian cells, the NFκB pathway centres around the formation of NFκB dimers containing Rel proteins, such as p50 and RelA (p65), which possess a C-terminal transcriptional activation domain. In resting cells, these dimers are maintained in the cytoplasm by binding of inhibitor of kappa B (IκB) proteins such as IκBα, and are thus unable to activate transcription. Upon activation however, cell surface receptors recruit an IκB kinase (IKK) complex containing catalytic subunits capable of phosphorylating IκBα, promoting its proteasomal degradation. This results in liberation of the NFκB dimers, facilitating their translocation to the nucleus and thus their ability to induce transcription of target genes[173,174]. Activation of NFκB in this

way is known as the canonical pathway of NFκB activation. An alternative pathway, known as the non-canonical pathway, exists in which RelB is maintained in the cytoplasm in complex with the IκB protein, p100, preventing its ability to translocate to the nucleus and alter transcription. In this pathway, activation of IKK initiates partial degradation of p100 to generate p52-RelB complexes (NFκB dimers) which can translocate to the nucleus to control gene transcription[173,174]. Both the canonical and non-canonical NFκB pathways are illustrated in **Figure 1.2**.

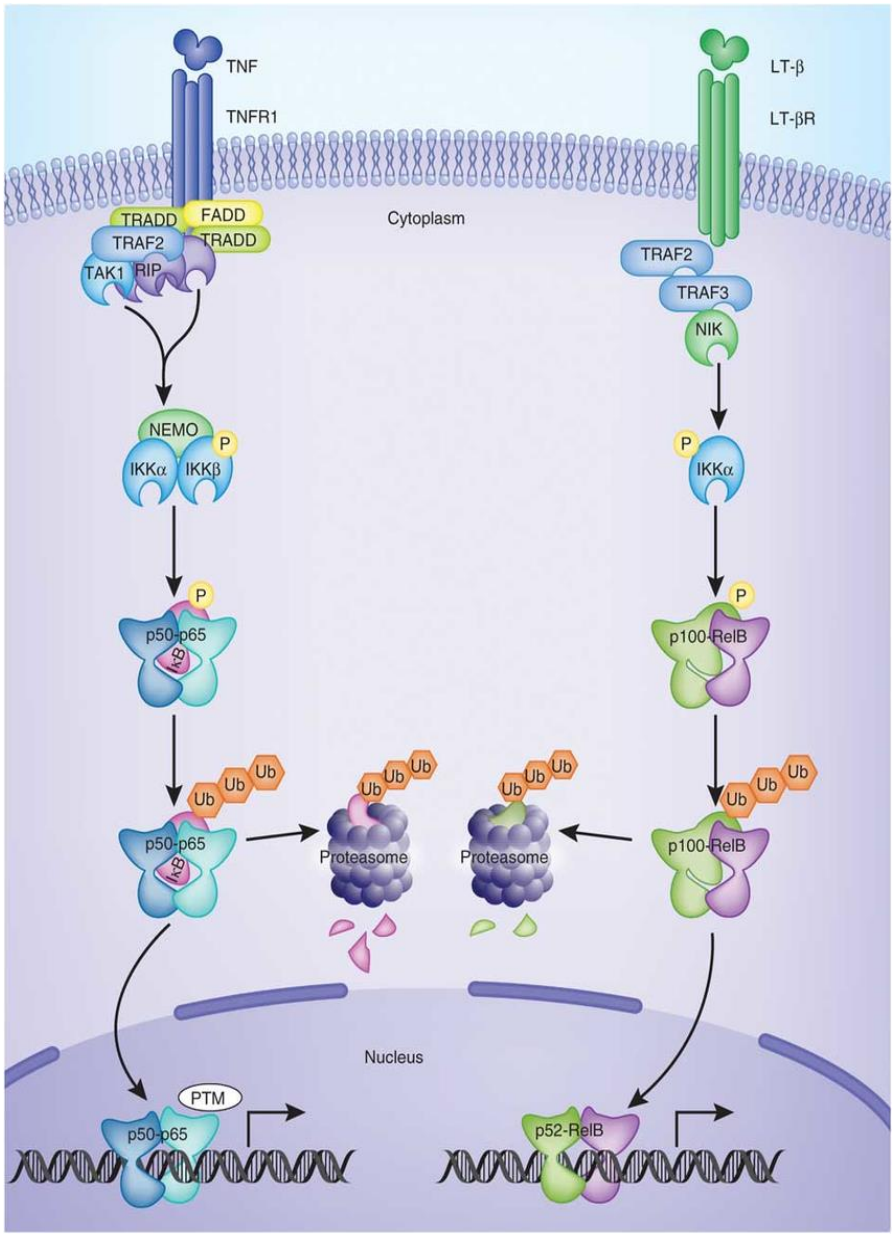

Figure 1.2: Canonical NFκB pathway (left) and non-canonical NFκB pathway (right).
Reproduced from Oeckinghaus 2011[174].

Attenuated activation of the canonical NFκB pathway has been associated with the anti-inflammatory properties of HCA in many *in vivo* and *in vitro* models of ARDS[132,157,159,175]. Its attenuated activation has also been associated with impaired wound closure of A549 cells *in vitro*[160]. Traditionally, HCA was believed to exert its effects through attenuated IκBα expression. However, more recent work in lipopolysaccharide (LPS)-stimulated A549 cells has elaborated on this mechanism, suggesting that attenuated IκBα expression occurs secondary to HCA-mediated inhibition of the IKKβ subunit[176]. Regardless of the upstream events however, the ultimate result is attenuated translocation of the strong transcriptional activator, p65, into the nucleus[176]. This results in attenuated transcriptional activation, namely of genes encoding inflammatory proteins.

The lesser-studied Rel family protein, RelB of the non-canonical pathway, may also play a role in mediating the effects of HCA. Early studies demonstrated that its hypercapnia-induced nuclear localisation was responsible for attenuated TNFα secretion by A549 cells[177]. Further work suggested that translocated RelB is truncated at the C-terminus in which its transcriptional activation domain is located. Its capacity to induce transcriptional activation is thus reduced[178]. This suggests that the effects of HCA may not depend solely on the canonical NFκB pathway, and that the non-canonical pathway is also involved. Overall, experimental evidence is strongly suggestive of the involvement of altered activation of the NFκB pathway in mediating the effects of HCA.

1.7.2 Mitochondrial function

Mitochondria are membrane-bound organelles best known for their role in facilitating energy production within the cell. Energy production begins in the cell cytoplasm with the process of glycolysis. This is an oxygen-independent process in which a small amount of energy is released in the form of adenosine triphosphate (ATP) during the breakdown of glucose to pyruvate[179]. Pyruvate is then transported into the mitochondrial matrix and oxidised to acetyl coenzyme A (CoA) which drives the subsequent tricarboxylic acid (TCA) cycle. The TCA cycle is a series of redox

reactions in which NADH and $FADH_2$ are produced from the reduction of NAD^+ and FAD, respectively[179]. NADH and $FADH_2$ are subsequently passed to the electron transport chain (ETC) located in the inner mitochondrial membrane. Here, the electrons they carry are utilised in the production of ATP by oxidative phosphorylation **(Figure 1.3)**[180].

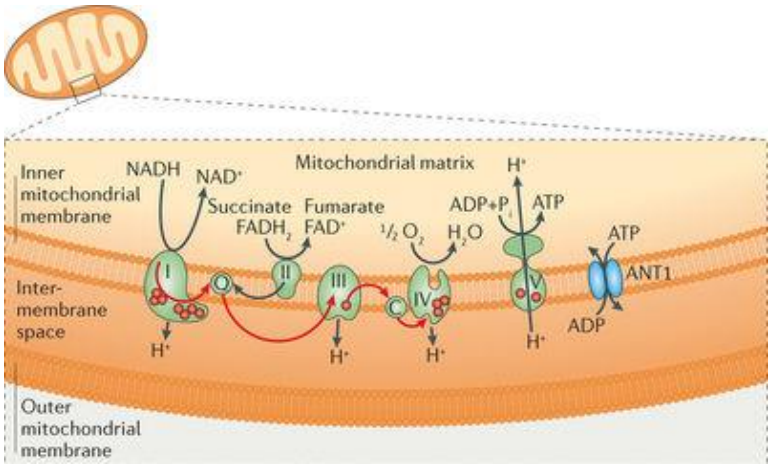

Figure 1.3: Oxidative phosphorylation via the electron transport chain located in the inner mitochondrial membrane. Reproduced from Suomalainen and Battersby, 2017[180].

As electrons are passed through the ETC, they establish a proton motive force – composed of a voltage gradient (mitochondrial membrane potential) and a proton concentration gradient – across the inner mitochondrial membrane which drives the activity of ATP synthase. The components of the proton motive force can therefore be indicative of mitochondrial function. In healthy cells, for example, mitochondrial membrane potential is normally maintained within an optimal range of approximately 100-120mV. Inside this range, ATP production is optimal. However, when the mitochondrial membrane potential falls, the function of the electron transport chain is

impaired and ATP production subsequently reduced[181]. Maintenance of mitochondrial membrane potential is therefore required for optimal energy production within the cell.

Aside from their role in oxidative metabolism, mitochondria also participate in other cellular processes. For example, they contribute to cell death by apoptosis through the release of cytochrome c from the intermembrane space into the cell cytoplasm. This is associated with enhanced mitochondrial membrane potential[181]. In the cytoplasm, cytochrome c induces caspase activation and subsequently promotes apoptosis[182].

Mitochondria are also an important source of reactive oxygen species (ROS), particularly superoxide and hydrogen peroxide (H_2O_2). These are largely generated during oxidative phosphorylation when mitochondrial membrane potential rises above approximately 150mV[181,183]. Normally, at the end of the ETC, each molecule of oxygen receives four electrons to form water. However premature electron leak from the ETC can result in the generation of ROS via partial reduction of oxygen to superoxide. Superoxide can subsequently be released into the cell cytoplasm via voltage-dependent channels in the outer mitochondrial membrane, or converted to H_2O_2 by superoxide dismutases in the mitochondrial matrix and intermembrane space. H_2O_2 may then also be released to the cytoplasm[184]. These ROS have the potential to exert a multitude of effects relevant to the pathophysiology of ARDS; they are important not only for host defence against pathogens, but also induce proinflammatory cytokine secretion, and induce damage by oxidation of the cells' proteins, lipids, and nucleic acids[184–186].

There have been some suggestions that mitochondria play a role in mediating the effects of HCA *in vitro*, although this mechanism is much less extensively studied than the involvement of the NFκB pathway. While inhibition of mitosis did not support a role for the process in the HCA-induced impairment of A549 wound repair[160], independent experiments demonstrated impaired proliferation of hypercapnia-exposed A549s not subjected to *in vitro* wounding[161]. Under these conditions, impaired proliferation resulted from delayed progression through the cell cycle. This

arose from impaired mitochondrial function occurring secondary to HCA-induced microRNA (miR)-183-mediated downregulation of isocitrate dehydrogenase expression – a key enzyme of the TCA cycle. Impaired bioenergetics has also been observed in HCA in isolated mitochondria[99], while neutrophil production of superoxide and H_2O_2 is also attenuated[140,155]. Given the role of mitochondria in the production of these ROS, this observation may also be indicative of impaired mitochondrial function. Therefore, together, these results support a role for altered mitochondrial function in driving the effects of HCA.

1.7.3 Alternative mechanisms

It should be noted that the precise molecular mechanisms mediating the effects of HCA in mammalian cells are likely to be complex and have not yet been fully elucidated. Transcription factors and other proteins not classically considered components of the NFκB pathway could also be influenced by HCA. For example, *in vivo* work in *Drosophila* has revealed that knockdown of the *zfh2* gene improved survival of hypercapnia-exposed flies infected with *S. aureus*. It is believed that improved survival resulted from dampening of hypercapnia-induced reductions in antimicrobial peptide gene expression[187]. Emerging data suggests that Zinc Finger Homeobox 3 (ZFHX3) – the mammalian homolog of *Drosophila zfh2* – may be involved in hypercapnia-induced alterations to immunomodulatory gene expression in macrophages[188], but the effects on antimicrobial gene expression have not yet been reported. This may open a potential avenue for investigation into the differential effects of HCA in the setting of infection.

1.8 Extracorporeal carbon dioxide removal ($ECCO_2R$)

Despite the use of low tidal volume mechanical ventilation, approximately 30% of patients with ARDS still develop lung injury as a result of alveolar over distension[189]. The use of even lower tidal volumes may help to reduce this statistic, but is likely to result in further development of HCA which, as discussed, may exert detrimental effects in ARDS. However, the use of extracorporeal carbon dioxide removal ($ECCO_2R$) devices, which effectively 'dialyse' CO_2 from the blood to normalise

$paCO_2$ and pH, could manage the potentially harmful effects of HCA to allow further reductions in tidal volume. In a small study of 32 patients with ARDS, the use of $ECCO_2R$ as an adjunct to mechanical ventilation with tidal volumes <6ml/kg predicted body weight (PBW) was associated with a reduction in proinflammatory cytokine concentrations, suggestive of a lesser degree of lung injury, when compared to conventional low tidal volume approaches of 6ml/kg PBW[190]. Additionally, posthoc analysis of the data from a randomised controlled trial in which the use very low tidal volumes of ~3ml/kg PBW in combination with $ECCO_2R$ was compared to the use of conventional tidal volumes of ~6ml/kg without $ECCO_2R$ support, revealed a potential increase in the number of ventilator free days in patients with more severe hypoxaemia in the very low tidal volume group[191]. A phase 1/2 trial (SUPERNOVA, clinicaltrials.gov identifier NCT02282657) investigating the feasibility and safety of $ECCO_2R$ in patients with moderate ARDS has recently been completed and its results are awaited. Other clinical trials investigating the use of $ECCO_2R$ are currently recruiting and include a multicentre phase 3 trial (REST, cinicaltrials.gov identifier NCT20654327) which is investigating whether the use of $ECCO_2R$ and lower tidal volume ventilation improves outcomes from acute hypoxaemic respiratory failure when compared to standard care in mechanically ventilated patients.

1.9 Summary and Aims of the Study

In summary, ARDS is a common and devastating clinical disorder for which there exists no effective pharmacological therapy. Mechanical ventilation strategies which are central to the management of patients with this condition can impair carbon dioxide removal, resulting in hypercapnic acidosis (HCA). The development of HCA has largely been regarded as safe, with secondary analysis of the data from a large ARDSNet study suggesting that it may reduce mortality in some patients. The development of HCA in mechanically ventilated patients with ARDS has since often been permitted by clinicians.

Despite *in vivo* data suggesting that HCA is largely protective, or at least safe, in the setting of inflammation, concerns have been raised with regards to its safety in

pneumonia. Insights have also been offered at the cellular level *in vitro* but this work has its limitations. The two key structural cells of the alveoli – alveolar epithelial cells and capillary endothelial cells – are key targets in the pathogenesis of ARDS. Investigations into the response of endothelial cells to HCA are few in number and have given rise to conflicting results. Studies investigating the response of epithelial cells to HCA have raised concerns regarding the potential for structural and functional recovery of the alveolar epithelium in this setting. However, these results are not necessarily corroborated by *in vivo* data which are largely suggestive of improved or unaltered barrier structure and function. This may, in part, be explained by the use of small animal models in *in vivo* studies where cellular responses do not necessarily recapitulate that of human cells. Reliance on immortalised cell lines as opposed to primary human cells to assess the response of the alveolar epithelium may be another contributing factor. Overall, due to the limitations of *in vivo* models and the limited knowledge which currently exists in primary human cells, the response to HCA of the primary human epithelial and endothelial cell types most relevant to the pathophysiology of ARDS requires investigation.

While no therapy exists for the treatment of ARDS, there is considerable interest in the potential use of mesenchymal stem cells (MSCs). Experimental data strongly support the therapeutic potential of MSCs for the treatment of ARDS. However, while MSCs are currently in clinical trials for the condition, much is still to be learned, particularly with regards to the effects of the surrounding environment on their biology and therapeutic capacity. Worryingly, despite the ability of MSCs to respond to local environmental changes and the possibility of encountering a hypercapnic acidotic environment in mechanically ventilated patients with ARDS, no data currently exist relating to the response of MSCs to HCA. This could have major implications for the efficacy of an MSC based therapy and is an issue which urgently needs to be addressed. Although the focus of this project is in the context of ARDS, MSCs are also being considered as a therapy for COPD and cystic fibrosis[192–195] – diseases in which they may also be exposed to HCA. The effects of HCA on the efficacy of an MSC-based therapy could therefore extend beyond ARDS to a diverse group of patients.

The aims of the project are therefore:

- To determine the effect of HCA on the inflammatory and reparative responses of the capillary endothelium and distal lung epithelium in an *in vitro* model of ARDS, using primary human pulmonary microvascular endothelial cells (HPMECs) and primary human small airway epithelial cells (SAECs)
- To determine the influence of HCA on the biological properties and therapeutic capacity of human MSCs in an *in vitro* model of ARDS
- To elucidate the mechanisms of any alterations observed with regards to the effects of HCA on the inflammatory and reparative responses of HPMECs and SAECs, and on the therapeutic potential of MSCs

Given the data currently available in *in vitro* cell lines, it is hypothesised that the inflammatory and reparative responses of HPMECs and SAECs will be attenuated in HCA. Given their capacity to respond to changes in their local environment, it is hypothesised that the therapeutic potential of MSCs will be altered in HCA. Finally, it is hypothesised that the mechanism of HCA-mediated effects will relate to alterations in the activation of the NFκB pathway, or to altered mitochondrial function.

Chapter Two – Materials and Methods

2.1 Cell Culture

2.1.1 Human Pulmonary Microvascular Endothelial Cells (HPMECs) and Small Airway Epithelial Cells (SAECs)

Primary Human Pulmonary Microvascular Endothelial Cells (HPMECs) and primary human Small Airway Epithelial Cells (SAECs) (both Promocell) were purchased as proliferating passage 2 cells and used to passage 7. HPMECs had been isolated from human lung parenchyma following removal of the macrovasculature and were characterised by their expression of Cluster of Differentiation 31 (CD31) and von Willebrand Factor (vWF), and their lack of expression of smooth muscle α-actin. SAECs had been isolated from the bronchoalveolar duct region of the lung and were characterised based on positive staining for cytokeratins.

HPMECs were maintained in endothelial cell growth medium MV (Promocell) and SAECs were maintained in small airway epithelial cell growth medium (Promocell), each supplemented with their respective supplied supplement mix **(Table 2.1)** and 50µg/ml Penicillin-Streptomycin (PS) (Gibco). These media are referred to herein as cell culture media. Both cell types were maintained at 37°C in a humidified incubator at 5% carbon dioxide (CO_2) until passaged or used for experimentation.

Endothelial Cell Growth Medium MV	Small Airway Epithelial Cell Growth Medium
0.05ml/ml foetal calf serum (FCS)	2.5mg/ml bovine serum albumin (fatty acid free)
0.004ml/ml endothelial cell growth supplement	0.004ml/ml bovine pituitary extract
10ng/ml recombinant human epidermal growth factor	10ng/ml recombinant human epidermal growth factor
90µg/ml heparin	5µg/ml recombinant human insulin
1µg/ml hydrocortisone	0.5µg/ml hydrocortisone
	0.5µg/ml adrenaline
	6.7ng/ml Triiodo-L-Thyronine
	10µg/ml human transferrin
	0.1ng/ml retinoic acid

Table 2.1: Final concentrations (after addition to basal medium) of supplements contained within the ready-to-use supplement mixes supplied with endothelial growth medium MV and small airway epithelial growth medium

HPMECS and SAECs were passaged when they reached approximately 80% confluency. All DetachKit (Promocell) reagents were brought to room temperature 30 minutes before use. Media was aspirated from the culture flask and the surface on which the cells were adhered was washed with 100µl 30mM HEPES Buffered Saline Solution (BSS)/cm^2. HEPES BSS was aspirated off and the cells were incubated with 100µl Trypsin/Ethylenediaminetetraacetic Acid (EDTA) (0.04%/0.03%) Solution/cm^2 for approximately 3 minutes at room temperature until the cells had detached from the culture surface. Trypsin activity was neutralised by adding a volume of Trypsin Neutralisation Solution (TNS) equal to the volume of trypsin already in the flask. Detached cells were collected and centrifuged at 220 x g for 3 minutes. Following centrifugation, the supernatant was aspirated off and the cell pellet was resuspended in 1ml of the appropriate cell culture medium. Cells were counted (see **Section 2.1.3** below) and seeded in well plates or culture flasks at a density of $1x10^4$ cells/cm^2.

2.1.2 Mesenchymal Stem Cells (MSCs)

Human bone marrow-derived Mesenchymal Stem/Stromal Cells (MSCs) were provided by the Institute for Regenerative Medicine at Texas A&M Health Science Centre, Baylor Scott and White Hospital, through a grant from NCCR of the National Institute of Health (NIH) (Grant# 40RR017477). These cells had been extensively characterised in accordance with the standards laid out by the International Society for Cellular Therapy (ISCT) and were shipped as cryopreserved cells at passage 1 or 2. Upon arrival, the cells were stored in liquid nitrogen until expanded in T175 culture flasks to passages 2 and 3 from a low density of 60 cells/cm^2. MSCs were used at passages 3-5 and were maintained in Alpha Minimal Essential Medium (αMEM) lacking ribonucleosides and deoxyribonucleosides (Gibco), but supplemented with 16.5% heat-inactivated foetal bovine serum (FBS), 50µg/ml PS, and 4mM L-glutamine (LG) (Gibco). This medium is herein denoted as $\alpha MEM_{16.5\%+PS+LG}$. Cultures were maintained at 37°C in a humidified tissue culture incubator at 5% CO_2 until used for experimentation.

MSCs were passaged when they reached approximately 70-80% confluency. Media was aspirated from the flask of cells and the cell layer was washed with Dulbecco's Phosphate Buffered Saline (DPBS) to remove any FBS-containing medium. The DPBS was then aspirated off and the cells were incubated with Trypsin-EDTA (diluted to a final concentration of 0.05% in DPBS) (Gibco) for up to 5 minutes at 37°C until the cells had detached from the culture surface. Trypsin activity was neutralised by addition of $\alpha MEM_{16.5\%+PS+LG}$ at a volume equal to that of the trypsin added to the flask. Detached cells were collected and centrifuged for 5 minutes at 1200 rpm. Following centrifugation, the supernatant was aspirated off and the cell pellet was resuspended in $\alpha MEM_{16.5\%+PS+LG}$. Cells were counted as described in **Section 2.1.3** below.

2.1.3 Cell counting

Following cell trypsinisation, centrifugation and resuspension, a small volume of the cell pellet was diluted to an appropriate density in trypan blue (Gibco). Trypan blue is a dye which is used to distinguish viable cells which exclude the dye, from non-

viable cells which take it up and appear blue. 20µl of diluted suspension was added to a haemocytometer (Neubauer model) to enable counting of cells. Viable cells were identified as those excluding the blue dye. The total number of viable cells in the four corners of the haemocytometer, including those which touched the top and left boundaries of the square, but not the bottom and right boundaries, were counted. The average count per square was multiplied by the dilution factor, and then by 10,000 to give the cell counter per millilitre of cell suspension.

2.1.4 Cell seeding

Following trypsinisation and counting of cells as described in **Sections 2.1.1** to **2.1.3** above, 1 million cells in 1ml freezing medium were added to cryovials for long term storage. The freezing medium used differed according to cell type. For MSCs, the freezing medium contained 65% αMEM, 30% FBS and 5% Dimethyl Sulfoxide (DMSO). For HPMECs, CryoSFM (Promocell) – a serum-free cryopreservation medium – was used. A number of attempts were made to store SAECs including the use of a freezing medium containing 90% FBS and 10% DMSO, and two commercially-available serum-free cryopreservation media; Cellbanker 2 (Amsbio) and CryoSFM. However, few viable cells were ever recovered following resuscitation. SAECs were therefore used continuously and not stored. Cryovials containing MSCs or HPMECs were stored overnight at -80°C in a Mr. Frosty freezing container filled with isopropanol before transfer to liquid nitrogen for long-term storage.

When required, cryovials were transported on dry ice from liquid nitrogen storage and thawed for 2-3 minutes in a 37°C waterbath until just thawed. The 1ml suspension was then transferred into 10ml pre-warmed cell culture medium. HPMECs were centrifuged at 220 x g for 3 minutes, and MSCs were centrifuged at 1200 rpm for 5 minutes to remove DMSO. The supernatant was aspirated off and the cell pellet was resuspended in 1ml cell culture medium. The cell suspension was transferred to an appropriately sized flask (T25 for HPMECs or T175 for MSCs) containing pre-warmed cell culture medium and allowed to adhere overnight at 37°C and 5% CO_2.

2.1.5 Alveolar Type II (ATII) Epithelial Cells

2.1.5.1 Collagen coating well plates

In preparation for the culture of isolated alveolar type II (ATII) cells, well plates were coated with type IV human collagen (Sigma-Aldrich) on the morning of isolation. Collagen was diluted to a final concentration of 10µg/ml in 1x phosphate buffered saline (PBS) (Gibco). 500µl was added to each well of a 24 well plate and 75µl was added per well of a 96 well plate. Plates were incubated at 37°C until required. Excess collagen was aspirated off and the wells were washed with 1x PBS immediately prior to use.

2.1.5.2 Isolation of ATII Cells

Human alveolar type II (ATII) epithelial cells were isolated from donor human lungs which had been rejected for transplantation within the Belfast Health and Social Care Trust. Four blocks of lung tissue approximately $5cm^3$ in size were dissected from the upper lobe of one lung and flushed by PBS injections until the lavage fluid ran clear. Trypsin-EDTA (diluted to a concentration of 0.05% in DPBS) was injected into the tissue blocks and incubated at 37°C in 5% CO_2 for 15 minutes. Trypsin instillation and incubation were repeated twice, bringing the total incubation time to 45 minutes. The digested tissue was cut into blocks as small as possible and added to a 250ml beaker containing 7ml FBS per block and 250µg/ml DNase I (Sigma-Aldrich). The tissue was minced by hand using scissors until a homogenous mixture was obtained. The mixture was added to 50ml falcons and shaken vigorously by hand for 5 minutes to loosen the cells before being passed through pores of reducing size (100µm cell strainer followed by 40µm cell strainer, both Corning) to remove debris and cell clumps. The resulting cell suspension was centrifuged at 800rpm for 7 minutes at 12°C. The cell pellet was resuspended in a solution made up of 50% DPBS and 50% unsupplemented DMEM/F12 (Gibco) together containing 100µg/ml DNase I. The cell suspension was incubated in T175 culture flasks at 37°C in 5% CO_2 for 1.5 hours to allow differential adherence of contaminating macrophages to the flask.

After 1.5 hours, the non-adherent ATII-enriched cell population was removed from the flask and centrifuged at 800rpm for 7 minutes at 12°C. The cell pellet was then resuspended in red cell lysis buffer (4.15g NH_4Cl, 500mg $KHCO_3$ and 18.6mg EDTA in 500ml 1N deionised water, pH 7.4) for 3 minutes. After this time, enough DPBS was added to bring the volume up to 30ml and the suspension was centrifuged at 800rpm for 7 minutes at 12°C. Cell culture medium was prepared by supplementing DMEM/F12 with 10% FBS, 50µg/ml penicillin-streptomycin, 50µg/ml gentamicin (Life Technologies), and 2.5µg/ml amphotericin B (ThermoFisher). The cell pellet was resuspended in pre-warmed cell culture medium and the cells were counted as described in **Section 2.1.3**. The cells were seeded onto culture plates pre-coated with type IV collagen at the densities laid out in **Table 2.2** and incubated at 37°C and 5% CO_2 untouched for 3 days.

	Growth Area	**Volume of Media per Well**	**Cell Density**
96 well plate	$0.32cm^2$	100µl	1×10^6
24 well plate	$1.9cm^2$	500µl	$1\text{-}2 \times 10^5$

Table 2.2: Densities of isolated cells added to cell culture plates

After 3 days, confluent monolayers were washed 3 times with Hanks' Balanced Salt Solution (HBSS) containing magnesium and calcium (Gibco) to remove debris. The media was either replaced with fresh cell culture medium and the cells were placed back into culture for future staining to determine the purity of the isolated cells, or they were used immediately for experimentation.

2.1.5.3 Immunofluorescent staining of cells present within the isolated cell population

Isolated cells were stained for the ATII marker, pro-surfactant protein-C (pro-SPC), to determine cell purity at 4 days post-isolation – the time at which a 24 hour timepoint would be taken. Cell monolayers were washed 3 times with 200µl 1x PBS and fixed

with 50µl 4% paraformaldehyde (PFA) (Sigma) per well at room temperature for 15 minutes. PFA was aspirated off and the wash step was repeated. Cells were blocked with 50µl strong block (0.1% Triton-X (Sigma) and 10% normal goat serum (NGS) (Sigma) in 1x PBS) for 1 hour at room temperature. Strong block was aspirated off and the wash step was repeated. Primary antibody against pro-surfactant protein-C (pro-SPC) was diluted in weak block (0.01% Triton-X and 2% NGS in 1x PBS) **(Table 2.3)**. Rabbit IgG monoclonal isotype control (Abcam) was diluted in weak block to the same concentration as the pro-SPC antibody. 50µl diluted primary antibody or isotype control was added per well and incubated overnight at 4°C.

Following overnight incubation, primary antibodies were aspirated off and the wells were washed 3 times with PBS. Secondary antibody was diluted in weak block **(Table 2.3)** and 50µl was added per well for 1 hour at room temperature. Secondary antibody was aspirated off and the wash step was repeated. Cells were counterstained with 50µl Hoechst (Sigma-Aldrich) diluted 1:2500 in weak block for 5-10 minutes. Hoechst was aspirated off and the wash step repeated. 200µl 1x PBS was added per well and the plates were stored at 4°C until imaged at x10 magnification using the EVOS FL Auto inverted epifluorescent microscope (Life Technologies).

	Manufacturer	**Dilution**
Primary: Pro-Surfactant Protein C (SPC)	Abcam	1:50
Secondary: Donkey Anti-Rabbit Alexa Fluor 647	Abcam	1:200

Table 2.3: Primary and secondary antibody dilutions

Cell purity was quantified using Image J, v1.48 (National Institute of Health). A grid of individual squares each of 100,000 pixels^2 in size was created for each image taken. Four randomly-selected squares were chosen and the number of total cells (identified by Hoechst nuclear stain) and the number of pro-SPC-positive cells were counted using the multipoint tool. The percentage of positive cells was calculated from this information.

2.1.6 Characterisation of cell types present within SAECs

Unstimulated SAECs were cultured in 5% CO_2 for 72 hours prior to fixation. After 72 hours, cell monolayers were washed 3 times with 200µl 1x PBS and fixed with 50µl 4% PFA per well at room temperature for 15 minutes. PFA was aspirated off and the wash step was repeated. Cells were blocked with 50µl strong block (0.1% Triton-X and 10% NGS in 1x PBS) for 1 hour at room temperature. Strong block was aspirated off and the wash step was repeated. Primary antibodies against pro-surfactant protein-C (pro-SPC) (ATI marker) and aquaporin-5 (AQP-5) (ATII marker) were diluted in weak block (0.01% Triton-X and 2% NGS in 1x PBS) **(Table 2.4)**. Rabbit IgG monoclonal isotype control (Abcam) was diluted in weak block to the same concentration as the pro-SPC antibody. Goat IgG polyclonal isotype control (Abcam) was diluted in weak block to the same concentration as the AQP-5 antibody. 50µl diluted primary antibody or isotype control was added per well and incubated overnight at 4°C.

Following overnight incubation, primary antibodies were aspirated off and the wells were washed 3 times with PBS. Secondary antibodies were diluted in weak block **(Table 2.4)** and 50µl was added to the appropriate wells for 1 hour at room temperature. Secondary antibodies were aspirated off and the wash step was repeated. Cells were counterstained with 50µl Hoechst diluted 1:2500 in weak block for 5-10 minutes. Hoechst was aspirated off and the wash step repeated. 200µl 1x PBS was added per well and the plates were stored at 4°C until imaged at x20 magnification using the Leica DMi8 microscope (Leica microsystems).

	Manufacturer	**Dilution**
Primary: Pro-Surfactant Protein C (pro-SPC)	Abcam	1:100
Primary: Aquaporin-5 (AQP-5)	Santa Cruz Biotechnology	1:200
Secondary: Donkey Anti-Rabbit Alexa Fluor 647	Abcam	1:500
Secondary: Donkey Anti-Goat Alexa Fluor 488	Abcam	1:500

Table 2.4: Primary and secondary antibody dilutions

Cell purity was quantified using Image J, v1.48. A grid of individual squares each of 100,000 pixels^2 in size was created for each image taken. Four randomly-selected squares were chosen and the number of total cells (identified by Hoechst nuclear stain) and the number of pro-SPC- or AQP-5-positive cells were counted using the multipoint tool. The percentage of positive cells was calculated from this information.

2.2 Experimental Conditions

2.2.1 Induction of Hypercapnic Acidosis (HCA)

Normocapnic and hypercapnic conditions were achieved using Panasonic MCO-230AIC CO_2 incubators with CO_2 set to 5% and 15%, respectively. All media used for experiments were pre-equilibrated under these conditions overnight in T25 cell culture flasks in the absence of cells. pH and pCO_2 were analysed using a Cobas b 221 blood gas analyser (Roche).

2.2.2 Stimulation of cells with cytomix

Unless otherwise stated, HPMECs or SAECs were allowed to reach 80% confluence prior to use for experimentation. A cytomix of proinflammatory cytokines composed of Tumour Necrosis Factor alpha (TNFα) (Peprotech), Interleukin 1 beta (IL1β) (Peprotech) and Interferon gamma (IFNγ) (R&D Systems), each at a concentration of 50ng/ml, was prepared. Cytomix was prepared separately in pre-equilibrated cell culture media for cells to be exposed to normocapnia and for cells to be exposed to HCA. Cells were washed with DPBS, and cytomix or media – the volume of which depended on the size of the wells used **(Table 2.5)** – was added. Following stimulation, cells were incubated at 5% CO_2 or 15% CO_2 for a period of time specific to each experiment.

Well Plate	Volume of Media
6 well	2ml
24 well	1ml
48 well	500µl
96 well	100µl

Table 2.5: Volumes of media or cytomix added to culture plates

2.3 Quantification of cytokines and growth factors

2.3.1 Enzyme-Linked Immunosorbent Assay (ELISA)

An Enzyme-Linked Immunosorbent Assay (ELISA) is an immunologic technique used to facilitate the quantification of antibodies and small proteins present within a solution. Commercially available Duoset sandwich ELISAs (R&D Systems), in which small proteins are detected using immobilised antibodies, were used to measure human C-X-C Motif Chemokine Ligand 8 (CXCL8) (also known as Interleukin 8 or IL-8), C-X-C Motif Chemokine Ligand 5 (CXCL5) (also known as Epithelial Neutrophil-Activating Protein-78 or ENA-78), Angiopoietin-1 (Ang-1), Keratinocyte Growth Factor (KGF), Interleukin 1 receptor antagonist (IL-1ra) and Interleukin 10 (IL-10) concentrations in cell-free supernatants.

All assays were performed following the manufacturer's standard instructions for Duoset ELISAs. Working concentrations of the antibodies provided with each kit were analyte- and lot-specific. Briefly, capture antibody specific for the analyte of interest was diluted to the required working concentration in 1x Phosphate Buffered Saline (PBS). 100µl was added to each well of a 96 well Maxisorp ELISA plate (Nunc). The plate was sealed with parafilm and incubated at room temperature overnight.

Following overnight incubation, the plate was washed three times with wash buffer (1x PBS containing 0.05% Tween-20 (Sigma Aldrich)) and dried by gently blotting against paper towels. 300µl reagent diluent (1x PBS containing 1% bovine serum albumin (BSA) (Sigma Aldrich)) was added per well and incubated for 1 hour at room temperature to prevent non-specific binding. The wash step was repeated. Two-fold serial dilutions were used to prepare seven standard concentrations in reagent diluent (see **Table 2.6** for standard range of each analyte). Samples were also diluted in reagent diluent if necessary and 100µl of each standard or sample was added in duplicate to the plate. 100µl reagent diluent was also added in duplicate to be used as a blank. The plate was incubated for 2 hours at room temperature with gentle agitation from a plate rocker. The wash step was repeated. Detection antibody was diluted to the required concentration in reagent diluent and 100µl per well was added to the plate. Following a further 2 hour incubation at room temperature, the wash step was repeated. Streptavidin-horse radish peroxidase (HRP) was diluted 1:40 in reagent diluent and 100µl was added to each well. The plate was wrapped in tinfoil and incubated for 20 minutes at room temperature in the dark. The wash step was repeated. 100µl 3,3',5,5'-tetramethylbenzidine (TMB) (Life Technologies) was added and incubated at room temperature in the dark until the top two standards had developed a medium-to-dark blue colour. At this point, 50µl 2M sulphuric acid was added to stop the reaction. Absorbance was read immediately at 450nm with a wavelength correction of 540nm using a FLUOstar Omega microplate reader (BMG Labtech). The concentration of each unknown sample was extrapolated from a 4-parameter curve generated using MARS data analysis software (BMG Labtech) and, where appropriate, dilutions were accounted for.

	Standard Concentration Range
Ang-1	10,000 – 156pg/ml
CXCL5	1,000 – 15.60pg/ml
CXCL8	2,000 – 31.25pg/ml
KGF	2,000 – 31.25pg/ml
IL10	2,000 – 31.25pg/ml
IL1ra	2,500 – 39.10pg/ml

Table 2.6: Range of standards prepared for analyte-specific Duoset ELISAs

2.4 Assessment of endothelial adhesion molecule expression by HPMECs

Flow cytometry is a technique which can be used to characterise cell populations based on the size of cells and the proteins they express. This technique was used to assess the effects of hypercapnic acidosis (HCA) on HPMEC expression of the adhesion molecules Endothelial-selectin (E-selectin), Intercellular Adhesion Molecule-1 (ICAM-1) and Vascular Cell Adhesion Molecule-1 (VCAM-1), both in the presence and the absence of cytomix stimulation.

After 24 hour or 72 hour incubation in 5% or 15% CO_2 with 50ng/ml cytomix or media, HPMEC monolayers were washed with 1ml 1x PBS. The PBS was aspirated from the wells and the cells were gently scraped from the surface in 1ml 1x PBS. The cell suspension was transferred into 5ml polystyrene flow tubes (Sarstedt, Fisher Scientific) and centrifuged for 5 minutes at 800 rpm and 4°C to pellet the cells. The supernatant was aspirated off and the pellet resuspended in 200µl 1x PBS. To prevent non-specific binding of antibodies, 20µl human FcR binding inhibitor (eBioscience) was added and incubated with the cells on ice for 20 minutes. Appropriate volumes of antibodies directed against the proteins of interest **(Table 2.7)** were added to the experimental groups and incubated on ice for 30 minutes in the dark. Unstained controls, isotype controls for each fluorophore used, and single stain controls for each

fluorophore were also included. All controls were performed in unstimulated HPMECs which had been incubated in 5% CO_2 for the duration of the experiment. Following incubation, the cell suspensions were topped up with 1ml PBS, the cells were centrifuged using the same settings as before, and the supernatant was discarded. The cell pellet was resuspended in 1ml 1x PBS and the centrifugation step was repeated to wash the cells of any excess fluorophore. Again, the supernatant was aspirated off and the wash step was repeated once more. Following the final wash step, the cell pellet was resuspended in 500µl 1x PBS and kept on ice. The samples were processed immediately using a FACSCantoII flow cytometer and FACSDiva software (BD Biosciences). If necessary, compensation was set up, using FACSDiva, between two fluorophores based on overlap in the single stain controls. All data were analysed using FlowJo Version 10 software (Treestar).

Protein of Interest	Fluorophore	Manufacturer	Dilution
Anti-human CD62E (E-selectin)	APC	BioLegend	1:100
Anti-human CD54 (ICAM-1)	FITC	BioLegend	1:100
Anti-human CD106 (VCAM-1)	PE	BioLegend	1:100

Table 2.7: Antibodies used to assess HPMEC adhesion molecule expression by flow cytometry

2.5 *In vitro* scratch assay

An *in vitro* scratch assay was used to assess the effects of HCA on epithelial and endothelial wound repair. Horizontal lines were created across the under surface of the wells of 24 well plates prior to cell seeding. HPMECs or SAECs were seeded on these plates at a density of $1x10^4$ cells/cm^2 and cultured until monolayer formation occurred. ATII cells were seeded at a density of $1x10^6$ cells/cm^2 and confluent monolayers were used at 4 days post-seeding. At this point, a single vertical 'scratch' wound was made from the top to the bottom of each well, running through the horizontal line, using a P1000 pipette tip. The edge of a ruler was used to guide a straight line. Cells were washed twice with DPBS to remove cell debris and 500µl 1% supplemented medium (see negative control in **Table 2.8**) was added to each of

the wells. For ATII cells, cell culture medium was added instead. The wound sites were imaged at x10 magnification using the Axiovert 25 inverted light microscope (Zeiss) and AxioVision Rel. 4.8 software (Zeiss). Two images were taken from each well; one was taken just above the horizontal line and one just below it to allow for re-imaging of the same area of each wound later in the experiment. Medium was aspirated off and replaced with 500µl of the appropriate condition, prepared in pre-equilibrated media **(Table 2.8)**. To limit bias when calculating wound closure, each of the conditions were blinded by an independent researcher unrelated to the project prior to their addition to the cells. Wounded cells were incubated under these conditions for 24 hours at 37°C in either 5% CO_2 or 15% CO_2.

	HPMECs (*Endothelial cell growth medium MV*)	**SAECs** (*Small airway epithelial cell growth medium*)	**ATII Cells** *(DMEM/F12)*
Vehicle	10% supplemented	10% supplemented	Cell culture medium containing 10% FBS
Cytomix	50ng/ml cytomix (TNFα, IL1β, IFNγ) in vehicle	50ng/ml cytomix (TNFα, IFNγ) in vehicle	N/A
Negative Control	1% supplemented	1% supplemented	N/A
Positive Control	100% supplemented	100% supplemented	N/A

Table 2.8: Conditions added to wounded HPMECs, SAECs, or ATII cells

For HPMECs and SAECs, percentage supplement refers to the percentage of the supplement added to the standard culture medium for each cell type.

Wounds were re-imaged, as before, in the same areas as baseline wounds following 24 hour incubation. Image J, v1.48 (National Institute of Health) was used to measure the area of the wound site at baseline and again at 24 hours. The percentage wound closure at 24 hours was calculated from these values. Only at this stage were the conditions un-blinded to permit interpretation of the results.

2.6 Determination of cell viability by lactate dehydrogenase (LDH) assay

Lactate dehydrogenase (LDH) is a cytoplasmic enzyme which is constitutively produced by most mammalian cells. Following disruption of membrane integrity, it is released into the surrounding environment where it can be used in colorimetric analysis as an indicator of cell death. The commercially available Cytotoxicity Detection Kit (Roche), which is based on the activity of LDH in cell-free supernatants, was used to assess the impact of HCA on HPMEC, SAEC and MSC cell death in both inflammatory and non-inflammatory environments.

After 24 hours, 48 hours or 72 hours of culture in 5% or 15% CO_2, cell supernatants were collected and centrifuged to remove cell debris. A positive control was included in which cells were lysed with a final concentration of 2% Triton-X (Sigma-Aldrich) 10 minutes before the collection of supernatants. 50µl samples were plated in triplicate into a 96 well plate (Nunc). Reaction mixture was prepared by adding 125µl diaphorase/NAD^+ (catalyst) to 5.6ml dye solution. 50µl of this mixture was added to the samples in the plate. The well contents were mixed on a plate shaker for 1 minute and the plate was incubated for approximately 30 minutes (until the positive control had developed a deep red colour) in the dark at room temperature. Optical densities were measured at 405nm using a FLUOstar Omega microplate reader. Data were analysed using MARS data analysis software. Results are presented relative to the positive control.

2.7 Nuclear Factor kappa B (NFκB) activation

2.7.1 Stimulation of cells

MSCS were seeded on 6 well plates at a density of $2x10^5$ per well and allowed to adhere overnight in $\alpha MEM_{16.5\%FBS+PS+LG}$. HPMECs or SAECs were seeded on 6 well plates at a density of $1x10^5$ per well and cultured in their respective cell culture media until monolayer formation was achieved. On the day of experimentation, the cells were washed with 1ml pre-warmed DPBS which was immediately aspirated off. 2ml $\alpha MEM_{1\%FBS+PS+LG}$, which had been pre-equilibrated in 5% CO_2 or 15% CO_2 overnight,

was added to the MSCs and the cells were left to rest for 2 hours in 5% or 15% CO_2 at 37°C due to the sensitivity of NFκB activation. For HPMECs or SAECs, their respective cell culture medium was used. After 2 hour incubation, 100µl media was removed from each well. Cytomix was prepared to a concentration of 1µg/ml in pre-equilibrated $\alpha MEM_{1\%FBS+PS+LG}$ for MSCs or cell culture medium for HPMECs and SAEC. 100µl was added to the 1.9ml media already in the appropriate wells, bringing the final concentration to 50ng/ml. For unstimulated cells and for the zero-minute control, 100µl pre-equilibrated media only was added instead of cytomix. The plates were incubated at 37°C and either 5% CO_2 or 15% CO_2 for zero minutes, 30 minutes, or 60 minutes. At the end of each incubation period, the medium was aspirated from the wells and the cells were scraped from the surface in 1ml ice cold PBS. Replicate cell suspensions of each condition were pooled and kept on ice in preparation for nuclear extraction.

2.7.2 Preparation of nuclear extracts

Nuclear extracts were prepared from chilled cell suspensions using the NE-PER Nuclear and Cytoplasmic Extraction Reagents kit (Pierce) following the instructions laid out by the manufacturer. Briefly, the cells were pelleted by centrifugation at 800 x g for 3 minutes at 4°C and the supernatant was discarded. The cell pellet was resuspended in 200µl CERI containing HALT protease inhibitor cocktail (EDTA-free) (Pierce), vortexed, and incubated for 10 minutes on ice before addition of 11µl CERII. Samples were vortexed at the highest setting for 5 seconds, incubated on ice for 1 minute, and vortexed again, before centrifugation at 16000 x g for 5 minutes at 4°C. Supernatants, containing cytoplasmic extracts, were collected into ice cold eppendorfs and kept on ice until the end of the extraction protocol.

The insoluble pellet was resuspended in 100µl ice cold NER containing HALT protease inhibitor cocktail (EDTA-free), and vortexed at the highest setting for 15 seconds. Samples were incubated on ice for 40 minutes, with the vortexing step repeated every 10 minutes until the time was up. Supernatants, containing the nuclear extracts, were collected into fresh ice-cold eppendorfs immediately following

centrifugation of the samples at 16000 x g for 10 minutes at 4°C. All extracts were stored at -80°C for future use.

2.7.3 Protein quantification

Protein concentrations in nuclear extracts were quantified using the Coomassie (Bradford) Protein Assay Kit (Pierce). BSA standards ranging in concentration from 0-2000µg/ml were prepared following the manufacturer's instructions. 5µl of each standard or sample were pipetted in duplicate into the wells of a 96 well plate, followed by 250µl Coomassie Reagent. Well contents were mixed on a plate shaker for 30 seconds and the plate was incubated at room temperature for 5 minutes, protected from light. Absorbance was measured at 595nm using a FLUOstar Omega microplate reader and the concentration of protein in each unknown sample was extrapolated from a second polynomial curve generated using MARS data analysis software.

2.7.4 TransAM NFκB p65 assay

The TransAM NFκB p65 Assay Kit (Active Motif) is a DNA-binding ELISA which facilitates the detection of active NFκB p65 subunits in nuclear extracts. In this assay, active p65 subunits bind to their consensus oligonucleotides which have been immobilised on a 96 well plate supplied with the kit. Bound subunits can be detected thereafter in a principle similar to that of an ELISA. This assay was used, following the manufacturer's instructions, to detect active p65 subunits in the nuclear extracts of HPMECs, SAECs or MSCs cultured in 5% or 15% CO_2.

Nuclear extracts were diluted in complete lysis buffer to a protein concentration of 150µg/ml (for MSCs) or 100µg/ml (for HPMECs or SAECs). Jurkat extract (positive control supplied with the kit) was also diluted to a protein concentration of 125µg/ml or 100µg/ml in complete lysis buffer. 30µl complete lysis buffer was added to the wells of the 96 well plate supplied, followed by 20µl Jurkat extract or unknown sample (containing 3µg protein for MSCs or 2µg protein for HPMECs and SAECs). 20µl complete lysis buffer was included as a blank control and the plate was incubated at

room temperature for 1 hour with mild agitation from a plate rocker. The plate was washed three times using the wash buffer supplied with the kit and gently blotted against paper towels to dry. Primary antibody (rabbit anti-NFκB p65) was diluted 1:1000 and 100µl was added per well. The plate was incubated at room temperature for 1 hour in the absence of agitation from a plate rocker. The wash step was repeated and 100µl HRP-conjugated anti-rabbit secondary antibody (diluted 1:1000) was added per well. The plate was incubated again for 1 hour at room temperature without agitation. The wash step was repeated four times. 100µl developing solution was added per well and incubated at room temperature protected from light until the colour of the sample wells had turned medium-to-dark blue. 100µl stop solution was added to stop the reaction and the optical density was measured within 5 minutes at 450nm using a FLUOstar Omega plate reader.

2.8 Assessment of mitochondrial function

2.8.1 Measurement of mitochondrial membrane potential using JC-1 dye

5,5',6,6'-tetrachloro-1,1',3,3'-tetraethylbenzimidazolylcarbocyanine iodide (JC-1) is a lipophilic, cationic dye which accumulates within mitochondria in a manner dependent on mitochondrial membrane potential. When mitochondrial membrane potential is low, JC-1 accumulates within mitochondria in low concentrations and persists in a monomeric form, fluorescing green. At higher mitochondrial membrane potential, JC-1 accumulation within the mitochondria is increased. Red fluorescing aggregates begin to form. Higher red/green fluorescence ratio is therefore proportional to mitochondrial membrane potential. JC-1 was used to assess the impact of HCA on mitochondrial membrane potential in HPMECs, SAECs, and MSCs under both inflammatory and non-inflammatory conditions.

After 24 hours of cytomix stimulation and culture in 5% or 15% CO_2, cells were stained with JC-1 (Sigma-Aldrich) at a concentration of 0.5µg/ml for 45 minutes (SAECs) or 1 hour (HPMECs and MSCs). A control was included in which 1µM carbonyl cyanide p-trifluoromethoxyphenylhydrazone (FCCP) was simultaneously

added to the cells at the time of JC-1 staining to induce mitochondrial depolarisation (collapse of mitochondrial membrane potential). Following staining, wells were washed 3 times using 1x PBS. 100µl 1x PBS was added per well and live cells were immediately imaged at x20 magnification, using the EVOS FL Auto epifluorescent microscope. Red and green fluorescence intensity of each image was measured in ImageJ and the red/green ratio was calculated.

2.8.1.1 JC-1staining of MSCs cultured in buffered hypercapnia

Experiments in which acidosis was buffered to determine the individual contributions of CO_2 and pH to HCA-induced effects on mitochondrial membrane potential were also performed in MSCs. The experimental setup was as before with both unstimulated and cytomix-stimulated MSCs cultured in 5% or 15% CO_2 for 24 hours. However, an additional two groups – one unstimulated and one cytomix-stimulated – in which the pH was buffered to that in 5% CO_2, were included in 15% CO_2. To achieve this, pre-equilibrated medium containing 0.02M sodium bicarbonate ($NaHCO_3$) (Sigma-Aldrich) was used. To ensure all groups were equi-osmolar, pre-equilibrated medium containing 0.02M sodium chloride (NaCl) (Sigma-Aldrich) was used for all other groups, in both 5% and 15% CO_2. Cells were cultured in the presence or absence of 50ng/ml cytomix in 5% or 15% CO_2 for 24 hours prior to JC-1 staining as described in **Section 2.8.1**.

2.8.2 ATP assay

The majority of cellular adenosine triphosphate (ATP) originates from the mitochondrial electron transport chain. ATP production is therefore indicative of mitochondrial function. Intracellular ATP levels were measured after culture of MSCs in 5% or 15% CO_2 in the presence or absence of 50ng/ml cytomix for 24 hours using a luminescent ATP detection assay kit (Abcam), following the manufacturer's instructions. All reagents were brought to room temperature prior to use. 50µl supplied detergent was added to each well containing the conditions of interest and to each well containing 90µl $\alpha MEM_{1\%+PS+LG}$ only in preparation for a standard curve. The plate was incubated at room temperature on an orbital shaker for 5 minutes.

Standards ranging in concentration from 10µM to 0.1nM were prepared. 10µl prepared standard was added to 90µl $\alpha MEM_{1\%+PS+LG}$ already in the wells reserved for the standard curve. The plate was incubated at room temperature for 5 minutes on an orbital shaker. 50µl of the supplied Substrate Solution was then added per well. The plate was incubated again at room temperature for 5 minutes on an orbital shaker. Luminescence was measured immediately using a FLUOstar Omega microplate reader.

2.9 Co-culture experiments

2.9.1 Mitochondrial transfer

MitoTracker® dyes are cell-permeable probes that react with the thiol groups of and thus label, mitochondria. To investigate whether mitochondria are transferred from MSCs to SAECs, MSCs were stained with 125ng/ml MitoTracker® Green FM for 45 minutes at 37°C in 5% CO_2. SAECs were pre-stained with 125ng/ml MitoTracker® Deep Red for 1 hour at 37°C in 5% CO_2. Stained cells were washed three times with 1x PBS. A sample of the third MSC wash was retained for use as a leak control to rule out unspecific staining. Pre-stained MSCs were seeded on Transwell inserts with 0.4µm pores (Greiner) at a ratio of 1 MSC to every 5 SAECs and co-cultured indirectly for 24 hours in 5% or 15% CO_2 in the presence of 50ng/ml cytomix with pre-stained SAECs seeded on the well surface below. For the leak control, MSCs were replaced with an equal volume of the MSC wash retained earlier.

After 24 hours, the transwells were removed and the SAECs were washed three times with PBS. Live SAECs were immediately imaged at x20 magnification on an EVOS FL Auto epifluorescence microscope to visualise uptake of MSC-derived green mitochondria by SAECs.

2.9.2 Co-culture *in vitro* scratch assay

To assess the effects of MSCs on SAEC wound closure in normocapnia and HCA, MSCs were co-cultured with SAECs wounded in an *in vitro* scratch assay. Horizontal lines were drawn across the under surface of 24 well plates prior to cell seeding.

SAECs were seeded on these culture plates at a density of $1x10^4$ cells/cm^2 and allowed to reach confluence at 37°C in 5% CO_2. A single vertical 'scratch' wound was made using a P1000 tip from the top to bottom of each well, running through the horizontal line. Cells were washed twice with DPBS to remove cell debris and 500µl 1% supplemented small airway epithelial cell growth medium was added to each well. The wound area of each well just above and just below the horizontal line was imaged using the Axiovert 25 inverted light microscope and AxioVision Rel. 4.8 software.

Media was aspirated from each of the wells and replaced with 500µl 10% supplemented small airway epithelial cell growth medium (pre-equilibrated in 5% or 15% CO_2) with or without the addition of 50ng/ml cytomix. For positive control wells, pre-equilibrated 100% supplemented small airway epithelial cell growth medium (i.e. cell culture medium) was added. For negative control wells, pre-equilibrated 1% supplemented small airway epithelial cell growth medium was added. MSCs were trypsinised and counted as described in **Sections 2.1.2 and 2.1.3**. In wells where MSCs were to be co-cultured with SAECs, MSCs were seeded on transwell inserts with 0.4µm pores in pre-equilibrated 10% supplemented small airway epithelial cell growth medium containing 50ng/ml cytomix at ratio of 1 MSC to every 5 SAECs. Plates were incubated at 37°C in 5% or 15% CO_2 for 24 hours.

Transwell inserts were removed and the wound areas above and below the horizontal lines were re-imaged at 24 hours. The area of the wound site at baseline and 24 hours was measured using ImageJ v1.48. The values obtained were used to calculate the percentage wound closure over 24 hours.

2.9.3 Ki67 staining

Ki67 is a cellular marker of proliferation. SAECs wounded in an *in vitro* scratch assay and co-cultured with MSCs **(Section 2.9.2)** were immunofluorescently stained for this marker. SAECs were washed 3 times with 1x PBS and fixed with 4% PFA at room temperature for 15 minutes. Excess PFA was aspirated and the wash step was

repeated. Cells were permeabilised by incubation with 0.5% Triton-X for 20 minutes at room temperature. The wash step was repeated. Cells were blocked with 200µl 1% BSA (prepared in 1x PBS) for 2 hours at room temperature. The wash step was repeated. The primary antibody, Ki67 monoclonal antibody (SolA15) (eBioscience), was diluted 1:200 in 1% BSA. 100µl primary antibody was added per well and incubated at 4°C overnight. For a secondary-only control, 100µl 1% BSA only was added.

After overnight incubation, cells were washed three times with 1x PBS. Goat anti-mouse/rat alexa fluor 594 was diluted 1:200 in 1% BSA. 100µl was added per well and incubated in the dark for 1 hour at room temperature. For a primary-only control, 100µl 1% BSA only was used. The wash step was repeated. 100µl Hoechst nuclear stain (undiluted) (Sigma-Aldrich) was added per well and incubated in the dark at room temperature for 20 minutes. The wash step was repeated. 200µl 1x PBS was added to the wells and the plates were stored at 4°C in the dark until imaging.

Images were taken at x5 magnification using a Leica DMi8 microscope (Leica Microsystems). One image was taken above and one below the horizontal line running across the under surface of the wells. To quantify Ki67 staining, a grid of individual squares each of 100,000 pixels^2 in size was drawn over each image using ImageJ v1.48. Four wells at the edge of the wound were selected from each image and the number of cells stained positively for Ki67 were counted using the multipoint tool. The average number of Ki67-positive cells per 100,000 pixels^2 was determined.

2.9.4 Loss-of-function experiment

A loss-of-function experiment were performed to determine the contribution of mitochondria to the ability of MSCs to promote SAEC wound closure in normocapnia. To induce mitochondrial dysfunction, confluent MSCs were treated with 1µg/ml Rhodamine 6G (R6G) (Sigma-Aldrich), prepared in $\alpha MEM_{16.5\%+PS+LG}$, for 48 hours at 37°C in 5% CO_2. Media was supplemented with 50µg/ml uridine (Sigma-Aldrich)

and 2.5mM sodium pyruvate (Sigma-Aldrich) to support glycolysis. At the same time, the media in another flask of MSCs at the same passage and confluence was replaced with fresh $\alpha MEM_{16.5\%+PS+LG}$. After 48 hours, the media were aspirated from both flasks of MSCs and the cells were washed three times with PBS. The MSCs were trypsinised and counted as described as described in **Sections 2.1.2** and **2.1.3**. The *in vitro* scratch assay in **Section 2.9.2** was repeated, including an additional group in normocapnia in which R6G-treated MSCs were co-cultured with SAECs.

2.10 Statistical analysis

Statistical analysis was performed on GraphPad Prism 5.01 (GraphPad Software Inc.). All data are presented as mean ± standard deviation and were tested for normal distribution using the Kolmogorov-Smirnov test, the D'Agostino and Pearson Omnibus normality test, or the Shapiro-Wilk normality test. Parametric data were analysed by one-way ANOVA with Bonferroni posthoc analysis while non-parametric data were analysed by Kruskal-Wallis with Dunn's posthoc analysis. Grouped data were analysed by two-way ANOVA. p-values of <0.05 were considered statistically significant.

Chapter Three – Hypercapnic acidosis attenuates the inflammatory response of, and wound closure by, primary human pulmonary microvascular endothelial cells

3.1 Overview of chapter

Endothelial cells are key cells in the pathophysiology of Acute Respiratory Distress Syndrome (ARDS). In this chapter, their response to hypercapnic acidosis (HCA) will be investigated. The rationale for this study will first be discussed in the context of the contributions of endothelial cells to the key hallmarks of ARDS and of the existent literature on their response to HCA. The aims and objectives of the study will be highlighted. The results will then be presented and their implications for the pathophysiology of ARDS subsequently discussed.

3.2 Introduction

The capillaries surrounding the alveoli, like much of the vascular network, are formed by a continuous layer of endothelial cells tethered to a proteinaceous basement membrane via integrin binding[196]. In the lung, this basement membrane is composed largely of laminins which contribute to signal transduction[197], and type IV collagen which confers resistance to mechanical stress[198]. Pericytes are also found scattered through the endothelial basement membrane where, among several roles, they provide stability to the capillary wall[199]. On the luminal side, the endothelium is lined by a negatively charged glycocalyx composed of proteoglycans, glycoproteins, and glycosaminoglycans (GAGs) which regulate accessibility of the endothelium to blood cells and macromolecules[196,200].

In the healthy lung, the endothelial cells themselves typically exhibit a relatively non-inflammatory phenotype. However, upon recognition of stimuli such as lipopolysaccharide (LPS), tumour necrosis factor-alpha (TNF-α), or interleukin-1 (IL-1) in their local environment, the inflammatory NFκB pathway becomes activated[201]. Mitochondrial dysfunction may also be induced, resulting in increased production of ROS which can subsequently activate inflammasomes and promote additional NFκB activation[202]. These intracellular signaling mechanisms ultimately induce a proinflammatory phenotype characterised by new or increased synthesis of inflammatory cytokines and neutrophil adhesion molecules[203]. As such, endothelial cells isolated from the lungs of patients with ARDS secrete more of the potent

neutrophil chemoattractant CXCL8 and express higher levels of the neutrophil adhesion molecules intercellular adhesion molecule-1 (ICAM-1) and vascular cell adhesion molecule-1 (VCAM-1) than control cells from individuals without ARDS[204]. Despite the mechanism, activated endothelial cells possessing an inflammatory phenotype are primed to contribute to the major hallmarks of ARDS – inflammation (including neutrophil recruitment to the alveoli), and accumulation of protein-rich alveolar oedema fluid.

Neutrophils are key contributors to the pathophysiology of ARDS[1]. In the lung, their extravasation from the bloodstream is unique in that it occurs at the capillary level rather than at the level of the post-capillary venules, as in other organs[205,206]. In health, this process is tightly regulated, and neutrophils primed by inflammatory mediators are de-primed at the endothelium and returned to the systemic circulation[207]. However, this depriming process is disrupted in ARDS, resulting in greater abundance of hyper-responsive neutrophils in the circulation which may be recruited to the lung[207].

In most organs, the initial stage of neutrophil extravasation from the bloodstream involves loose attachment of neutrophils to the endothelium via interactions between their surface glycoproteins and endothelial selectins, including E-selectin and P-selectin. In larger vessels, these interactions promote neutrophil rolling along the endothelial surface to slow their passage through the vessel. However, the diameter of the pulmonary capillaries is small relative to that of neutrophils[208]. Therefore, to continue in the circulation, neutrophil deformation is inevitably required to pass through the capillaries and into the post-capillary venules[209]. In inflammatory states, such as that in ARDS and sepsis, neutrophil deformability is reduced[210]. This is thought to be the key mechanism behind initial neutrophil sequestration in the pulmonary capillaries and may be induced by inflammatory mediators, specifically CXCL8 which is known to be secreted in higher concentrations by the pulmonary endothelium of patients with ARDS compared to that from individuals without ARDS[204,211]. Although neutrophil rolling does not occur in the pulmonary capillaries,

endothelial selectins are thought to increase subsequent retention of sequestered neutrophils[212].

Following sequestration and retention in the pulmonary capillaries, neutrophils firmly adhere to the endothelium via binding of their β1 and β2 integrins to endothelial VCAM-1 and ICAM-1, respectively[213]. ICAM-1, in particular, is important not only for neutrophil entrapment within the capillaries, but also for subsequent recruitment into the alveoli[214,215]. While there exists evidence that VCAM-1 is also important for neutrophil recruitment to the lung in the settings of endotoxin-induced lung injury and acute pancreatitis[216,217], its contribution in the setting of sepsis has been questioned[218]. Nonetheless, expression of both these adhesions molecules is increased on endothelial cells isolated from the lungs of patients with ARDS[204].

Neutrophils migrate through interendothelial gaps in a process termed diapedesis following their retention at the endothelium. This occurs in response to a chemotactic gradient and is facilitated by homophilic interactions between platelet and endothelial cell adhesion molecule-1 (PECAM-1) molecules on the neutrophils and their surrounding endothelial cells[219,220]. The neutrophils themselves also possess the ability to create an environment facilitatory of their passage through obstruction and so, once they have evaded the endothelial barrier, can then make their way through the interstitium to accumulate within the alveoli[220,221].

In addition to promoting alveolar neutrophil recruitment, activation of endothelial cells, as mentioned, also promotes the formation of protein-rich alveolar oedema fluid. In its non-activated state, the endothelium forms a semi-permeable barrier which regulates the paracellular transport of water and solutes out of the capillaries to prevent alveolar flooding. Integrity of this barrier is maintained predominantly by adherens junctions through the interactions of transmembrane vascular endothelial (VE)-cadherin molecules on adjacent endothelial cells[222] and is dependent on mitochondrial function, particularly energy production[223]. The ability of endothelial cells to spread and migrate is also important for the maintenance of barrier integrity, by ensuring the

adjacent cells come into close enough contact to form such intercellular junctions[224,225]. In the inflammatory setting, intercellular junctions can be broken down by direct phosphorylation of VE-cadherin and its associated intracellular proteins[226]. Endothelial activation also induces cytoskeletal remodelling and actomyosin contraction which further forces cells apart, resulting in the formation of gaps between neighbouring endothelial cells. These gaps increase paracellular permeability to macromolecules such as plasma proteins which should otherwise be restricted in passing through the capillary walls. As a result, inflammation-induced endothelial permeability promotes oedema formation in ARDS[222].

To date there exists only two reports on the response of endothelial cells to hypercapnic acidosis (HCA). While both lack *in vitro* evidence of the effects of HCA on endothelial permeability and did not address the potential involvement of mitochondrial function, the first, published in 2003 by Takeshita *et al.,* demonstrates HCA-induced attenuation of CXCL8 secretion, ICAM-1 expression, neutrophil adhesion, and NFκB activation[227]. To the contrary, Liu *et al.* more recently demonstrated increases in all of these parameters in response to HCA[158].

A number of factors may have contributed to these conflicting responses. Firstly, the degree of hypercapnia differed between both studies; the endothelial response to 15% CO_2 (equivalent to 75mmHg) was assessed by Takeshita *et al.*, while Liu *et al.* more recently assessed the response to 10% CO_2 (equivalent to 64mmHg). Additionally, the degree of endothelial injury between the two studies also differed with Takeshita *et al.* using 1µg/ml lipopolysaccharide (LPS) to induce endothelial activation, and Liu *et al.* inducing activation with a much higher concentration of LPS (minimum of 1ng/ml) or a different stimulus altogether (minimum 5ng/ml TNFα). Of particular note however are the cell types used to model the pulmonary endothelium in these studies; human pulmonary artery endothelial cells (HPAECs) were used by Takeshita *et al.,* while human pulmonary microvascular endothelial cells (HPMECs) were used by Liu *et al*.

A common limitation of many *in vitro* studies of the pulmonary capillary endothelium is the use of HPAECs or human umbilical vein endothelial cells (HUVECs) as a model. These are macrovascular endothelial cells, whereas the pulmonary capillaries are composed of microvascular cells. Significant heterogeneity exists between endothelial cell types both within organs and between organs. Specifically, microvascular endothelial cells are well known to differ from macrovascular endothelial cells from both the same and different organs in a number of respects including expression of cytokine receptors[228], cytokine secretion[228–231], adhesion molecule expression[228,232], and the integrity of the barriers they form[233]. The use of macrovascular cells to study the pulmonary capillary endothelium in ARDS may therefore limit the translational value of *in vitro* work.

These differences between endothelial cell types suggest that, of the two HCA studies discussed, the results of the more recent study by Liu *et al.* are the post representative of the response of the pulmonary capillary endothelium in ARDS. However, of concern in this study is the *in vivo* data which are presented alongside the *in vitro* data. These data corroborate the *in vitro* findings, demonstrating increased CXCL8 concentrations in lung tissue homogenates, increased adhesion molecule expression, and recovery of more neutrophils from the BALF of hypercapnic rabbits[158]. However, they also contradict a large body of *in vivo* evidence to the contrary[129,132,234,235]. While these *in vivo* discrepancies may be explained by differences in the degree of HCA, the animal species used, or the stimulus and/or concentration of that stimulus used to induce lung injury, many *in vivo* studies have been performed to date covering a range of CO_2 concentrations, species and stimuli. Concerns are thus raised regarding the reliability of the data in this study, necessitating the confirmation of the *in vitro* response of HPMECs to HCA.

3.3 Aims and Objectives

The overall objective of this chapter is to study the response of the pulmonary capillary endothelium to hypercapnic acidosis in the setting of inflammation. This will be achieved using the primary cell type most relevant to the pathophysiology of ARDS –

human pulmonary microvascular endothelial cells (HPMECs) – in an *in vitro* model of the condition in which the inflammatory environment is modelled by a cytomix of proinflammatory cytokines implicated in its pathogenesis. The specific aims of this study are:

- To determine the effects of HCA on the inflammatory response of HPMECs to cytomix stimulation
- To determine the effects of HCA on the reparative potential of HPMECs in an inflammatory environment
- To investigate the mechanism(s) responsible for any observed effects

3.4 HCA develops and stabilises within 4 hours of incubation of cell culture medium in 15% CO_2

Many patients with ARDS who develop hypercapnia also develop acidosis[54]. However, as the decision to buffer this acidosis is open to clinical discretion, its persistence may be significantly altered in some patients and not others. Acidosis itself may alter cell behaviour and, therefore, it is important to determine whether the *in vitro* results gathered pertain to a hypercapnic or a hypercapnic acidotic environment. In addition, initial fluctuations in pH and pCO_2 *in vitro* have the potential to influence experimental readouts. This can be overcome by pre-equilibrating the media used for experiments in either 5% or 15% CO_2 prior to use. However, it is important to determine when the pH and pCO_2 of these media have stabilised to ensure that no further alterations in these parameters occur.

Endothelial cell culture medium (in the absence of cells) was exposed to 5% or 15% CO_2 for up to 72 hours. During this time, pH and pCO_2 were measured at various intervals using a blood gas analyser. Results demonstrate an initial increase in pCO_2 from baseline (0 hours) to 4 hours in both 5% and 15% CO_2 (1.7± 0.1kPa at baseline to 3.4 ± 0.1kPa in 5% CO_2, and to 9.0 ± 0.2kPa in 15% CO_2). pCO_2 remained relatively stable thereafter **(Figure 3.1A)**. Similarly, pH declines within the first 4

hours of incubation (7.6 ± 0.0 at baseline to 7.3 ± 0.0 in 5% CO_2, and to 7.0 ± 0.0 in 15% CO_2), and remained constant thereafter **(Figure 3.1B)**. Together these results demonstrate both that the *in vitro* condition under investigation is hypercapnic acidosis, and that media should be pre-equilibrated in 5% or 15% CO_2 for not less than 4 hours prior to use.

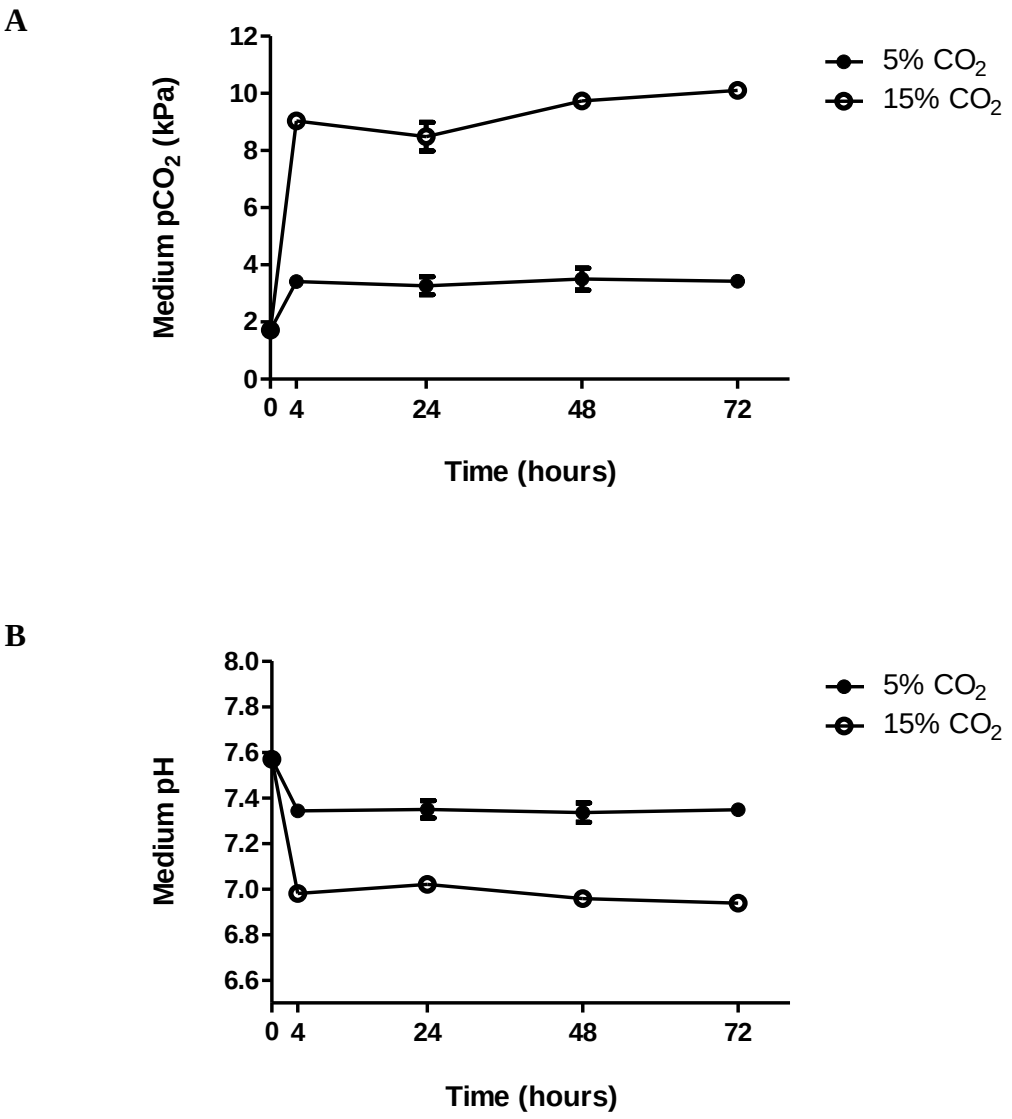

Figure 3.1: HCA develops and stabilises within 4 hours of incubation of cell culture medium in 15% CO_2

Endothelial cell culture medium was exposed to 5% or 15% CO_2. pCO_2 (A) and pH (B) were measured at intervals up to 72 hours using a blood gas analyser. Error bars represent standard deviation (SD). (n=2 for all conditions; no statistical analysis performed).

3.5 HCA attenuates secretion of the neutrophil chemoattractants CXCL8 and CXCL5 by HPMECs

HPMECs were stimulated with 50ng/ml cytomix and cultured in 5% or 15% CO_2 for up to 72 hours. Supernatants were collected and analysed by ELISA to quantify alterations in HPMEC secretion of the potent neutrophil chemoattractants CXCL8 and CXCL5 in response to HCA. CXCL8 secretion by HPMECs increased progressively across all conditions analysed from 24 hours to 72 hours **(Figure 3.2A-C)**. Secretion of CXCL8 by cytomix-stimulated HPMECs was not significantly influenced by HCA in comparison to normocapnia at 24 hours **(Figure 3.2A)**. However, when compared to normocapnia, its secretion was significantly attenuated at 48 hours (85.5 ± 18.5ng/ml in normocapnia vs. 59.9 ± 10.9ng/ml in HCA) **(Figure 3.2B)**. This difference became more pronounced at 72 hours (105.7 ± 12.5ng/ml in normocapnia vs. 66.3 ± 8.2ng/ml in HCA) **(Figure 3.2C)**.

Secretion of CXCL5 by HPMECs was assessed at 72 hours only. The concentrations of both basal and cytomix-induced CXCL5 secreted were considerably lower than that of CXCL8. However, similar to CXCL8, CXCL5 secretion in HCA was also significantly attenuated at 72 hours when compared to normocapnia (21.1 ± 7.1ng/ml in normocapnia vs. 5.5 ± 1.5ng/ml in HCA) **(Figure 3.2D)**. In this case, the degree of attenuation was such that cytomix no longer significantly enhanced CXCL5 secretion in HCA **(Figure 3.2D)**.

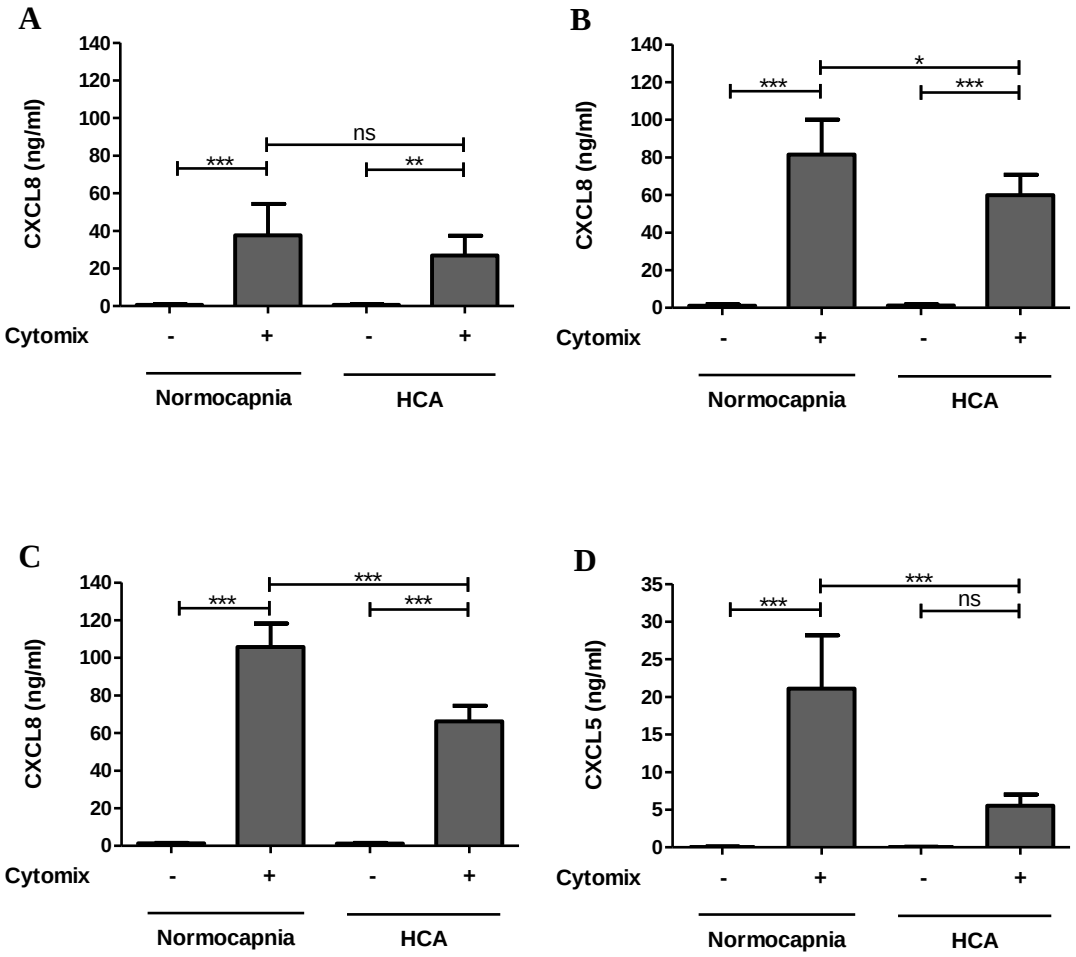

Figure 3.2: HCA attenuates secretion of the neutrophil chemoattractants CXCL8 and CXCL5 by HPMECs

Unstimulated or cytomix-stimulated HPMECs were cultured in 5% or 15% CO_2 for up to 72 hours. CXCL8 concentrations in cell culture supernatants were quantified by ELISA at 24 hours (A), 48 hours (B), and 72 hours (C). CXCL5 concentrations were quantified by ELISA at 72 hours only (D). Error bars represent standard deviation (SD). (n=5 for all conditions; one-way ANOVA with Bonferroni posthoc analysis; ns = $p>0.05$; * = $p<0.05$; ** = $p<0.01$; *** = $p<0.001$).

3.6 HCA attenuates cytomix-induced expression of ICAM-1 by HPMECs

HPMEC monolayers in the presence or absence of 50ng/ml cytomix were cultured in 5% or 15% CO_2 for 24 hours or 72 hours. Cell surface expression of E-selectin, ICAM-1 and VCAM-1 was assessed by flow cytometry to determine the effects of HCA on endothelial adhesion molecule expression. Results demonstrate a low basal expression of ICAM-1 (17.0 ± 11.2% of total unstimulated cells in normocapnia), which was significantly upregulated by cytomix (to 94.3 ± 4.2 % of total cytomix-stimulated cells in normocapnia) at 24 hours **(Figure 3.3B)**. Cytomix stimulation also induced HPMEC expression of both E-selectin (1.1 ± 1.3% of total unstimulated cells vs. 64.8 ± 19.9% of total stimulated cells, both in normocapnia) and VCAM-1 (2.0 ± 1.5% of total unstimulated cells vs. 84.5 ± 6.6% of cytomix-stimulated cells, both in normocapnia) at this time point **(Figures 3.3A and 3.3C)**. When compared to normocapnia, HCA did not significantly alter cytomix-induced expression of any of the three adhesion molecules at 24 hours **(Figures 3.3A-C)**. However, in contrast, while neither median fluorescence intensity (MFI) (a measure of the level of expression per cell) nor the percentage of cells staining positively for E-selectin or VCAM-1 were altered by HCA at 72 hours **(Figures 3.3D and 3.3F)**, the MFI for ICAM-1 was significantly attenuated when compared to normocapnia (17008 ± 3501 in normocapnia vs. 9183 ± 2551 in HCA) **(Figure 3.3E)**.

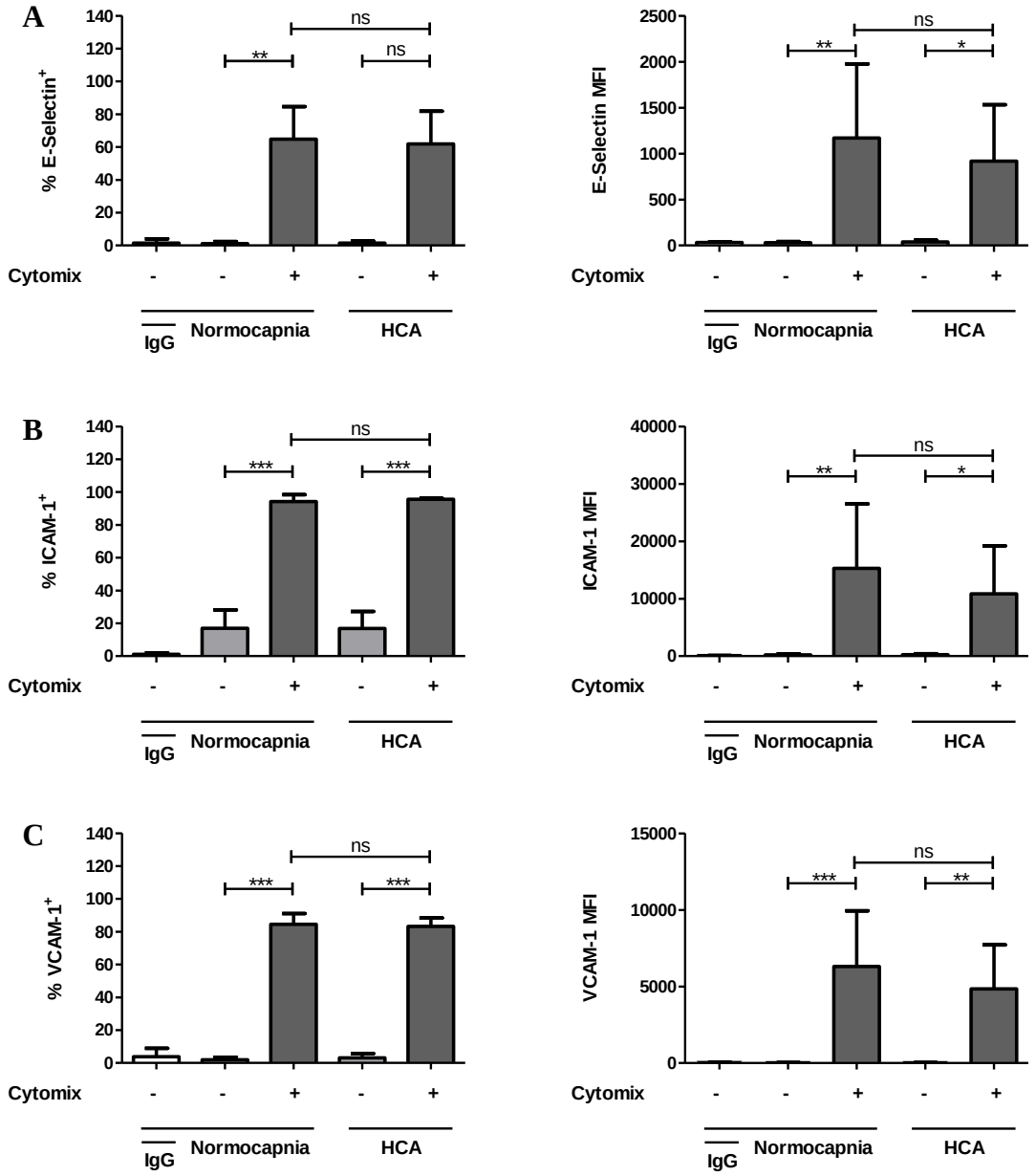

Figure 3.3: HCA attenuates cytomix-induced expression of ICAM-1 by HPMECs (continued overleaf)

Unstimulated or cytomix-stimulated HPMECs were cultured in 5% or 15% CO_2. Expression of the adhesion molecules E-selectin (A), ICAM-1 (B), and VCAM-1 (C) was assessed by flow cytometry at 24 hours. Both percentage positive cells and MFI are presented for each adhesion molecule. Error bars represent standard deviation (SD). (n=5 for all conditions; one-way ANOVA with Bonferroni posthoc analysis for all except E-selectin % positive cells which was analysed by Kruskal Wallis with Dunn's posthoc test; ns = $p>0.05$; * = $p<0.05$; ** = $p<0.01$; *** = $p<0.001$).

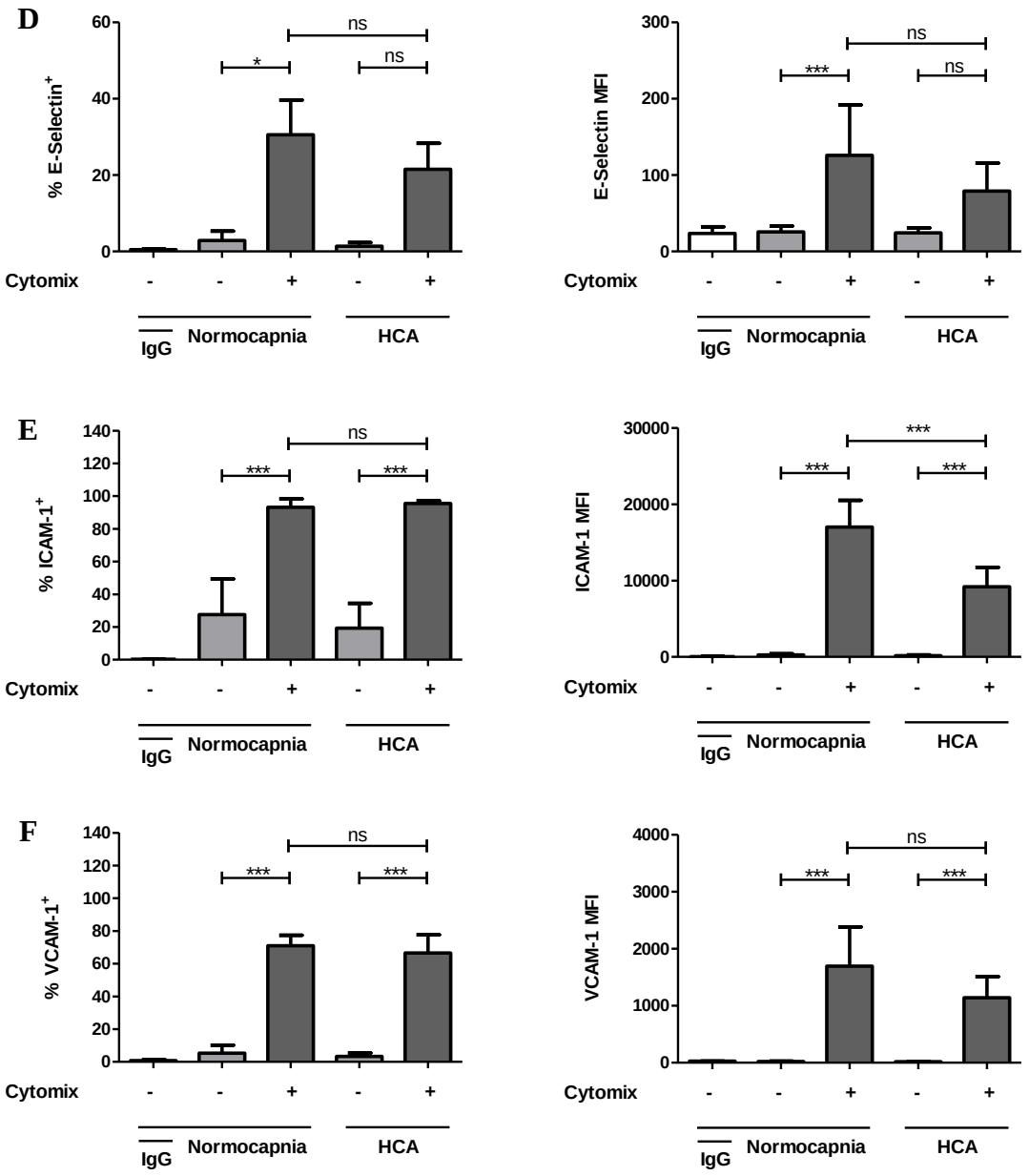

Figure 3.3: (continued) HCA attenuates cytomix-induced expression of ICAM-1 by HPMECs

Unstimulated or cytomix-stimulated HPMECs were cultured in 5% or 15% CO_2. Expression of the adhesion molecules E-selectin (D), ICAM-1 (E), and VCAM-1 (F) was assessed by flow cytometry at 72 hours. Both percentage positive cells and MFI are presented for each adhesion molecule. Error bars represent standard deviation (SD). (n=5 for all conditions; one-way ANOVA with Bonferroni posthoc analysis for all except E-selectin % positive cells which was analysed by Kruskal Wallis with Dunn's posthoc test; ns = $p>0.05$; * = $p<0.05$; ** = $p<0.01$; *** = $p<0.001$).

3.7 HCA attenuates HPMEC wound closure

To assess the reparative capacity of the endothelium in response to HCA, HPMEC monolayers were wounded in an *in vitro* scratch assay and cultured in 5% or 15% CO_2 in the presence or absence of 50ng/ml cytomix for 24 hours. Results demonstrate that HPMEC wound closure was impaired by HCA in a non-inflammatory setting (48.8 ± 13.4% in normocapnia vs. 28.4 ± 13.1% in HCA) **(Figures 3.4A and 3.4C)**. In the inflammatory setting of cytomix, wound closure was almost completely inhibited in normocapnia. The degree of wound closure in this inflammatory setting was not altered by HCA (8.9 ± 8.6% in normocapnia vs. 9.4 ± 12.1% in HCA) **(Figures 3.4B and 3.4C)**.

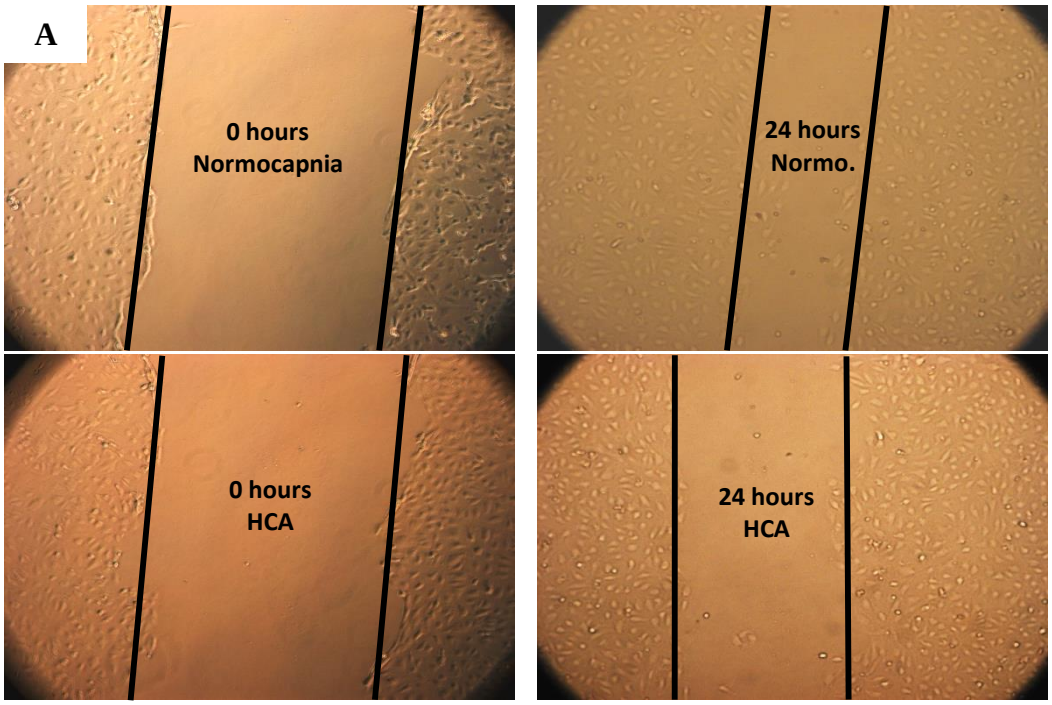

Figure 3.4: HCA attenuates HPMEC wound closure (continued overleaf)

HPMEC monolayers were wounded in an *in vitro* scratch assay and cultured in 5% or 15% CO_2 for 24 hours in the presence or absence of cytomix. Representative images depicting approximate wound areas at 0 hours and at 24 hours are presented for the non-inflammatory environment (vehicle) (A) (Normo = normocapnia).

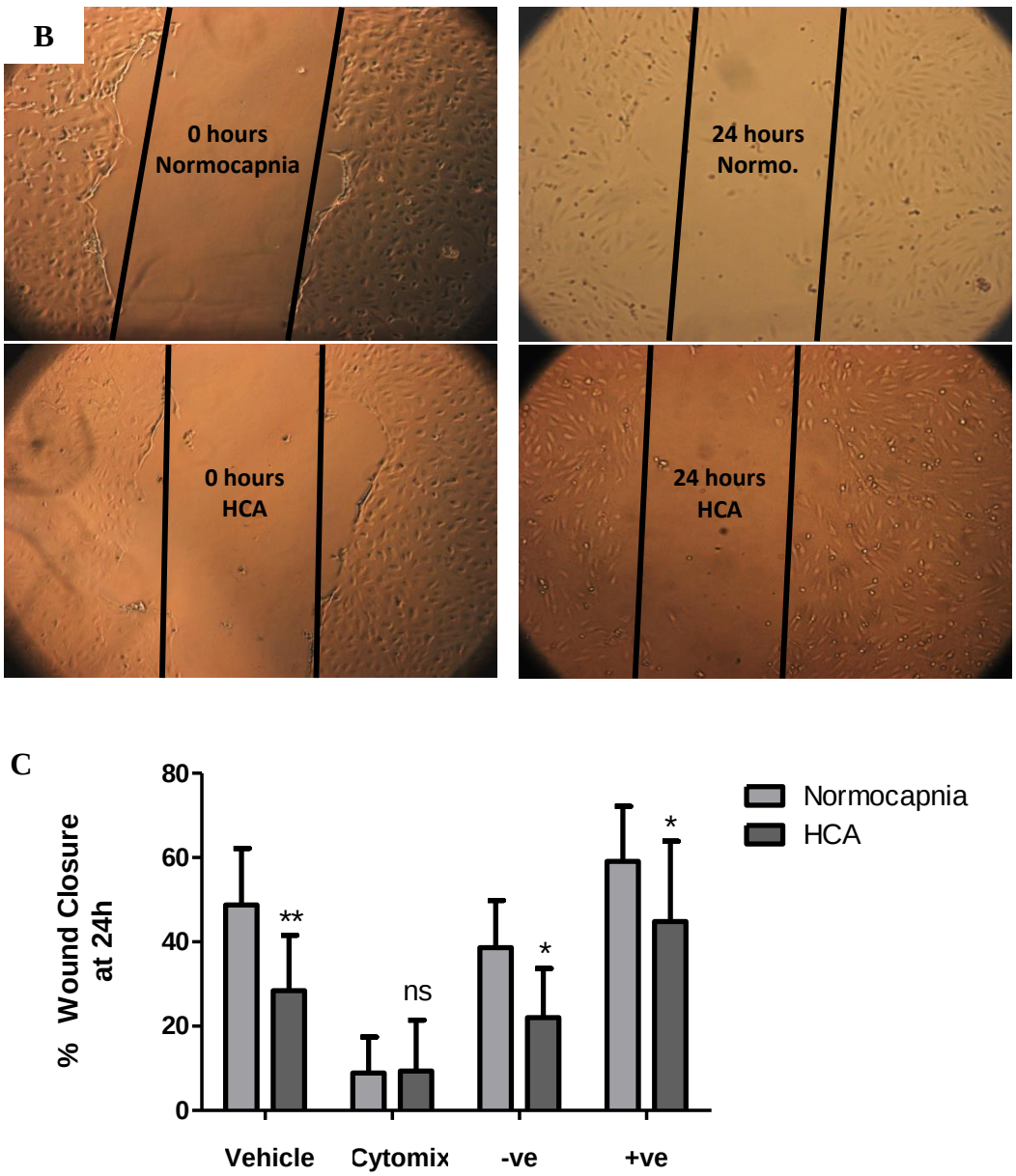

Figure 3.4 (continued): HCA attenuates HPMEC wound closure

HPMEC monolayers were wounded in an *in vitro* scratch assay and cultured in 5% or 15% CO_2 for 24 hours in the presence or absence of cytomix. Representative images depicting approximate wound areas at 0 hours and at 24 hours are presented for the inflammatory environment (cytomix) (B) (Normo = normocapnia). Percentage wound closure over 24 hours was calculated for each condition, including positive (+ve) and negative (-ve) controls (C). Error bars represent standard deviation (SD). (n=4 for all conditions; two-way ANOVA with Bonferroni posthoc analysis; ns = $p>0.05$; * = $p<0.05$; ** = $p<0.01$; *** = $p<0.001$).

3.8 HCA does not alter HPMEC viability

To investigate the mechanism behind HCA-induced attenuation of chemokine secretion, ICAM-1 expression, and endothelial wound closure, HPMEC viability was assessed by lactate dehydrogenase (LDH) assay using the supernatants analysed by ELISA in **Section 3.5**. A positive control in which cell death was induced using 2% Triton-X was included and the results are presented as percentage relative to this control.

Results demonstrate trends suggestive of cytomix-induced cell death across all three timepoints studied (24 hours, 48 hours, and 72 hours) in both normocapnia and HCA **(Figure 3.5)**. However, these differences did not reach statistical significance when compared to unstimulated counterparts. The degree of cell viability did not differ between cytomix-stimulated HPMECs exposed to 5% or 15% CO_2 at 24 hours (41.5 ± 2.0% in normocapnia vs. 29.6 ± 4.3% in HCA), 48 hours (43.4 ± 1.2% in normocapnia vs. 34.6 ± 3.0% in HCA), or 72 hours (38.9 ± 7.9% in normocapnia vs. 29.2 ± 5.05 in HCA) **(Figure 3.5)**. Similarly, no statistically significant HCA-induced alterations in the viability of unstimulated HPMECs were observed in comparison to normocapnia at 24 hours (24.5 ± 4.2% in normocapnia vs. 17.9 ± 2.4% in HCA), 48 hours (26.2 ± 6.6% in normocapnia vs. 21.5 ± 3.4% in HCA), or 72 hours (36.7 ± 6.0% in normocapnia vs. 20.6 ± 3.8% in HCA) **(Figure 3.5)**.

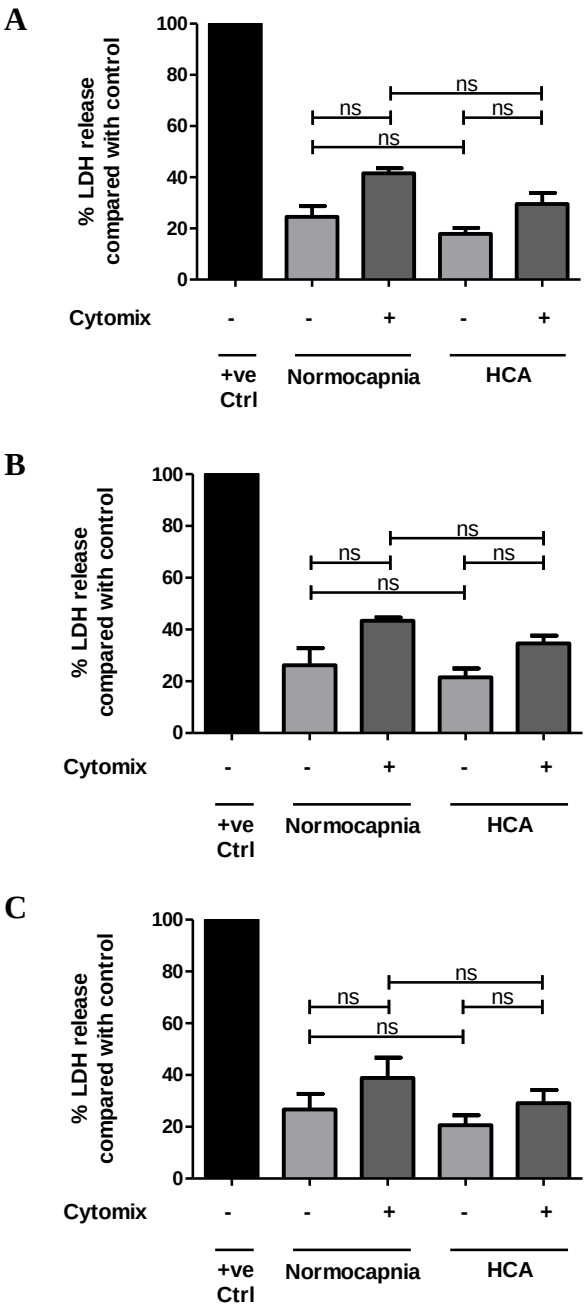

Figure 3.5: HCA does not alter HPMEC viability

Unstimulated or cytomix-stimulated HPMECs were cultured in 5% or 15% CO_2 for up to 72 hours. Cell viability was assessed by LDH release into cell culture supernatants at 24 hours (A), 48 hours (B), and 72 hours (C). Results are presented as percentage relative to the positive control (+ve Ctrl). Error bars represent standard deviation (SD). (n=5 for all conditions; Kruskal-Wallis with Dunn's posthoc analysis; ns = P>0.05).

3.9 NFκB activation in HPMECs is not altered in response to HCA

To further probe the mechanism responsible for the observed endothelial responses to HCA, HPMECs in the presence or absence of 50ng/ml cytomix were cultured in 5% or 15% CO_2 for 0, 30 or 60 minutes. Nuclear extracts were collected and activation status of the NFκB pathway was assessed by p65 TransAM assay. This assay is a DNA-binding ELISA which detects active NFκB p65 subunits in nuclear extracts via their binding to consensus oligonucleotides immobilised on a 96 well plate.

Results demonstrate marked induction of NFκB activation by cytomix stimulation of HPMECs for 30 or 60 minutes **(Figure 3.6)**. A small trend towards attenuated NFκB activation was observed in HCA at 30 minutes post-stimulation (optical density (OD) 1.3 ± 0.2 in normocapnia vs. 1.0 ± 0.2 in HCA). However, this difference did not reach statistical significance **(Figure 3.6)**. The degree of NFkB activation also did not differ between normocapnia and HCA at 60 minutes post-stimulation (optical density (OD) 1.1 ± 0.1 in normocapnia vs. 1.2 ± 0.1 in HCA) **(Figure 3.6)**.

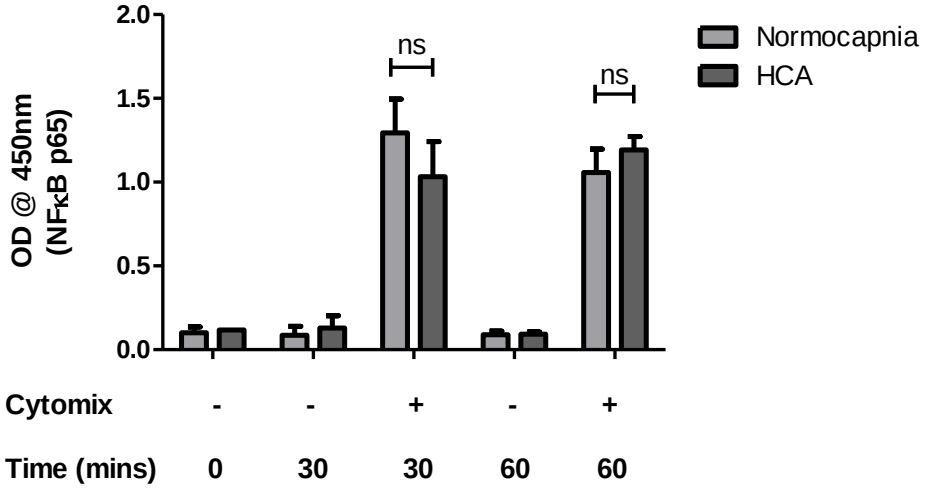

Figure 3.6: NFκB activation in HPMECs is not altered in response to HCA

HPMECs were cultured in 5% or 15% CO_2 in the presence or absence of cytomix stimulation for 0, 30, and 60 minutes. The degree of NFκB activation was assessed by TransAM assay. Results are presented as optical density (OD) at 450nm. Error bars represent standard deviation (SD). (n=1 for 0 minutes in HCA; n=2 for 0 minutes in normocapnia, 30 minutes + cytomix in normocapnia, and 60 minutes – cytomix in HCA; n=3 for all other conditions; two-way ANOVA with Bonferroni posthoc analysis; ns = $p>0.05$).

3.10 HCA attenuates HPMEC mitochondrial membrane potential

To explore the effect of HCA on mitochondrial function as a potential mechanism behind the attenuated inflammatory and reparative responses of HPMECs to HCA, mitochondrial membrane potential was assessed. HPMECs, in the presence or absence of cytomix, were cultured in 5% or 15% CO_2 for 24 hours. Cells were then stained with the mitochondrial membrane potential indicator, JC-1. JC-1 accumulates in mitochondria at low concentrations when their membrane potential is low and persists in a monomeric form exhibiting green fluorescence. When mitochondrial membrane potential is increased, JC-1 accumulates in higher concentrations and forms aggregates which exhibit red fluorescence. The degree of JC-1 aggregation – which is therefore proportional to mitochondrial membrane potential - was subsequently assessed by fluorescence microscopy. Control wells were included in which HPMECs were treated with the mitochondrial oxidative phosphorylation uncoupler, FCCP, simultaneously to JC-1 staining to induce mitochondrial depolarisation. Results are presented as the ratio of red (JC-1 aggregates) / green (JC-1 monomers), normalised to unstimulated cells in normocapnia.

Mitochondrial depolarisation was significantly induced by FCCP (normalised red/green ratio 0.2 ± 0.3) when compared to untreated cells in normocapnia (normalised red/green ratio 1.0 ± 0.0) **(Figure 3.7)**. Cytomix stimulation did not significantly alter mitochondrial membrane potential in either normocapnia or HCA when compared to unstimulated cells cultured under the same conditions **(Figure 3.7)**. However, mitochondrial membrane potential of stimulated cells in HCA was significantly attenuated in comparison to stimulated cells cultured under normocapnic conditions (2.6 ± 2.2 in normocapnia vs. 0.7 ± 0.5 in HCA) **(Figure 3.7)**. HCA also attenuated mitochondrial membrane potential in unstimulated HPMECs when compared to normocapnia (1.0 ± 0.0 in normocapnia vs. 0.5 ± 0.3 in HCA) **(Figure 3.7)**.

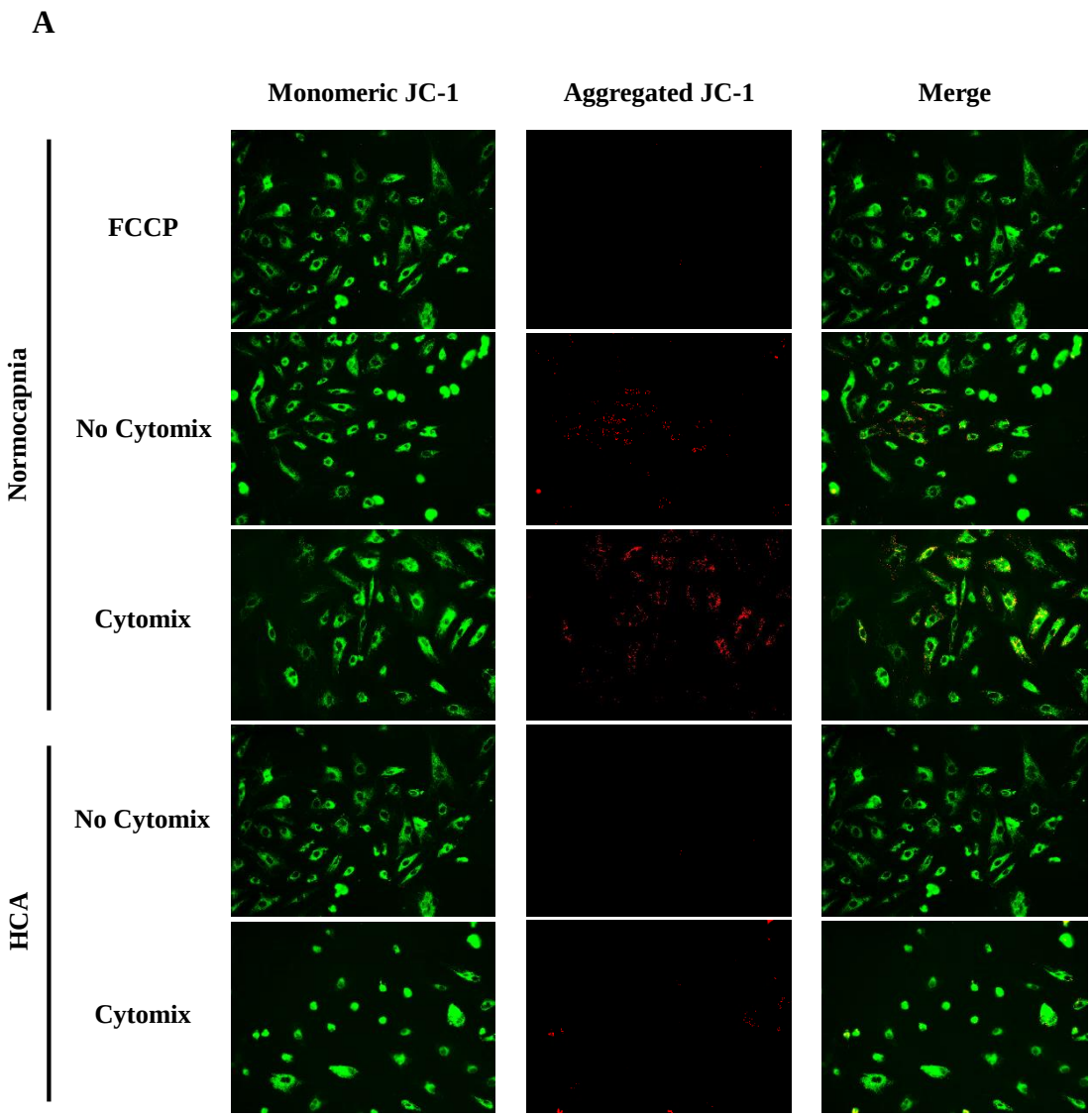

Figure 3.7: HCA attenuates HPMEC mitochondrial membrane potential (continued overleaf)

HPMECs were cultured in 5% or 15% CO_2 in the presence or absence of cytomix stimulation for 24 hours before staining with the mitochondrial membrane potential indicator, JC-1. A control was included in which FCCP was used to induce mitochondrial depolarisation. Representative images are presented (A).

B

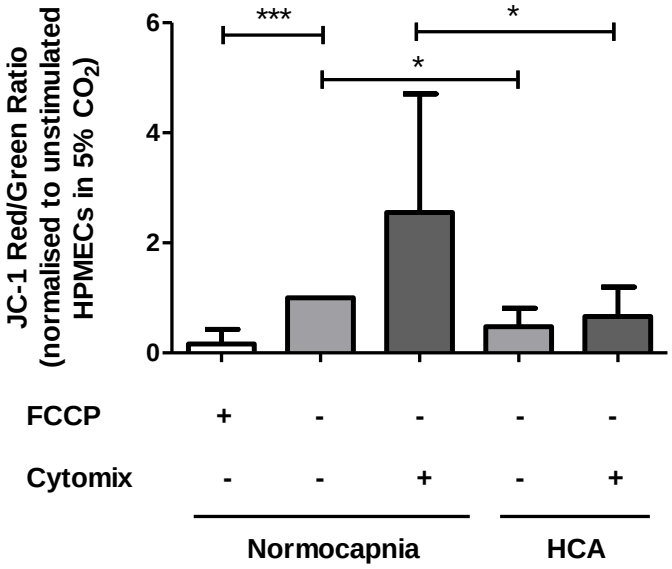

Figure 3.7 (continued): HCA attenuates HPMEC mitochondrial membrane potential

HPMECs were cultured in 5% or 15% CO_2 in the presence or absence of cytomix stimulation for 24 hours before staining with the mitochondrial membrane potential indicator, JC-1. A control was included in which FCCP was used to induce mitochondrial depolarisation. The JC-1 red (aggregate) / green (monomer) ratio was measured and presented relative to unstimulated cells in normocapnia (B). Error bars represent standard deviation (SD). (n=5 for all conditions; Kruskal-Wallis with Dunn's posthoc analysis; * = $p<0.05$; *** = $p<0.001$).

3.11 Discussion

To date, data on the response of the capillary endothelium to HCA is limited, with only two papers having been published on the subject. The first of these, by Takeshita *et al.*, used a macrovascular endothelial cell type which, as discussed in **Section 3.2**, is of limited translational value in ARDS[227]. The second, by Liu *et al.*, used human pulmonary microvascular endothelial cells (HPMECs) – the most appropriate endothelial cell type for studying ARDS[158]. However, as also discussed in **Section 3.2**, some concerns have arisen with regard to the results of the latter study. The aim of the work in this chapter was therefore to determine the effects of HCA on the injured pulmonary capillary endothelium in ARDS, using an *in vitro* model whereby HPMECs were stimulated with a cytomix of proinflammatory cytokines (IL1β, IFNγ and TNFα) implicated in the pathogenesis of the condition.

The inflammatory response of cytomix-stimulated HPMECs to HCA was first assessed. Neutrophils are key mediators of inflammation and damage in ARDS, and their recruitment to the alveoli depends in part on the presence of chemotactic stimuli[1]. CXCL5 and CXCL8 are important chemokines in this respect[236–239]. The results of the present study demonstrate attenuated HPMEC secretion of both these chemokines in HCA. This is the first time that the secretion of CXCL5 by HPMECs has been assessed in the hypercapnic setting. However, the effects of HCA on CXCL8 secretion have previously been reported: while the results of the present study do not support the findings of Liu *et al.* who demonstrated increased CXCL8 secretion by HPMECs in HCA, they do support the findings of Takeshita *et al.* who demonstrated attenuated secretion, albeit in pulmonary macrovascular cells[158,227]. Of note, however, is that in comparison to the work of Takeshita *et al.* in which CXCL8 secretion was attenuated in HCA at 24 hours post-stimulation, its secretion was not attenuated until at least 48 hours post-stimulation in the current study. While it is perceivable that the two endothelial cell types may differ in their sensitivity to HCA, the pCO_2 did differ slightly between the two studies (9kPa in the current study vs. 10kPa in the study by Takeshita *et al.*), suggesting that the delayed response in HPMECs may have arisen as a result of less pronounced hypercapnia and that a dose-response effect may occur. Attenuation of CXCL8 secretion was again more pronounced at 72 hours post-

stimulation, suggesting that the effects of HCA on HPMEC chemokine secretion are not transient.

Endothelial adhesion molecule expression is, as discussed in **Section 3.2**, another important element of neutrophil recruitment to the alveoli during ARDS. In the present study, the percentage of HPMECs expressing the adhesion molecules E-selectin, ICAM-1 or VCAM-1, was not altered in response to HCA. While there were also no differences in the degree of expression of any of these three adhesion molecules on the surface of positive cells (as reflected in the MFI) at 24 hours post-stimulation, the degree of ICAM-1 expression was significantly attenuated in HCA at 72 hours post-stimulation. Again, while this work is in accordance with the work of Takeshita *et al.*, the time it takes to see such attenuation in delayed in the current study[227].

Numerous *in vivo* studies have reported attenuated bronchoalveolar lavage fluid (BALF) neutrophilia in HCA[129,132,234,235]. The attenuation of both chemokine secretion and ICAM-1 expression observed in the current study suggest that HPMECs contribute to this response by attenuating neutrophil extravasation from the capillaries. However, this work lacks a functional assay in which neutrophil migration across the endothelial barrier is assessed to confirm this theory. This is an assay which would require the formation of an endothelial monolayer on a transwell insert. While the formation of such a monolayer has been successfully achieved using HPMECs in the past[240], insufficiently tight and consistent monolayers were achieved in the current study to permit such assessments.

The inability of HPMECs to achieve a sufficiently tight, consistent monolayer also hindered the ability to study the response of endothelial barrier integrity to HCA. Such information is currently absent from the published literature. As highlighted in **Section 3.2**, the endothelium forms a semi-permeable barrier, the integrity of which is disrupted in ARDS to promote the accumulation of a protein-rich oedema fluid within the alveoli. Considerable time and effort were put into establishing a suitable *in vitro*

model to assess endothelial barrier integrity. Among the techniques utilised was the measurement of transendothelial electrical resistance (TEER) using an EndOhm meter (World Precision Instruments, USA). TEER measurements, in which the resistance of a cellular monolayer to an electric current is quantitatively measured, is a commonly used approach to assessing barrier integrity. In this model, electrical resistance is proportional to the integrity of the barrier[241]. Using this technique, HPMECs have previously been reported to form tighter barriers than other cell types commonly used to model the pulmonary capillary endothelium, including HUVECs[242]. Typical resistances across HPMEC monolayers of approximately 25-40Ω/cm^2 have been reported [242,243]. Despite numerous modifications to the protocol, including alterations in the original number of cells seeded, the use of smaller pore sizes, coating of the inserts with different cell matrix components, and lengthening of the time the cells were cultured on the inserts, maximum resistances across HPMEC monolayers rarely peaked above 9Ω/cm^2 in the current study **(Section 8.1, Supplement 1)**. Significant TEERs of 75 Ω/cm^2 were eventually achieved using inserts with a smaller growth area, but peak resistances were not maintained and fell rapidly **(Section 8.2, Supplement 1)**. This would have made it difficult to determine whether any reductions in resistance observed were naturally-occurring or a result of the experimental conditions under investigation. The Electric Cell Substrate Impedance System (ECIS) - which facilitates real-time continuous monitoring of electrical resistance – was also trialled. However, again, using this system, resistances were found to be low and peaked only transiently (data not shown). On the basis of the results from both these systems, it was decided that resistance measurements would not be appropriate for studying the effects of HCA on the integrity of the endothelial barrier in this study.

Functionally, permeability can be assessed by measuring the movement of fluorescently-labelled macromolecules, such as FITC-dextran, across endothelial monolayers[244–246]. Unfortunately, compared to a control in which FITC-dextran was permitted to pass through a transwell insert unobstructed by endothelial cells (taken as 100% passage through the cell layer), 69.2 ± 17.1% of FITC-dextran still passed through unstimulated HPMEC monolayers in the current study **(Section 8.2, Supplement 2)**. This indicates that HPMEC monolayer integrity was also

insufficiently tight to permit the functional assessment of endothelial barrier integrity using this model.

With few alternatives remaining with which to *directly* study endothelial barrier integrity, it was concluded that the effects of HCA on the structural and functional integrity of the endothelial barrier could not be accurately determined in the current study. However, the formation of intercellular gaps in response to endothelial activation triggers cytoskeletal remodelling which may promote cell migration in an attempt to regain integrity of the endothelial barrier[247,248]. Cellular migration may contribute to wound repair and, as such, *in vitro* scratch assays are often considered a surrogate measure of barrier integrity. Using this assay, the results of the current study demonstrate impaired wound closure in HCA in a non-inflammatory, but not inflammatory, environment. In the presence of 50ng/ml cytomix, the cells may have been too injured to respond to HCA, resulting in no difference in the degree of wound repair in comparison to normocapnia. The impaired wound closure observed in response to HCA in the non-inflammatory environment, however, suggests that in a healthy or less injured lung, HCA may hinder endothelial repair and, although TEER measurements or a functional permeability assay would be required for confirmation, subsequently impact upon restoration of barrier integrity.

An *in vitro* scratch assay has previously been used to assess HUVEC wound repair in response to hypoxia and HCA[249]. This study demonstrated no effect of HCA on wound repair in the absence of an inflammatory stimulus. However, wound repair was attenuated in response to hypoxia. Notably, concomitant exposure to HCA improved the degree of wound closure by hypoxic HUVECs. These results contrast not only with those of the current study, but also to many studies which have consistently demonstrated that hypoxia (1%), in the absence of HCA, promotes wound repair[250–252]. The results should therefore be interpreted with caution. As previously discussed, HUVECs are not necessarily representative of the pulmonary capillary endothelium. While this may have accounted for the contrasting results in comparison to the current study, the findings highlight an important limitation of all *in vitro* work. That is, that no *in vitro* culture system can completely recapitulate the *in vivo*

environment. *In vivo*, endothelial cells do not exist in isolation, exposed only to an inflammatory and hypercapnic acidotic environment. Instead, they are surrounded by an extracellular matrix and lie in close apposition to the alveolar epithelium which may in itself influence their functions[253]. They are also subjected to a continuous blood flow and a hypoxic environment in which they are exposed to not only three, but multiple, cytokines and growth factors as well as reactive oxygen species, damage-associated molecular patterns, and pathogens to name a few[1].

Having identified that HCA attenuates the inflammatory response of HPMECs and impairs endothelial wound closure, further work was carried out to determine the mechanism responsible. Importantly, cell death was not altered in response to HCA, indicating that the reductions observed did not result from loss of cell viability and subsequently the presence of fewer cells to secrete chemokines and express adhesion molecules.

The transcriptional regulation of CXCL5, CXCL8 and ICAM-1 is mediated by the NFκB pathway[254–260]. As discussed in **Section 1.7.1**, HCA has consistently been associated with attenuated activation of this pathway as a result of reduced IκBα degradation. In the study by Takeshita *et al.*, this was confirmed as the mechanism responsible for the attenuated inflammatory response of HPAECs to HCA[158]. Interestingly however, while NFκB activation was markedly induced by cytomix stimulation in the current study, the degree of activation was not altered in HCA. This suggests that the altered inflammatory response observed in HCA was independent of alterations in NFκB activation in this case.

To date, although evidence in endothelial cells is lacking, only one alternative mechanism has been proposed as the mediator of HCA-driven effects *in vitro*; impaired mitochondrial function. Vohwinkel *et al.* demonstrated impaired proliferation of A549 cells and N12 human lung fibroblasts in the setting of hypercapnia[161]. This resulted from hypercapnia-induced expression of microRNA-183 (miR-183) which downregulated the expression of isocitrate dehydrogenase 2

(IDH2). IDH2 is an enzyme which catalyses the oxidative decarboxylation of isocitrate to α-ketoglutarate and is therefore important for progression through the tricarboxylic acid (TCA) cycle. Its attenuated expression induced mitochondrial dysfunction which was responsible for the attenuated proliferation observed in the study.

In the current study, mitochondrial membrane potential in HPMECs was attenuated in HCA, suggesting induction of mitochondrial dysfunction. This was associated with attenuated inflammatory responses, and with impaired wound closure. Wound closure, in particular, is a highly energy-demanding process, requiring constant rearrangement of the cytoskeleton[261]. Changes in mitochondrial function, particularly energy production, may therefore attenuate the migratory capacity of cells. It could therefore be hypothesised that mitochondrial dysfunction is at least partially responsible for the attenuated inflammatory response and impaired wound closure observed in this study. However, further studies are required to further elucidate whether this is the case, and to identify the molecular pathways responsible for HCA-induced mitochondrial dysfunction.

3.12 Summary and Conclusions

From this chapter it can be concluded that:

- HPMEC secretion of the potent neutrophil chemoattractants CXCL8 and CXCL5 is attenuated in HCA
- HPMEC surface expression of the adhesion molecule ICAM-1 is attenuated in HCA
- HPMEC wound closure is impaired in HCA
- While NFκB activation in HPMECs was not significantly altered in HCA, mitochondrial membrane potential was attenuated

Together these results suggest that, via attenuated HPMEC chemokine secretion and adhesion molecule expression, the pulmonary microvascular endothelium may contribute to HCA-induced attenuation of BALF neutrophilia which has previously been demonstrated in *in vivo*. However, impaired endothelial wound closure in HCA raises concerns with regards to the reparative capacity of the endothelium. While the results suggest that the attenuated inflammatory response of, and attenuated wound repair by, HPMECs may arise from HCA-induced mitochondria dysfunction, further studies are required to directly link the observations and to elucidate the molecular mechanisms responsible.

Chapter Four – Hypercapnic acidosis attenuates chemokine secretion and wound repair by primary human small airway epithelial cells

4.1 Overview of chapter

Alveolar epithelial cells are key cells in the pathophysiology of Acute Respiratory Distress Syndrome (ARDS). In this chapter, their response to hypercapnic acidosis (HCA) will be investigated. The rationale for this study will first be discussed in the context of the contributions of epithelial cells to the key hallmarks of ARDS and of the existent literature on their response to HCA. The aims and objectives of the study will be highlighted. The results will then be presented and their implications for the pathophysiology of ARDS subsequently discussed.

4.2 Introduction

The alveoli form the most distal portion of the lung and are best described as the small air sacs where gas exchange occurs. The lining of the alveolar wall is comprised primarily of two epithelial cell types – alveolar type I (ATI) and alveolar type II (ATII) cells – tethered to a basement membrane underneath. ATI cells line the majority (>90%) of the alveolar wall. Their thin, squamous morphology provides the ideal surface over which effective gas exchange can be facilitated by means of diffusion[262]. ATII cells are more abundant than ATI cells but, by comparison, line only a small area of the alveolar wall (5-10%). Although they exhibit their own highly-specialised functions, ATII cells are more cuboidal in nature, making them less effective in facilitating gas exchange[262].

ATII cells can be identified ultrastructurally by the presence of lamellar bodies[111]. These are small membrane-bound compartments where the lipid components of surfactant are stored[111,263]. Surfactant is a phospholipoprotein synthesised and stored in ATII cells. It is subsequently secreted into the alveolar space where it is responsible for reducing alveolar surface tension to prevent alveolar collapse. It may also exert a protective role against infection[111,263]. Surfactant dysfunction has been noted in ARDS. However, this appears not to be a key driving factor in the pathogenesis of the condition itself and instead arises from alterations in its composition and/or activity which occur secondary to inflammation and pulmonary oedema[264]. This therefore

suggests that surfactant function could be restored by first addressing the primary underlying mechanisms driving the pathogenesis of ARDS.

In addition to the secretion of surfactant, ATII cells also play a role in the regulated secretion of chemokines. In the absence of inflammation, low basal concentrations of chemokines are secreted by ATII cells[265]. However, upon epithelial activation by inflammatory cytokines such as those implicated in the pathogenesis of ARDS, chemokine secretion is markedly enhanced[260,265,266], making ATII cells a major cellular source of chemokines within the alveoli[265]. Activation of the NFκB pathway is classically involved in this response[201]. However, mitochondria may also contribute[267] by inducing activation of either the NFκB pathway or the NLRP3 inflammasome[202,268]. As previously discussed, neutrophils are key contributors to inflammation in the pathophysiology of ARDS[1]. ATII-derived chemokines promote neutrophil migration *in vitro*, suggesting that ATII cells may indirectly contribute to inflammation in ARDS by promoting alveolar neutrophil recruitment[265].

Aside from the secretory functions of ATII cells, the alveolar epithelium, much like the capillary endothelium, forms a functional barrier which regulates access of fluid and macromolecules to the alveoli. In contrast to the endothelium, the tight junction proteins occludin and claudin form the basis of the inter-epithelial junctions maintaining the integrity of the alveolar epithelial barrier[269]. In ARDS, the epithelial barrier breaks down, resulting in increased permeability and the accumulation of alveolar oedema fluid[270]. However, the contribution of intercellular junctions to this increase in permeability and subsequent oedema formation is likely to be overridden by the cell death and denudation of the alveolar basement membrane experienced in the condition[14,271]. Mitochondria play a well-recognised role in mediating death of alveolar epithelial cells by apoptosis[272,273].

In the healthy lung, excess alveolar fluid is cleared in a process termed alveolar fluid clearance (AFC). While some evidence supports a role for ATI cells in this process, their involvement is not well recognised or characterised, and AFC is typically

considered a function of ATII cells[274,275]. AFC is the process by which excess alveolar fluid is driven across the epithelium and into the interstitium where it is removed by the lymphatic system[276]. It is driven by two epithelial sodium transporters located in the membrane of ATII cells; the apically expressed epithelial sodium channel (ENaC) which facilitates the uptake of sodium from the alveolar space, and the basolaterally expressed Na,K-ATPase which transports sodium out of the epithelial cells and into the interstitium in exchange for potassium. This sodium flux across the epithelium creates an osmotic gradient which ultimately drives the removal of fluid from the alveoli[270,277]. AFC is often impaired in ARDS as a result of cell death and attenuated expression and activity of the sodium transporters, the remaining functional capacity of which is likely to be overwhelmed by excessive fluid influx[20,277]. As a result, excess fluid accumulates in the alveoli at a faster rate than it can be removed. In sepsis this is associated with impaired mitochondrial function[278,279].

The resolution of alveolar oedema in ARDS therefore requires restoration of epithelial barrier integrity to limit further alveolar fluid accumulation, and recovery of effective AFC to remove remaining excess alveolar fluid. In this context, recovery of barrier integrity requires two events: (1) re-epithelialisation of the denuded basement membrane in a process involving cell migration, and expansion and differentiation of ATII cells to ATI cells, and (2) reformation of intercellular junctions between neighbouring cells of the alveolar epithelium[21,23]. Only after structural recovery of the alveolar epithelial barrier can complete alveolar function be restored.

In comparison to the response of the capillary endothelium to hypercapnia/hypercapnic acidosis (HCA), the response of the alveolar epithelium is somewhat better understood. Hypercapnia, in a non-inflammatory environment, impairs A549 wound closure in a pH-independent manner by attenuating cell migration via reduced NFκB activity[160]. Although no functional assay has definitively linked the two observations, this may also involve altered matrix metalloproteinase (MMP) / tissue inhibitor of matrix metalloproteinase (TIMP) balance[160]. While the contribution of potential alterations in proliferation to the attenuated cell migration was not addressed, an independent study has reported that hypercapnia impairs

proliferation of A549 cells, again in a manner independent of acidosis[161]. This resulted from hypercapnic induction of the microRNA miR-183 which downregulated the isocitrate dehydrogenase 2 (IDH2) enzyme of the tricarboxylic acid (TCA) cycle, subsequently inducing mitochondrial dysfunction. These results raise concerns regarding the reparative potential, particularly re-epithelialisation, of the alveolar epithelium in the setting of hypercapnia/hypercapnic acidosis.

As discussed, following alveolar re-epithelisation, the successful formation of stable intercellular junctions is critical for complete recovery of the alveolar epithelial barrier. The effects of HCA on the expression of the adherens and tight junction proteins, and on their ability to form effective intercellular junctions, has never been directly characterised. However, hypercapnia impairs cell-cell adhesion in A549 cells as a result of CO_2-induced proteasomal degradation of the Na,K-ATPase β1 subunit[280]. This may result from destabilisation of the epithelial adherens junctions as the β1 subunit is required for the stable association of Na,K-ATPase with β-catenin, a key protein of the adherens junction complex[281]. To date, however, there remains no suggestions as to the effects of HCA on epithelial tight junction formation. Although impaired migration and/or proliferation may prevent cells coming into close enough contact with each other to form intercellular junctions in the first place, these findings raise concerns for the recovery of epithelial barrier function.

The effects of HCA on AFC have been particularly well studied. Hypercapnia impairs AFC in isolated rat lungs *ex vivo* independently of acidosis[164,282,283]. *In vitro* work has demonstrated that this occurs downstream of AMP-activated protein kinase (AMPK) activation which is induced by Ca^{2+}/calmodulin-dependent protein kinase kinase-β (CaMKKβ) or extracellular signal-regulated kinase (ERK)[282,284]. Activated AMPK activates protein kinase C (PKC)-ζ, ultimately resulting in endocytosis of Na,K-ATPase from the basolateral membrane of alveolar epithelial cells[282]. To date, two pathways have been identified through which this may occur. Firstly, PKC-ζ may induce phosphorylation of the α_1 subunit of Na,K-ATPase, promoting its endocytosis[164]. Alternatively, PKC may activate c-June N-terminal kinase (JNK). JNK phosphorylates LIM domain only 7b (LMO7b), promoting its interaction with

both Na,K-ATPase and proteins of the endocytic pathway. In this way it promotes endocytosis of Na,K-ATPase without phosphorylating the ion channel itself[285]. Although less extensively explored, more recent data suggest that ERK activation in the setting of hypercapnia may also promote ubiquitination of βENaC, reducing its cell surface expression[286]. Taken together, these data raise concerns regarding the potential for resolution of alveolar oedema in the hypercapnic setting.

Despite the concerning effects of hypercapnia on the reparative potential of the alveolar epithelium and on alveolar fluid clearance, not all epithelial responses to HCA may be detrimental: CXCL8 secretion by A549s is attenuated in HCA[159,287]. While this suggests that HCA may have the potential to attenuate neutrophil chemoattraction to the alveoli during ARDS, CXCL8 is only one chemokine involved in the pathogenesis of the condition. It is unknown whether this effect extends beyond CXCL8 to other chemokines.

The major limitations of the *in vitro* work assessing the response of the alveolar epithelium to HCA lie in the choice of cell type used. Ideally, such work should be performed on primary human alveolar epithelial cells, specifically a co-culture of ATI and ATII cells in which ATII predominate. However, no reliable and reproducible method for the isolation of pure ATI cultures has yet been reported. While it is possible to isolate highly pure yields of ATII cells, their use for experimental research is hampered by a number of factors including infrequent availability of suitable human donor lung tissue, as well as the difficult and time-consuming isolation process. In addition, difficult culture of isolated cells poses a further problem; due to spontaneous differentiation to an ATI-like phenotype over 1-2 weeks, these cells have to be used quickly and only for short-term culture[266,288–290].

Cell lines are often used to overcome the limitations of primary cells as they are more readily available and generally easier to culture. A549s are a cell line originating from a lung adenocarcinoma. They were first isolated in 1973 and have since become one of the most widely used models of the alveolar epithelium[291]. Indeed, the majority of

the *in vitro* studies discussed above were performed using this cell type. However, while generally considered representative of ATII cells, concerns have arisen regarding the consistency of the A549 phenotype with that of primary ATII cells. Discrepancy exists among studies as to whether or not A549s maintain an ATII phenotype in culture – some suggest that they express high levels of the ATII marker, surfactant protein C (SPC), while other have been unable to detect its presence[266,289,292]. Additionally, unlike ATII cells, it appears that A549s lack the capacity to differentiate into ATI-like cells; regardless of the expression level of SPC, A549s either do not or only weakly express caveolins (ATI marker)[289,292,293]. A549s also do not form electrically tight monolayers and subsequently exhibit much lower transepithelial electrical resistance (TEER) measurements than primary ATII cells, rendering them unsuitable for the assessment of permeability[294,295]. Results obtained using this cell type should therefore be interpreted with caution and ideally confirmed in primary cells.

Small airway epithelial cells (SAECs) isolated from the 1mm bronchiole area of the human distal lung epithelium have been used as an alternative to A549 cells. Although not pure cultures of ATI or ATII cells, these offer a number of benefits over the use of A549 cells where primary alveolar epithelial cells are unavailable; they are untransformed primary cells which, importantly, like A549s, are readily available. They are also considered to be representative of the alveolar epithelium in that they express markers typically expressed by alveolar epithelial cells, including aquaporins and surfactant proteins[296–298]. Although rarely used to study barrier function and permeability *in vitro*, SAECs express intercellular junction proteins including zonula occludins-1 (ZO-1), and appear to be a better model of the epithelial barrier than A549s, exhibiting reasonable TEERs of approximately $600\Omega/cm^2$ [299]. This, however, is not to say that SAECs are without their limitations; as primary cells, they have a limited lifespan and are difficult to transfect[298]. In addition, the cells are derived from multiple donors, leaving experimental results subject to significant variation. However, it can be argued that such variation is not a limitation of the use of primary cells, but rather a major advantage as it provides the opportunity to obtain results more representative of the natural variation which exists between individuals.

4.3 Aims and Objectives

The overall objective of this chapter is to study the response of the small airway epithelium to hypercapnic acidosis in the setting of inflammation. This will be achieved using primary human small airway epithelial cells (SAECs) in an *in vitro* model of ARDS in which the inflammatory environment is modelled by a cytomix of proinflammatory cytokines implicated in the pathogenesis of the condition. The specific aims of this study are:

- To determine the effects of HCA on the inflammatory response of SAECs to cytomix stimulation
- To determine the effects of HCA on the reparative potential of SAECs in an inflammatory environment
- To investigate the mechanism(s) responsible for any observed effects
- To confirm important findings in primary human alveolar type II (ATII) epithelial cells

4.4 SAECs contain a population of alveolar epithelial cells

To confirm that commercially available SAEC preparations contain alveolar epithelial cells, unstimulated SAECs were cultured in 5% CO_2. Cells were then fixed and stained for the ATI marker aquaporin-5 (AQP-5) and the ATII marker pro-surfactant protein C (pro-SPC). Unstained cells were identified by nuclear staining with Hoechst. The percentage of cells stained positively for each marker was quantified. Alveolar epithelial cells comprised almost 45% of the total cells: 22.0 ± 2.8% stained positively for the ATI marker AQP-5, while 25.0 ± 1.4% stained positively for the ATII marker pro-SPC **(Figure 4.1)**. These data confirm that SAECs are a suitable model of the primary human alveolar epithelium.

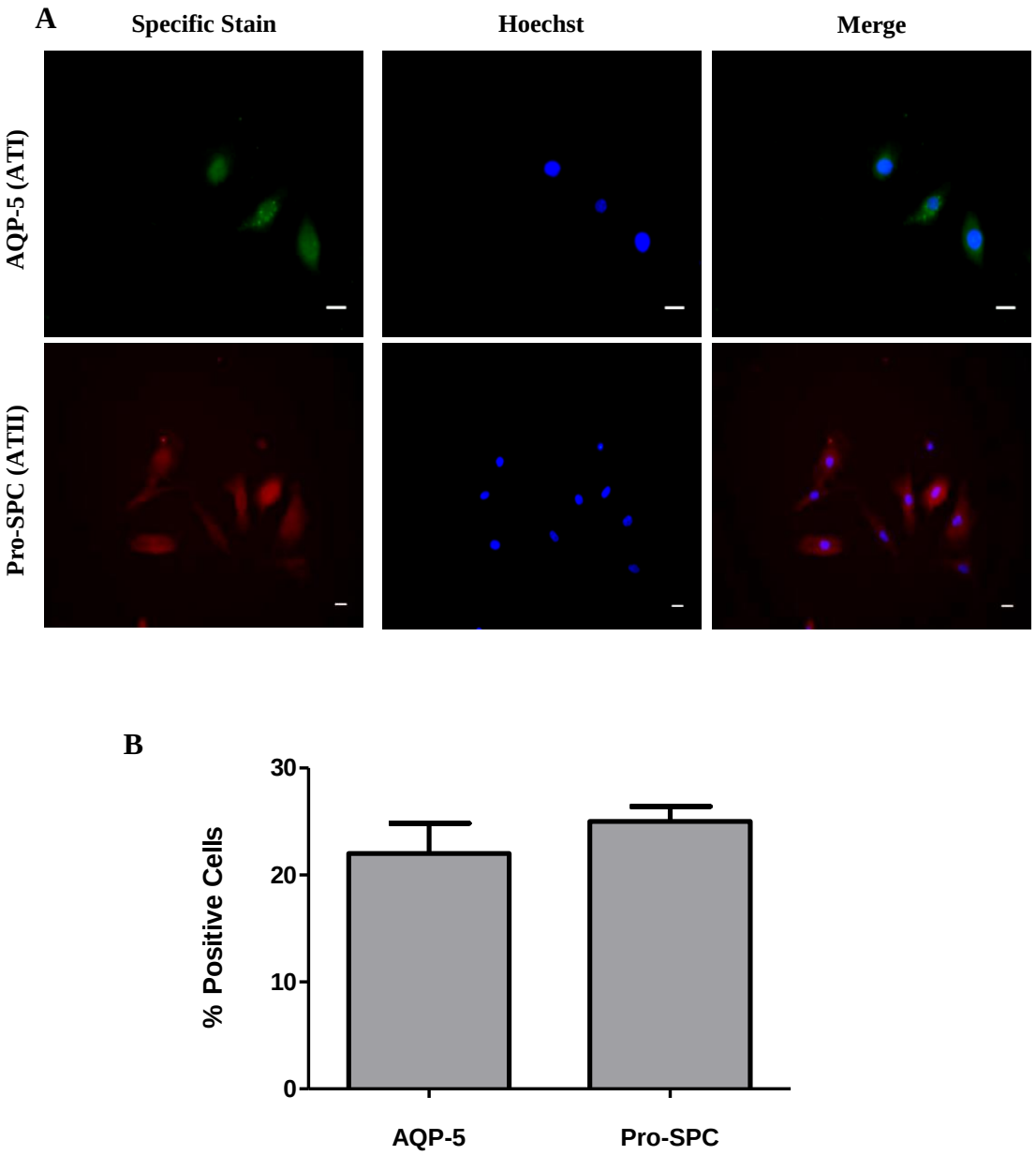

Figure 4.1: SAECs contain a population of alveolar epithelial cells

Unstimulated SAECs were cultured in 5% CO_2 prior to fixation. Cells were stained for aquaporin (AQP-5) and pro-surfactant protein C (pro-SPC). All cells were identified by nuclear staining with Hoechst. Images demonstrating positive staining for each marker are presented (A). Each image represents a small area of a larger field taken at x20 magnification. Scale bar = 50 microns. The percentage of total cells positive for each marker was quantified (B). Error bars represent standard deviation. (n=2 for both markers; no statistical analysis performed).

4.5 HCA attenuates secretion of the neutrophil chemoattractants CXCL8 and CXCL5 by SAECs

SAECs were stimulated with 50ng/ml cytomix and cultured in 5% or 15% CO_2 for 24 hours. To determine the effect of HCA on SAEC chemokine secretion, supernatants were collected and the concentrations of the potent neutrophil chemoattractants CXCL8 and CXCL5 were measured by ELISA.

Cytomix induced a 50-fold increase in CXCL8 secretion by SAECs in normocapnia (1.1 ± 0.4ng/ml in unstimulated SAECs to 53.2 ± 19.4ng/ml in cytomix-stimulated SAECs) **(Figure 4.2A)**. Secretion by cytomix-stimulated cells was significantly reduced in HCA to 29.5 ± 6.9ng/ml **(Figure 4.2A)**. CXCL5 secretion by SAECs was also increased by cytomix in normocapnia (0.3 ± 0.1ng/ml in unstimulated SAECs vs. 15.1 ± 8.7ng/ml in cytomix-stimulated SAECs), and was again significantly attenuated (to 5.3 ± 1.9ng/ml) in cytomix-stimulated cells in HCA **(Figure 4.2B)**.

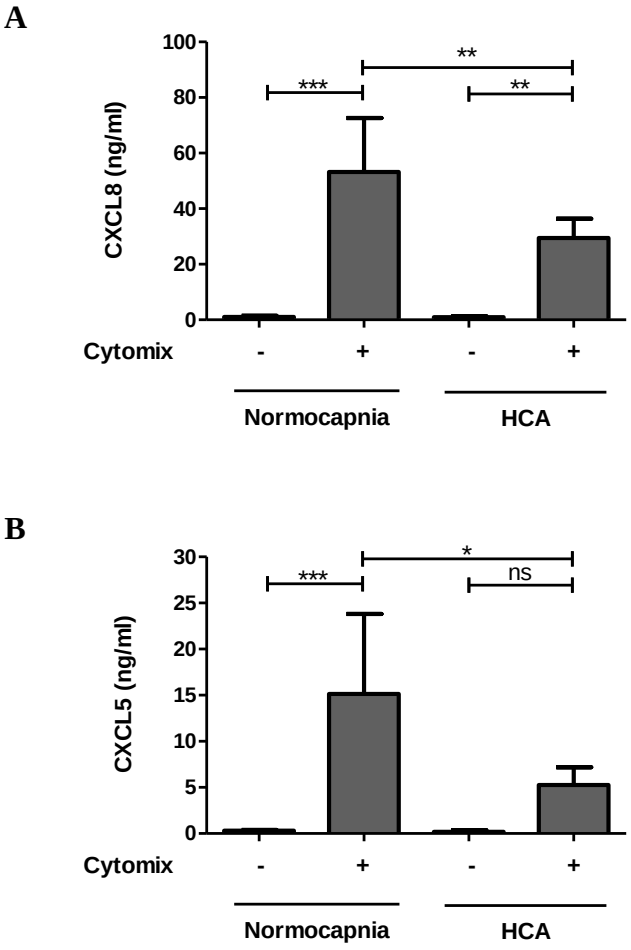

Figure 4.2: HCA attenuates secretion of the neutrophil chemoattractants CXCL8 and CXCL5 by HCA

Unstimulated or cytomix-stimulated SAECs were cultured in 5% or 15% CO_2 for 24 hours. CXCL8 (A) and CXCL5 (B) concentrations in cell culture supernatants were quantified by ELISA. Error bars represent standard deviation (SD). (n=5 for both analytes; one-way ANOVA with Bonferroni posthoc analysis; ns = $p>0.05$; * = $p<0.05$; ** = $p<0.01$; *** = $p<0.001$).

4.6 HCA attenuates SAEC wound closure

Using an *in vitro* scratch assay, SAEC monolayers were wounded and cultured in 5% or 15% CO_2 in the presence or absence of 50ng/ml cytomix for 24 hours. Percentage wound closure over the 24-hour period was measured to determine the reparative capacity of the epithelium in response to HCA. Results demonstrate that in a non-inflammatory environment, SAEC wound closure is impaired by HCA (59.4 ± 19.3% in normocapnia vs. 41.6 ± 15.8% in HCA) **(Figures 4.3A and 4.3C)**. In the inflammatory environment of cytomix, while a trend suggestive of attenuated wound repair was observed in HCA (38.2 ± 14.3% in normocapnia vs. 25.5 ± 15.2% in HCA), this did not reach statistical significance **(Figures 4.3 B and 4.3C)**.

A

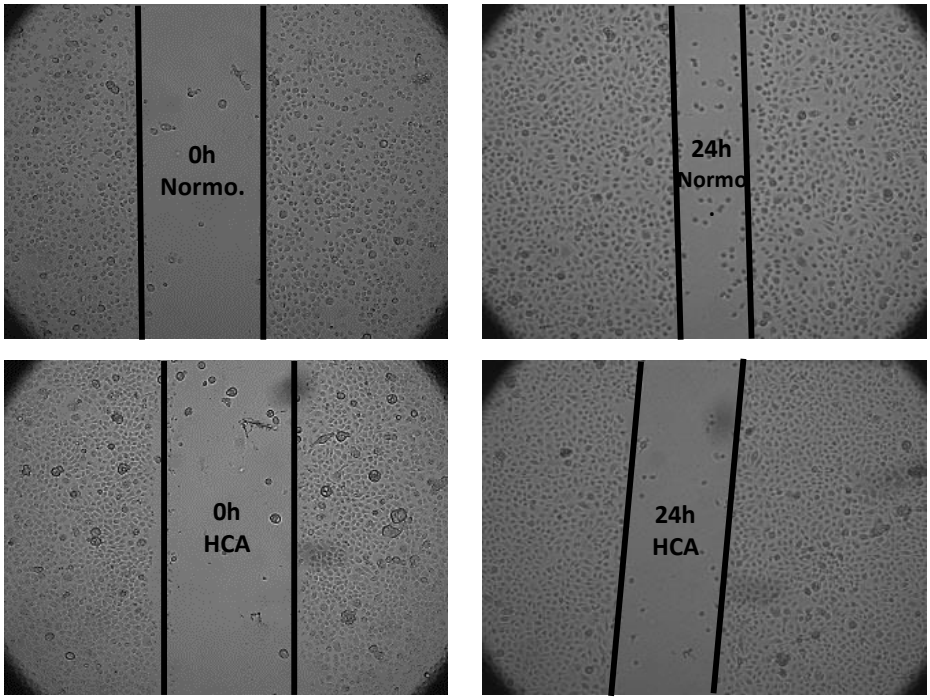

Figure 4.3: HCA attenuates SAEC wound closure (continued overleaf)

SAEC monolayers were wounded in an *in vitro* scratch assay and cultured in 5% or 15% CO_2 for 24 hours in the presence or absence of cytomix. Representative images illustrating approximate wound areas at 0 hours and 24 hours are presented for the non-inflammatory environment (vehicle) (A) (Normo = normocapnia).

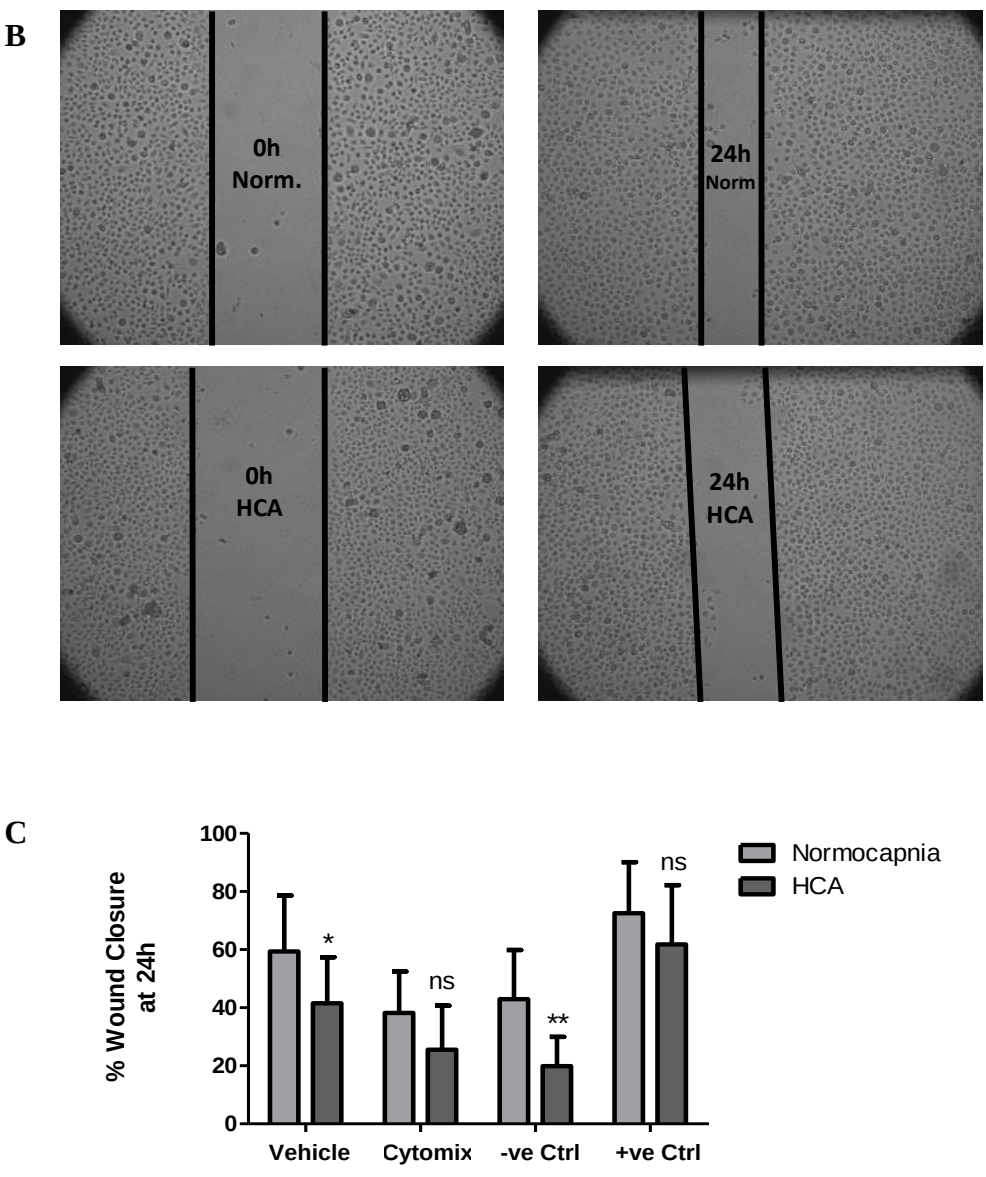

Figure 4.3 (continued): HCA attenuates SAEC wound closure

SAEC monolayers were wounded in an *in vitro* scratch assay and cultured in 5% or 15% CO_2 for 24 hours in the presence or absence of cytomix. Representative images illustrating approximate wound areas at 0 hours and 24 hours are presented for the inflammatory environment (cytomix) (B) (Norm = normocapnia). Percentage wound closure over 24 hours was quantified for each condition, including negative (-ve Ctrl) and positive (+ve Ctrl) controls (C). Error bars represent standard deviation (SD). (n=5 for all conditions; two-way ANOVA with Bonferroni posthoc analysis; ns = $p>0.05$; * = $p<0.05$; ** = $p<0.01$).

4.7 HCA does not alter SAEC viability

To assess the mechanism behind attenuated chemokine secretion and impaired epithelial wound closure, SAEC viability was assessed by lactate dehydrogenase (LDH) release into cell culture supernatants at regular intervals over 72 hours in 5% or 15% CO_2 in the presence or absence of cytomix. A positive control was included in which cells were lysed with 2% Triton-X. Results are presented as percentage relative to the positive control.

Results demonstrate no significant cytomix-induced cell death in either normocapnia or HCA across any of the time points studied **(Figure 4.4)**. Additionally, when the degree of cell viability was compared between cytomix-stimulated SAECs cultured in 5% CO_2 and cytomix-stimulated SAECs cultured in 15% CO_2, no statistically significant differences were observed at 24 hours (38.4 ± 9.4% in normocapnia vs. 30.8 ± 10.8% in HCA) **(Figure 4.4A)**, 48 hours (35.5 ± 7.5% in normocapnia vs. 25.6 ± 8.7% in HCA) **(Figure 4.4B)**, or 72 hours (53.4 ± 8.7% in normocapnia vs. 43.6 ± 9.6% in HCA) **(Figure 4.4C)**. Similarly, no statistically significant differences were observed between unstimulated SAECs cultured in 5% or 15% CO_2 for 24 hours (32.6 ± 9.3% in normocapnia vs. 25.0 ± 8.6% in HCA) **(Figure 4.4A)**, 48 hours (36.5 ± 13.8% in normocapnia vs. 18.6 ± 3.9% in HCA) **(Figure 4.4B)**, or 72 hours (45.9 ± 12.1% in normocapnia vs. 40.0 ± 6.7% in HCA) **(Figure 4.4C)**.

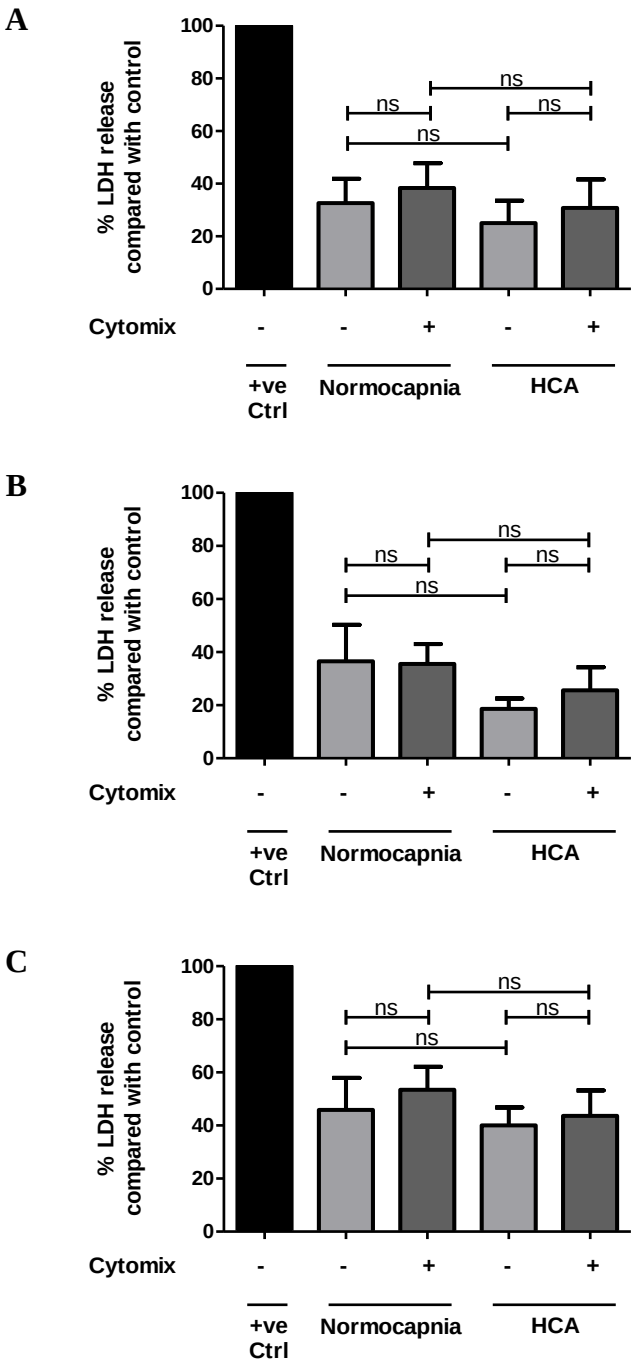

Figure 4.4: HCA does not alter SAEC viability

Unstimulated or cytomix-stimulated HPMECs were cultured in 5% or 15% CO_2 for up to 72 hours. Cell viability was assessed by LDH release at 24 hours (A), 48 hours (B), and 72 hours (C). Results are presented as percentage relative to the positive control (+ve Ctrl). Error bars represent standard deviation (SD). (n=5 for all conditions; Kruskal-Wallis with Dunn's posthoc analysis; ns = $p>0.05$).

4.8 NFκB activation in SAECs is not altered in response to HCA

To further investigate the mechanism responsible for attenuated chemokine secretion and epithelial wound closure in HCA, SAECs, stimulated or not with 50ng/ml cytomix, were cultured in 5% or 15% CO_2 for 0, 30, or 60 minutes. Nuclear extracts were analysed for NFκB activity using a p65 TransAM assay. This assay is a DNA-binding ELISA which detects active NFκB p65 subunits in nuclear extracts via their binding to consensus oligonucleotides immobilised on a 96 well plate.

Results demonstrate marked induction of NFκB activation by cytomix at both 30 minutes and 60 minutes post-stimulation **(Figure 4.5)**. The degree of activation in cytomix-stimulated SAECs did not differ between normocapnia and HCA at either 30 minutes (optical density (OD) 1.3 ± 0.3 in normocapnia vs. 1.1 ± 0.2 in HCA) or 60 minutes (OD 1.3 ± 0.2 in both normocapnia and HCA) post-stimulation **(Figure 4.5)**.

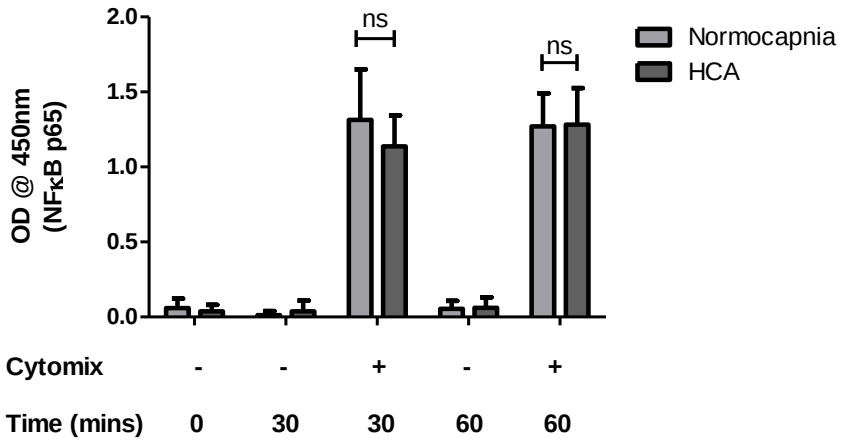

Figure 4.5: NFκB activation in SAECs is not altered in response to HCA

The degree of NFκB activation in nuclear extracts from SAECs cultured in the presence or absence of cytomix in 5% or 15% CO_2 for 0, 30, or 60 minutes, was assessed by TransAM assay. Results are presented as optical density (OD) at 450nm. Error bars represent standard deviation (SD). (n=5 for all timepoints, except 0 minutes in normocapnia which is n=6; two-way ANOVA with Bonferroni posthoc analysis; ns = $p>0.05$).

4.9 SAEC mitochondrial membrane potential is attenuated in HCA

To explore the effect of HCA on mitochondrial function as a potential mechanism behind the attenuated inflammatory and reparative responses to HCA, mitochondrial membrane potential was assessed. SAECs, in the presence or absence of cytomix, were cultured for 24 hours in 5% or 15% CO_2. Cells were subsequently stained with the mitochondrial membrane potential indicator, JC-1. When mitochondrial membrane potential is low, JC-1 accumulates within mitochondria at low concentrations and persists in a green fluorescent monomeric state. When mitochondrial membrane potential is increased, JC-1 accumulation increases and begins to form red fluorescent aggregates. Fluorescence microscopy was used to assess the degree of JC-1 aggregation. A control was included in which SAECs were treated with the mitochondrial oxidative phosphorylation uncoupler, FCCP, at the time of JC-1 staining to induce mitochondrial depolarisation. Results are presented as the ratio of red (JC-1 aggregates) / green (JC-1 monomers), normalised to unstimulated SAECs in normocapnia.

Significant induction of mitochondrial depolarisation by FCCP was observed in comparison to unstimulated SAECs in normocapnia (normalised red/green ratio 0.6 ± 0.2 vs. 1.0 ± 0.0, respectively). Mitochondrial membrane potential was not significantly altered by cytomix stimulation in either normocapnia or HCA **(Figure 4.6)**. However, when compared to normocapnia, significant attenuation of mitochondrial membrane potential in HCA was observed in both unstimulated (1.0 ± 0.0 in normocapnia vs. 0.7 ± 0.1 in HCA) and cytomix-stimulated (1.2 ± 0.1 in normocapnia vs. 0.7 ± 0.1 in HCA) SAECs **(Figure 4.6)**.

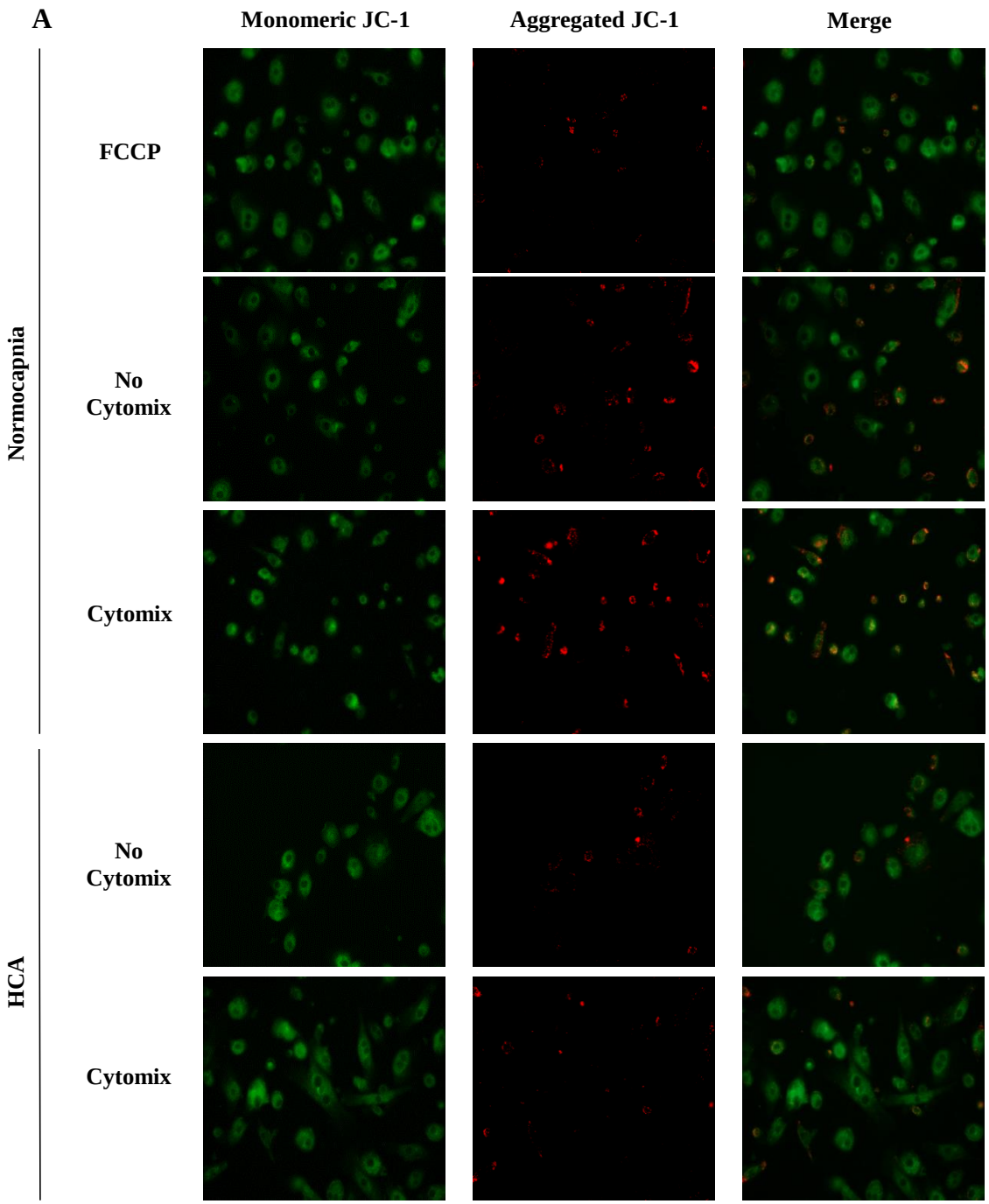

Figure 4.6: SAEC mitochondrial membrane potential is attenuated in HCA (continued overleaf)

SAECs cultured in 5% or 15% CO_2 for 24 hours in the presence or absence of cytomix were stained with JC-1 mitochondrial membrane potential indicator. FCCP was included as a control to induce mitochondrial depolarisation. Representative images are presented (A).

B

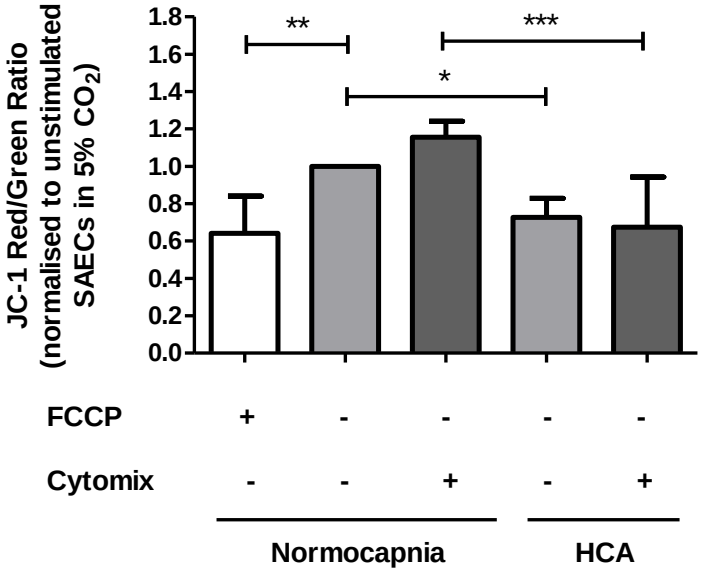

Figure 4.6 (continued): SAEC mitochondrial membrane potential is attenuated in HCA

SAECs cultured in 5% or 15% CO_2 for 24 hours in the presence or absence of cytomix were stained with JC-1 mitochondrial membrane potential indicator. FCCP was included as a control to induce mitochondrial depolarisation. The JC-1 red (aggregate) / green (monomer) ratio was measured and presented relative to unstimulated cells in normocapnia (B). Error bars represent standard deviation (SD). (n=4 for all conditions; one-way ANOVA with Bonferroni posthoc analysis; * = $p<0.05$; ** = $p<0.01$; *** = $p<0.001$).

4.10 HCA may attenuate wound closure by primary ATII-like cells

Alveolar epithelial cells were isolated from donor human lungs. 4 days post-seeding (the time at which a 24 hour timepoint would be taken), cell monolayers were fixed and stained for the presence of the ATII marker, pro-surfactant protein C (pro-SPC). Almost all cells stained positively for pro-SPC (99.6 ± 0.7%) **(Figure 4.7A)**.

Additionally, to confirm if the attenuated SAEC wound closure observed in HCA also applies to primary alveolar epithelial cells, isolated cell monolayers were wounded using an *in vitro* scratch assay at 3 days post-seeding. Wounded cells were cultured in 5% or 15% CO_2, in the absence of cytomix, for 24 hours. Percentage wound closure over the 24 hour period was measured. Results demonstrate a trend suggestive of attenuated wound repair in HCA (33.2% in normocapnia vs. 23.5% in HCA) **(Figures 4.7B and 4.7C)**.

A

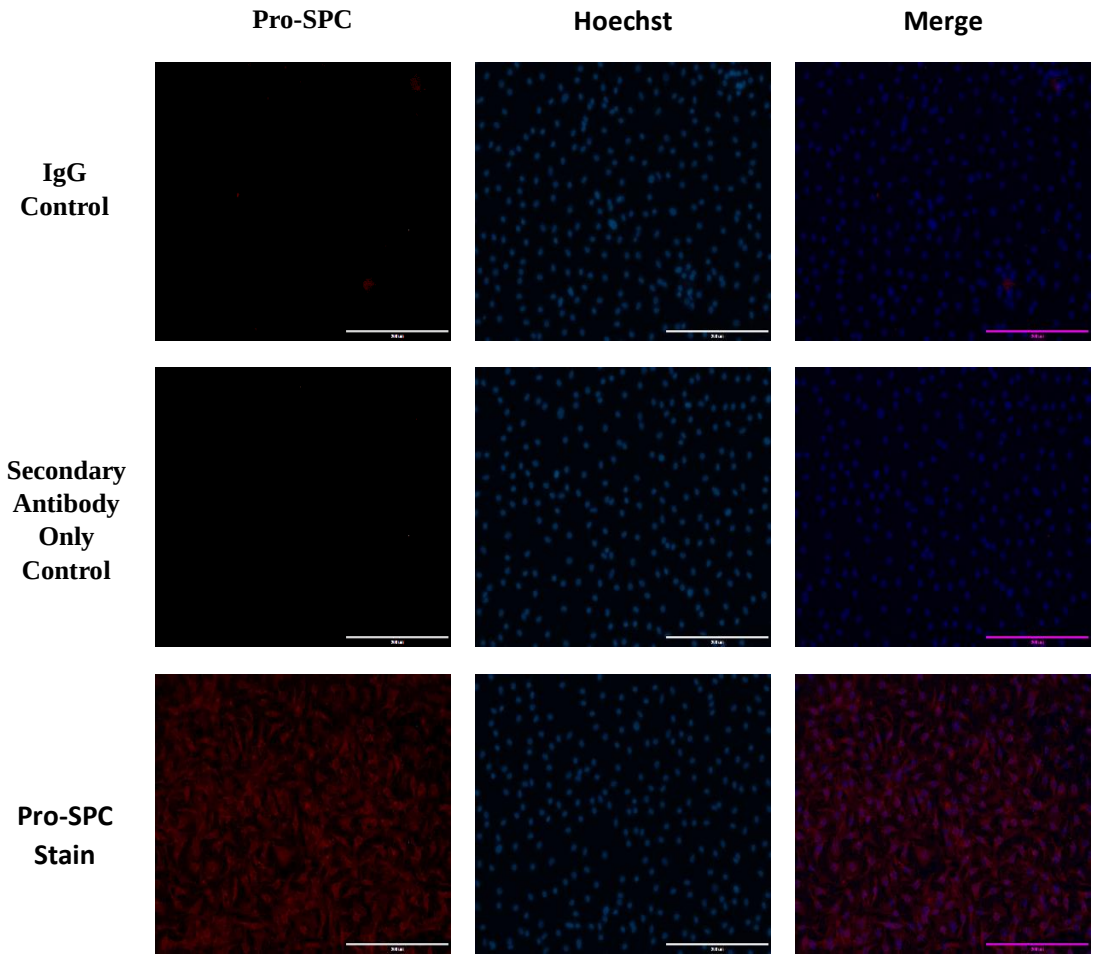

Figure 4.7: HCA may attenuate wound closure by primary ATII-like cells (continued overleaf)

ATII cells were isolated from donor human lungs. Isolated cells were fixed and stained for pro-surfactant protein C (pro-SPC) after 4 days in culture. Nuclei were identified by Hoechst staining (A). (n=1; no statistical analysis performed).

B

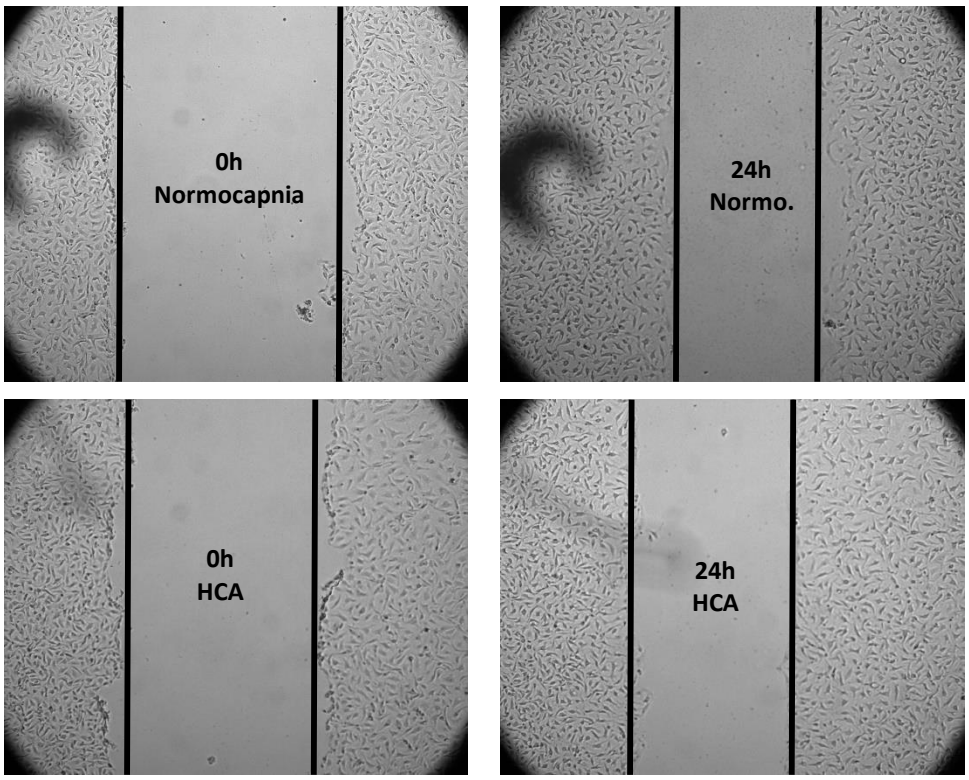

C

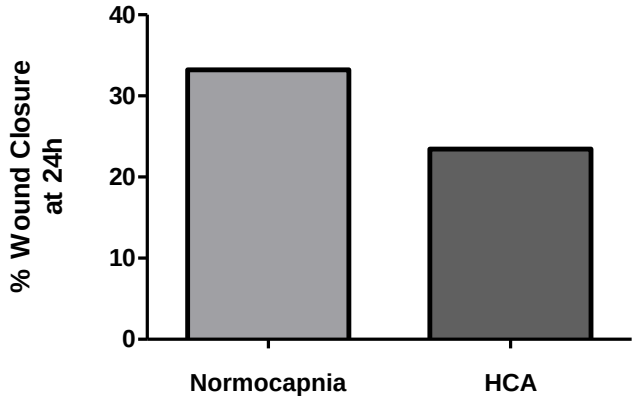

Figure 4.7 (continued): HCA may attenuate wound closure by primary ATII-like cells

ATII cells were isolated from donor human lungs. Monolayers of isolated cells were wounded in an *in vitro* scratch assay and cultured in 5% or 15% CO_2 for 24 hours without any inflammatory stimulus. Representative images illustrating approximate wound areas at 0 hours and 24 hours are presented (B) (Normo = normocapnia). Percentage wound closure over 24 hours was quantified (C). (n=1; no statistical analysis performed).

4.11 Discussion

To date, *in vitro* studies assessing the response of the alveolar epithelium to HCA have been limited to the use of cell lines or primary cells isolated from rat lungs, as a result of difficulties in the isolation and subsequent culture of human alveolar epithelial cells (discussed in **Section 4.2**). Notably, the A549 cell line, which has been most commonly, does not permit assessment of epithelial barrier integrity and therefore hampers accurate investigations into epithelial repair. The aim of the work in this chapter was therefore to determine the effects of HCA on chemokine secretion and the tissue reparative responses of the human distal lung epithelium. To achieve this, an *in vitro* model of ARDS in which primary human small airway epithelial cells (SAECs) were stimulated with a cytomix of proinflammatory cytokines (IL1β, IFNγ and TNFα) implicated in the pathogenesis of ARDS, was used. While SAECs are not pure cultures of alveolar epithelial cells themselves, as discussed in **Section 4.2**, they exhibit many characteristics of the alveolar epithelium and, importantly, are thought to facilitate better assessment of epithelial barrier integrity. Importantly, characterisation of the cellular composition of SAECs in the current study demonstrated the presence of both ATI and ATII cells, constituting over 40% of total SAECs.

Alterations in SAEC chemokine secretion in response to HCA were first assessed. As discussed previously, neutrophils are key mediators of inflammation and damage in ARDS, and their recruitment into the alveoli is driven in part by the presence of chemotactic stimuli[1]. Previous work has demonstrated that A549 secretion of the potent neutrophil chemoattractant, CXCL8, which is increased in the bronchoalveolar lavage fluid (BALF) of patients with ARDS, is attenuated in HCA[159,236–238,287]. However, until now, it had not been demonstrated whether this response extends beyond CXCL8 to other chemokines. CXCL5 is a potent neutrophil chemoattractant primarily secreted in the lung by ATII cells[260,300]. Like CXCL8, this chemokine drives neutrophil recruitment into the alveoli in inflammatory settings and is known to be present in higher quantities in the BALF of patients with ARDS[238,260]. The results of the present study demonstrate attenuated secretion of both CXCL5 and CXCL8 by SAECs following cytomix stimulation in HCA for 24 hours. This demonstrates, for

the first time, that the effects of HCA on primary epithelial chemokine secretion in the setting of inflammation extend beyond CXCL8 to other chemokines, specifically CXCL5. These data suggest that in the setting of HCA, the distal lung epithelium may be a key contributor to the attenuated BALF neutrophilia observed in HCA in many *in vivo* models of acute lung injury[129,132,234,235].

As discussed in **Section 4.2**, the alveolar epithelial basement membrane is denuded in ARDS by epithelial cell death, resulting in impaired barrier function and subsequently less-restricted access of neutrophils and oedema fluid to the alveoli[1]. Therefore, for the successful recovery of epithelial barrier function, remaining cells must migrate towards each other and proliferate to fill the gaps and re-epithelialise the basement membrane. Following alveolar re-epithelialisation, effective intercellular junctions must form to facilitate functional recovery of the epithelial barrier. To address the effects of HCA on the reparative capacity of the epithelium, an *in vitro* scratch assay was used to assess its effects on the initial aspect of this process -the ability of epithelial cells to migrate and/or proliferate in an attempt to structurally repair the epithelium. O'Toole *et al.* had already reported the effects of HCA on SAEC and A549 wound repair, but in a non-inflammatory setting only. Their work in A549 cells demonstrated that HCA impaired wound closure in a manner involving impaired migration as a result of attenuated NFκB activation and possibly altered MMP/TIMP balance[160]. However, while HCA also impaired wound closure in primary cells, the contributions of migration, NFκB activation, and MMP/TIMP balance were not confirmed in SAECs. Additionally, Vohwinkel *et al.* have demonstrated impaired proliferation of A549 cells in HCA[161]. The current study not only confirmed that SAEC wound closure is impaired in a non-inflammatory environment, but extended this result, demonstrating that, by comparison, the degree of wound closure is not altered in the inflammatory setting of cytomix. The difference in SAEC response to HCA in a non-inflammatory vs. inflammatory environment could be explained by the degree of epithelial damage. A trend towards attenuated wound closure in HCA exists in the inflammatory environment, raising the possibility that more injured cells take longer to respond in terms of their migratory and/or proliferative response to HCA. Unfortunately, this hypothesis could not be investigated in the present study as it would require lengthening the duration of the experiment, and this was not possible as

a result of complete wound closure by 48 hours post-stimulation. However, while these results further add to concerns regarding the effects of HCA on the reparative capacity of the epithelium, the lack of response of inflamed SAECs to HCA may at least offer some reassurance that in the most injured epithelium, HCA may not further worsen epithelial repair.

Permeability of SAEC monolayers to FITC-dextran was deemed the most appropriate *in vitro* model to study the functional response of epithelial barrier integrity to HCA **(Section 8.3, Supplement 3)**. SAEC monolayers sufficiently impermeable to FITC-dextran were obtained. However, despite numerous reports in which TNFα enhanced epithelial permeability to FITC-dextran, including by approximately 25% in alveolar epithelial cells[301,302], 50ng/ml TNFα was unable to induce significant permeability in the current study (compared to a positive control in which FITC-dextran was allowed to pass through a transwell insert unobstructed by SAECs, 33.0 ± 4.7% FITC-dextran passed through unstimulated SAECs vs. 41.1 ± 2.0% through TNFα-stimulated SAECs in normocapnia) **(Section 8.3, Supplement 3)**. Given that SAECs did not respond to either TNFα or HCA, it is difficult to determine whether the results obtained represent the true cellular response to HCA, or whether the SAECs had become unable to respond to their local environment. This model was therefore unable to reliably determine the effects of HCA on epithelial barrier function.

Having identified that HCA attenuates SAEC secretion of potent neutrophil chemoattractants in the setting of inflammation and impairs epithelial wound closure in a non-inflammatory setting, further work was performed to investigate the mechanism responsible. Importantly, cell viability was not altered in response to HCA in either an inflammatory or non-inflammatory environment, indicating that the attenuated CXCL5 and CXCL8 secretions did not occur secondary to reduced cell numbers as a result of increased cell death.

The transcriptional regulation of both CXCL5 and CXCL8 is mediated by the NFκB pathway[254,258,259,303]. Attenuated activation of this pathway in HCA has previously

been associated with attenuated CXCL8 secretion by A549 cells[159,287]. In addition, O'Toole *et al.* demonstrated that NFκB activation was required for optimal wound closure in A549s in normocapnia[160]. Interestingly, while NFκB activation was markedly enhanced upon cytomix stimulation in the present study, the degree of activation did not differ between normocapnia and HCA. This suggests that the effects of HCA observed in this study are not dependent on alterations in NFκB activation.

ATII cells are one of the biggest cellular sources of mitochondria within the lung and depend primarily on metabolism by oxidative phosphorylation[304]. Having already identified that HCA attenuated mitochondrial membrane potential in HPMECs **(Figure 3.7)**, together with the knowledge that proliferation of A549 cells is impaired in HCA via mitochondrial dysfunction[161], mitochondrial membrane potential was assessed in SAECs exposed to normocapnia or HCA. The measurement of mitochondrial membrane potential is often used as a measure of mitochondrial function. It was attenuated in HCA in both an inflammatory and non-inflammatory setting, suggesting that HCA induced mitochondrial dysfunction.

Low mitochondrial membrane potential is commonly associated with the induction of mitophagy – a process whereby damaged mitochondria are degraded in lysosomes and removed from the cell[304,305]. While its role in the lung is complex, mitophagy confers resistance to cell death in both alveolar epithelial cells and macrophages[306,307]. This suggests that the attenuated mitochondrial membrane potential observed in HCA may induce mitophagy to preserve cell viability, as observed in the current study. In addition, both low mitochondrial membrane potential and mitophagy impair proliferation of liver and kidney cells, respectively[308,309]. Low mitochondrial membrane potential has also been associated with impaired macrophage migration[310]. If these results are also applicable to alveolar epithelial cells, given that wound repair involves cell migration and proliferation, these data suggest that the attenuated mitochondrial membrane potential observed in HCA could explain the impairment of wound closure observed in the current study. In addition, reduced mitochondrial membrane potential has been associated with the development of an anti-inflammatory M2 macrophage phenotype[311]. While the effects of altered mitochondrial membrane

potential on inflammation do not appear to have been reported in alveolar epithelial cells, this suggests that attenuated SAEC mitochondrial membrane potential may also be linked to the attenuated chemokine secretion observed in HCA in the current study.

The final aim of the study was to confirm if the results obtained in SAECs were reproducible in primary human ATII cells. To achieve this, a protocol for the successful isolation of ATII cells from donor human lungs had to be set up within the lab. Initial attempts to isolate ATII cells using a previously published protocol in which elastase was used to digest the lung tissue, yielded very low cell numbers (usually much less than $1x10^6$ cells per isolation)[312]. However, after significant modifications to the isolation protocol based on another published method, high yields of pro-SPC-positive cells were obtained[313]. Surfactant protein C (SPC) is a marker of ATII cells. As ATII cells can differentiate to ATI cells, it is important to counterstain with an ATI marker such as Aquaporin-5 (AQP-5). Due to problems with the specificity of AQP-5 antibodies, it is unknown if the cells are true ATII cells or if they have begun to undergo differentiation and are of an intermediate phenotype. They must therefore be referred to as ATII-like cells. The current study demonstrates that HCA appears to impair wound closure of these ATII-like cells, as was the case with SAECs. This suggests that the results obtained using SAECs may be sufficiently representative of the alveolar epithelium. However, further replicates and the use of other readouts will be required before it can be confirmed that this is the case.

4.12 Summary and Conclusions

From this chapter it can be concluded that:

- SAEC secretion of the potent neutrophil chemoattractants CXCL8 and CXCL5 is attenuated in HCA
- SAEC wound closure is impaired in HCA
- While NFκB activation in SAECs was not significantly altered in HCA, mitochondrial membrane potential was attenuated
- Further work is required to definitively determine if these results are reproducible in primary human ATII cells

Together these results suggest that, via attenuated chemokine secretion, the small airway epithelium may contribute to dampening of inflammation which has previously been demonstrated in *in vivo* models in HCA. However, impaired SAEC wound closure in HCA raises concerns with regards to the reparative capacity of SAECs. While the results suggest that the attenuated inflammatory response of, and attenuated wound repair by, SAECs may arise from HCA-induced mitochondrial dysfunction, further studies are required to directly link the observations and to elucidate the molecular mechanisms responsible.

Chapter Five – Hypercapnic acidosis attenuates the therapeutic efficacy of MSCs in an *in vitro* model of ARDS via impaired mitochondrial function

5.1 Overview of chapter

This chapter will discuss the potential use of mesenchymal stem cells (MSCs) as a potential therapy for the treatment of ARDS and will highlight the lack of investigations into the potential implications a hypercapnic acidotic environment may exert on their therapeutic potential. The aims and objectives of the study will be highlighted. The results will then be presented and their implications for an MSC-based therapy for ARDS subsequently discussed.

5.2 Introduction

Despite decades of pre-clinical and clinical research, there remains no successful pharmacological therapy for the treatment of ARDS. However, in recent years, the potential use of a mesenchymal stem cell (MSC)-based therapy has been under intense investigation. MSCs are multipotent in nature and can be derived from numerous adult tissue sources including, but not limited to, the bone marrow, umbilical cord, and adipose tissue[314,315]. They are a heterogeneous population of cells and are characterised by three criteria proposed by the International Society for Cellular Therapy (ICST)[316]. These criteria dictate that MSCs must be capable of adhering to tissue culture plasticware, express a defined set of markers, and possess the capacity to differentiate into adipocytes, chondrocytes and osteoblasts under appropriate conditions identified by Pittenger *et al*. in 1999[316,317].

To date, MSCs have demonstrated therapeutic potential in preclinical models of a range of conditions including diabetes, hepatic disease and myocardial infarction[318–321]. Additionally, their use for the prophylaxis of graft-versus-host disease in a recently reported phase II clinical trial yielded encouraging results[322]. Importantly, MSCs have also demonstrated a capacity to modulate the major hallmarks of ARDS – inflammation and pulmonary oedema – in preclinical *in vivo* models of the condition. In this regard, their administration has been associated with attenuated pro-inflammatory and elevated anti-inflammatory cytokine concentrations, attenuated accumulation of pulmonary oedema fluid, improved oxygenation, and enhanced survival[56,59,60,62,323–328]. In preclinical models of sepsis- and pneumonia-induced

ARDS, enhanced survival has also been associated with improved bacterial clearance[57,58,323,324,329]. Furthermore, many of these therapeutic effects of MSCs have been reproducible in a human *ex vivo* lung perfusion (EVLP) model where their administration has been associated with attenuated proinflammatory cytokine concentrations, restoration of alveolar fluid clearance, and reduced bacterial load[64–66]. The results also appear to translate to patients with severe refractory ARDS: although compassionate administration of $2x10^6$ MSCs/kg predicted body weight has been reported only in a very small cohort of two patients, their use was associated with improvements in pulmonary oedema and in bronchoalveolar lavage fluid (BALF) and plasma concentrations of inflammatory markers[330].

In ARDS, the integrity of the alveolar epithelial barrier is compromised, in part as a result of alveolar epithelial cell death[1]. Although MSCs are multipotent and capable of differentiating into many cell types, low levels of pulmonary engraftment (<5%) have been reported[56,331–333]. As a result, it is thought that engraftment and differentiation of administered MSCs are not, at least solely, responsible for their therapeutic benefits. A number of alternative mechanisms, which are likely to act in concert with each other, have been proposed.

Of these mechanisms, the most extensively studied is the MSC secretion of paracrine soluble factors including inflammatory cytokines, growth factors, and antimicrobial peptides. Among these include keratinocyte growth factor (KGF) which contributes to MSC-mediated improvements in alveolar fluid clearance by improving the activity of the epithelial sodium channel ENaC[64,66,334], and angiopoietin-1 (Ang-1) which attenuates permeability of type II alveolar epithelial cells[335]. Other such paracrine factors include interleukin-10 (IL-10), interleukin-1 receptor antagonist (IL-1ra), lipocalin-2 (LCN-2), and prostaglandin E2 (PGE2), to name a few[336].

The therapeutic capacity of MSCs may also be mediated by transfer of their mitochondria to surrounding injured cells. This can occur via direct contact mediated by the formation of actin-based tunnelling nanotubules (TNTs) between MSCs and

nearby cells. MSCs use this mitochondrial transfer approach to rescue human umbilical vein endothelial cells (HUVECs) from apoptosis, and enhance the phagocytic capacity of macrophages[337,338]. Mitochondrial transfer to bronchial epithelial cells in this way has also been associated with therapeutic effects of MSCs in models of asthma and chronic obstructive pulmonary disease (COPD)[339,340].

Mitochondria can also be transferred, along with other biologically active molecules including microRNAs (miRNAs), independently of TNT formation through the MSC secretion of small membrane-bound compartments known as extracellular vesicles (EVs)[319,341]. EVs can be taken up by recipient cells via one of two processes – endocytosis, or direct fusion of their membranes[319]. *In vivo*, MSC-derived EVs reproduce, at least partially, many of the therapeutic benefits of MSCs themselves[341–345].

MSC-based therapies have already entered clinical trials for the treatment of ARDS and, encouragingly, the results to date attest to their safety. No infusion toxicities or serious adverse events were reported in a phase I randomised placebo-controlled trial in which patients with moderate-to-severe ARDS were administered a dose of $1x10^6$ adipose-derived MSCs/kg predicted body weight (PBW)[52]. Similarly, the results of a multi-centre phase I dose-escalation trial attest to the safe administration of up to $1x10^7$ bone marrow-derived MSCs/kg PBW to patients with moderate-to-severe ARDS[53]. However, these were very small studies with short-term follow-up. The results of larger trials currently planned or underway (clinicaltrails.gov NCT03042143 and NCT02097641) to confirm these results and investigate the efficacy of MSCs as a therapeutic option for ARDS are eagerly anticipated.

However, much is still to be learned about the optimal isolation, expansion, screening, and ultimately use of MSCs as a potential therapeutic for the treatment of human disease. Currently, MSC biology and the factors which influence it are incompletely understood, and the isolation and characterisation of MSCs exhibiting optimal and consistent therapeutic effects have not been standardised. It could therefore be argued

that the progression of MSCs from pre-clinical models to clinical trials has progressed too rapidly, certainly when compared to the considerable effort spanning more than half a century which was required to establish the successful transplantation of haematopoietic stem cells[346].

Of particular relevance to the current project, MSCs are well-known to respond to local environmental cues such as inflammation and hypoxia[347–351]. It is therefore perceivable that they will also respond to altered CO_2 concentrations in their local environment. However, despite the knowledge that patients with ARDS often develop hypercapnic acidosis[352], the effects of HCA on MSC biology and their therapeutic efficacy has never been studied pre-clinically. This could have profound implications when delivered for the treatment of ARDS to patients presenting with HCA.

5.3 Aims and Objectives

The overall objective of this chapter is to determine the effects of HCA on MSC biology and subsequently their therapeutic potential in ARDS. This will be achieved using human bone marrow-derived MSCs in an *in vitro* model in which the inflammatory environment of ARDS is modelled by a cytomix of proinflammatory cytokines implicated in the pathogenesis of the condition. The specific aims of this study are:

- To determine the effects of HCA on the aspects of MSC biology key to their therapeutic potential, including cell viability, their capacity for paracrine secretion, and mitochondrial function
- To assess the therapeutic efficacy of MSCs in the setting of HCA, specifically their capacity to alter SAEC wound repair
- To investigate the mechanisms mediating any observed effects

5.4 HCA does not alter MSC viability

To assess the effect of HCA on MSC viability, release of lactate dehydrogenase (LDH) into cell culture supernatants was measured following exposure of MSCs to 5% or 15% CO_2 for 24 hours in the presence or absence of cytomix. A positive control was included in which cells were lysed using 2% Triton-X. Results are presented as percentage relative to this control.

Results demonstrate no apparent induction of cell death by cytomix in either normocapnia or HCA **(Figure 5.1)**. While further replicates are required to perform statistical analysis, the degree of cell viability does not appear to differ between cytomix-stimulated MSCs cultured in 5% CO_2 (22.5 ± 3.2% of positive control) or 15% CO_2 (18.7 ± 2.7% of positive control). This is also true of unstimulated MSCs cultured in 5% CO_2 (20.1 ± 4.2% of positive control) or 15% CO_2 (17.7 ± 1.7% of positive control) **(Figure 5.1)**.

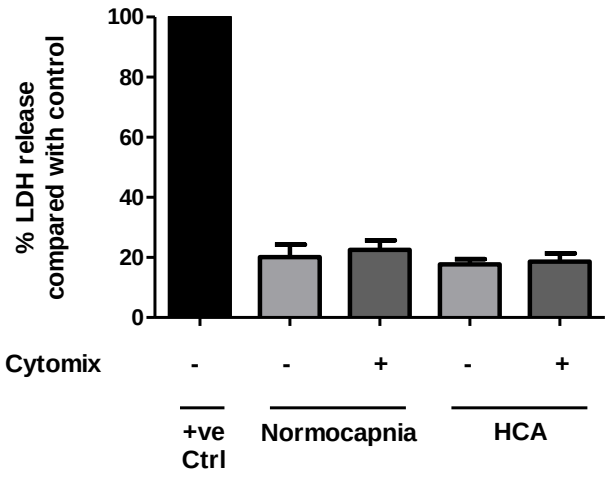

Figure 5.1: HCA does not alter MSC viability

MSCs were cultured in 5% or 15% CO_2 in the presence or absence of cytomix for 24 hours. Cell viability was assessed by measurement of LDH release into cell culture supernatants. Results are presented as percentage relative to positive control (+ve Ctrl). Error bars represent standard deviation (SD). (n=2 for all conditions; no statistical analysis performed).

5.5 HCA does not alter the capacity of MSCs to secreted paracrine soluble factors and does not alter NFκB activation

MSCs, in the presence or absence of 50ng/ml cytomix, were cultured in 5% or 15% CO_2 for 24 hours. To determine the response of MSCs to HCA in terms of their ability to secrete paracrine soluble factors, the concentrations of a selection of MSC-secreted factors which have previously been associated with the therapeutic benefits of MSC-based therapies, were measured in cell culture supernatants by ELISA. Results demonstrate that the secretion of Ang-1 by MSCs was not significantly altered by cytomix stimulation **(Figure 5.2A)**. Notably, the concentration of Ang-1 secreted by cytomix-stimulated MSCs also did not differ between normocapnia and HCA (247.5 ± 101.8pg/ml in normocapnia vs. 222.6 ± 110.4pg/ml in HCA) **(Figure 5.2A)**. In contrast, cytomix significantly enhanced IL1ra secretion by MSCs in both normocapnia and HCA (<39.1pg/ml in unstimulated MSCs vs. 294.9 ± 152.4pg/ml in stimulated cells in normocapnia and 250.2 ± 148.8pg/ml in stimulated cells in HCA). However, again, no statistically significant difference in the concentration of IL1ra present in cell culture supernatants from cytomix-stimulated MSCs was observed between normocapnia and HCA **(Figure 5.2B)**. Concentrations of KGF and IL-10 in MSC supernatants were also measured by ELISA, but were below the lower limit of detection of the assays (31.25pg/ml for both analytes) (data not shown).

Activation status of the NFκB pathway was assessed by p65 TransAM assay using nuclear extracts from MSCs cultured in 5% or 15% CO_2 for 0, 30 or 60 minutes. The NFκB assay is a DNA-binding ELISA which detects active NFκB p65 subunits in nuclear extracts via their binding to consensus oligonucleotides immobilised on a 96 well plate. Results demonstrate marked induction of NFκB activation in response to cytomix stimulation for 30 minutes or 60 minutes **(Figure 5.2C)**. The degree of activation did not differ between cells cultured in 5% or 15% CO_2 for either 30 minutes (optical density (OD) 0.9 ± 0.3 in normocapnia vs. 1.1 ± 0.2 in HCA) or 60 minutes (OD 0.9 ± 0.3 in normocapnia vs. 0.8 ± 0.3 in HCA) post-stimulation **(Figure 5.2C)**.

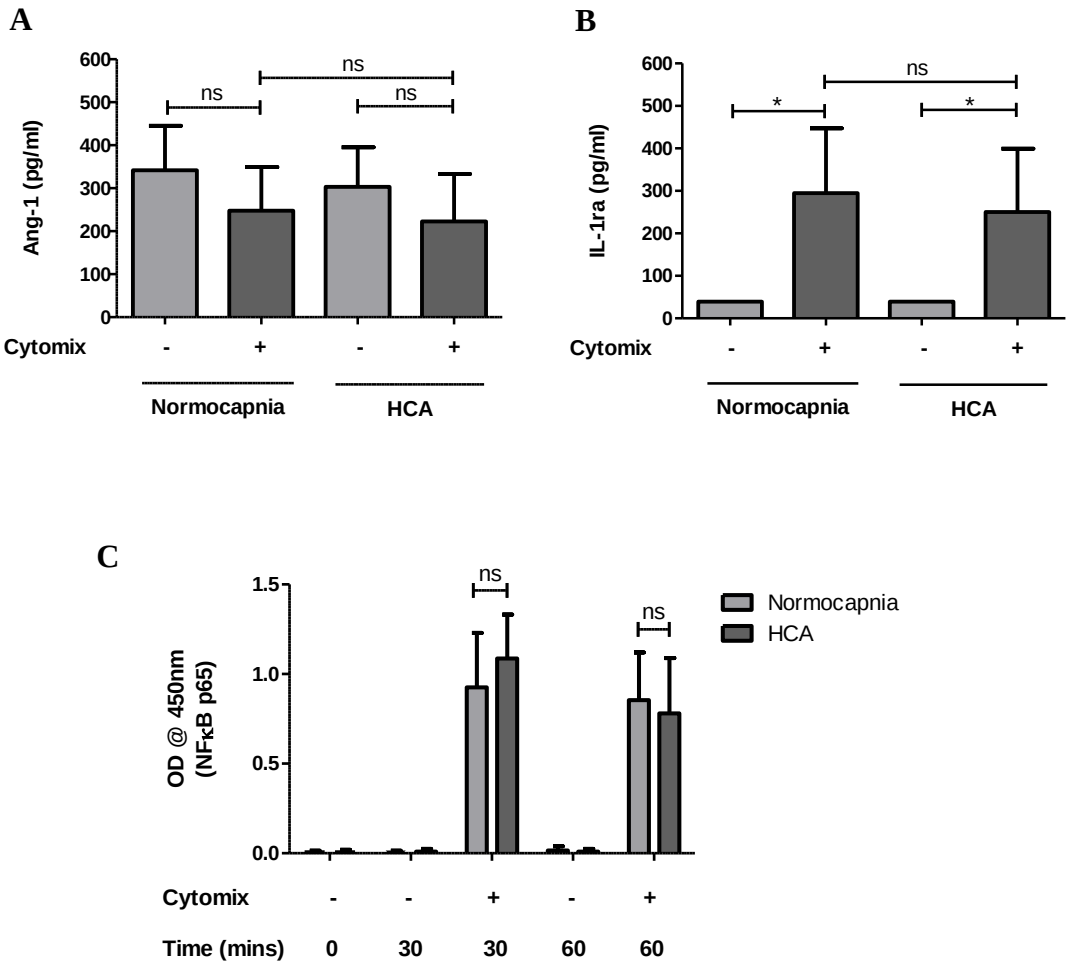

Figure 5.2: HCA does not alter the capacity of MSCs to secrete paracrine soluble factors and does not alter NFκB activation

Unstimulated or cytomix-stimulated MSCs were cultured in 5% or 15% CO_2 for 24 hours. MSC secretion of Ang-1 (A) and IL-1ra (B) was quantified by ELISA (n=5 for all conditions; Kruskal-Wallis with Dunn's posthoc analysis). MSCs were cultured in 5% or 15% CO_2 in the presence or absence of cytomix stimulation for 0, 30, or 60 minutes (B). NFκB activation was assessed by p65 TransAM assay and results are presented as optical density (OD). (n=5 for 0 and 60 minutes; n=4 for 30 minutes; two-way ANOVA with Bonferroni posthoc analysis). Error bars represent standard deviation (SD) (ns = not significant; * = $p<0.05$).

5.6 HCA attenuates MSC mitochondrial membrane potential in a pH-independent manner

To investigate the effects of HCA on MSC mitochondrial function, its effects on mitochondrial membrane potential were assessed. MSCs were cultured in 5% or 15% CO_2 in the presence or absence of cytomix for 24 hours. For experiments in which the contribution of pH to the effects of HCA were investigated, acidosis was buffered by addition of 0.02M sodium bicarbonate ($NaHCO_3$) to the medium in which the MSCs were cultured throughout the experiment. Cells were then stained with the mitochondrial membrane potential indicator, JC-1. When mitochondrial membrane potential is low, low concentrations of JC-1 enter the mitochondria where they remain in a monomeric form exhibiting green fluorescence. Higher mitochondrial membrane potential allows more JC-1 to accumulate within mitochondria. At higher concentrations, JC-1 forms aggregates which fluorescence red. The degree of JC-1 aggregation was assessed by fluorescence microscopy. MSCs treated with FCCP at the time of JC-1 staining to induce mitochondrial depolarisation were included as a control. Results are presented as the ratio of red (JC-1 aggregates) / green (JC-1 monomers), normalised to unstimulated MSCs in normocapnia and are proportional to mitochondrial membrane potential.

Mitochondrial depolarisation was successfully induced by FCCP when compared to unstimulated MSCs in normocapnia (normalised red/green ratio 0.6 ± 0.3 vs. 1.0 ± 0.0, respectively). Mitochondrial membrane potential was not significantly altered by cytomix stimulation in either normocapnia or HCA **(Figures 5.3A and 5.3B)**. However, HCA significantly attenuated mitochondrial membrane potential in both unstimulated (1.0 ± 0.0 in normocapnia vs. 0.6 ± 0.2 in HCA) and cytomix-stimulated MSCs (0.9 ± 0.2 in normocapnia vs. 0.6 ± 0.2 in HCA) **(Figures 5.3A and 5.3B)**. In separate experiments, although it did not reach statistical significance, mitochondrial membrane potential in 15% CO_2 did not differ between buffered and unbuffered conditions either in unstimulated MSCs (0.6 ± 0.2 unbuffered vs. 0.6± 0.1 buffered) or cytomix-stimulated MSCs (0.6 ± 0.3 unbuffered vs. 0.7 ± 0.2 buffered) **(Figure 5.3C)**.

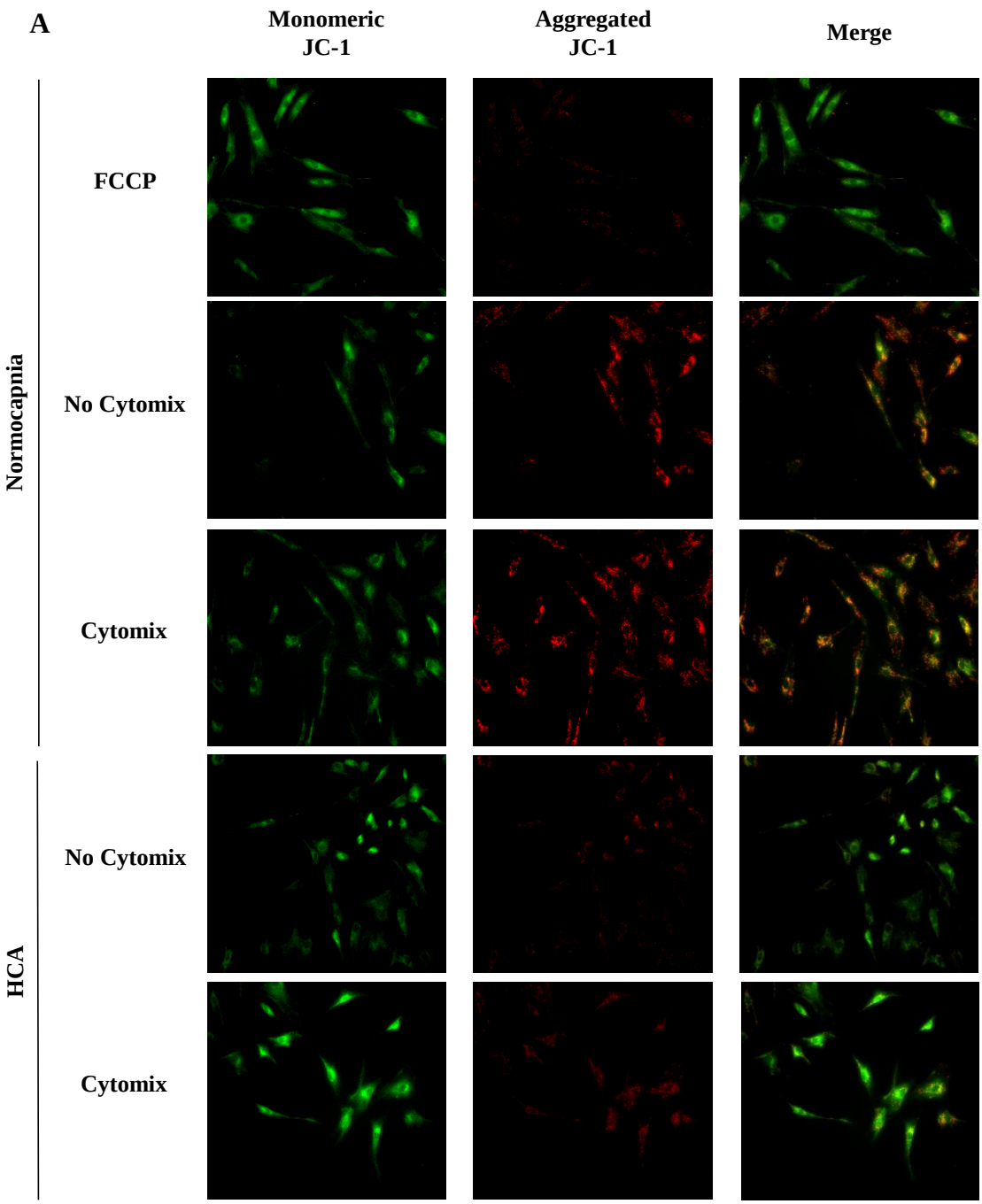

Figure 5.3: HCA attenuates MSC mitochondria membrane potential in a pH-independent manner

MSCs cultured in 5% or 15% CO_2 for 24 hours in the presence or absence of cytomix were stained with the mitochondrial membrane potential indicator, JC-1. A control was included in which mitochondrial depolarisation was induced using FCCP. JC-1 staining was visualised by fluorescence microscopy. Representative images are presented (A).

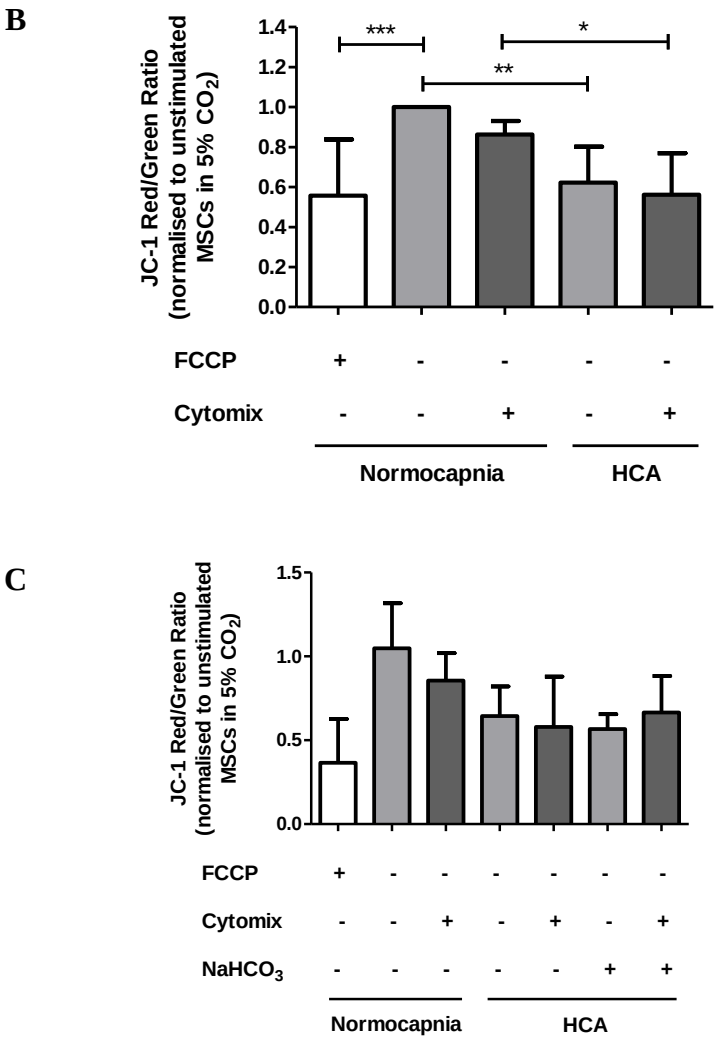

Figure 5.3 (continued): HCA attenuates MSC mitochondria membrane potential in a pH-independent manner

MSCs cultured in 5% or 15% CO_2 for 24 hours in the presence or absence of cytomix were stained with the mitochondrial membrane potential indicator, JC-1 (B) (n=5 for all conditions; one-way ANOVA with Bonferroni posthoc analysis; * = $p<0.05$; ** = $p<0.01$; *** = $p<0.001$). In separate experiments, acidosis was buffered by addition of $NaHCO_3$ and JC-1 staining was performed (C) (n=3 for all conditions except FCCP and all unstimulated groups in 15% CO_2 which are n=2; Kruskal-Wallis with Dunn's posthoc analysis). A control was included in which mitochondrial depolarisation was induced using FCCP. JC-1 staining was visualised by fluorescence microscopy and the red (aggregate) / green (monomer) ratio was calculated. Results are presented relative to unstimulated MSCs in normocapnia. Error bars represent standard deviation (SD).

5.7 HCA attenuates MSC ATP production

MSCs were cultured in 5% or 15% CO_2 in the presence or absence of cytomix for 24 hours. To determine if the attenuated mitochondrial membrane potential observed in HCA is associated with loss of mitochondrial function, ATP production was measured by luminescent assay. Results demonstrate that cytomix attenuates ATP production by MSCs in normocapnia (0.6 ± 0.1 in cytomix relative to unstimulated MSCs in normocapnia). ATP production by cytomix-stimulated MSCs was further impaired in HCA (0.6 ± 0.1 in cytomix in normocapnia vs 0.3 ± 0.1 in cytomix in HCA, both relative to unstimulated MSCs in normocapnia) **(Figure 5.4)**.

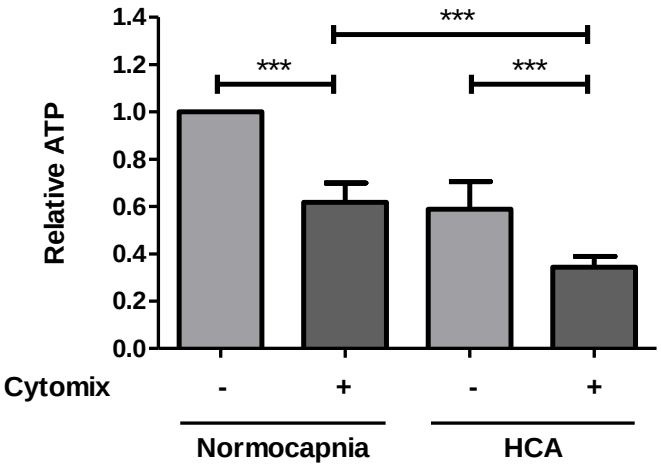

Figure 5.4: HCA attenuates MSC ATP production

Unstimulated or cytomix-stimulated MSCs were cultured in 5% or 15% CO_2 for 24 hours. MSC ATP production was assessed by luminescent assay. Results are presented relative to unstimulated MSCs in normocapnia. Error bars represent standard deviation (SD) (n=5 for all conditions; one-way ANOVA with Bonferroni posthoc analysis; *** =$p<0.001$).

5.8 MSCs promote SAEC wound closure in normocapnia, but not HCA, independently of cell proliferation

To assess the effects of HCA on the therapeutic potential of MSCs, SAECs were wounded in an *in vitro* scratch assay and cultured in the presence of cytomix either alone or in indirect contact with MSCs seeded on transwell inserts, for 24 hours in 5% or 15% CO_2. A control in which SAECs were not stimulated with cytomix or co-cultured with MSCs was included in normocapnia. Results demonstrate that MSCs promote SAEC wound closure in normocapnia (55.0 ± 20.0% in the presence of MSCs vs. 33.9 ± 8.1% in their absence) but that this effect is lost in HCA (30.1 ± 12.9% in the presence of MSCs vs. 24.9 ± 13.4% in their absence) **(Figures 5.5A and 5.5B)**.

The SAECs used for these *in vitro* scratch assays were fixed and stained for the proliferation marker, Ki67, to determine whether the reparative effect of MSCs is associated with altered proliferation. Ki67 staining in SAECs was not influenced by MSCs in either normocapnia (3.3 ± 2.8 Ki67-positive cells in SAECs cultured in the absence of MSCs vs. 1.5 ± 1.6 in the presence of MSCs) or HCA (3.6 ± 3.2 Ki67-positive cells in SAECs cultured in the absence of MSCs vs. 3.5 ± 3.7 in the presence of MSCs) **(Figure 5.5C)**.

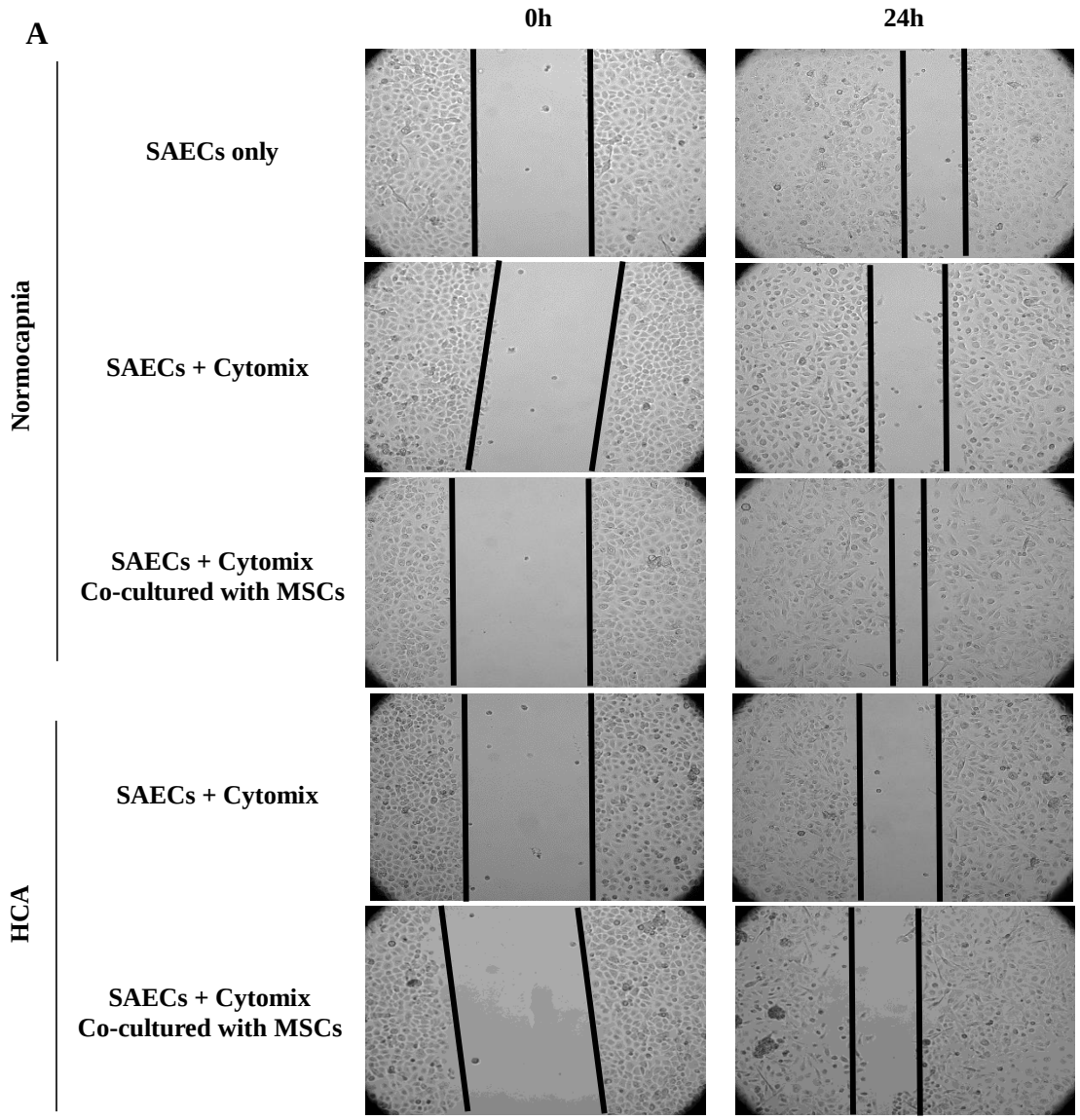

Figure 5.5: MSCs promote SAEC wound closure in normocapnia, but not HCA, independently of cell proliferation (continued overleaf)

SAEC monolayers were wounded in an *in vitro* scratch assay and cultured in 5% or 15% CO_2 in the presence of cytomix, either alone or in indirect contact with MSCs. A control in which SAECs were not stimulated with cytomix or co-cultured with MSCs was included. Representative images illustrating approximate wound areas at 0 hours and 24 hours are presented for each condition (A).

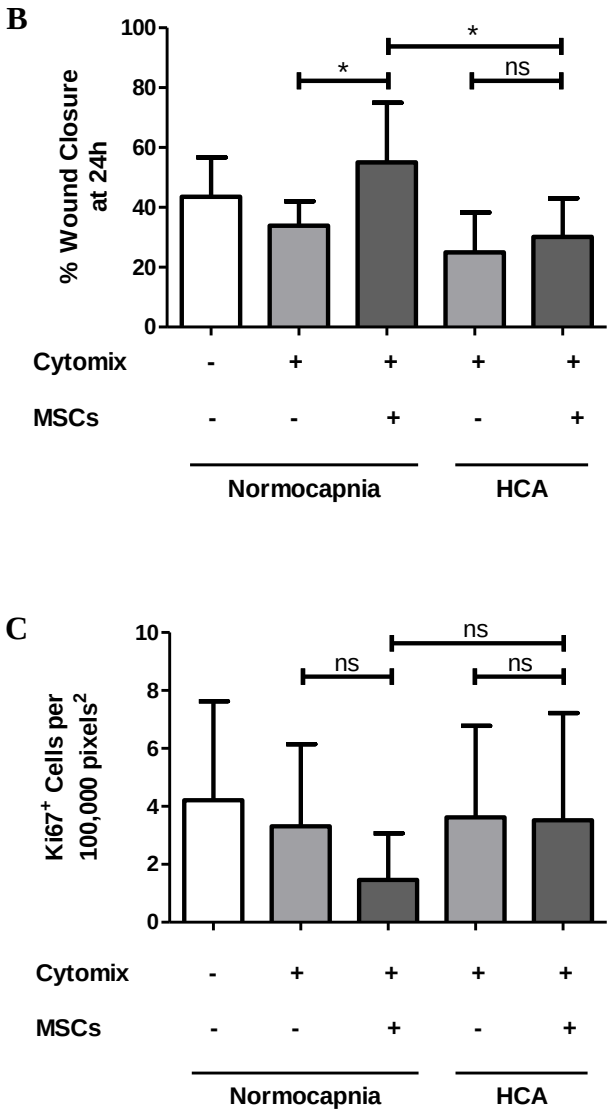

Figure 5.5 (continued): MSCs promote SAEC wound closure in normocapnia, but not HCA, independently of cell proliferation

SAEC monolayers were wounded in an *in vitro* scratch assay and cultured in 5% or 15% CO_2 in the presence of cytomix, either alone or in indirect contact with MSCs. A control in which SAECs were not stimulated with cytomix or co-cultured with MSCs was included. Percentage wound closure over 24 hours was quantified for each condition (B). (n=4 for all conditions; one-way ANOVA with Bonferroni posthoc analysis; ns = not significant; * = $p<0.05$). SAECs from the *in vitro* scratch assay were fixed and stained for the proliferation marker, Ki67 (C). (n=3 for all conditions; Kruskal-Wallis with Dunn's posthoc analysis; ns = $p>0.05$). Error bars represent standard deviation (SD).

5.9 MSCs transfer their mitochondria to SAECs

It has previously been reported that transfer of MSC mitochondria in extracellular vesicles (EVs) was responsible for the paracrine-mediated effects of MSCs on macrophage modulation[341]. To investigate if MSC mitochondria are transferred to SAECs through a paracrine mechanism, mitochondria in MSCs were stained with MitoTracker Green (a fluorescent dye specific for functional mitochondria) and SAECs were stained with MitoTracker Red. To determine whether MSCs transfer their mitochondria to SAECs, the stained MSCs were subsequently washed and seeded on transwell inserts placed over the stained SAECs. The two cell types were co-cultured in the presence of cytomix for 24 hours in 5% or 15% CO_2. To rule out unspecific staining due to unbound MitoTracker Green, a leak test was included which involved taking PBS from the third wash of MSCs and adding it to a transwell insert in place of the MSCs themselves. Mitochondrial transfer from MSCs to SAECs was visualised by fluorescence microscopy. Uptake of MSC mitochondria into the SAEC mitochondrial network is evidenced by the colocalisation of red and green fluorescence, producing a yellow hue **(Figure 5.6, arrows)**. Results demonstrate that MSC-derived mitochondria are transferred to SAECs in a paracrine manner in the settings of both normocapnia and HCA **(Figure 5.6)**.

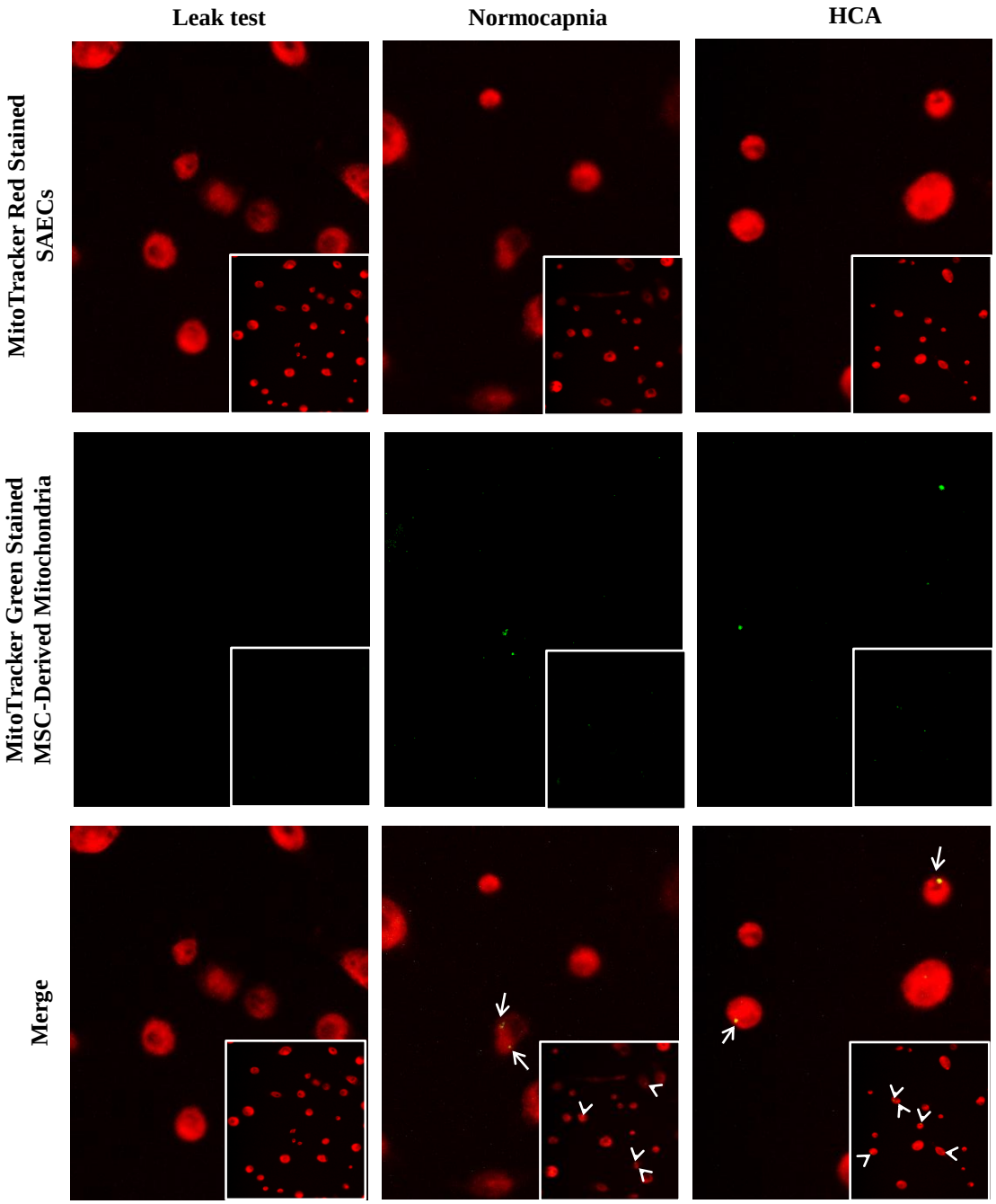

Figure 5.6: MSCs transfer their mitochondria to SAECs

MSC mitochondria were stained with MitoTracker Green while SAECs were labelled using MitoTracker Red. Stained MSCs were seeded in transwell inserts and co-cultured in indirect contact with stained SAECs in 5% or 15% CO_2 for 24 hours in the presence of cytomix stimulation. Mitochondrial transfer from MSCs to SAECs was visualised by fluorescence microscopy. Representative images are presented. Inset are full images taken at x20 magnification. Lager images are smaller area of the field.

5.10 MSCs may increase ATP production by SAECs

To determine whether mitochondrial transfer from MSCs to SAECs is associated with altered ATP production, SAECs were cultured for 24 hours in 5% or 15% CO_2 either alone or in indirect contact with MSCs seeded on transwell inserts. ATP production by SAECs was quantified using a luminescent ATP detection assay kit. Although it did not reach statistical significance, the results demonstrate a small trend towards enhanced ATP production by SAECs in normocapnia (149.9 ± 54.9nM in SAECs cultured alone vs. 175.8 ± 51.8nM in SAECs co-cultured with MSCs) **(Figure 5.7)**. This trend was less pronounced in HCA (92.0 ± 28.4nM in SAECs cultured alone vs. 102.0 ±28.1nM in SAECs cultured in indirect contact with MSCs) **(Figure 5.7)**.

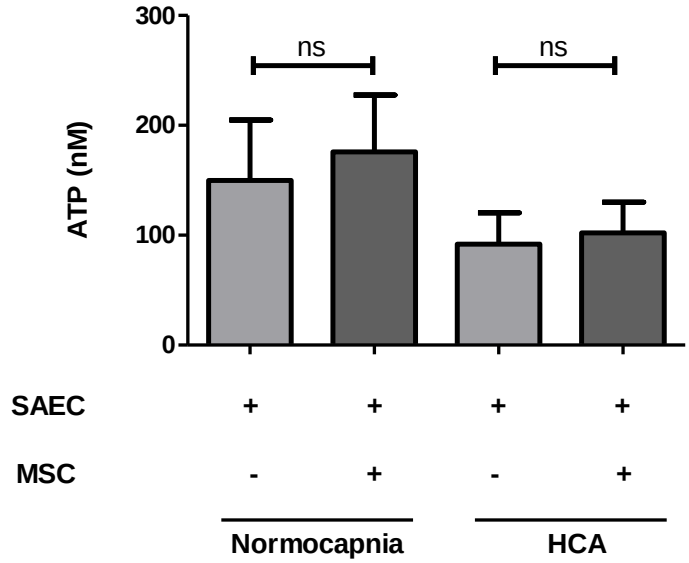

Figure 5.7: MSCs may increase ATP production by SAECs

SAECs were cultured for 24 hours in 5% or 15% CO_2 either alone or in indirect contact with MSCs. ATP production was quantified at 24 hours using a luminescent ATP detection assay kit. Error bars represent standard deviation (SD). (n=3 for all conditions; Kruskal-Wallis with Dunn's posthoc analysis; ns = $p>0.05$).

5.11 Functional mitochondria are required for MSCs to promote SAEC wound closure

To determine whether functional mitochondria are required for the ability of MSCs to promote SAEC wound closure, MSCs were pre-treated with rhodamine 6G (R6G) for 48 hours. R6G induces mitochondrial dysfunction by irreversibly impairing oxidative phosphorylation without significantly altering MSC paracrine secretion[341]. SAECs were then wounded in an *in vitro* scratch assay and cultured in the presence of cytomix either alone or in indirect contact with MSCs (either untreated or pre-treated with R6G) seeded on inserts for 24 hours in 5% or 15% CO_2. A control in which wounded SAECs were cultured alone, in the absence of cytomix or MSCs, was included. Percentage wound closure over the 24 hour period was measured.

Results demonstrate that while MSCs not treated with R6G promote SAEC wound closure in normocapnia when compared to cytomix-stimulated SAECs cultured in the absence of MSCs (21.4 ± 4.6% in SAECs not co-cultured with MSCs vs. 35.4 ± 7.3% in SAECs co-cultured with MSCs), this effect is lost upon co-culture with MSCs pre-treated with R6G (14.8 ± 8.2%) **(Figure 5.8)**. SAEC wound closure did not differ between cells co-cultured with MSCs pre-treated with R6G in normocapnia and cells co-cultured with untreated MSCs in HCA (12.8 ± 2.5 in HCA) **(Figure 5.8)**.

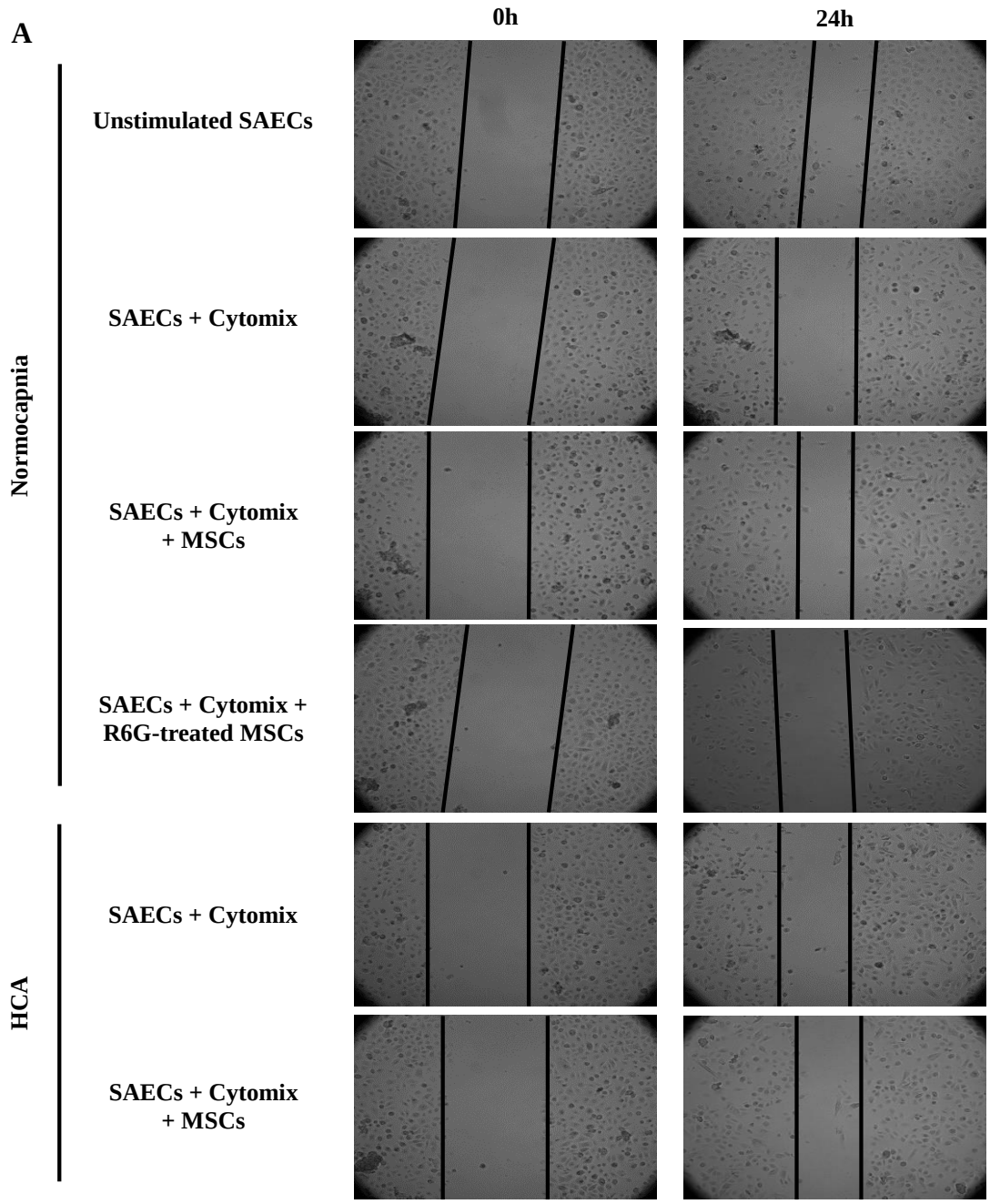

Figure 5.8: Functional mitochondria are required for MSCs to promote SAEC wound closure (continued overleaf)

MSCs were pre-treated with rhodamine 6G (R6G). SAEC monolayers were wounded in an *in vitro* scratch assay and cultured in the presence of cytomix either alone or in indirect contact with MSCs (pre-treated or not with R6G) for 24 hours in 5% or 15% CO_2. A control in which wounded SAECs were cultured in the absence of cytomix or MSCs was included in normocapnia. Representative images illustrating wound areas at 0 hours and 24 hours are presented (A).

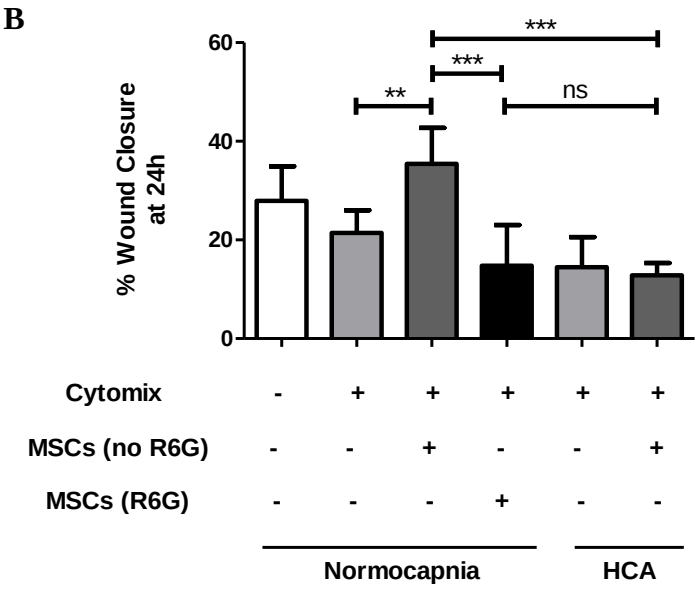

Figure 5.8 (continued): Functional mitochondria are required for MSCs to promote SAEC wound closure

MSCs were pre-treated with rhodamine 6G (R6G). SAEC monolayers were wounded in an *in vitro* scratch assay and cultured in the presence of cytomix either alone or in indirect contact with MSCs (pre-treated or not with R6G) for 24 hours in 5% or 15% CO_2. A control in which wounded SAECs were cultured in the absence of cytomix or MSCs was included in normocapnia. Percentage wound closure over 24 hours was quantified for each condition (B). Error bars represent standard deviation (SD). (n=3 for all conditions; one-way ANOVA with Bonferroni posthoc analysis; ns = $p>0.05$; ** = $p<0.01$; *** = $p<0.001$).

5.12 Discussion

Mesenchymal Stem Cells (MSCs) represent a promising potential therapeutic option for the treatment of ARDS[353]. However, there is still much to be learned in the field of MSC-based therapies for the treatment of human disease. Despite the occurrence of hypercapnic acidosis (HCA) in mechanically ventialtion patients with ARDS[352], and the known capacity of MSCs to respond to their local environment[347–351], the therapeutic potential of MSCs has never been studied in the setting of HCA. The aims of the work in this chapter were therefore to determine the effects of HCA on MSC biology and subsequently to investigate how therapeutically efficacious MSCs are in such an environment. To achieve these aims, MSCs were cultured either alone or in indirect co-culture with SAECs in *in vitro* assays in which the inflammatory environment of ARDS was modelled using a cytomix of proinflammatory cytokines (IFNγ, IL1β, and TNFα) implicated in the pathogenesis of the condition.

To assess the effects of HCA on MSC biology, its effect on MSC viability was first assessed by LDH assay. Importantly, cell viability was not altered by HCA.

It is well-established that MSCs respond to their local environment to secrete a plethora of cytokines, growth factors, and antimicrobial peptides[336,353]. One of these soluble mediators is the vascular growth factor, Angiopoietin-1 (Ang-1). Ang-1 secretion by MSCs attenuates protein permeability of the alveolar epithelium *in vitro* and is thought to contribute to the reduction of LPS-induced BALF protein concentrations observed *in vivo*[335,354]. Interleukin-1 receptor antagonist (IL-1ra) is another soluble factor secreted by MSCs. It competitively prevents binding of interleukin-1 (IL-1) to its receptor[355]. In doing so, IL-1ra secretion by MSCs prevents IL-1-induced TNFα secretion by macrophages and induces macrophage polarisation towards an anti-inflammatory M2 phenotype[356,357]. Given that macrophages are the initial drivers of inflammation in ARDS and that the accumulation of a protein-rich oedema fluid is one of the main characteristics of the condition[2], the capacity of MSCs to secrete these soluble mediators is of importance for their therapeutic potential.

The transcriptional regulation of both Ang-1 and IL1-ra involves the NFκB pathway[358,359]. Attenuated activation of this pathway has previously been demonstrated in HCA both *in vivo* and in multiple cell types *in vitro*[132,159,160,227], raising concerns regarding the ability of MSCs to secrete soluble mediators and subsequently exert their paracrine-mediated therapeutic effects in HCA. However, reassuringly, the results of the current study demonstrate that MSC secretions of neither Ang-1 nor IL-1ra are altered in such an environment. Additionally, no difference in the degree of NFκB activation was observed between normocapnia and HCA. These results demonstrate that MSCs retain their capacity to secrete at least some of the soluble mediators they are known to produce. However, while this suggests that the capacity of MSCs to exert therapeutic effects mediated by soluble mediators is retained in HCA, these results do not imply that the therapeutic effects actually exerted by such soluble mediators are also retained: the ability of MSC-secreted soluble mediators to exert their effects could still be influenced by the target cells themselves, for example via altered expression of target receptors. Further investigations will be required to properly probe whether or not this is the case.

Another important aspect to the biology of any cell is its ability to produce adenosine triphosphate (ATP) to meet energy demands. In the presence of oxygen, the majority of cellular ATP is produced during oxidative phosphorylation which is powered by the electron transport chain (ETC) located within the inner membrane of mitochondria[360]. Mitochondria are membrane-bound organelles found in eukaryotic cells. As electrons are passed through their ETC, protons are pumped out of the mitochondrial matrix and into the intermembrane space. In addition to creating a chemical gradient, this proton movement also creates an electrical gradient across the inner mitochondrial membrane which constitutes the mitochondrial membrane potential[360]. The protons eventually re-enter the matrix through ATP synthase which utilises them in the phosphorylation of adenosine diphosphate (ADP) to ATP[360]. The activities of both ATP synthase and adenine nucleotide translocase (ANT) - which exports ATP from the mitochondrial matrix in exchange for ADP - are dependent on mitochondrial membrane potential[360–362]. The measurements of mitochondrial membrane potential and intracellular ATP levels are therefore often used as indicators of mitochondrial function. In the current study, both measurements were attenuated

by HCA, suggesting that HCA induced mitochondrial dysfunctional in MSCs. The inability of buffered media to prevent attenuation of mitochondrial membrane potential suggests that these effects occur in a pH-independent manner.

In the absence of oxygen, ATP is produced by glycolysis which is a mitochondria-independent cytoplasmic process generating much fewer ATP molecules than aerobic oxidative phosphorylation. Bone marrow-derived MSCs – as used in this study - are adapted for glycolytic metabolism as a result of their hypoxic natural niche[363]. However, outside of this environment they can exhibit high oxygen consumption rates and utilise oxidative phosphorylation, although it is uncertain if this is a result of energy-dependent processes such as proliferation, or whether it results from adaptation to a change in environmental conditions[364,365]. It is therefore uncertain how profoundly HCA-induced mitochondrial dysfunction may affect MSC biology itself as the dependency of MSCs on oxidative metabolism outside of their natural niche is poorly understood. It is perceivable that in the setting of HCA, MSCs may revert back to glycolytic metabolism to maintain metabolic homeostasis. However, given that mitochondrial transfer to injured cells – which do depend on oxidative phosphorylation to meet their energy demands – contributes to the therapeutic effects of MSCs in experimental disease models[337–340], the MSC mitochondrial dysfunction observed in the current study raises concerns regarding the therapeutic potential of an MSC-based therapy in the setting of HCA.

Given these concerns, the ability of MSCs to promote SAEC wound closure was compared in normocapnia and HCA. MSCs have previously been shown to promote SAEC wound closure through a contact-independent mechanism via enhanced SAEC migration[366]. The results of the current study confirm these findings in normocapnia, demonstrating enhanced SAEC wound closure in a manner independent of proliferation. This indicates that MSCs, similarly to the previous observations[366], promoted SAEC wound closure via enhanced migration. However, the capacity of MSCs to promote SAEC wound closure via a contact-independent mechanism was lost in the setting of HCA. This is the first time that the therapeutic capacity of MSCs has been reported in such an environment. The findings are concerning as they suggest

that MSCs may lose their therapeutic efficacy in patients with ARDS who present with HCA.

To investigate why the capacity of MSCs to promote SAEC wound closure is lost in HCA, the mechanism for the MSC-mediated effect was first investigated. The transfer of mitochondria from MSCs to SAECs was first to be investigated given that HCA had induced mitochondrial dysfunction and the concerns that this raised regarding the therapeutic potential of MSCs. In the current study, mitochondrial transfer from MSCs to SAECs was observed in both normocapnia and HCA. This was associated with increased ATP production in SAECs. This is the first time that mitochondrial transfer to SAECs has been reported *in vitro* and suggests that MSCs promote SAEC wound closure via the transfer of functional mitochondria.

To further investigate whether mitochondrial transfer from MSCs to SAECs is the mechanism mediating SAEC wound closure in normocapnia, a loss-of-function experiment was performed. To induce mitochondrial dysfunction, MSCs were pre-treated with rhodamine 6G (R6G) which irreversibly inhibits the activity of adenine nucleotide translocase (ANT) and thus prevents the exchange of ATP for ADP across the inner mitochondrial membrane[367]. Pre-treatment of R6G does not significantly influence the MSC secretion of soluble mediators[341]. The *in vitro* scratch assay used to assess SAEC wound closure was then repeated using SAECs with both functional and dysfunctional mitochondria. The results demonstrate that functional mitochondria are required for the ability of MSCs to promote SAEC wound closure in normocapnia, suggesting that the induction of mitochondrial dysfunction in HCA was responsible for loss of the therapeutic benefit of MSCs.

Taken together, the results of this study demonstrate that, in normocapnia, MSCs promote SAEC wound closure by a mechanism dependent on functional MSC mitochondria. This is likely to occur via the transfer of functional mitochondria to SAECs in extracellular vesicles (EVs). However, the results also demonstrate that the therapeutic capacity of MSCs to promote SAEC wound closure is lost in HCA,

suggesting that MSCs lose their ability to promote structural – and therefore ultimately functional – recovery of the epithelial barrier in HCA.

This study is limited by the lack of investigation into whether differences in the extent of mitochondrial transfer exist between normocapnic and hypercapnic acidotic conditions. The results of the current study support the view that the mitochondria transferred to SAEC in HCA were dysfunctional as a result of attenuated mitochondrial membrane potential and therefore did not benefit the SAECs in the same way as functional mitochondria transferred in normocapnia. However, this should be subject to further investigation.

5.13 Summary and Conclusions

From this chapter it can be concluded that:

- HCA does not alter viability of MSCs or their capacity to secrete NFκB-regulated soluble mediators
- HCA induces MSC mitochondrial dysfunction in a pH-independent manner
- MSCs promote SAEC wound repair in normocapnia but not HCA, independently of proliferation
- Mitochondria are transferred from MSCs to SAECs in the settings of both normocapnia and HCA
- Transfer of MSC mitochondria is associated with a trend towards increased ATP production in SAECs
- Functional mitochondria are required for the ability of SAECs to promote SAEC wound repair

Together these results demonstrate that MSCs promote SAEC wound closure in normocapnia via a mechanism dependent on the presence of functional MSC mitochondria. The results suggest that this may occur through the transfer of

functional mitochondria to SAECs. However, they also demonstrate that this therapeutic capacity of MSCs is lost in HCA. HCA, in a pH-independent manner, induced mitochondrial dysfunction in MSCs. This is likely to result in the transfer of fewer functional mitochondria to the SAECs and thus attenuate the therapeutic benefits on wound closure. These results are concerning from a clinical perspective as they suggest that the therapeutic efficacy of an MSC-based therapy for ARDS may be adversely impacted by HCA. This suggests that patients with established HCA are not likely to benefit from MSC treatment, and is important for the design of future MSC-based clinical trials not only in ARDS, but also in other conditions complicated by HCA, for example chronic obstructive pulmonary disease (COPD) and cystic fibrosis.

Chapter Six – Final conclusions and future directions

6.1 Final conclusions

Acute Respiratory Distress Syndrome (ARDS) is a devastating clinical disorder common in intensive care units[133]. It is characterised by a diffuse inflammatory response and impaired function of the endothelial-epithelial blood-air barrier, resulting in the formation of pulmonary oedema and subsequently impaired gas exchange[3]. Currently, there exists no effective pharmacological therapy for the treatment of ARDS and so its management relies primarily on the use of supportive care approaches, particularly low tidal volume mechanical ventilation which may induce hypercapnic acidosis (HCA)[54]. Despite a lack of trials investigating the effects of HCA on clinical outcomes in ARDS, its development is largely considered safe for the patient and so has come to be accepted by many clinicians.

As the alveolar epithelium and capillary endothelium are keys targets in the pathogenesis of ARDS, it is important that the influence of the surrounding environment on their potential for recovery from the condition is characterised. To date only two studies have investigated the response of endothelial cells to HCA. The first used human pulmonary artery endothelial cells (HPAECs) and demonstrated attenuated inflammatory responses[157]. In contrast, the second study used human pulmonary microvascular endothelial cells (HPMECs) – the endothelial cell type most relevant to the pathophysiology of ARDS – but demonstrated the opposite response[158]. While the difference in results between the two studies may be explained by differences in the cell types used or in the concentration of CO_2, the results of the more relevant cell type – the HPMECs - are corroborated by *in vivo* findings which contradict a large body of *in vivo* evidence, raising concerns with regards to their validity. Both studies were also limited by lack of assessment of the reparative potential of the endothelium in HCA and of the contributions of mitochondria to the HCA-induced effects.

The response of the alveolar epithelium to HCA has been more extensively studied in comparison to the endothelium. It is concerning that while data demonstrate attenuated inflammatory responses in HCA, they also suggest that re-epithelialisation

and the capacity of alveolar epithelial cells to facilitate alveolar fluid clearance is impaired **(Section 4.2)**. However, much of this work has been performed in the immortalised A549 cell line which differs phenotypically from primary alveolar epithelial cells in a number of respects. The results obtained using this cell line should therefore be interpreted with caution, especially given that much of the *in vivo* evidence to date suggests that HCA either improves or does not affect epithelial-endothelial barrier function.

The first aim of the current study was designed to address the lack of clarity in relation to the responses of the alveolar epithelium and capillary endothelium to HCA. The aim was to determine the effects of HCA on the inflammatory and reparative responses of primary human pulmonary microvascular endothelial cells (HPMECs) and primary human small airway epithelial cells (SAECs) in an *in vitro* model of ARDS.

The results demonstrate that HCA attenuated inflammatory cytokine secretion by both cell types. Both cytokines measured – CXCL8 and CXCL5 - are potent neutrophil chemoattractants[238,239], suggesting that in the setting of HCA, the alveolar epithelium and capillary endothelium may help to dampen inflammatory responses within the alveoli by attenuating neutrophil recruitment. In this respect, both cell types may therefore contribute to recovery from ARDS by attenuating inflammation. These results are in keeping with previous observations demonstrating attenuated cytokine secretions by A549 cells and HPAECs. However, unsurprisingly given the concerns previously raised, they do not support the findings of Liu *et al.* who demonstrated enhanced inflammatory cytokine secretion by HPMECs[158].

It is concerning that the results of the current study also demonstrate attenuated wound repair in HCA by both HPMECs and SAECs. These findings are in keeping with previous reports in both A549 cells and SAECs[160], but are the first report of the response of endothelial cells to HCA in this regard and are the first report of the effects of HCA on wound repair in an inflammatory environment in either cell type. These findings are concerning as proliferation and migration are key to wound repair and are

important for recovery of the structural and subsequently functional integrity of the alveolar epithelial-capillary endothelial barrier. While the results of the current study are limited in that SAECs were used to model the epithelium instead of primary alveolar epithelial cells themselves, the results demonstrate that SAECs do contain a population of alveolar epithelial cells. The use of primary isolated ATII cells was limited by the availability of suitable donor human lungs. However, the limited data collected do demonstrate a trend suggestive of attenuated wound repair by these cells in the setting of HCA. Together these results suggest that while the epithelium and endothelium may exert potentially beneficial effects in response to HCA, their response may also be detrimental for subsequent recovery from ARDS. These results are concerning and highlight the need for randomised trials investigating the effects of HCA on clinical outcomes in the condition.

Despite decades of research, no pharmacological therapy currently exists for the treatment of ARDS[37]. The potential use of mesenchymal stem cells (MSCs) has generated considerable interest and is supported by an ever-increasing body of preclinical research. However, while MSCs are known to respond to their local environment – which may involve HCA when administered to mechanically ventilated patients with ARDS - their therapeutic capacity in the setting of HCA has never been investigated. HCA could have important implications for the efficacy of an MSC-based therapy and so the second aim of the current project was to determine the influence of HCA on the biological properties and therapeutic capacity of MSCs.

The results demonstrate that MSCs promote SAEC wound repair via enhanced cell migration under normocapnic conditions. However, this reparative capacity of MSCs is lost in HCA. This is the first time that the therapeutic capacity of MSCs in response to HCA has been investigated and suggests that HCA may attenuate the therapeutic capacity of MSCs in ARDS. These findings could have important implications in the interpretation of clinical trial data. They suggest that *a priori* posthoc analyses of data from patients with and without HCA should be planned as the presence of HCA may mask any MSC-driven improvements observed in patients in whom HCA is not present. This may allow for the identification of an effective therapy for at least a

subset of patients with ARDS where clinical trial data may otherwise demonstrate that an MSC-based therapy may be ineffective. Subsequently, it may allow the prospective identification of HCA to be developed as an exclusion criteria useful in the identification of patients with ARDS who are more likely to benefit from an MSC-based therapy.

The third aim of the current study was to elucidate the mechanisms of the effects of HCA on the inflammatory and reparative responses of HPMECs and SAECs, and on the therapeutic potential of MSCs. While considerable evidence supports a role for the NFκB pathway in mediating the effects of HCA in preclinical models of ARDS **(Section 1.7.1)**, the current study found no difference in the degree of activation of this pathway in any of the three cell types studied. However, the effects of HCA were associated with mitochondrial dysfunction in all three cell types. Importantly, functional mitochondria were required for the ability of MSCs to promote SAEC wound closure. MSCs have previously been shown to transfer mitochondria to surrounding cells where they enhance bioenergetics and are associated with therapeutic outcomes such as increased surfactant production by alveolar epithelial cells, improved barrier integrity, and enhanced phagocytosis by macrophages[338,341,368–370]. Mitochondrial transfer from MSCs to SAECs was observed in the current study, in both normocapnia and HCA. Additionally, a trend suggestive of enhanced ATP production by SAECs co-cultured with MSCs was observed in normocapnia. MSCs in which mitochondrial function has been inhibited with rhodamine 6G were not able to recapitulate the effect of uninhibited MSCs. Together these results suggest that MSCs improved SAEC wound closure in normocapnia via the transfer of functional mitochondria to SAECs where they augmented energy production within the cell. However, it appears that mitochondria transferred to SAECs in the setting of HCA were less functional and not capable of mounting the same response. HCA-induced attenuation of mitochondrial membrane potential occurred in a pH-independent manner, suggesting that clinical buffering of acidosis will not reverse this effect. These data represent a novel mechanism of the therapeutic effects of MSCs in ARDS and provide mechanistic insight which may pave the way for future improvements of an MSC-based therapy which may be more effective in patients with ARDS.

It is particularly noteworthy that HCA attenuated cell functions across all three cell types used in this study. These cells arise from different areas within the embryonic germ layer during development: while SAECs are of endodermal origin, HPMECs and MSCs are of mesodermal origin[371,372]. This suggests that HCA exerts a general effect on target cells, regardless of cell lineage. Previously reported data also support this theory as HCA impairs phagocytosis by both macrophages and neutrophils[140,152], while attenuated inflammatory responses have been reported across all four cell types relevant to the pathophysiology of ARDS: neutrophils, macrophages, epithelial cells, and endothelial cells[150,152,155,159,227]. Given the presence of mitochondria in most mammalian cells, the ability of HCA to induce mitochondrial dysfunction may explain this general effect on cell phenotype.

6.2 Future Directions

The current study demonstrated that HCA attenuated inflammatory cytokine secretion and wound repair by HPMECs and SAECs. These effects were associated with impaired mitochondrial function, but the results are limited by the lack of a definitive link between the two observations. Further work, for example repetition of cytokine analysis experiments with an additional group added in which mitochondrial depolarisation is induced by FCCP, will be required to bridge this gap in knowledge.

In addition, the current study did not address the individual contributions of pH and CO_2 to the effects of HCA on the inflammatory and reparative responses of HPMECs and SAECs. Clinically, the degree of acidosis can be reduced by the administration of buffers such as sodium bicarbonate. It is important that the individual contributions of pH and CO_2 are investigated in future studies as, if the negative effects of HCA observed in the current study are driven by acidosis rather than CO_2 *per se*, buffering could help lessen these effects and permit continuation of low tidal volume mechanical ventilation in patients with ARDS.

Of considerable importance, the results of the current study have also raised concerns with regard to the therapeutic potential of MSCs in the setting of HCA. Mitochondria were required for the ability of MSCs to promote SAEC wound closure. In the normocapnic setting mitochondria were transferred to SAECs. Transfer was also observed in the setting of HCA, but MSC mitochondrial function was impaired in this setting, suggesting that the mitochondria transferred in HCA were less functional. While a contact-independent mechanism of transfer was demonstrated, the exact mechanism of transfer was not elucidated. The transfer of mitochondria inside extracellular vesicles (EVs) has been demonstrated previously[341,373]. Further studies should investigate whether extracellular vesicles facilitate the transfer of mitochondria from MSCs to SAECs, and, if so, should confirm whether the attenuated therapeutic potential of MSCs in HCA results from the transfer of less functional mitochondria, and/or whether the capacity of the recipient cells to take them up is impaired in HCA.

CD44 expression on the surface of MSC-derived extracellular vesicles has been reported as important for their uptake by alveolar epithelial cells and macrophages[341,343]. Although it has not yet been studied, it is possible that HCA may attenuate EV expression of CD44 and subsequently attenuate their uptake by recipient cells. However, it is also possible that EV uptake by target cells is not altered by HCA and that the impaired therapeutic potential observed in the current study simply results from the transfer of less functional mitochondria within the EVs. Such investigations may open an avenue for the future development of an MSC-derived therapy which is independent of the cells themselves. For example, if it were found that fewer mitochondria were transferred to SAECs and that this was independent of the capacity of SAECs to take up EVs, MSC-generated EVs could be produced in normocapnia, collected and administered to patients with HCA in place of the cells themselves. There is currently interest in utilising EVs for the treatment of a number of conditions, and to date their clinical use appears to be feasible.

Chapter Seven – References

1. Ware, L. B. & Matthay, M. A. The Acute Respiratory Distress Syndrome. *N. Engl. J. Med.* **342,** 1334–1349 (2000).

2. Mac Sweeney, R. & McAuley, D. F. Acute respiratory distress syndrome. *Lancet* **388,** 2416–2430 (2016).

3. Thompson, B. T., Chambers, R. C. & Liu, K. D. Acute Respiratory Distress Syndrome. *N Engl J Med* **377,** 562–572 (2017).

4. Ashbaugh, D. G., Bigelow, D. B., Petty, T. L. & Levine, B. E. Acute Respiratory Distress in Adults. *Lancet* **2,** 319–323 (1967).

5. Bernard, G. R. *et al.* The American-European Consensus Conference on ARDS. Definitions, mechanisms, relevant outcomes, and clinical trial coordination. *Am J Respir Crit Care Med.* **149,** 818–824 (1994).

6. Ferguson, N. D. *et al.* The Berlin definition of ARDS: an expanded rationale, justification, and supplementary material. *Intensive Care Med.* **38,** 1573–1582 (2012).

7. The ARDS Definition Task Force. Acute Respiratory Distress Syndrome: The Berlin Definition. *JAMA* **307,** 2526–2533 (2012).

8. Armstrong, L., Jordan, N. & Millar, A. Interleukin 10 (IL-10) regulation of tumour necrosis factor alpha (TNF-alpha) from human alveolar macrophages and peripheral blood monocytes. *Thorax* **51,** 143–149 (1996).

9. Kobayashi, A. *et al.* Expression of inducible nitric oxide synthase and inflammatory cytokines in alveolar macrophages of ARDS following sepsis. *Chest* **113,** 1632–1639 (1998).

10. Williams, A. E. & Chambers, R. C. The mercurial nature of neutrophils: still an enigma in ARDS? *Am J Physiol Lung Cell Mol Physiol.* **306,** L217-230 (2014).

11. Williams, A. E. *et al.* Evidence for chemokine synergy during neutrophil migration in ARDS. *Thorax* **72,** 66–73 (2017).

12. Cox, G., Gauldie, J. & Jordana, M. Bronchial epithelial cell-derived cytokines (G-CSF and GM-CSF) promote the survival of peripheral blood neutrophils in vitro. *Am J Respir Cell Mol Biol.* **7,** 507–513 (1992).

13. Aggarwal, A., Baker, C. S., Evans, T. W. & Haslam, P. L. G-CSF and IL-8 but not GM-CSF correlate with severity of pulmonary neutrophilia in acute respiratory distress syndrome. *Eur Respir J.* **15,** 895–901 (2000).

14. Matute-Bello, G. *et al.* Soluble Fas ligand induces epithelial cell apoptosis in humans with acute lung injury (ARDS). *J Immunol.* **163,** 2217–2225 (1999).

15. Serrao, K. L., Fortenberry, J. D., Owens, M. L., Harris, F. L. & Brown, L. A. S. Neutrophils induce apoptosis of lung epithelial cells via release of soluble Fas ligand. *Am J Physiol Lung Cell Mol Physiol.* **280,** L298-305 (2001).

16. Saffarzadeh, M. *et al.* Neutrophil extracellular traps directly induce epithelial and endothelial cell death: a predominant role of histones. *PLoS One* **7,** e32366 (2012).

17. Seybold, J. *et al.* Tumor necrosis factor-alpha-dependent expression of phosphodiesterase 2: role in endothelial hyperpermeability. *Blood* **105,** 3569–3576 (2005).

18. Lopez-Ramirez, M. A. *et al.* Role of caspases in cytokine-induced barrier breakdown in human brain endothelial cells. *J Immunol.* **189,** 3130–3139 (2012).

19. Wessel, F. *et al.* Leukocyte extravasation and vascular permeability are each controlled in vivo by different tyrosine residues of VE-cadherin. *Nat. Immunol.* **15,** 223–230 (2014).

20. Ware, L. B. & Matthay, M. A. Alveolar fluid clearance is impaired in the majority of patients with acute lung injury and the acute respiratory distress syndrome. *Am J Respir Crit Care Med.* **163,** 1376–1383 (2001).

21. Barkauskas, C. E. *et al.* Type 2 alveolar cells are stem cells in adult lung. *J Clin Invest.* **132,** 3025–3036 (2013).

22. Zhao, J. *et al.* Autotaxin induces lung epithelial cell migration through lysoPLD activity-dependent and -independent pathways. *Biochem J.* **439,** 45–55 (2011).

23. Desai, T. J., Brownfield, D. G. & Krasnow, M. A. Alveolar progenitor and stem cells in lung development, renewal and cancer. *Nature* **507,** 190–194 (2014).

24. Schilders, K. A. A. *et al.* Regeneration of the lung: Lung stem cells and the development of lung mimicking devices. *Respir. Res.* **17,** 44 (2016).

25. Beers, M. F. & Morrisey, E. E. The three R's of lung health and disease: repair, remodeling, and regeneration. *J Clin Invest.* **121,** 2065–2073 (2011).

26. Millar, F. R., Summers, C., Griffiths, M. J., Toshner, M. R. & Proudfoot, A. G. The pulmonary endothelium in acute respiratory distress syndrome: insights and therapeutic opportunities. *Thorax* **71,** 462–473 (2016).

27. Marshall, R. P. *et al.* Fibroproliferation occurs early in the acute respiratory distress syndrome and impacts on outcome. *Am J Respir Crit Care Med.* **162,** 1783–1788 (2000).

28. Bellani, G. *et al.* Epidemiology, Patterns of Care, and Mortality for Patients With Acute Respiratory Distress Syndrome in Intensive Care Units in 50 Countries. *JAMA* **315,** 788–800 (2016).

29. McAuley, D. F. *et al.* Simvastatin in the acute respiratory distress syndrome. *N Engl J Med.* **371,** 1695–1703 (2014).

30. Rubenfeld, G. D. *et al.* Incidence and outcomes of acute lung injury. *N Engl J Med.* **353,** 1685–1693 (2005).

31. Weinert, C. R., Gross, C. R., Kangas, J. R., Bury, C. L. & Marinelli, W. A. Health-related quality of life after acute lung injury. *Am J Respir Crit Care Med.* **156,** 1120–1128 (1997).

32. Herridge, M. S. *et al.* One-year outcomes in survivors of the acute respiratory distress syndrome. *N. Engl. J. Med.* **348,** 683–693 (2003).

33. Hopkins, R. O. *et al.* Two-year cognitive, emotional, and quality-of-life outcomes in acute respiratory distress syndrome. *Am J Respir Crit Care Med.* **171,** 340–347 (2005).

34. Herridge, M. S. *et al.* Functional Disability 5 Years after Acute Respiratory Distress Syndrome. *N. Engl. J. Med.* (2011). doi:10.1056/NEJMoa1011802

35. Mikkelsen, M. E. *et al.* The adult respiratory distress syndrome cognitive outcomes study: long-term neuropsychological function in survivors of acute

lung injury. *Am J Respir Crit Care Med.* **185,** 1307–1315 (2012).

36. Pfoh, E. R. *et al.* Physical declines occurring after hospital discharge in ARDS survivors: a 5-year longitudinal study. *Intensive Care Med.* **42,** 1557–1566 (2016).

37. Boyle, A. J., Mac Sweeney, R. & McAuley, D. F. Pharmacological treatments in ARDS; a state-of-the-art update. *BMC Med.* **11,** 166 (2013).

38. The National Heart, Lung, and B. I. A. R. D. S. (ARDS) & Clinical Trials Network. Efficacy and safety of corticosteroids for persistent acute respiratory distress syndrome. *N Engl J Med.* **354,** 1671–1684 (2006).

39. Meduri, G. U. *et al.* Methylprednisolone infusion in early severe ARDS: results of a randomized controlled trial. *Chest* **131,** 954–963 (2007).

40. The National Heart, Lung, and B. I. A. R. D. S. (ARDS) C. T. N. Randomized, placebo-controlled clinical trial of an aerosolized β2-agonist for treatment of acute lung injury. *Am J Respir Crit Care Med.* **184,** 561–568 (2011).

41. Smith, F. G. *et al.* Effect of intravenous β-2 agonist treatment on clinical outcomes in acute respiratory distress syndrome (BALTI-2): a multicentre, randomised controlled trial. *Lancet* **379,** 229–235 (2012).

42. Gates, S. *et al.* Beta-Agonist Lung injury TrIal-2 (BALTI-2): a multicentre, randomised, double-blind, placebo-controlled trial and economic evaluation of intravenous infusion of salbutamol versus placebo in patients with acute respiratory distress syndrome. *Heal. Technol Assess.* **17,** 1–87 (2013).

43. The National Heart, Lung, and B. I. & ARDS Clinical Trials Network. Rosuvastatin for sepsis-associated acute respiratory distress syndrome. *N Engl J Med.* **370,** 2191–2200 (2014).

44. Sakuma, T. *et al.* Beta-adrenergic agonist stimulated alveolar fluid clearance in ex vivo human and rat lungs. *Am J Respir Crit Care Med.* **155,** 506–512 (1997).

45. McAuley, D. F., Frank, J. A., Fang, X. & Matthay, M. A. Clinically relevant concentrations of beta2-adrenergic agonists stimulate maximal cyclic adenosine monophosphate-dependent airspace fluid clearance and decrease

pulmonary edema in experimental acid-induced lung injury. *Crit Care Med.* **32,** 1470–1476 (2004).

46. Perkins, G. D., Gao, F. & Thickett, D. R. In vivo and in vitro effects of salbutamol on alveolar epithelial repair in acute lung injury. *Thorax* **63,** 215–220 (2008).

47. Smith, F. G. *et al.* Effect of intravenous β-2 agonist treatment on clinical outcomes in acute respiratory distress syndrome (BALTI-2): a multicentre, randomised controlled trial. *Lancet* **379,** 229–235 (2012).

48. Prescott, H. C., Calfee, C. S., Thompson, B. T., Angus, D. C. & Liu, V. X. Toward Smarter Lumping and Smarter Splitting: Rethinking Strategies for Sepsis and Acute Respiratory Distress Syndrome Clinical Trial Design. *Am J Respir Crit Care Med.* **194,** 147–155 (2016).

49. Jabaudon, M. *et al.* Recent directions in personalised acute respiratory distress syndrome medicine. *Anaesth Crit Care Pain Med.* (2017).

50. Calfee, C. S. *et al.* Subphenotypes in acute respiratory distress syndrome: latent class analysis of data from two randomised controlled trials. *Lancet Respir Med.* **2,** 611–620 (2014).

51. Famous, K. R. *et al.* Acute Respiratory Distress Syndrome Subphenotypes Respond Differently to Randomized Fluid Management Strategy. *Am J Respir Crit Care Med.* **195,** 331–338 (2017).

52. Zheng, G. *et al.* Treatment of acute respiratory distress syndrome with allogeneic adipose-derived mesenchymal stem cells: a randomized, placebo-controlled pilot study. *Respir Res.* **15,** 39 (2014).

53. Wilson, J. G. *et al.* Mesenchymal stem (stromal) cells for treatment of ARDS: a phase 1 clinical trial. *Lancet Respir Med.* **3,** 24–32 (2015).

54. The Acute Respiratory Distress Syndrome Network. Ventilation with lower tidal volumes as compared with traditional tidal volumes for acute lung injury and the acute respiratory distress syndrome. *N Engl J Med.* **342,** 1301–1308 (2000).

55. The National Heart, Lung, and B. I. A. R. D. & Syndrome (ARDS) Clinical Trials Network. Comparison of two fluid-management strategies in acute lung injury. *N Engl J Med.* **354,** 2564–2575 (2006).

56. Gupta, N. *et al.* Intrapulmonary delivery of bone marrow-derived mesenchymal stem cells improves survival and attenuates endotoxin-induced acute lung injury in mice. *J Immunol.* **179,** 1855–1863 (2007).

57. Nemeth, K. *et al.* Bone marrow stromal cells attenuate sepsis via prostaglandin E(2)-dependent reprogramming of host macrophages to increase their interleukin-10 production. *Nat Med.* **15,** 42–49 (2009).

58. Krasnodembskaya, A. *et al.* Antibacterial effect of human mesenchymal stem cells is mediated in part from secretion of the antimicrobial peptide LL-37. *Stem Cells* **28,** 2229–2238 (2010).

59. Curley, G. F. *et al.* Mesenchymal stem cells enhance recovery and repair following ventilator-induced lung injury in the rat. *Thorax* **67,** 496–501 (2012).

60. Gupta, N. *et al.* Mesenchymal stem cells enhance survival and bacterial clearance in murine Escherichia coli pneumonia. *Thorax* **67,** 533–539 (2012).

61. Krasnodembskaya, A. *et al.* Human mesenchymal stem cells reduce mortality and bacteremia in gram-negative sepsis in mice in part by enhancing the phagocytic activity of blood monocytes. *Am J Physiol Lung Cell Mol Physiol.* **302,** L1003-1013 (2012).

62. Asmussen, S. *et al.* Human mesenchymal stem cells reduce the severity of acute lung injury in a sheep model of bacterial pneumonia. *Thorax* **69,** 819–825 (2014).

63. Curley, G. F. *et al.* Cryopreserved, Xeno-Free Human Umbilical Cord Mesenchymal Stromal Cells Reduce Lung Injury Severity and Bacterial Burden in Rodent Escherichia coli-Induced Acute Respiratory Distress Syndrome. *Crit Care Med.* **45,** e202-212 (2017).

64. Lee, J. W., Fang, X., Gupta, N., Serikov, V. & Matthay, M. A. Allogeneic human mesenchymal stem cells for treatment of E. coli endotoxin-induced acute lung injury in the ex vivo perfused human lung. *Proc Natl Acad Sci U S*

A **106,** 16357–16362 (2009).

65. Lee, J. W. *et al.* Therapeutic Effects of Human Mesenchymal Stem Cells in Ex Vivo Human Lungs Injured with Live Bacteria. *Am J Respir Crit Care Med.* **187,** 751–760 (2013).

66. McAuley, D. F. *et al.* Clinical grade allogeneic human mesenchymal stem cells restore alveolar fluid clearance in human lungs rejected for transplantation. *Am J Physiol Lung Cell Mol Physiol.* **306,** L809-815 (2014).

67. The Acute Respiratory Distress Syndrome Network. Ventilation with Lower Tidal Volumes as Compared with Traditional Tidal Volumes for Acute Lung Injury and the Acute Respiratory Distress Syndrome. *N. Engl. J. Med.* **342,** 1301–1308 (2000).

68. Dreyfuss, D., Soler, P., Basset, G. & Saumon, G. High inflation pressure pulmonary edema. Respective effects of high airway pressure, high tidal volume, and positive end-expiratory pressure. *Am Rev Respir Dis.* **137,** 1159–1164 (1988).

69. Dreyfuss, D. & Saumon, G. Ventilator-induced lung injury: lessons from experimental studies. *Am J Respir Crit Care Med.* **157,** 294–323 (1998).

70. Gattinoni, L. & Pesenti, A. The concept of 'baby lung'. *Intensive Care Med.* **31,** 776–784 (2005).

71. Slutsky, A. S. & Tremblay, L. N. Multiple system organ failure. Is mechanical ventilation a contributing factor? *Am J Respir Crit Care Med.* **157,** 1721–1725 (1998).

72. Liu, Y.-Y. *et al.* Spillover of cytokines and reactive oxygen species in ventilator-induced lung injury associated with inflammation and apoptosis in distal organs. *Respir Care.* **59,** 1422–1432 (2014).

73. Beitler, J. R., Malhotra, A. & Thompson, B. T. Ventilator-induced Lung Injury. *Clin Chest Med.* **37,** 633–646 (2016).

74. Curley, G. F., Laffey, J. G., Zhang, H. & Slutsky, A. S. Biotrauma and Ventilator-Induced Lung Injury: Clinical Implications. *Chest* **150,** 1109–1117

(2016).

75. Gajic, O. *et al.* Ventilator-associated lung injury in patients without acute lung injury at the onset of mechanical ventilation. *Crit Care Med.* **32,** 1817–1824 (2004).

76. Gajic, O., Frutos-Vivar, F., Esteban, A., Hubmayr, R. D. & Anzueto, A. Ventilator settings as a risk factor for acute respiratory distress syndrome in mechanically ventilated patients. *Intensive Care Med.* **31,** 922–926 (2005).

77. Amato, M. B. P. *et al.* Effect of a protective-ventilation strategy on mortality in the acute respiratory distress syndrome. *N Engl J Med.* **338,** 347–354 (1998).

78. Fan, E. *et al.* An Official American Thoracic Society/European Society of Intensive Care Medicine/Society of Critical Care Medicine Clinical Practice Guideline: Mechanical Ventilation in Adult Patients with Acute Respiratory Distress Syndrome. *Am J Respir Crit Care Med.* **195,** 1253–1263 (2017).

79. Laffey, J. G. & Kavanagh, B. P. Carbon dioxide and the critically ill--too little of a good thing? *Lancet* **354,** 1283–1286 (1999).

80. Groenewegen, K. H., Schols, A. M. & Wouters, E. F. Mortality and mortality-related factors after hospitalization for acute exacerbation of COPD. *Chest* **124,** 459–467 (2003).

81. Belkin, R. A. *et al.* Risk factors for death of patients with cystic fibrosis awaiting lung transplantation. *Am J Respir Crit Care Med.* **173,** 659–666 (2006).

82. Kregenow, D. A., Rubenfeld, G. D., Hudson, L. D. & Swenson, E. R. Hypercapnic acidosis and mortality in acute lung injury. *Crit Care Med.* **34,** 1–7 (2006).

83. Tiruvoipati, R., Pilcher, D., Buscher, H., Botha, J. & Bailey, M. Effects of Hypercapnia and Hypercapnic Acidosis on Hospital Mortality in Mechanically Ventilated Patients. *Crit Care Med.* **45,** e649-656 (2017).

84. Arthurs, G. J. & Sudhakar, M. Carbon dioxide transport. *Contin. Educ. Anaesth. Crit. Care Pain* **5,** 207–210 (2005).

85. Musa-Aziz, R., Chen, L.-M., Pelletier, M. F. & Boron, W. F. Relative CO2/NH3 selectivities of AQP1, AQP4, AQP5, AmtB, and RhAG. *Proc Natl Acad Sci U S A* **106,** 5406–5411 (2009).

86. Shigemura, M., Lecuona, E. & Sznajder, J. I. Effects of hypercapnia on the lung. *J Physiol.* **595,** 2431–2437 (2017).

87. Tresguerres, M., Buck, J. & Levin, L. R. Physiological carbon dioxide, bicarbonate, and pH sensing. *Eur J Physiol* **460,** 953–964 (2010).

88. Zippin, J. H. *et al.* Compartmentalization of bicarbonate-sensitive adenylyl cyclase in distinct signaling microdomains. *FASEB J.* **17,** 82–84 (2003).

89. Geng, W. *et al.* Cloning and characterization of the human soluble adenylyl cyclase. *Am J Physiol Cell Physiol.* **288,** C1305-1316 (2005).

90. Schmid, A. *et al.* Soluble adenylyl cyclase is localized to cilia and contributes to ciliary beat frequency regulation via production of cAMP. *J Gen Physiol.* **130,** 99–109 (2007).

91. Schmid, A. *et al.* Decreased soluble adenylyl cyclase activity in cystic fibrosis is related to defective apical bicarbonate exchange and affects ciliary beat frequency regulation. *J Biol Chem.* **285,** 29998–30007 (2010).

92. Obiako, B. *et al.* Bicarbonate disruption of the pulmonary endothelial barrier via activation of endogenous soluble adenylyl cyclase, isoform 10. *Am J Physiol Lung Cell Mol Physiol.* **305,** L185–L192 (2013).

93. Lecuona, E. *et al.* Protein kinase A-Iα regulates Na,K-ATPase endocytosis in alveolar epithelial cells exposed to high CO(2) concentrations. *Am J Respir Cell Mol Biol.* **48,** 626–634 (2013).

94. An, S., Tsai, C. & Goetzl, E. J. Cloning, sequencing and tissue distribution of two related G protein-coupled receptor candidates expressed prominently in human lung tissue. *FEBS Lett.* **375,** 121–124 (1995).

95. Chen, A. *et al.* Activation of GPR4 by acidosis increases endothelial cell adhesion through the cAMP/Epac pathway. *PLoS One* **6,** e27586 (2011).

96. Dong, L. *et al.* Acidosis Activation of the Proton-Sensing GPR4 Receptor

Stimulates Vascular Endothelial Cell Inflammatory Responses Revealed by Transcriptome Analysis. *PLoS One* **8,** e61991 (2013).

97. Castellone, R. D., Leffler, N. R., Dong, L. & Yang, L. V. Inhibition of tumor cell migration and metastasis by the proton-sensing GPR4 receptor. *Cancer Lett.* **312,** 197–208 (2011).

98. Kregenow, D. A. & Swenson, E. R. The lung and carbon dioxide: implications for permissive and therapeutic hypercapnia. *Eur Respir J.* **20,** 6–11 (2002).

99. Hillered, L., Ernster, L. & Siesjo, B. K. Influence of in vitro lactic acidosis and hypercapnia on respiratory activity of isolated rat brain mitochondria. *J Cereb Blood Flow Metab.* **4,** 430–437 (1984).

100. Akca, O. *et al.* Hypercapnia improves tissue oxygenation. *Anesthesiology* **97,** 801–806 (2002).

101. Akca, O. *et al.* Tissue oxygenation response to mild hypercapnia during cardiopulmonary bypass with constant pump output. *Br J Anaesth.* **96,** 708–714 (2006).

102. Brugniaux, J. V., Hodges, A. N. H., Hanly, P. J. & Poulin, M. J. Cerebrovascular responses to altitude. *Respir Physiol Neurobiol.* **158,** 212–223 (2007).

103. Ainslie, P. N. & Duffin, J. Integration of cerebrovascular CO2 reactivity and chemoreflex control of breathing: mechanisms of regulation, measurement, and interpretation. *Am J Physiol Regul Integr Comp Physiol.* **296,** R1473-1495 (2009).

104. Grubb, R. L., Raichle, M. E., Eichling, J. O. & Ter-Pogossian, M. M. The effects of changes in PaCO2 on cerebral blood volume, blood flow, and vascular mean transit time. *Stroke* **5,** 630–639 (1974).

105. Vannucci, R. C., Towfighi, J., Heitjan, D. F. & Brucklacher, R. M. Carbon dioxide protects the perinatal brain from hypoxic-ischemic damage: an experimental study in the immature rat. *Pediatrics* **95,** 868–874 (1995).

106. Brambrink, A. & Orfanakis, A. 'Therapeutic hypercapnia' after ischemic brain

injury: is there a potential for neuroprotection? *Anesthesiology* **112,** 274–276 (2010).

107. Zhou, Q. *et al.* Effects of permissive hypercapnia on transient global cerebral ischemia-reperfusion injury in rats. *Anesthesiology* **112,** 288–297 (2010).

108. Keenan, R. J., Todd, T. R. J., Demajo, W. & Slutsky, A. S. Effects of hypercarbia on arterial and alveolar oxygen tensions in a model of gram-negative pneumonia. *J Appl Physiol* **68,** 1820–1825 (1990).

109. Brogan, T. V., Robertson, H. T., Lamm, W. J. E. & Souders, J. E. Carbon dioxide added late in inspiration reduces ventilation-perfusion heterogeneity without causing respiratory acidosis. *J Appl Physiol* **96,** 1894–1898 (2004).

110. Sinclair, S. E. *et al.* Therapeutic hypercapnia and ventilation-perfusion matching in acute lung injury: low minute ventilation vs inspired CO2. *Chest* **130,** 85–92 (2006).

111. Andreeva, A. V., Kutuzov, M. A. & Voyno-Yasenetskaya, T. A. Regulation of surfactant secretion in alveolar type II cells. *Am J Physiol Lung Cell Mol Physiol.* **293,** L259-271 (2007).

112. Petty, T. L., Silvers, G. W., Paul, G. W. & Stanford, R. E. Abnormalities in lung elastic properties and surfactant function in adult respiratory distress syndrome. *Chest* **75,** 751–754 (1979).

113. Hallman, M., Spragg, R., Harrell, J. H., Moser, K. M. & Gluck, L. Evidence of lung surfactant abnormality in respiratory failure. Study of bronchoalveolar lavage phospholipids, surface activity, phospholipase activity, and plasma myoinositol. *J Clin Invest.* **70,** 673–683 (1982).

114. Gunther, A. *et al.* Surfactant alterations in severe pneumonia, acute respiratory distress syndrome, and cardiogenic lung edema. *Am J Respir Crit Care Med.* **153,** 176–184 (1996).

115. Contreras, M., Masterson, C. & Laffey, J. G. Permissive hypercapnia: what to remember. *Curr Opin Anaesthesiol.* **28,** 26–37 (2015).

116. Emery, M. J., Eveland, R. L., Min, J.-H., Hildebrandt, J. & Swenson, E. R. CO2

relaxation of the rat lung parenchymal strip. *Respir Physiol Neurobiol.* **186,** 33–39 (2013).

117. Lele, E. E. *et al.* Bronchoconstriction during alveolar hypocapnia and systemic hypercapnia in dogs with a cardiopulmonary bypass. *Respir Physiol Neurobiol.* **175,** 140–145 (2011).

118. Tashkin, D. P. & Simmons, D. H. Effect of Carbon Dioxide Breathing on Specific Airway Conductance in Normal and Asthmatic Subjects. *Am Rev Respir Dis.* **106,** 729–739 (1972).

119. D'Angelo, E., Calderini, I. S. & Tavola, M. The effects of CO2 on respiratory mechanics in anesthetized paralyzed humans. *Anesthesiology* **94,** 604–610 (2001).

120. Finucane, K. E. & Singh, B. Role of bronchodilation and pattern of breathing in increasing expiratory flow during progressive hypercapnia in chronic obstructive pulmonary disease. *J Appl Physiol* (2017).

121. Fard, N. *et al.* Acute respiratory distress syndrome induction by pulmonary ischemia–reperfusion injury in large animal models. *J Surg Res.* **189,** 274–284 (2014).

122. Caruso, P. & Gomes, S. Ischemia/reperfusion-induced lung injury prevention: many options, no choices. *J Bras Pneumol.* **42,** 7–8 (2016).

123. Shibata, K. *et al.* Hypercapnic acidosis may attenuate acute lung injury by inhibition of endogenous xanthine oxidase. *Am J Respir Crit Care Med.* **159,** 1578–1584 (1998).

124. Laffey, J. G. *et al.* Therapeutic hypercapnia reduces pulmonary and systemic injury following in vivo lung reperfusion. *Am J Respir Crit Care Med.* **162,** 2287–2294 (2000).

125. Laffey, J. G. *et al.* Effects of therapeutic hypercapnia on mesenteric ischemia-reperfusion injury. *Am J Respir Crit Care Med.* **168,** 1383–1390 (2003).

126. Wu, S.-Y. *et al.* Hypercapnic acidosis attenuates reperfusion injury in isolated and perfused rat lungs. *Crit Care Med.* **40,** 553–559 (2012).

127. Wu, S.-Y. *et al.* Protective effect of hypercapnic acidosis in ischemia-reperfusion lung injury is attributable to upregulation of heme oxygenase-1. *PLoS One* **8,** e74742 (2013).

128. Broccard, A. F. *et al.* Protective effects of hypercapnic acidosis on ventilator-induced lung injury. *Am J Respir Crit Care Med.* **164,** 802–806 (2001).

129. Sinclair, S. E. *et al.* Hypercapnic acidosis is protective in an in vivo model of ventilator-induced lung injury. *Am J Respir Crit Care Med.* **166,** 403–408 (2002).

130. Halbertsma, F. *et al.* Hypercapnic acidosis attenuates the pulmonary innate immune response in ventilated healthy mice. *Crit. Care Med.* **36,** 2403–2406 (2008).

131. Peltekova, V. *et al.* Hypercapnic acidosis in ventilator-induced lung injury. *Intensive Care Med.* **36,** 869–878 (2010).

132. Contreras, M. *et al.* Hypercapnic acidosis attenuates ventilation-induced lung injury by a nuclear factor-κB-dependent mechanism. *Crit Care Med.* **40,** 2622–2630 (2012).

133. Bellani, G. *et al.* Epidemiology, Patterns of Care, and Mortality for Patients With Acute Respiratory Distress Syndrome in Intensive Care Units in 50 Countries. *JAMA* **315,** 788–800 (2016).

134. Emori, T. G. & Gaynes, R. P. An overview of nosocomial infections, including the role of the microbiology laboratory. *Clin Microbiol Rev*. **6,** 428–442 (1993).

135. O'Croinin, D. F. *et al.* Hypercapnic acidosis does not modulate the severity of bacterial pneumonia–induced lung injury. *Crit Care Med.* **33,** 2606–2612 (2005).

136. Ni Chonghaile, M., Higgins, B. D., Costello, J. F. & Laffey, J. G. Hypercapnic acidosis attenuates severe acute bacterial pneumonia-induced lung injury by a neutrophil-independent mechanism. *Crit Care Med.* **36,** 3135–3144 (2008).

137. Ni Chonghaile, M., Higgins, B. D., Costello, J. & Laffey, J. G. Hypercapnic Acidosis Attenuates Lung Injury Induced by Established Bacterial Pneumonia.

Anesthesiology **109,** 837–848 (2008).

138. Pugin, J. *et al.* Cyclic stretch of human lung cells induces an acidification and promotes bacterial growth. *Am J Respir Cell Mol Biol.* **38,** 362–370 (2008).

139. O'Croinin, D. F. *et al.* Sustained hypercapnic acidosis during pulmonary infection increases bacterial load and worsens lung injury. *Crit Care Med.* **36,** 2128–2135 (2008).

140. Gates, K. *et al.* Hypercapnia impairs lung neutrophil function and increases mortality in murine pseudomonas pneumonia. *Am J Respir Cell Mol Biol.* **49,** 821–828 (2013).

141. Lewis, A. J., Seymour, C. W. & Rosengart, M. R. Current Murine Models of Sepsis. *Surg Infect (Larchmt).* **17,** 385–393 (2016).

142. Toscano, M. G., Ganea, D. & Gamero, A. M. Cecal ligation puncture procedure. *J Vis Exp.* **51,** e2860 (2011).

143. Ruiz, S. *et al.* Sepsis modeling in mice: ligation length is a major severity factor in cecal ligation and puncture. *Intensive Care Med Exp.* **4,** 22 (2016).

144. Higgins, B. D. *et al.* Differential Effects of Buffered Hypercapnia versus Hypercapnic Acidosis on Shock and Lung Injury Induced by Systemic Sepsis. *Anesthesiology* **111,** 1317–1326 (2009).

145. Costello, J. *et al.* Hypercapnic acidosis attenuates shock and lung injury in early and prolonged systemic sepsis. *Crit Care Med.* **37,** 2412–2420 (2009).

146. Garrido, A. G., De Figueiredo, L. F. P. & Silva, M. R. Experimental models of sepsis and septic shock: an overview. *Acta Cir. Bras.* **19,** (2004).

147. Wang, Z., Su, F., Bruhn, A., Yang, X. & Vincent, J.-L. Acute Hypercapnia Improves Indices of Tissue Oxygenation More than Dobutamine in Septic Shock. *Am J Respir Crit Care Med.* **177,** 178–183 (2008).

148. Bastarache, J. A. & Blackwell, T. S. Development of animal models for the acute respiratory distress syndrome. *Dis Model Mech.* **2,** 218–223 (2009).

149. Martin, T. R. & Frevert, C. W. Innate Immunity in the Lungs. *Proc Am Thorac Soc.* **2,** 403–411 (2005).

150. Lang, C. J., Dong, P., Hosszu, E. K. & Doyle, I. R. Effect of CO2 on LPS-induced cytokine responses in rat alveolar macrophages. *Am J Physiol Lung Cell Mol Physiol.* **289,** L96-103 (2005).

151. Wang, N. *et al.* Elevated CO2 selectively inhibits interleukin-6 and tumor necrosis factor expression and decreases phagocytosis in the macrophage. *FASEB J.* **24,** 2178–2190 (2010).

152. Wang, N. *et al.* Elevated CO2 selectively inhibits interleukin-6 and tumor necrosis factor expression and decreases phagocytosis in the macrophage. *FASEB J.* **24,** 2178–90 (2010).

153. Casalino-Matsuda, S. M., Nair, A., Beitel, G. J., Gates, K. L. & Sporn, P. H. S. Hypercapnia Inhibits Autophagy and Bacterial Killing in Human Macrophages by Increasing Expression of Bcl-2 and Bcl-xL. *J Immunol* **194,** 5388–5396 (2015).

154. Virgin, H. W. & Levine, B. Autophagy genes in immunity. *Nat Immunol.* **10,** 461–470 (2009).

155. Coakley, R. J., Taggart, C., Greene, C., MvElvaney, N. G. & O'Neill, S. J. Ambient pCO2 modulates intracellular pH, intracellular oxidant generation, and interleukin-8 secretion in human neutrophils. *J Leukoc Biol.* **71,** 603–610 (2002).

156. Dahlgren, C., Karlsson, A. & Bylung, J. Measurement of respiratory burst products generated by professional phagocytes. *Methods Mol Biol.* **412,** 349–363 (2007).

157. Takeshita, K. *et al.* Hypercapnic acidosis attenuates endotoxin-induced nuclear factor-κB activation. *Am. J. Respir. Cell Mol. Biol.* **29,** 124–132 (2003).

158. Liu, Y. *et al.* Modulatory effects of hypercapnia on in vitro and in vivo pulmonary endothelial-neutrophil adhesive responses during inflammation. *Cytokine* **44,** 108–17 (2008).

159. Horie, S. *et al.* Hypercapnic acidosis attenuates pulmonary epithelial stretch-induced injury via inhibition of the canonical NF-κB pathway. *Intensive Care Med Exp.* **4,** (2016).

160. O'Toole, D. *et al.* Hypercapnic acidosis attenuates pulmonary epithelial wound repair by an NF-kappaB dependent mechanism. *Thorax* **64,** 976–982 (2009).

161. Vohwinkel, C. U. *et al.* Elevated CO2 Levels Cause Mitochondrial Dysfunction and Impair Cell Proliferation. *J Biol Chem.* **286,** 37067–37076 (2011).

162. Vadasz, I., Hubmayr, R. D., Min, N., Sporn, P. H. S. & Sznajder, J. I. Hypercapnia: a nonpermissive environment for the lung. *Am J Respir Cell Mol Biol.* **46,** 417–421 (2012).

163. Laffey, J. G., Engelberts, D. & Kavanagh, B. P. Buffering hypercapnic acidosis worsens acute lung injury. *Am J Respir Crit Care Med.* **161,** 141–146 (2000).

164. Briva, A. *et al.* High CO2 levels impair alveolar epithelial function independently of pH. *PLoS One* **2,** e1238 (2007).

165. Caples, S. M., Rasmussen, D. L., Lee, W. Y., Wolfert, M. Z. & Hubmayr, R. D. Impact of buffering hypercapnic acidosis on cell wounding in ventilator-injured rat lungs. *Am J Physiol Lung Cell Mol Physiol.* **296,** L140-144 (2009).

166. Velissaris, D., Karamouzos, V., Ktenopoulos, N., Pierrackos, C. & Karanikolas, M. The Use of Sodium Bicarbonate in the Treatment of Acidosis in Sepsis: A Literature Update on a Long Term Debate. *Crit. Care Res. Pract.* (2015).

167. Nahas, G. G. *et al.* Guidelines for the Treatment of Acidaemia with THAM. *Drugs* **55,** 191–224 (1998).

168. Kallet, R. H., Jasmer, R. M., Luce, J. M., Lin, L. H. & Marks, J. D. The Treatment of Acidosis in Acute Lung Injury with Tris-Hydroxymethyl Aminomethane (THAM). *Am J Respir Crit Care Med.* **161,** 1149–1153 (2000).

169. Hoffman, E., Dittrich-Breiholz, O., Holtmann, H. & Kracht, M. Multiple control of interleukin-8 gene expression. *J Leukoc Biol.* **72,** 847–855 (2002).

170. Liu, H. *et al.* TNF-alpha gene expression in macrophages: regulation by NF-kappa B is independent of c-Jun or C/EBP beta. *J Immunol.* **164,** 4277–4285 (2000).

171. Melotti, P. *et al.* Activation of NF-kB mediates ICAM-1 induction in respiratory cells exposed to an adenovirus-derived vector. *Gene Ther.* **8,** 1436–

1442 (2001).

172. Hadad, N., Tuval, L., Elgazar-Carmom, V., Levy, R. & Levey, R. Endothelial ICAM-1 protein induction is regulated by cytosolic phospholipase A2α via both NF-κB and CREB transcription factors. *J Immunol.* **186,** 1816–1827 (2011).

173. Oeckinghaus, A. & Ghosh, S. The NF-kappaB family of transcription factors and its regulation. *Cold Spring Harbor perspectives in biology* (2009).

174. Oeckinghaus, A., Hayden, M. S. & Ghosh, S. Crosstalk in NF-κB signaling pathways. *Nat Immunol.* **12,** 695–708 (2011).

175. Cummins, E. P. *et al.* NF-κB links CO2 sensing to innate immunity and inflammation in mammalian cells. *J Immunol.* **185,** 4439–4445 (2010).

176. Masterson, C. *et al.* Effects and Mechanisms by Which Hypercapnic Acidosis Inhibits Sepsis-Induced Canonical Nuclear Factor-κB Signaling in the Lung. *Crit. Care Med.* **44,** e207-217 (2015).

177. Oliver, K. M. *et al.* Hypercapnia induces cleavage and nuclear localization of RelB protein, giving insight into CO2 sensing and signaling. *J Biol Chem.* **287,** 14004–14011 (2012).

178. Keogh, C. E. *et al.* Carbon dioxide-dependent regulation of NF-κB family members RelB and p100 gives molecular insight into CO2-dependent immune regulation. *J Biol Chem.* **292,** 11561–11571 (2017).

179. Shaughnessy, D. T. *et al.* Mitochondria, energetics, epigenetics, and cellular responses to stress. *Env. Heal. Perspect.* **122,** 1271–1278 (2014).

180. Suomalainen, A. & Battersby, B. J. Mitochondrial diseases: the contribution of organelle stress responses to pathology. *Nat Rev Mol Cell Biol.* (2017).

181. Huttemann, M. *et al.* Regulation of mitochondrial respiration and apoptosis through cell signaling: cytochrome c oxidase and cytochrome c in ischemia/reperfusion injury and inflammation. *Biochim Biophys Acta.* **1817,** 598–609 (2012).

182. Tait, S. W. G. & Green, D. R. Mitochondria and cell death: outer membrane permeabilization and beyond. *Nat Rev Mol Cell Biol.* **11,** 621–632 (2010).

183. Korshunov, S. S., Skulachev, V. P. & Starkov, A. A. High protonic potential actuates a mechanism of production of reactive oxygen species in mitochondria. *FEBS Lett.* **416,** 15–18 (1997).

184. West, A. P., Shadel, G. S. & Ghosh, S. Mitochondria in innate immune responses. *Nat Rev Immunol.* **11,** 389–402 (2011).

185. Bulua, A. C. *et al.* Mitochondrial reactive oxygen species promote production of proinflammatory cytokines and are elevated in TNFR1-associated periodic syndrome (TRAPS). *J Exp Med.* **208,** 519–533 (2011).

186. West, A. P. *et al.* TLR signalling augments macrophage bactericidal activity through mitochondrial ROS. *Nature* **472,** 476–480 (2011).

187. Helenius, I. T. *et al.* Identification of Drosophila Zfh2 as a Mediator of Hypercapnic Immune Regulation by a Genome-Wide RNA Interference Screen. *J Immunol.* **196,** 655–667 (2016).

188. Casalino-Matsuda, S. *et al.* ZFHX3 selectively modulates hypercapnia-regulated gene expression in lipopolysaccharide-stimulated macrophages. *Am. J. Respir. Crit. Care Med.* (2013).

189. Terragni, P. P. *et al.* Tidal hyperinflation during low tidal volume ventilation in acute respiratory distress syndrome. *Am J Respir Crit Care Med.* **175,** 160–166 (2007).

190. Terragni, P. P. *et al.* Tidal volume lower than 6 ml/kg enhances lung protection: role of extracorporeal carbon dioxide removal. *Anesthesiology* **111,** 826–835 (2009).

191. Bein, T. *et al.* Lower tidal volume strategy (≈3 ml/kg) combined with extracorporeal CO2 removal versus 'conventional' protective ventilation (6 ml/kg) in severe ARDS. *Intensive Care Med.* **39,** 847–856 (2013).

192. Bonfield, T. L. *et al.* Cell based therapy aides in infection and inflammation resolution in the murine model of cystic fibrosis lung disease. *Stem Cell Discov.* **3,** 139–153 (2013).

193. Sutton, M. T. *et al.* Antimicrobial Properties of Mesenchymal Stem Cells:

Therapeutic Potential for Cystic Fibrosis Infection, and Treatment. *Stem Cells Int.* (2016).

194. Antunes, M. A., Lapa e Silva, J. R. & Rocco, P. R. M. Mesenchymal stromal cell therapy in COPD: from bench to bedside. *Int J Chron Obs. Pulmon Dis.* **12,** 3017–3027 (2017).

195. Cheng, S.-L., Lin, C.-H. & Yao, C.-L. Mesenchymal Stem Cell Administration in Patients with Chronic Obstructive Pulmonary Disease: State of the Science. *Stem Cells Int.* (2017).

196. Mehta, D. & Malik, A. B. Signaling Mechanisms Regulating Endothelial Permeability. *Physiol. Rev.* **86,** 279–367 (2006).

197. Yousif, L., Di Russo, J. & Sorokin, L. Laminin isoforms in endothelial and perivascular basement membranes. *Cell Adhes. Migr.* **7,** 101–110 (2013).

198. West, J. Thoughts on the pulmonary blood-gas barrier. *Am J Physiol Lung Cell Mol Physiol.* **285,** L501-513 (2003).

199. Barron, L., Gharib, S. & Duffield, J. Lung Pericytes and Resident Fibroblasts: Busy Multitaskers. *Am J Pathol* **186,** 2519–2531 (2016).

200. Schmidt, E. P. *et al.* The pulmonary endothelial glycocalyx regulates neutrophil adhesion and lung injury during experimental sepsis. *Nat. Med.* **18,** 1217–1223 (2012).

201. Tak, P. P. & Firestein, G. S. NF-κB: a key role in inflammatory diseases. *J Clin Invest.* **107,** 7–11 (2001).

202. Lopez-Armada, M. J., Riveiro-Naveira, R. R., Vaamonde-Garcia, C. & Valcarcel-Ares, M. N. Mitochondrial dysfunction and the inflammatory response. *Mitochondrion* **13,** 106–118 (2013).

203. Pober, J. S. & Sessa, W. C. Evolving functions of endothelial cells in inflammation. *Nat. Rev. Immunol.* **7,** 803–815 (2007).

204. Grau, G. E. *et al.* Phenotypic and functional analysis of pulmonary microvascular endothelial cells from patients with acute respiratory distress syndrome. *Lab Invest* **74,** 761–770 (1996).

205. Aird, W. C. Phenotypic heterogeneity of the endothelium: I. Structure, function, and mechanisms. *Circ. Res.* **100,** 158–173 (2007).

206. Aird, W. C. Phenotypic heterogeneity of the endothelium: II. Representative vascular beds. *Circ. Res.* **100,** 174–190 (2007).

207. Summers, C. *et al.* Pulmonary retention of primed neutrophils: a novel protective host response, which is impaired in the acute respiratory distress syndrome. *Thorax* **69,** 623–629 (2014).

208. Doerschuk, C. M., Beyers, N., Coxson, H. O., Wiggs, B. & Hogg, J. C. Comparison of neutrophil and capillary diameters and their relation to neutrophil sequestration in the lung. *J. Appl. Physiol.* **74,** 3040–3045 (1993).

209. Gebb, S. A. *et al.* Sites of leukocyte sequestration in the pulmonary microcirculation. *J. Appl. Physiol.* **79,** 493–497 (1995).

210. Skoutelis, A. T. *et al.* Neutrophil deformability in patients with sepsis, septic shock, and adult respiratory distress syndrome. *Crit. Care Med.* **28,** 2355–2359 (2000).

211. Drost, E. M. & MacNee, W. Potential role of IL-8, platelet-activating factor and TNF-α in the sequestration of neutrophils in the lung: effects on neutrophil deformability, adhesion receptor expression, and chemotaxis. *Eur. J. Immunol.* **32,** 393–403 (2002).

212. Kubo, H. *et al.* L- and P-selectin and CD11/CD18 in intracapillary neutrophil sequestration in rabbit lungs. *Am. J. Respir. Crit. Care Med.* **159,** 267–274 (1999).

213. Diamond, M. S., Staunton, D. E., Marlin, S. D. & Springer, T. A. Binding of the integrin Mac-1 (CD11b/CD18) to the third immunoglobulin-like domain of ICAM-1 (CD54) and its regulation by glycosylation. *Cell* **65,** 961–971 (1991).

214. Moreland, J. G., Fuhrman, R. M., Pruessner, J. A. & Schwartz, D. A. CD11b and intercellular adhesion molecule-1 are involved in pulmonary neutrophil recruitment in lipopolysaccharide-induced airway disease. *Am J Respir Cell Mol Biol.* **27,** 474–480 (2002).

215. Miyao, N. *et al.* Various adhesion molecules impair microvascular leukocyte kinetics in ventilator-induced lung injury. *Am J Physiol Lung Cell Mol Physiol.* **290,** L1059-1068 (2006).

216. Callicutt, C. S. *et al.* Diminished lung injury with vascular adhesion molecule-1 blockade in choline-deficient ethionine diet-induced pancreatitis. *Surgery* **133,** 186–196 (2003).

217. Nolte, D., Kuebler, W. M., Muller, W. A., Wolff, K. D. & Messmer, K. Attenuation of leukocyte sequestration by selective blockade of PECAM-1 or VCAM-1 in murine endotoxemia. *Eur Surg Res.* **36,** 331–337 (2004).

218. Laudes, I. J. *et al.* Disturbed homeostasis of lung intercellular adhesion molecule-1 and vascular cell adhesion molecule-1 during sepsis. *Am J Pathol.* **164,** 1435–1445 (2004).

219. Vaporciyan, A. A. *et al.* Involvement of platelet-endothelial cell adhesion molecule-1 in neutrophil recruitment in vivo. *Science (80-.).* **262,** 1580–1582 (1993).

220. Orfanos, S. ., Mavrommati, I., Korovesi, I. & Roussos, C. Pulmonary endothelium in acute lung injury: from basic science to the critically ill. *Intensive Care Med.* **30,** 1702–1714 (2004).

221. Kaynar, A. M., Houghton, A. M., Lum, E. H., Pitt, B. R. & Shapiro, S. D. Neutrophil Elastase Is Needed for Neutrophil Emigration into Lungs in Ventilator-Induced Lung Injury. *Am J Respir Cell Mol Biol.* **39,** 53–60 (2008).

222. Kása, A., Csortos, C. & Verin, A. D. Cytoskeletal mechanisms regulating vascular endothelial barrier function in response to acute lung injury. *Tissue Barriers* **3,** e974448 (2015).

223. Bongard, R. D. *et al.* Depleted energy charge and increased pulmonary endothelial permeability induced by mitochondrial complex I inhibition are mitigated by coenzyme Q1 in the isolated perfused rat lung. *Free Radic Biol Med.* **65,** 1455–1463 (2014).

224. Yamazaki, D. *et al.* WAVE2 is required for directed cell migration and cardiovascular development. *Nature* **424,** 452–456 (2003).

225. Mooren, O. L., Li, J., Nawas, J. & Cooper, J. A. Endothelial cells use dynamic actin to facilitate lymphocyte transendothelial migration and maintain the monolayer barrier. *Mol Biol Cell.* **25,** 4115–4129 (2014).

226. Angelini, D. J. *et al.* TNF-alpha increases tyrosine phosphorylation of vascular endothelial cadherin and opens the paracellular pathway through fyn activation in human lung endothelia. *Am J Physiol Lung Cell Mol Physiol* **291,** L1232–L1245 (2006).

227. Takeshita, K. *et al.* Hypercapnic acidosis attenuates endotoxin-induced nuclear factor-[kappa]B activation. *Am J Respir Cell Mol Biol.* **29,** 124–132 (2003).

228. Hillyer, P., Mordelet, E., Flynn, G. & Male, D. Chemokines, chemokine receptors and adhesion molecules on different human endothelia: discriminating the tissue-specific functions that affect leucocyte migration. *Clin Exp Immunol.* **134,** 431–441 (2003).

229. Beck, G. C., Yard, B. A., Breedijk, A. J., van Ackern, K. & van der Woude, F. J. Release of CXC-chemokines by human lung microvascular endothelial cells (LMVEC) compared with macrovascular umbilical vein endothelial cells. *Clin Exp Immunol.* **118,** 298–303 (1999).

230. Burg, J., Krump-Konvalinkova, V., Bittinger, F. & Kirkpatrick, C. J. GM-CSF expression by human lung microvascular endothelial cells: in vitro and in vivo findings. *Am J Physiol Lung Cell Mol Physiol.* **283,** L460-467 (2002).

231. Rydkina, E., Turpin, L. C. & Sahni, S. K. Rickettsia rickettsii infection of human macrovascular and microvascular endothelial cells reveals activation of both common and cell type-specific host response mechanisms. *Infect Immun.* **78,** 2599–2606 (2010).

232. Muller, A. M., Hermanns, M. I., Cronen, C. & Kirkpatrick, C. J. Comparative study of adhesion molecule expression in cultured human macro- and microvascular endothelial cells. *Exp Mol Pathol.* **73,** 171–180 (2002).

233. Shelton, J. L. *et al.* Albumin leak across human pulmonary microvascular vs. umbilical vein endothelial cells under septic conditions. *Microvasc Res.* **71,** 40–47 (2006).

234. Higgins, B. D. *et al.* Differential effects of buffered hypercapnia versus hypercapnic acidosis on shock and lung injury induced by systemic sepsis. *Anesthesiology* **111,** 1317–1326 (2009).

235. Nardelli, L. M. *et al.* Effects of acute hypercapnia with and without acidosis on lung inflammation and apoptosis in experimental acute lung injury. *Respir Physiol Neurobiol.* **205,** 1–6 (2015).

236. Jorens, P. G. *et al.* Interleukin 8 (IL-8) in the bronchoalveolar lavage fluid from patients with the adult respiratory distress syndrome (ARDS) and patients at risk for ARDS. *Cytokine* **4,** 592–597 (1992).

237. Miller, E. J. *et al.* Elevated levels of NAP-1/interleukin-8 are present in the airspaces of patients with the adult respiratory distress syndrome and are associated with increased mortality. *Am Rev Respir Dis.* **146,** 427–432 (1992).

238. Goodman, R. B. *et al.* Inflammatory cytokines in patients with persistence of the acute respiratory distress syndrome. *Am J Respir Crit Care Med.* **154,** 602–611 (1996).

239. Fitzgerald, M., McAuley, D. F. & O'Kane, C. M. Oncostatin M is a novel mediator of human pulmonary endothelial chemokine and protease activity in the lung in ARDS. *Thorax* **71,** A47 (2016).

240. Shelton, J. L., Wang, L., Cepinskas, G., Inculet, R. & Mehta, S. Human neutrophil-pulmonary microvascular endothelial cell interactions in vitro: differential effects of nitric oxide vs. peroxynitrite. *Microvasc Res.* **76,** 80–88 (2008).

241. Srinivasan, B. *et al.* TEER Measurement Techniques for In Vitro Barrier Model Systems. *J Lab Autom.* **20,** 107–126 (2015).

242. van der Heijden, M. *et al.* Opposing effects of the angiopoietins on the thrombin-induced permeability of human pulmonary microvascular endothelial cells. *PLoS One* **6,** e23448 (2011).

243. Jurczyluk, J., Brown, D. & Stanley, K. K. Polarised secretion of cytokines in primary human microvascular endothelial cells is not dependent on N-linked glycosylation. *Cell Biol Int.* **27,** 997–1003 (2003).

244. Pati, S. *et al.* Bone Marrow Derived Mesenchymal Stem Cells Inhibit Inflammation and Preserve Vascular Endothelial Integrity in the Lungs after Hemorrhagic Shock. *PLoS One* **6,** e25171 (2011).

245. Bischoff, I. *et al.* Pitfalls in assessing microvascular endothelial barrier function: impedance-based devices versus the classic macromolecular tracer assay. *Sci Rep.* **6,** 23671 (2016).

246. Singla, S. *et al.* Hemin Causes Lung Microvascular Endothelial Barrier Dysfunction by Necroptotic Cell Death. *Am J Respir Cell Mol Biol.* **57,** 307–314 (2017).

247. Dudek, S. M. & Garcia, J. G. N. Cytoskeletal regulation of pulmonary vascular permeability. *J Appl Physiol* **91,** 1487–1500 (2001).

248. Csortos, C., Kolosova, I. & Verin, A. D. Regulation of vascular endothelial cell barrier function and cytoskeleton structure by protein phosphatases of the PPP family. *Am J Physiol Lung Cell Mol Physiol.* **293,** L843-854 (2007).

249. Tsuji, T., Aoshiba, K., Itoh, M., Nakamura, H. & Yamaguchi, K. Hypercapnia Accelerates Wound Healing in Endothelial Cell Monolayers Exposed to Hypoxia. *Open Respir Med J.* **7,** 6–12 (2013).

250. Inoue, T. *et al.* Cross-enhancement of ANGPTL4 transcription by HIF1 alpha and PPAR beta/delta is the result of the conformational proximity of two response elements. *Genome Biol.* **15,** R63 (2014).

251. Yang, L. *et al.* Melatonin suppresses hypoxia-induced migration of HUVECs via inhibition of ERK/Rac1 activation. *Int J Mol Sci.* **15,** 14102–14121 (2014).

252. Wang, F. *et al.* T7 peptide inhibits angiogenesis via downregulation of angiopoietin-2 and autophagy. *Oncol. Rep.* **33,** 675–684 (2015).

253. Wang, L. *et al.* Human alveolar epithelial cells attenuate pulmonary microvascular endothelial cell permeability under septic conditions. *PLoS One* **8,** e55311 (2013).

254. Mukaida, N., Okamoto, S., Ishikawa, Y. & Matsushima, K. Molecular mechanism of interleukin-8 gene expression. *J Leukoc Biol.* **56,** 554–558

(1994).

255. Collins, T. *et al.* Transcriptional regulation of endothelial cell adhesion molecules: NF-kappa B and cytokine-inducible enhancers. *FASEB J.* **9,** 899–909 (1995).

256. Rahman, A., Anwar, K. A., True, A. L. & Malik, A. B. Thrombin-induced p65 homodimer binding to downstream NF-kappa B site of the promoter mediates endothelial ICAM-1 expression and neutrophil adhesion. *J Immunol.* **162,** 5466–5476 (1999).

257. Roebuck, K. A. & Finnegan, A. Regulation of intercellular adhesion molecule-1 (CD54) gene expression. *J Leukoc Biol.* **66,** 876–888 (1999).

258. Keates, A. C. *et al.* ZBP-89, Sp1, and nuclear factor-kappa B regulate epithelial neutrophil-activating peptide-78 gene expression in Caco-2 human colonic epithelial cells. *J Biol Chem.* **276,** 43713–43722 (2001).

259. Hoffmann, E., Dittrich-Breiholz, O., Holtmann, H. & Kracht, M. Multiple control of interleukin-8 gene expression. *J Leukoc Biol.* **72,** 847–855 (2002).

260. Liu, Y. *et al.* IL-17A and TNF-a Exert Synergistic Effects on Expression of CXCL5 by Alveolar Type II Cells In Vivo and In Vitro. *J Immunol.* **186,** 3197–3205 (2011).

261. Schuler, M.-H. *et al.* Miro1-mediated mitochondrial positioning shapes intracellular energy gradients required for cell migration. *Mol Biol Cell.* **28,** 2159–2169 (2017).

262. Weibel, E. R. On the tricks alveolar epithelial cells play to make a good lung. *Am J Respir Crit Care Med.* **191,** 504–513 (2015).

263. Fehrenbach, H. Alveolar epithelial type II cell: defender of the alveolus revisited. *Respir Res.* **2,** 33–46 (2001).

264. Bellingan, G. J. The pulmonary physician in critical care • 6: The pathogenesis of ALI/ARDS. *Thorax* **57,** 540–546 (2002).

265. Thorley, A. J. *et al.* Differential Regulation of Cytokine Release and Leukocyte Migration by Lipopolysaccharide-Stimulated Primary Human Lung Alveolar

Type II Epithelial Cells and Macrophages. *J Immunol* **178,** 463–473 (2007).

266. Witherden, I. R. *et al.* Primary human alveolar type II epithelial cell chemokine release: effects of cigarette smoke and neutrophil elastase. *Am J Respir Cell Mol Biol.* **30,** 500–509 (2004).

267. Hoffmann, R., Brandenburg, S., ten Hacken, N., van Oosterhout, A. & Heijink, I. Mitochondrial dysfunction in airway epithelium increases pro-inflammatory IL-8, impairs barrier function and reduces glucocorticoid responsiveness. *Eur. Respir. J.* **38,** 773 (2011).

268. Dunn, J. D., Alvarez, L. A. J., Zhang, X. & Soldati, T. Reactive oxygen species and mitochondria: A nexus of cellular homeostasis. *Redox Biol.* **6,** 472–485 (2015).

269. Vandenbroucke, E., Mehta, D., Minshall, R. & Malik, A. B. Regulation of endothelial junctional permeability. *Ann N Y Acad Sci.* **1123,** 134–145 (2008).

270. Matthay, M. A., Folkesson, H. G. & Clerici, C. Lung epithelial fluid transport and the resolution of pulmonary edema. *Physiol Rev.* **82,** 569–600 (2002).

271. Morales, M. M. B. *et al.* Small airway remodeling in acute respiratory distress syndrome: a study in autopsy lung tissue. *Crit Care.* **15,** R4 (2011).

272. Panduri, V., Weitzman, S. A., Chandel, N. S. & Kamp, D. W. Mitochondrial-derived free radicals mediate asbestos-induced alveolar epithelial cell apoptosis. *Am J Physiol Lung Cell Mol Physiol.* **286,** L1220-1227 (2004).

273. Kiefmann, M. *et al.* IDH3 mediates apoptosis of alveolar epithelial cells type 2 due to mitochondrial Ca2+ uptake during hypocapnia. *Cell Death Dis.* **8,** e3005 (2017).

274. Johnson, M. D., Widdicombe, J. H., Allen, L., Barbry, P. & Dobbs, L. G. Alveolar epithelial type I cells contain transport proteins and transport sodium, supporting an active role for type I cells in regulation of lung liquid homeostasis. *Proc. Natl. Acad.* **99,** 1966–1971 (2002).

275. Flodby, P. *et al.* Knockout Mice Reveal a Major Role for Alveolar Epithelial Type I Cells in Alveolar Fluid Clearance. *Am J Respir Cell Mol Biol.* **55,** 395–

406 (2016).

276. Wiener-Kronish, J. P. *et al.* Relationship of pleural effusions to increased permeability pulmonary edema in anesthetized sheep. *J Clin Invest.* **82,** 1422–1429 (1988).

277. Matthay, M. A. Resolution of pulmonary edema. Thirty years of progress. *Am J Respir Crit Care Med.* **189,** 1301–1308 (2014).

278. Campos, R. *et al.* N-acetylcysteine prevents pulmonary edema and acute kidney injury in rats with sepsis submitted to mechanical ventilation. *Am J Physiol Lung Cell Mol Physiol.* **302,** L640-650 (2012).

279. Eisenhut, M. Role of nitric oxide metabolites in reduction of sodium potassium ATPase dependent pulmonary edema clearance. *Am J Physiol Lung Cell Mol Physiol* **303,** L487 (2012).

280. Kryvenko, V. *et al.* Hypercapnia Impairs Cell Junction Formation by Promoting Ubiquitination and Proteasomal Degradation of the Na,K-ATPase β-Subunit in Alveolar Epithelial Cells [abstract]. *Am. J. Respir. Crit. Care Med.* **193,** A5765 (2016).

281. Vagin, O., Tokhtaeva, E. & Sachs, G. The Role of the β1 Subunit of the Na,K-ATPase and Its Glycosylation in Cell-Cell Adhesion. *J Biol Chem.* **281,** 39573–39587 (2006).

282. Vadasz, I. *et al.* AMP-activated protein kinase regulates CO2-induced alveolar epithelial dysfunction in rats and human cells by promoting Na,K-ATPase endocytosis. *J Clin Invest.* **118,** 752–762 (2008).

283. Vadasz, I. *et al.* Evolutionary conserved role of c-Jun-N-terminal kinase in CO2-induced epithelial dysfunction. *PLoS One* **7,** e46696 (2012).

284. Welch, L. C. *et al.* Extracellular signal-regulated kinase (ERK) participates in the hypercapnia-induced Na,K-ATPase downregulation. *FEBS Lett.* **584,** 3985–3989 (2010).

285. Dada, L. A. *et al.* High CO2 Leads to Na,K-ATPase Endocytosis via c-Jun Amino-Terminal Kinase-Induced LMO7b Phosphorylation. *Mol. Cell. Biol.* **35,**

3962–3973 (2015).

286. Gwozdzinska, P. *et al.* Hypercapnia Impairs ENaC Cell Surface Stability by Promoting Phosphorylation, Polyubiquitination and Endocytosis of β-ENaC in a Human Alveolar Epithelial Cell Line. *Front Immunol.* **8,** (2017).

287. Wu, S.-Y. *et al.* Protective Effect of Hypercapnic Acidosis in Ischemia-Reperfusion Lung Injury Is Attributable to Upregulation of Heme Oxygenase-1. *PLoS One* **8,** e74742 (2013).

288. Elbert, K. J. *et al.* Monolayers of human alveolar epithelial cells in primary culture for pulmonary absorption and transport studies. *Pharm Res.* **16,** 601–308 (1999).

289. Fuchs, S. *et al.* Differentiation of human alveolar epithelial cells in primary culture: morphological characterization and synthesis of caveolin-1 and surfactant protein-C. *Cell Tissue Res.* **311,** 31–45 (2003).

290. Bove, P. F. *et al.* Human alveolar type II cells secrete and absorb liquid in response to local nucleotide signaling. *J Biol Chem.* **285,** 34939–34949 (2010).

291. Giard, D. J. *et al.* In vitro cultivation of human tumors: establishment of cell lines derived from a series of solid tumors. *J Natl Cancer Inst.* **51,** 1417–1423 (1973).

292. Swain, R. J., Kemp, S. J., Goldstraw, P., Tetley, T. D. & Stevens, M. M. Assessment of cell line models of primary human cells by Raman spectral phenotyping. *Biophys J.* **98,** 1703–1711 (2010).

293. Campbell, L. *et al.* Caveolin-1 expression and caveolae biogenesis during cell transdifferentiation in lung alveolar epithelial primary cultures. *Biochem Biophys Res Commun.* **262,** 744–751 (1999).

294. Godfrey, R. W. A. Human airway epithelial tight junctions. *Microsc Res Tech.* **38,** 488–499 (1997).

295. Geys, J. *et al.* In vitro study of the pulmonary translocation of nanoparticles: a preliminary study. *Toxicol Lett.* **160,** 218–226 (2006).

296. Hall-Stoodley, L. *et al.* Mycobacterium tuberculosis Binding to Human

Surfactant Proteins A and D, Fibronectin, and Small Airway Epithelial Cells under Shear Conditions. *Infect Immun.* **74,** 3587–3596 (2006).

297. Verkman, A. S. Role of aquaporins in lung liquid physiology. *Respir Physiol Neurobiol.* **159,** 324–330 (2007).

298. Bhowmick, R. & Gappa-Fahlenkamp, H. Cells and Culture Systems Used to Model the Small Airway Epithelium. *Lung* **194,** 419–428 (2016).

299. Damian, S., Smithhisler, M. R. & Klarmann, G. J. *An air-liquid interface culture system for small airway epithelial cells*. (2011).

300. Jayaseelan, S. *et al.* Induction of CXCL5 during inflammation in the rodent lung involves activation of alveolar epithelium. *Am J Respir Cell Mol Biol.* **32,** 531–539 (2005).

301. Lacherade, J. C. *et al.* Evaluation of basement membrane degradation during TNF-alpha-induced increase in epithelial permeability. *Am J Physiol Lung Cell Mol Physiol.* **281,** L134-143 (2001).

302. Tang, M. *et al.* TNF-α Mediated Increase of HIF-1α Inhibits VASP Expression, Which Reduces Alveolar-Capillary Barrier Function during Acute Lung Injury (ALI). *PLoS One* **9,** e102967 (2014).

303. Liu, Y. *et al.* IL-17A and TNF-α exert synergistic effects on expression of CXCL5 by alveolar type II cells in vivo and in vitro. *J Immunol.* **186,** 3197–3205 (2011).

304. Piantadosi, C. A. & Suliman, H. B. Mitochondrial Dysfunction in Lung Pathogenesis. *Annu Rev Physiol.* **79,** 495–515 (2017).

305. Youle, R. J. & Narendra, D. P. Mechanisms of mitophagy. *Nat Rev Mol Cell Biol.* **12,** 9–14 (2011).

306. Patel, A. S. *et al.* Epithelial cell mitochondrial dysfunction and PINK1 are induced by transforming growth factor-beta1 in pulmonary fibrosis. *PLoS One* **10,** e0121246 (2015).

307. Larson-Casey, J. L., Deshane, J. S., Ryan, A. J., Thannickal, V. J. & Carter, A. B. Macrophage Akt1 Kinase-Mediated Mitophagy Modulates Apoptosis

Resistance and Pulmonary Fibrosis. *Immunity* **44,** 582–596 (2016).

308. Niu, Z. *et al.* Mitophagy inhibits proliferation by decreasing cyclooxygenase-2 (COX-2) in arsenic trioxide-treated HepG2 cells. *Env. Toxicol Pharmacol.* **45,** 212–221 (2016).

309. Martinez-Reyes, I. *et al.* TCA Cycle and Mitochondrial Membrane Potential Are Necessary for Diverse Biological Functions. *Mol. Cell* **61,** 199–209 (2016).

310. Wu, G.-J. *et al.* Propofol specifically inhibits mitochondrial membrane potential but not complex I NADH dehydrogenase activity, thus reducing cellular ATP biosynthesis and migration of macrophages. *Ann N Y Acad Sci.* **1042,** 168–176 (2005).

311. Mills, E. L. *et al.* Succinate Dehydrogenase Supports Metabolic Repurposing of Mitochondria to Drive Inflammatory Macrophages. *Cell* **167,** 457–470 (2016).

312. Lee, J. W. *et al.* Acute lung injury edema fluid decreases net fluid transport across human alveolar epithelial type II cells. *J Biol Chem.* **282,** 24109–24119 (2007).

313. Zheng, S. *et al.* ResolvinD 1 stimulates epithelial wound repair and inhibits TGF- β -induced EMT whilst reducing fibroproliferation and collagen production. *Lab. Investig.* (2017).

314. Wagner, W. *et al.* Comparative characteristics of mesenchymal stem cells from human bone marrow, adipose tissue, and umbilical cord blood. *Exp. Hematol.* **33,** 1402–1416 (2005).

315. Ullah, I., Subbarao, R. B. & Rho, G. J. Human mesenchymal stem cells - current trends and future prospective. *Biosci Rep.* **35,** e00191 (2015).

316. Dominici, M. *et al.* Minimal criteria for defining multipotent mesenchymal stromal cells. The International Society for Cellular Therapy position statement. *Cytotherapy* **8,** 315–317 (2006).

317. Pittenger, M. F. *et al.* Multilineage potential of adult human mesenchymal stem cells. *Science (80-.).* **284,** 143–147 (1999).

318. Timmers, L. *et al.* Reduction of myocardial infarct size by human mesenchymal stem cell conditioned medium. *Stem Cell Res.* **1,** 129–137 (2007).

319. Monsel, A., Zhu, Y.-G., Gudapati, V., Lim, H. & Lee, J. W. Mesenchymal Stem Cell Derived Secretome and Extracellular Vesicles for Acute Lung Injury and Other Inflammatory Lung Diseases. *Expert Opin Biol Ther.* **16,** 859–871 (2016).

320. Lou, G., Chen, Z., Zheng, M. & Liu, Y. Mesenchymal stem cell-derived exosomes as a new therapeutic strategy for liver diseases. *Exp Mol Med.* **49,** e346 (2017).

321. Zang, L. *et al.* Mesenchymal stem cell therapy in type 2 diabetes mellitus. *Diabetol Metab Syndr.* **36,** (2017).

322. Gao, L. *et al.* Phase II Multicenter, Randomized, Double-Blind Controlled Study of Efficacy and Safety of Umbilical Cord-Derived Mesenchymal Stromal Cells in the Prophylaxis of Chronic Graft-Versus-Host Disease After HLA-Haploidentical Stem-Cell Transplantation. *J Clin Oncol.* **34,** 2843–2850 (2016).

323. Mei, S. H. J. *et al.* Mesenchymal stem cells reduce inflammation while enhancing bacterial clearance and improving survival in sepsis. *Am J Respir Crit Care Med.* **182,** 1047–1057 (2010).

324. Krasnodembskaya, A. *et al.* Human mesenchymal stem cells reduce mortality and bacteremia in gram-negative sepsis in mice in part by enhancing the phagocytic activity of blood monocytes. *Am J Physiol Lung Cell Mol Physiol.* **302,** L1003-1013 (2012).

325. Curley, G. F. *et al.* Effects of intratracheal mesenchymal stromal cell therapy during recovery and resolution after ventilator-induced lung injury. *Anesthesiology* **118,** 924–932 (2013).

326. Shalaby, S. M. *et al.* Mesenchymal stromal cell injection protects against oxidative stress in Escherichia coli–induced acute lung injury in mice. *Cytotherapy* **16,** 764–775 (2014).

327. Devaney, J. *et al.* Human mesenchymal stromal cells decrease the severity of

acute lung injury induced by E. coli in the rat. *Thorax* **70,** 625–635 (2015).

328. Hayes, M. *et al.* Therapeutic efficacy of human mesenchymal stromal cells in the repair of established ventilator-induced lung injury in the rat. *Anesthesiology* **122,** 363–373 (2015).

329. Gupta, N. *et al.* Mesenchymal stem cells enhance survival and bacterial clearance in murine Escherichia coli pneumonia. *Thorax* **67,** 533–539 (2012).

330. Simonson, O. E. *et al.* In Vivo Effects of Mesenchymal Stromal Cells in Two Patients With Severe Acute Respiratory Distress Syndrome. *Stem Cells Transl Med.* **4,** 1199–1213 (2015).

331. Ortiz, L. *et al.* Mesenchymal stem cell engraftment in lung is enhanced in response to bleomycin exposure and ameliorates its fibrotic effects. *Proc Natl Acad Sci U S A* **100,** 8407–8411 (2003).

332. Pierro, M. *et al.* Short-term, long-term and paracrine effect of human umbilical cord-derived stem cells in lung injury prevention and repair in experimental bronchopulmonary dysplasia. *Thorax* **68,** 475–484 (2013).

333. Liu, L. *et al.* Intranasal versus intraperitoneal delivery of human umbilical cord tissue-derived cultured mesenchymal stromal cells in a murine model of neonatal lung injury. *Am J Pathol.* **184,** 3344–3358 (2014).

334. Goolaerts, A. *et al.* Conditioned media from mesenchymal stromal cells restore sodium transport and preserve epithelial permeability in an in vitro model of acute alveolar injury. *Am. J. Physiol. - Lung Cell. Mol. Physiol.* **306,** L975–L985 (2014).

335. Fang, X., Neyrinck, A. P., Matthay, M. A. & Lee, J. W. Allogeneic human mesenchymal stem cells restore epithelial protein permeability in cultured human alveolar type II cells by secretion of angiopoietin-1. *J Biol Chem.* **285,** 26211–26222 (2010).

336. Morrison, T., McAuley, D. F. & Krasnodembskaya, A. Mesenchymal stromal cells for treatment of the acute respiratory distress syndrome: The beginning of the story. *J. Intensive Care Soc.* **16,** 320–329 (2015).

337. Liu, K. *et al.* Mesenchymal stem cells rescue injured endothelial cells in an in vitro ischemia-reperfusion model via tunneling nanotube like structure-mediated mitochondrial transfer. *Microvasc Res.* **92,** 10–18 (2014).

338. Jackson, M. V. *et al.* Mitochondrial Transfer via Tunneling Nanotubes is an Important Mechanism by Which Mesenchymal Stem Cells Enhance Macrophage Phagocytosis in the In Vitro and In Vivo Models of ARDS. *Stem Cells* **34,** 2210–2223 (2016).

339. Ahmad, T. *et al.* Miro1 regulates intercellular mitochondrial transport & enhances mesenchymal stem cell rescue efficacy. *EMBO J.* **33,** 994–1010 (2014).

340. Li, X. *et al.* Mitochondrial transfer of induced pluripotent stem cell-derived mesenchymal stem cells to airway epithelial cells attenuates cigarette smoke-induced damage. *Am J Respir Cell Mol Biol.* **51,** 455–465 (2014).

341. Morrison, T. J. *et al.* Mesenchymal Stromal Cells Modulate Macrophages in Clinically Relevant Lung Injury Models by Extracellular Vesicle Mitochondrial Transfer. *Am J Respir Crit Care Med.* (2017).

342. Zhu, Y.-G. *et al.* Human Mesenchymal Stem Cell Microvesicles for Treatment of E.coli Endotoxin-Induced Acute Lung Injury in Mice. *Stem Cells* **32,** 116–125 (2014).

343. Monsel, A. *et al.* Therapeutic Effects of Human Mesenchymal Stem Cell-derived Microvesicles in Severe Pneumonia in Mice. *Am J Respir Crit Care Med.* **192,** 324–336 (2015).

344. Tang, X.-D. *et al.* Mesenchymal Stem Cell Microvesicles Attenuate Acute Lung Injury in Mice Partly Mediated by Ang-1 mRNA. *Stem Cells* **35,** 1849–1859 (2017).

345. Willis, G. R. *et al.* Mesenchymal Stromal Cell Exosomes Ameliorate Experimental Bronchopulmonary Dysplasia and Restore Lung Function Through Macrophage Immunomodulation. *Am J Respir Crit Care Med.* (2017).

346. Prockop, D. J., Prockop, S. E. & Bertoncello, I. Are Clinical Trials With Mesenchymal Stem/ Progenitor Cells too Far Ahead of the Science? Lessons

From Experimental Hematology. *Stem Cells* **32,** 3055–3061 (2014).

347. Rosova, I., Dao, M., Capoccia, B., Link, D. & Nolta, J. A. Hypoxic preconditioning results in increased motility and improved therapeutic potential of human mesenchymal stem cells. *Stem Cells* **26,** 3173–3182 (2008).

348. Carrero, R. *et al.* IL1β Induces Mesenchymal Stem Cells Migration and Leucocyte Chemotaxis Through NF-κB. *Stem Cell Rev.* **8,** 905–916 (2012).

349. Fan, H. *et al.* Pre-treatment with IL-1β enhances the efficacy of MSC transplantation in DSS-induced colitis. *Cell Mol Immunol.* **9,** 473–481 (2012).

350. Beegle, J. *et al.* Hypoxic preconditioning of mesenchymal stromal cells induces metabolic changes, enhances survival, and promotes cell retention in vivo. *Stem Cells* **33,** 1818–1828 (2015).

351. Saparov, A., Ogay, V., Nurgozhin, T., Jumabay, M. & Chn, W. C. W. Preconditioning of Human Mesenchymal Stem Cells to Enhance Their Regulation of the Immune Response. *Stem Cells Int.* (2016).

352. Kregenow, D. a, Rubenfeld, G. D., Hudson, L. D. & Swenson, E. R. Hypercapnic acidosis and mortality in acute lung injury. *Crit. Care Med.* **34,** 1–7 (2006).

353. Horie, S. & Laffey, J. G. Recent insights: mesenchymal stromal/stem cell therapy for acute respiratory distress syndrome. *F1000 Res.* **5,** 1532 (2016).

354. Mei, S. H. J. *et al.* Prevention of LPS-Induced Acute Lung Injury in Mice by Mesenchymal Stem Cells Overexpressing Angiopoietin 1. *PLoS Med.* **4,** e269 (2007).

355. Dinarello, C. A., Simon, A. & van der Meer, J. W. M. Treating inflammation by blocking interleukin-1 in a broad spectrum of diseases. *Nat Rev Drug Discov.* **11,** 633–652 (2012).

356. Ortiz, L. A. *et al.* Interleukin 1 receptor antagonist mediates the antiinflammatory and antifibrotic effect of mesenchymal stem cells during lung injury. *Proc Natl Acad Sci U S A* **104,** 11002–11007 (2007).

357. Luz-Crawford, P. *et al.* Mesenchymal Stem Cell-Derived Interleukin 1

Receptor Antagonist Promotes Macrophage Polarization and Inhibits B Cell Differentiation. *Stem Cells* **34,** 483–492 (2016).

358. Smith, M. F., Eidlen, D., Arend, W. P. & Gutierrez-Hartmann, A. LPS-induced expression of the human IL-1 receptor antagonist gene is controlled by multiple interacting promoter elements. *J Immunol.* **153,** 3584–3593 (1994).

359. Scott, B. B. *et al.* TNF-alpha modulates angiopoietin-1 expression in rheumatoid synovial fibroblasts via the NF-kappa B signalling pathway. *Biochem Biophys Res Commun.* **328,** 409–414 (2005).

360. Santo-Domingo, J. & Demaurex, N. The renaissance of mitochondrial pH. *J Gen Physiol.* **139,** 415–423 (2012).

361. Dimroth, P., Kaim, G. & Matthey, U. Crucial role of the membrane potential for ATP synthesis by F(1)F(o) ATP synthases. *J Exp Biol.* **203,** 51–59 (2000).

362. Klingenberg, M. The ADP and ATP transport in mitochondria and its carrier. *Biochim Biophys Acta.* **1778,** 1978–2021 (2008).

363. Chen, C.-T., Shih, Y.-R. V., Huo, T. K., Lee, O. K. & Wei, Y.-H. Coordinated changes of mitochondrial biogenesis and antioxidant enzymes during osteogenic differentiation of human mesenchymal stem cells. *Stem Cells* **26,** 960–968 (2008).

364. Pattappa, G., Heywood, H. K., de Bruijn, J. D. & Lee, D. A. The metabolism of human mesenchymal stem cells during proliferation and differentiation. *J Cell Physiol.* **226,** 2562–2570 (2011).

365. Shyh-Chang, N., Daly, G. Q. & Cantley, L. C. Stem cell metabolism in tissue development and aging. *Development* **140,** 2535–2547 (2013).

366. Akram, K. M., Samad, S., Spiteri, M. A. & Forsyth, N. R. Mesenchymal stem cells promote alveolar epithelial cell wound repair in vitro through distinct migratory and paracrine mechanisms. *Respir Res.* **14,** 9 (2013).

367. Gear, A. R. L. Rhodamine 6G. A potent inhibitor of mitochondrial oxidative phosphorylation. *J Biol Chem.* **249,** 3628–3637 (1974).

368. Islam, M. N. *et al.* Mitochondrial transfer from bone marrow-derived stromal

cells to pulmonary alveoli protects against acute lung injury. *Nat Med.* **18,** 759–765 (2012).

369. Ahmad, T. *et al.* Miro1 regulates intercellular mitochondrial transport & enhances mesenchymal stem cell rescue efficacy. *EMBO J.* **33,** 994–1010 (2014).

370. Liu, K. *et al.* Mesenchymal stem cells rescue injured endothelial cells in an in vitro ischemia-reperfusion model via tunneling nanotube like structure-mediated mitochondrial transfer. *Microvasc Res.* **92,** (2014).

371. Vodyanik, M. A. *et al.* A mesoderm-derived precursor for mesenchymal stem and endothelial cells. *Cell Stem Cell* **7,** 718–729 (2010).

372. Kadzik, R. S. & Morrisey, E. E. Lessons from development for directing lung endoderm differentiation in pluripotent stem cells. *Cell Stem Cell* **10,** 355–361 (2012).

373. Phinney, D. G. *et al.* Mesenchymal stem cells use extracellular vesicles to outsource mitophagy and shuttle microRNAs. *Nat Commun.* **6,** 2472 (2015).

Chapter Eight – Supplement

8.1 Supplement 1

To assess endothelial barrier integrity, human pulmonary microvascular endothelial cells (HPMECs) were seeded on transwell inserts and cultured in cell culture medium in 5% CO_2. Transendothelial electrical resistance (TEER) measurements were taken throughout the culture period using an EndOhm meter (World Precision Instruments, USA) to monitor the integrity of the forming barrier. However, TEERs obtained were consistently much lower than expected, even when microscopically the HPMECs appeared to be in a good monolayer. A number of modifications were made to the protocol in an attempt to improve the integrity of the barriers formed. Modifications to the original protocol included:

- Reduction of pore sizes from 3.0µm to 0.4µm
- Switch from polycarbonate membranes to polyethylene terephthalate (PET) membranes
- Increase in the number of cells seeded – minimum density was $1x10^4/cm^2$ (as recommended by the cell supplier), and maximum density was $1x10^5/cm^2$
- Inserts coated with collagen – either type I bovine collagen (Purecol®) or type IV human collagen (both Sigma)
- Cells were maintained in culture for up to 2 weeks, with media changes every 2-3 days

Despite modifications to the original protocol, maximum resistances across HPMEC monolayers rarely peaked above $9\Omega/cm^2$. In a representative experiment, maximum resistance of $8.93\Omega/cm^2$ was obtained 72 hours post-seeding on inserts coated with type IV human collagen **(Figure 8.1A)**. On one occasion, significant TEERs of $75\Omega/cm^2$ were achieved 24 hours post-seeding of $2.5x10^4$ HPMECs/cm^2 on type IV human collagen-coated PET inserts with 0.4µm suitable for a 12 well plate. However, resistances fell rapidly **(Figure 8.1B)** and would have made it difficult to determine the results of experimental conditions.

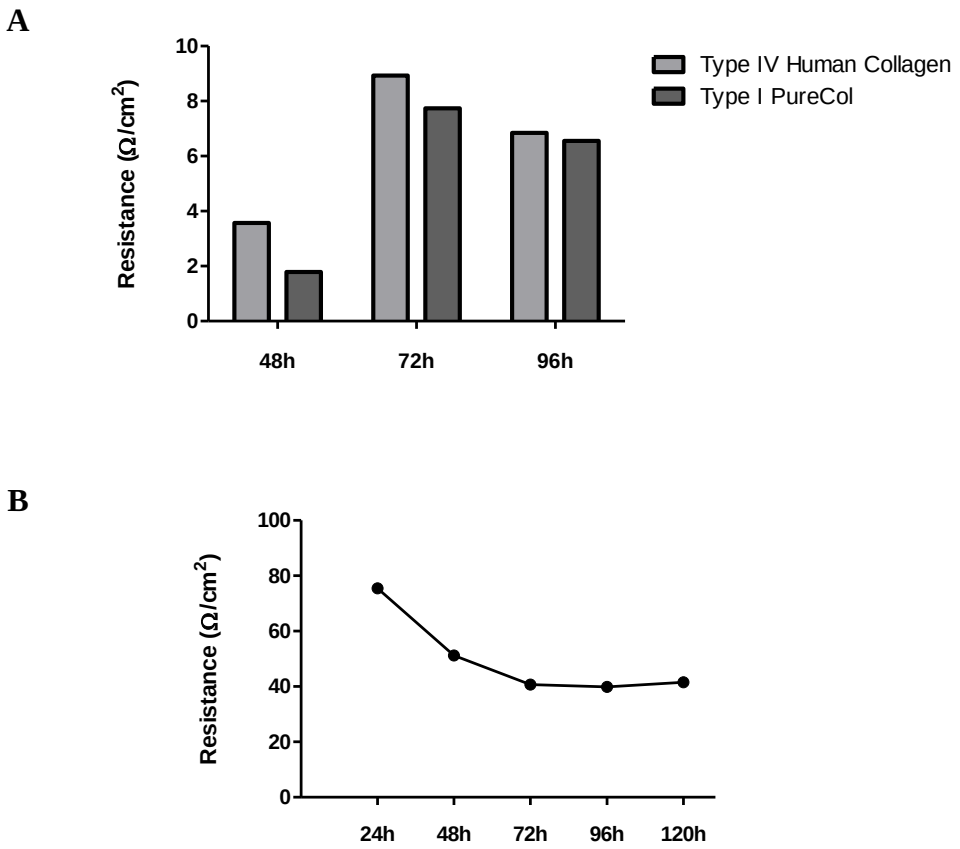

Figure 8.1: Transendothelial electrical resistance (TEER) measurements across HPMEC layers

HPMECs were seeded on collagen-coated polyethylene terephthalate (PET) inserts with 0.4µm pores and cultured in 5% CO_2. TEERs were measured every 24 hours. TEERs across HPMECs seeded on inserts coated with type IV human collagen were compared with those seeded on inserts coated with type I bovine collagen (A) (one representative experiment). On one occasion, significant resistances were obtained across cells seeded on type IV human collagen-coated inserts with 0.4µm pores, but these fell rapidly (B). (n=1; no statistical analysis performed).

8.2 Supplement 2

Human pulmonary microvascular endothelial cells (HPMECs) were seeded at a density of $2.5x10^4/cm^2$ on transwell inserts with 0.4µm pores suitable for a 24 well plate (Greiner). Cells were cultured in 5% CO_2 until monolayer formation, with medium changes every 2-3 days. Following monolayer formation, the medium was replaced with fresh medium; 100µl was added to the upper chamber and 500µl to the lower chamber. 10µl 40kDa FITC-Dextran (Sigma) was added to the upper chamber of inserts on which cells had been seeded. A positive control in which FITC-dextran was also added to inserts on which no cells had been seeded was included. A blank in which PBS was added in place of FITC-dextran to the upper chamber of inserts containing no cells was also included. Cells were cultured in the presence of FITC-dextran in 5% or 15% CO_2 for 30 minutes. After 30 minutes, 100µl samples were collected and added to a black 96 well plate with transparent bottom (Corning). Fluorescence intensity was read immediately using a FLUOstar Omega microplate reader at 485nm excitation and 520nm emission. Results are presented as % of positive control.

The results demonstrate that 69.2 ± 17.1% of FITC-dextran still passed through unstimulated HPMEC monolayers when compared to the positive control **(Figure 8.2)**, indicating that monolayer integrity was insufficiently tight to permit functional assessment of barrier integrity in this model.

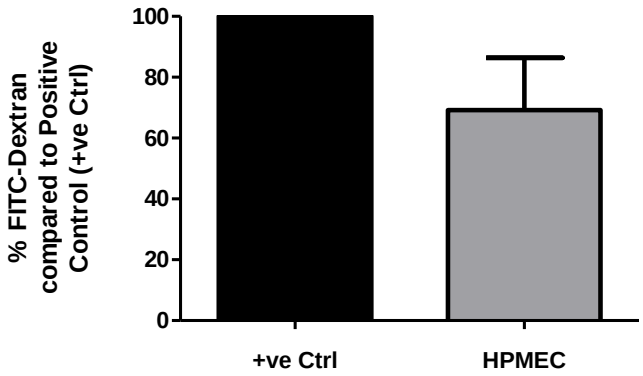

Figure 8.2: HPMEC permeability to FITC-Dextran

HPMECs were seeded on transwell inserts and cultured in 5% CO_2 until monolayer formation. FITC-dextran was added to the upper chamber and the cells were cultured for a further 30 minutes in 5% or 15% CO_2. A positive control was included in which FITC-dextran was added to a transwell insert on which no cells had been seeded. 100µl samples of the medium in the bottom chambers were collected after 30 minutes and fluorescence intensity was measured. Results are presented at % of positive control. Error bars represent standard deviation (SD) (n=2; no statistical analysis performed).

8.3 Supplement 3

Small airway epithelial cells (SAECs) were seeded at a density of $1x10^5/cm^2$ on transwell inserts with 0.4µm pores suitable for a 24 well plate (Greiner). Cells were cultured in 5% CO_2 for two weeks to allow monolayer formation. After two weeks, the medium was replaced with fresh medium either containing or not containing 50ng/ml TNFα. These media had been pre-equilibrated in 5% or 15% CO_2 for 24 hours prior to use. 100µl was added to the upper chamber and 500µl to the lower chamber. Cells were cultured in 5% or 15% CO_2 for 24 hours. After 24 hours, 10µl 40kDa-FITC-Dextran was added to the upper chamber of inserts on which cells had been seeded. A positive control in which FITC-dextran was also added to inserts on which no cells had been seeded was also included. A blank in which PBS was added in place of FITC-dextran to the upper chamber of inserts containing no cells was also included. Cells were cultured in the presence of FITC-dextran in 5% or 15% CO_2 for 30 minutes. After 30 minutes, 100µl samples were collected and added to a black 96 well plate with transparent bottom (Corning). Fluorescence intensity was read immediately using a FLUOstar Omega microplate reader at 485nm excitation and 520nm emission. Results are presented as % of positive control.

Results demonstrate reasonable SAEC barrier function in unstimulated cells in normocapnia (33.0 ± 4.7% of positive control) **(Figure 8.3)**. However, 50ng/ml TNFα did not induce a significant increase in permeability to FITC-dextran in normocapnia (41.1 ± 2.0% of positive control) **(Figure 8.3)**. Given that permeability of unstimulated SAECs and TNFα-stimulated SAECs also did not differ significantly from any other experimental groups (38.8 ± 3.8% and 41.3 ± 5.1% of positive control, respectively) **(Figure 8.3)**, it is difficult to determine if the results obtained are true results or whether the SAECs did not respond to their environment to alter permeability to FITC-dextran.

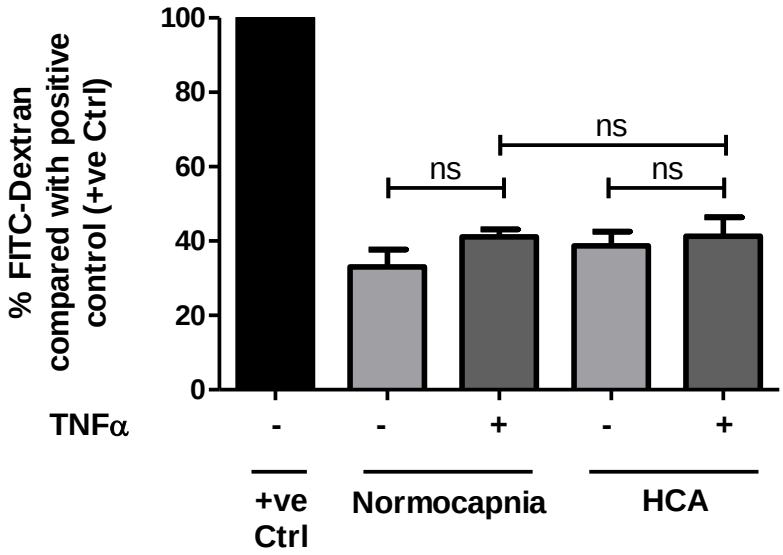

Figure 8.3: SAEC permeability to FITC-Dextran

SAECs were seeded on transwell inserts and cultured in 5% CO_2 for 2 weeks until monolayer formation. SAECs were then cultured in 5% or 15% CO_2 in the presence or absence of 50ng/ml TNFα for 24 hours. FITC-dextran was added to the upper chamber and the cells were cultured for a further 30 minutes in 5% or 15% CO_2. A positive control was included in which FITC-dextran was added to a transwell insert on which no cells had been seeded. 100µl samples of the medium in the bottom chambers were collected after 30 minutes and fluorescence intensity was measured. Results are presented at % of positive control. Error bars represent standard deviation (SD) (n=3; Kruskal-Wallis with Dunn's posthoc analysis; ns = $p>0.05$).